Imperial College London

MRC Centre for Molecular Bacteriology and Infection

Whole-genome analysis of sporulation and germination in *Clostridium difficile*

Marcin Dembek

A thesis submitted in fulfilment of the requirements for the Degree of Doctor of Philosophy

Imperial College London

Department of Life Sciences

MRC Centre for Molecular Bacteriology and Infection

February 2014

Declaration of Originality

The work presented in this thesis has been conducted by the author with all other work acknowledged or referenced appropriately.

Abstract

Clostridium difficile is a Gram-positive, obligate anaerobe and a leading cause of hospital-acquired diarrhoea in humans. Under conditions that are not favourable for growth, *C. difficile* triggers sporulation, producing metabolically dormant endospores through asymmetric cell division. These are regarded as the principal infective stage in the *C. difficile* life cycle, but must germinate to allow for vegetative cell growth and toxin production, representing an attractive target for intervention. A detailed understanding of sporulation and germination could thus have direct applications for disease prevention. While sporulation and germination in the model sporeformer *Bacillus subtilis* is well understood, little is known about these events in *C. difficile*. Therefore, the primary aim of this project was to provide a genome-wide overview of sporulation and germination in *C. difficile* and to identify genes that are essential in these processes using a combination of molecular microbiology, microscopy, transcriptomics and next-generation sequencing.

The first part of this thesis is devoted to the characterisation of *C. difficile* sporulation and germination dynamics, and is followed by a transcriptional analysis of temporal gene expression in germinating spores. A functional analysis of the 511 genes identified as differentially regulated during germination is provided and the results validated for a number of selected genes. One gene in particular, encoding a membrane associated cell wall protein Cwp7, is examined in more detail. In the second part of this thesis I describe the construction of the first comprehensive transposon mutant library which is then used to identify genes that are essential for sporulation and/or germination using Transposon-Directed Insertion Site Sequncing (TraDIS). The results of this study are validated by constructing in-frame deletions in four selected genes followed by a thorough analysis of the resulting phenotypes. Two genes: CD0125 encoding a homologue of *B. subtilis* SpoIIQ and CD3567 encoding a putative cell wall hydrolase are shown to be involved in spore formation while CD0106 encoding a homologues of *B. subtilis* CwlD is shown to be involved in germination.

Acknowledgements

First and foremost I would like to thank my supervisor Professor Neil Fairweather for his constant support, unwavering enthusiasm and giving me the freedom to pave my own path through research. Huge thanks to all the members of the Fairweather Lab (both past and present) for making the last four years such an enjoyable experience… Robert Fagan for spare brainstorming power and his seemingly endless knowledge of all things science-related; Stephanie Willing for being the cool-headed kindred spirit in tackling the day-to-day reality of Academia; Cate Reynolds, for taking me under her wing during the early days; Lucia de la Riva, for being the heart and soul of the group; as well as Allie Shaw and Zoë Seager, for reminding me that there is more to life than work and providing me with more cat-related trivia than I could ever hope for. I would also like to thank Ana Arbeloa Del Moral, Jo Monger, Paula Salgado, Mandy Fivian-Hughes, Johan Peltier, Tom Charlton, Aaron Dale, Ed Couchman and Emma Richards for being the most generous, supportive and friendly people I ever had the chance to eat crêpes with… I mean work with.

I would also like to acknowledge my collaborators at the London School of Hygiene and Tropical Medicine, Royal Holloway and the Sanger Institute for all their help throughout this project and providing me with a pretext to hit the road and change the scenery every once in a while, as well as the Wellcome Trust for the best start to a scientific career one could wish for.

Finally, I would not be in the position I am in today if it was not for my family and friends, keeping me going throughout the years. Thanks to the Wellcome Crew: Anna, Katie, Sorcha and Daniela for braving the course with me and making sure I don't take it all too seriously; Karotka and Kasia, for being my surrogate family in London (even if we still cannot agree on a single set of rules in Macao); Pauli, Sabina and Karolina for all the weekend getaways (getting lost in the wilderness of the Lake District would never be the same without you); and Ania, for pestering me with e-mails and being my musically-inclined pen pal. Most importantly however, I would like to thank my parents who have been my skype-mediated lifeline and the single constant beacon of sanity throughout the years. I dedicate this work to you.

Nie wiedziałem nic, trwając w niewzruszonej wierze,
I knew nothing, dwelling in unwavering belief
że nie minął czas okrutnych cudów.
that the time of cruel wonders has not yet passed.

Stanisław Lem – 'Solaris'

Contents

List of Figures

List of Tables

Abbreviations

ACE	allele-coupled exchange
ATc	anhydrotetracycline
BHI	brain heart infusion
CDDM	*C. difficile* defined medium
CDI	*C. difficile* infection
CDAD	*C. difficile*-associated disease
CFU	colony-forming unit
ci-di-AMP	cyclic diadenosine monophosphate
CLE	cortex lytic enzymes
CoIP	co-immunoprecipitation
CPE	cytopathic effect
CWB domain	cell wall binding domain
CWP	cell wall protein
DPA	dipicolinic acid
EIA	enzyme immunoassay
FC	5-fluorocysteine
FOA	5-fluoroorotic acid
FU	5-fluorouracil
GDH	glutamate dehydrogenase
HMW SLP	high molecular weight S-layer protein
IEP	intron-encoded protein
ITR	inverted terminal repeat
KEGG	Kyoto Encyclopedia of Genes and Genomes
GR	germination receptor
LCT	large Clostridial toxin
LMW SLP	low molecular weight S-layer protein
LTA	lipoteichoic acid
MAL	muramic-δ-lactam
Mes	morpholineethanesulfonic acid
MPS	massively parallel sequencing
MWCO	molecular weight cut-off
NAG	N-acetylglucosamine
NAM	N-acetylmuramic acid

O/N	overnight incubation
OD	optical density
ORF	open reading frame
PaLoc	pathogenicity locus
PBP	penicillin-binding protein
PBS	phosphate-buffered saline
PG	peptidoglycan
P_i	inorganic phosphate
PLG	phase lock gel
PMC	pseudomembraneus colitis
RAM	retrotransposition-acivated marker
RBS	ribosome binding site
RIN	RNA integrity number
ROS	reactive oxygen species
RT	room temperature
S-layer	surface layer
SLH domain	S-layer homology domain
SM	sporulation medium
SASP	small acid-soluble protein
SCWP	secondary cell wall polymer
TBS	Tris-buffered saline
TCA	trichloroacetic acid
Tch	taurocholate
TEM	transmission electron microscopy
TraDIS	transposon-directed insertion site sequencing
WTA	wall teichoic acid

Chapter I

Introduction

1.1. *Clostridium difficile* as a human pathogen

Clostridium difficile is a Gram-positive, spore-forming, obligate anaerobe and a leading cause of antibiotic-associated diarrhoea in humans. First isolated in 1935 from an infant's stool sample and initially named *Bacillus difficilis* to reflect the difficulties in culturing the organism (Hall and O'Toole, 1935), it was not until 1978 that the pathogen was discovered as the agent responsible for pseudomembraneus colitis (PMC), the most severe form of *C. difficile* infection (CDI) (George *et al*., 1978, Bartlett *et al*., 1978b, Bartlett *et al*., 1978c). Since then, the organism has continued to evolve into an adaptable, aggressive, 'hypervirulent' strain placing considerable economic pressure on healthcare systems worldwide (Dubberke and Olsen, 2012).

1.1.1. Epidemiology

For nearly 30 years, CDI has been a common complication of antibiotic use and, with the exception of occasional institutional outbreaks and the problem of relapsing disease following treatment, has been relatively easy to manage. However, the last decade has brought an unexpected change in *C. difficile* epidemiology, particularly in some locations, where *C. difficile*–associated disease (CDAD) has become more frequent, more serious, and more refractory to standard therapy.

1.1.1.1. The new epidemic

Alarming increases in CDI rates initially reported in Canada and the United States in 2002 were shortly followed by reports of similar outbreaks in Europe (Kuijper *et al*., 2006, Warny *et al*., 2005, Pepin *et al*., 2004), raising the possibility of a new strain of *C. difficile*, with unique properties accounting for enhanced virulence. Indeed, the increase in CDI severity and frequency

was shortly correlated with the emergence of a previously uncommon but more virulent strain known as *C. difficile* BI/NAP1, or ribotype 027 (McDonald *et al*., 2005, Warny *et al*., 2005). This trend continued during the following years, culminating in 2007 when more than 55,000 CDI cases were reported in England alone, resulting in 8,324 deaths, compared to 1,517 deaths caused by MRSA, a major nosocomial pathogen implicated in a number of high-profile outbreaks during that period (www.statistics.gov.uk). In response to public health needs, enhanced surveillance of CDI was implemented and mandatory reduction targets for CDI were established across the UK to help battle the escalating infection (Wilcox *et al*., 2012). As a result, CDI numbers have been falling steadily since 2008 with only 1,646 deaths reported in England and Wales in 2012 (www.statistics.gov.uk) (Figure 1.1).

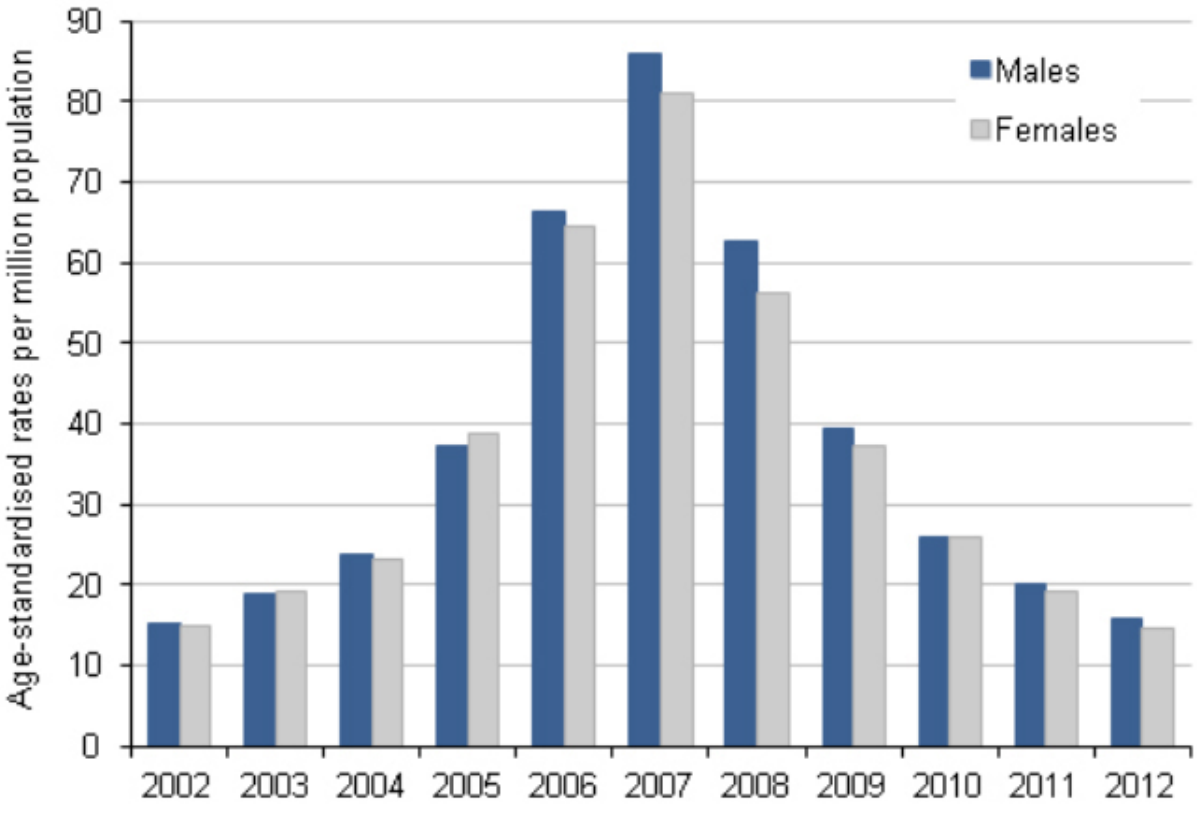

Figure 1.1. Mortality rates for deaths involving *C. difficile* registered in England and Wales between 2002 and 2012 (Office for National Statistics, 22 August 2013; http://www.ons.gov.uk/ons/dcp171778_323989.pdf).

1.1.1.2. Hospital-acquired infection

CDI typically occurs among elderly, hospitalized patients, whose natural intestinal microflora has been disrupted by prolonged treatment with broad-spectrum antibiotics, allowing the pathogen to colonize the compromised gastro-intestinal tract. While it remains unclear why *C. difficile* is particularly effective at colonising this niche compared to other organisms, it is estimated that 20-30% of cases of antibiotic-associated diarrhoea are caused by *C. difficile* making it the most common cause of the disease (McFarland, 2008). Many antibiotics have been linked to CDI, but some carry a higher risk than others including clindamycin, cephalosporins and fluoroquinolones (Johnson *et al*., 1999, Pepin *et al*., 2005). While the use of clindamycin and cephalosporins, to which virtually all *C. difficile* strains are resistant, has been implicated as a CDI risk factor in hospitals for several decades (Johnson *et al*., 1999), the rise in fluoroquinolone-associated risk is more recent, and has been attributed to the rising incidence of *C. difficile* ribotype 027 and other strains that carry high-level fluoroquinolone resistance (Pepin *et al*., 2005). Hospitalisation remains the primary cause of CDI however, as it brings together multiple risks factors, including exposure to antibiotics, a spore-contaminated environment, poor hygiene among health care workers and a highly susceptible elderly population of patients, unable to mount an effective immune response upon infection (reviewed in Rupnik *et al*., 2009).

1.1.1.3. Community-acquired infection

It is estimated that approx. 1 - 3% of the healthy adult population and 40 – 60% of neonates carry *C. difficile* as a commensal bacterium (Kuipers and Surawicz, 2008, McFarland *et al*., 2000). However, community-acquired CDI has always been thought to be rare, leading researchers to focus on hospital settings as the primary backdrop for *C. difficile*-associated disease. Nevertheless, while elderly, hospitalized patients receiving antibiotics are still considered the main group at risk of infection, recent studies revealed an increase in CDI among populations with no previous contact either with the hospital environment or with antibiotics, including children (Kim *et al*., 2008) and

pregnant women (Rouphael *et al*., 2008). The paradigm of a hospital-acquired infection has been further challenged by Eyre *et al*., (2013) who used whole-genome sequencing to illustrate the genetic diversity of *C. difficile* isolates, suggesting a considerable, community-driven reservoir of the pathogen and forcing researcher to consider the role of non-symptomatic carriers in spreading CDI.

1.1.2. Pathogenesis

CDI is a toxin-mediated, intestinal disease with clinical outcomes ranging from asymptomatic colonisation through mild, self-limiting diarrhoea to more severe disease syndromes, including abdominal pain, severe diarrhoea, fever and leukocytosis. Fulminant CDI is characterized by inflammatory lesions and the formation of pseudomembranes in the colon (typical for the aforementioned PMC) (Figure 1.2) which can progress to toxic megacolon and sepsis syndrome causing significant morbidity and mortality (reviewed in Rupnik *et al*., 2009).

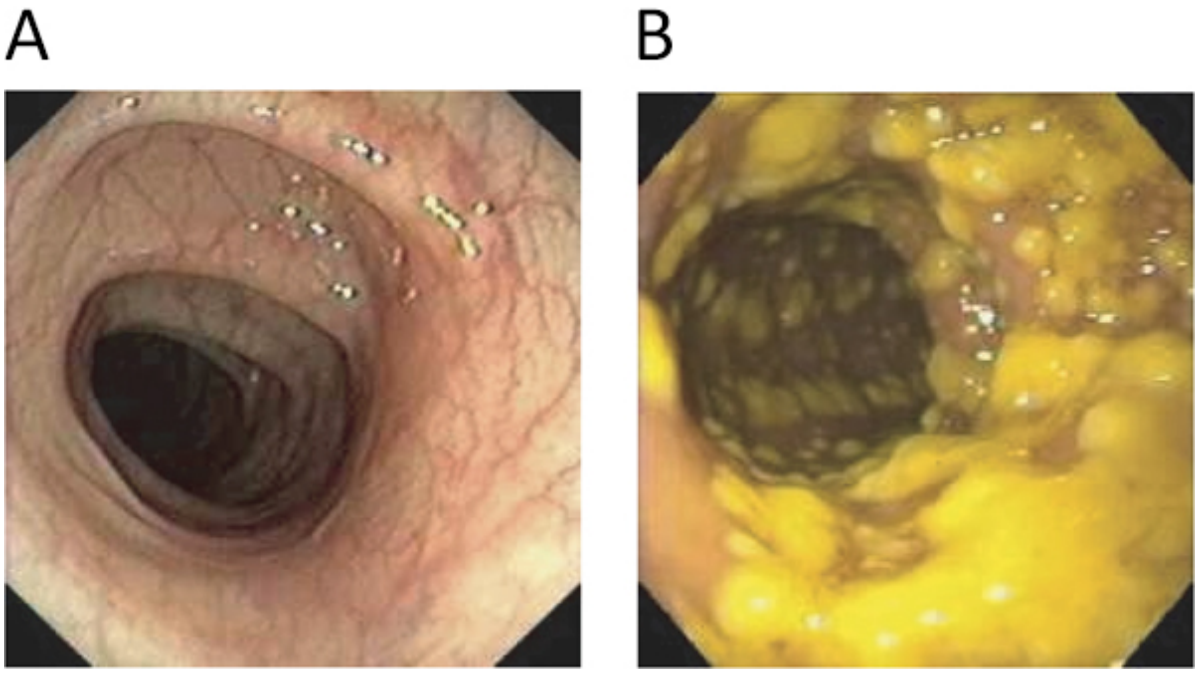

Figure 1.2. Endoscopic visualisation of pseudomembranous colitis. (**A**) Image of a healthy colon. (**B**) Image from a CDAD patient. Classic pseudomembranes are visible as raised yellow plaques, which range from 2-10 mm in diameter and are scattered over the colorectal mucosa. Adapted from Yassin *et al.* (2009).

1.1.2.1. *C. difficile* toxins

It is widely accepted that symptoms of CDI are caused by the action of enterotoxins, as most can be reproduced in animal models by purified toxins alone. Early studies with *Clostridium sordellii* antitoxin showed neutralisation of the *C. difficile* toxins in cell rounding assays (Chang *et al*., 1978, Willey and Bartlett, 1979) and alleviation of CDI symptoms in hamsters, with a reduction in mortality by 75% and reduction in toxicity in faecal filtrates (Allo *et al*., 1979). Two major toxins have been implicated in *C. difficile* pathogenicity: the enterotoxin TcdA and cytotoxin TcdB.

TcdA (308 kDa) and TcdB (269 kDa) are among the largest bacterial toxins known to date and belong to a group of large clostridial toxins (LCTs) that includes the *Clostridium sordellii* lethal toxin (TcsL) and hemorrhagic toxin (TcsH), *Clostridium novyi* alpha toxin (Tcnα) and two types of *Clostridium perfringens* toxin (TcpL). Both TcdA and TcdB are single-chain proteins with similar activity conferred by three main functional regions: an C-terminal binding domain with characteristic repeats, a N-terminal catalytic domain and a putative translocation domain (reviewed in Popoff and Bouvet, 2009) (Figure 1.3A). They enter the cell by receptor-mediated endocytosis and require an acidified endosome for translocation. While TcdA has been shown to bind cell-surface carbohydrates including Gal-α1,3-Gal-β1,4-GlcNAc, the receptor for TcdB has been more elusive. Upon translocation, the N-terminal catalytic domains are released into the cytosol where they glycosylate small GTPases of the Rho and Ras families, rendering them inactive and leading to disruption of the actin cytoskeleton and tight junctions. This results in decreased transepithelial resistance, fluid accumulation and eventual destruction of the intestinal epithelium (reviewed in Jank *et al*., 2007).

Both TcdA and TcdB are expressed from genes located within a 19.6 kb pathogenicity locus (PaLoc) which also contains three other genes important in regulation of toxin activity: *tcdR*, *tcdE* and *tcdC* (Figure 1.3A). Due to its homology to DNA-binding proteins, TcdR is predicted to be a positive regulator of toxin expression, with its presence enhancing toxin promoter activity in *E. coli* (Moncrief *et al*., 1997). TcdE is speculated to be a holin-like protein involved in toxin secretion (Govind and Dupuy, 2012). The *tcdC* gene shows high expression during exponential phase, and a

decrease in transcription when the rest of the PaLoc is up-regulated, suggesting it to be a negative regulator of toxin production (Carter *et al*., 2011, Hundsberger *et al*., 1997, Saujet *et al*., 2011). Mutation of *tcdC* in some ribotype 027 strains was believed to cause constitutive expression of toxins, resulting in 'hypervirulence' (Curry *et al*., 2007). However, this view has been recently challenged, as no link between *tcdC* mutations and toxin production was observed following restoration of the WT *tcdC* allele in a ribotype 027 strain (Cartman *et al*., 2012).

Not all strains produce both toxins and the exact role of each protein has long been disputed. Early experiments indicated that TcdA alone had enterotoxic effects and was able to evoke the symptoms of *C. difficile* infection in hamsters, while toxin B was unable to do so unless mixed with sub-lethal concentrations of TcdA (Lyerly *et al*., 1985). In a later study, a different group demonstrated the importance of both toxins by creating isogenic toxin mutants, both of which showed cytotoxic activity *in vivo* and *in vitro*, as well as a toxin null-mutant which was found to be avirulent (Kuehne *et al*., 2010). In contrast, a study by Lyras *et al*. (2009) indicated that TcdB is essential for *C. difficile* virulence and that a strain producing TcdA alone was avirulent, consistent with experiments on human colonic tissue in which TcdB was shown to be more potent than TcdA in causing mucosal necrosis (Riegler *et al*., 1995). To date, a consensus on the role of each individual protein has not been reached.

In addition to the TcdA and TcdB, some strains also produce the so called binary toxin CTD (Stubbs *et al*., 2000), a homologue of actin-specific ADP-ribosyltransferases found in other clostridial species (Figure 1.3B). Binary toxin genes, *ctdA* and *ctdB* are located away from PaLoc on the chromosome and toxin production is controlled by *ctdR* (Carter *et al*., 2007). The exact function of binary toxin remains to be elucidated, although some studies have found a positive correlation with the severity of diarrhoea (Bacci *et al*., 2011, Barbut *et al*., 2005) and at least one study suggests that CTD might be involved in modulating the epithelial layer to allow for increased colonisation of the gut (Schwan *et al*., 2009).

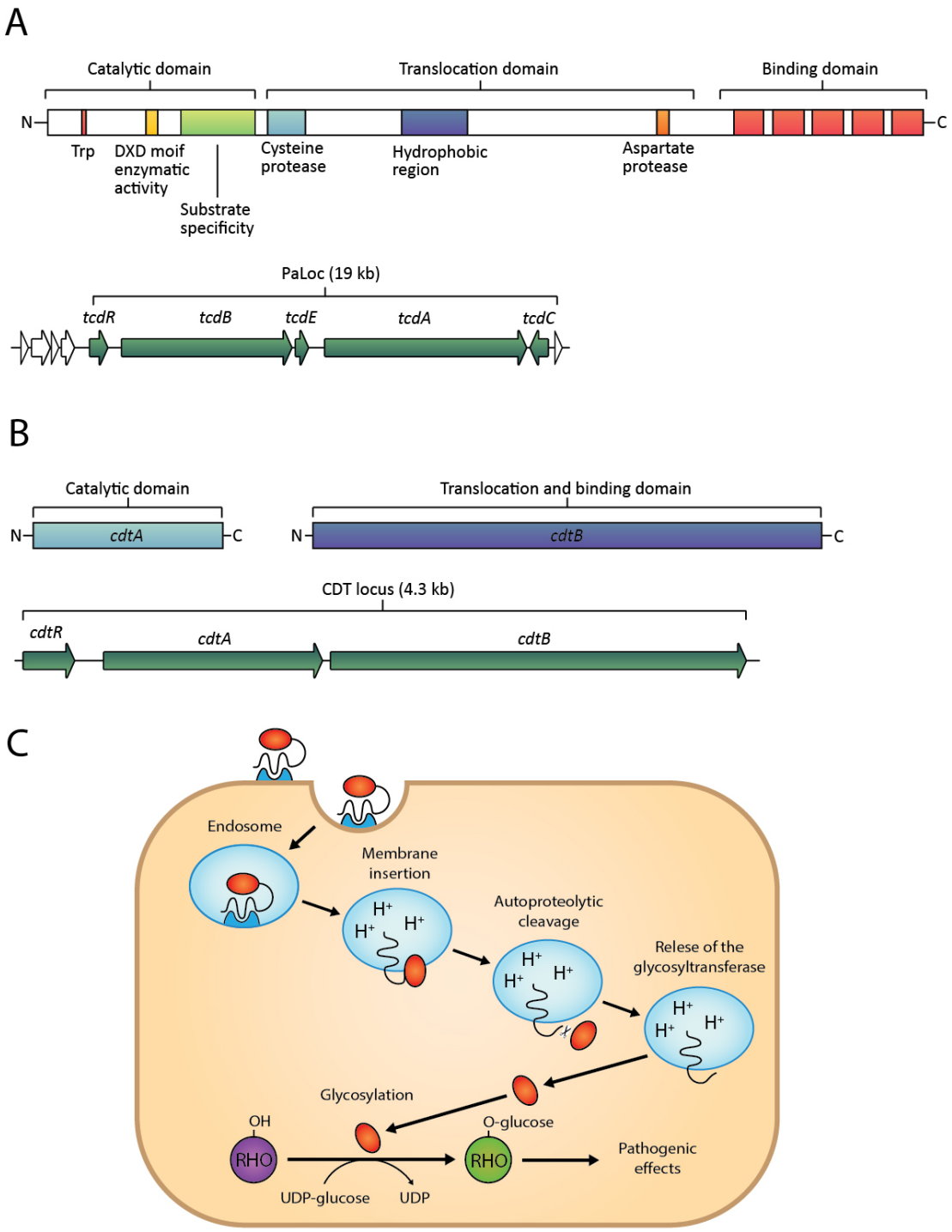

Figure 1.3. Toxins produced by *C. difficile*. (A) Toxin A and toxin B (TcdA and TcdB), are single chain proteins, with several functional domains and motifs (TcdB shown in detail). The genes are located within the pathogenicity locus (PaLoc), which apart from *tcdA* and *tcdB* contains three genes involved in regulation of toxin expression and secretion: *tcdC, tcdE* and *tcdR*. In non-toxigenic strains, this region is replaced by a short 115 bp sequence. **(B)** A third toxin, the binary toxin or CDT, is encoded within a separate region of the chromosome (CdtLoc) and comprises three genes. Two of these encode the binary toxin, composed of two unlinked proteins, CdtB and CdtA. CdtB has a binding function and CdtA is the enzymatic component. The third gene, encoding CtdR is involved in regulation of toxin expression. **(C)** Mechanism of toxin action. The toxin binds with its C terminus to the cell surface receptor, resulting in endocytosis of the toxin–receptor complex. The low pH of endosomes results in a structural change in the toxin, allowing membrane insertion. After translocation of the glucosyltransferase and protease domains into the cytosol, the cysteine protease domain is activated. The protease domain autocatalytically cleaves the toxin and releases the glucosyltransferase domain into the cytosol, where RHO-family proteins are then glucosylated. Adapted from Rupnik *et al.* (2009).

1.1.3. Diagnosis

Rapid and accurate diagnosis of CDI is critical in successful management of the disease, improving patient outcome and ensuring that correct infection control measures are put in place to reduce the chances of horizontal transmission in health care facilities. An early indication of CDI is diarrhoea with a characteristic, foul-smelling odour (Bartlett and Gerding, 2008). While not sufficient for a definitive diagnosis, odour assessment can be a useful tool when determining priority for isolation in settings where isolation capacity is limited, particularly when rapid laboratory diagnostics are not available. All patients with diarrhoea that are at risk of CDI should be further tested. Historically, detection of toxin in stool has been the gold standard in *C. difficile* diagnostics and a number of such methods have been developed over the years, including the cell culture cytotoxicity neutralisation assay, first described in 1978, shortly after the association between *C. difficile* and PMC was made (Bartlett *et al*., 1978a). In this assay the patient's stool filtrate is inoculated onto a monolayer of a particular cell line and tested for toxin-mediated cytopathic effect (CPE). Once CPE is observed, the result is validated by neutralisation with an antiserum. While being highly specific, the CPE test does have certain limitations as it requires 24-48h to carry out and is both costly and labour-intensive (Ticehurst *et al*., 2006). Furthermore, recent comparisons with toxigenic culture tests, in which the pathogen is first cultured form a patients stool sample and then tested for toxin production, as well as with PCR-based assays, have shown the CPE test to have unacceptably low sensitivity (Stamper *et al*., 2009), forcing health care professionals to re-evaluate its usefulness as a reference method in CDI diagnostics (Crobach *et al*., 2009). Some of these issues have been solved with the introduction of enzyme immunoassays (EIAs) which are now commonly used by most laboratories to detect toxin A or both toxins A and toxin B. These are particularly attractive because they do not require cell culture and are technically easier to carry out with a turnaround time of approx. two hours. Several studies have shown however, that EIAs are less sensitive than tissue culture assays, which combined with a poor positive predictive value, particularly in low-prevalence populations, makes them suboptimal for diagnosis of CDI (reviewed in Planche *et al*., 2008). Finally,

indirect detection of toxin is also possible using PCR-based assays specific for conserved regions of *tcdB*, or PaLoc itself. In general PCR-based testing is rapidly replacing other methods in clinical microbiology laboratories, particularly where the required instrumentation is already in place. However, these new technologies are yet to be endorsed by professional society guidelines (Cohen *et al*., 2010, Crobach *et al*., 2009).

Alternative diagnostic methods rely on detection of the pathogen by culture, by PCR or by testing for conserved antigens such as glutamate dehydrogenase (GDH) (Riley *et al*., 1995, Ticehurst *et al*., 2006, van den Berg *et al*., 2006), although all of these suffer from high frequency of false-positive results as 10 - 30% of hospitalised patients are non-symptomatic carriers. Many laboratories have now adopted a two-step approach in which a high negative predictive values test such as the GDH assay is performed first, and if negative, no further testing is required. If the GDH test is positive, a toxin test follows. Due to its high sensitivity (>90%), this two-step method is currently recommended by professional societies in both Europe and America (Cohen *et al*., 2010, Crobach *et al*., 2009).

1.1.4. Treatment

Prior to the emergence of hypevirulent *C. difficile* strains and the corresponding increase in CDI frequency and severity there was little interest in developing new treatments against the pathogen. In most patients, CDI responded to antibiotic therapy, severe complicated cases of CDI were infrequent and while recurrent disease was common, it was also more easily managed. During the past decade, the limitations of current treatment options have become more apparent urging researcher to revisit this once-forgotten problem and develop new methods for battling *C. difficile*.

1.1.4.1. Standard therapy

Since their introduction in the early 1980's, metronidazole and vancomycin have remained the first-line treatment for CDI (Silva *et al*., 1981, Teasley *et al*., 1983). Metroniodazole is

primarily used in mild to moderate cases while vancomycin is reserved for more severe and recurrent CDI as the emergence of vancomycin-resistant enterococci has prompted the reduction of vancomycin usage. While both antibiotics are effective at killing *C. difficile*, between 20 and 30% of patients suffer from recurring infection (Johnson *et al*., 1989). Such Individuals typically respond to further treatment but their symptoms resume within days to weeks after the treatment has stopped. Patients who have one recurrence have up to a 40% chance of a second recurrence, and after their seconds recurrence, up to 65% of patients will suffer a third (Huebner and Surawicz, 2006). Approx. 60% of recurrent infections are classified as relapses caused by the same strain of *C. difficile*, suggesting that antibiotic treatment fails to eradicate the pathogen. The remaining cases represent new infections, caused by a different strain of *C. difficile* (O'Neill *et al*., 1991). There are no effective means to deal with these multiple recurrences, and most are treated with prolonged tapering and pulse dosing of vancomycin given every other or every third day in the hope of keeping *C. difficile* from re-growing while the normal flora recovers. Similarly, there is currently no effective treatment for severe complicated CDI and if antibiotic therapy fails, surgical removal of the colon can be the only remaining life-saving measure (Lamontagne *et al*., 2007).

Better agents for treatment of multiple relapsing and fulminant CDI are desperately needed, and several approaches are currently under investigation. Alternative antibiotics are being developed to deal with the threat of resistance to vancomycin and metronidazole. Possibly the most prominent of these is fidaxomicin, a macrocyclic antibiotic with potent *in vitro* activity against *C. difficile* and limited activity against the normal gut flora (Louie *et al*., 2011). When compared to oral vancomycin, fidaxomicin is equally effective in treating acute CDI, while being associated with significantly lower risk of recurrent infection (Mullane *et al*., 2011). Such promising results led the FDA to approve the drug in 2011 as a routine treatment for CDAD.

1.1.4.2. Faecal transplant therapy

Possibly the most interesting method of treatment that is currently under investigation is the restoration of normal gut flora through faecal transplant therapy. It is now widely accepted that disruption of the indigenous gut flora is a major risk for both primary CDI and recurrent disease. Restoration of the gut flora using stool from a healthy donor has thus been long considered as a viable therapeutic strategy. While the method has been successfully used in the treatment of PMC as early as 1958 (Eiseman *et al*., 1958), it has not gained public attention until recently, when several studies were published showing the therapeutic potential of faecal microbiota in treating fulminant and recurring CDI (Chang *et al*., 2008, Grehan *et al*., 2010, Khoruts *et al*., 2010). Although current literature on the effectiveness of faecal transplant therapy is limited, in all studies published to date approx. 92% of patients that underwent treatment recovered from recurrent CDI (reviewed in Gough *et al*., 2011). The only long-term multicentre follow-up study reported a cure rate of 98% (Brandt *et al*., 2012).

Despite its effectiveness, availability of faecal transplant therapy is still limited and a number of issues need to be addressed before it can be accepted as a standard therapy. The logistics of the treatment are relatively complex, particularly with regard to donor selection and screening as there is a significant risk of donor infection transmission. The timing of collection and preparation of the specimen as well as the route and means of administration are also critical and need to be standardised (reviewed in Smits *et al.*, 2013). Finally, the unusual nature of the treatment is met with an understandable reluctance among the general public. In order to overcome these problems research has begun in defining the bacterial species necessary for recovery, to produce a more palatable treatment. In a recent study, six phylogenetically distinct bacterial species were shown to be sufficient to regain microbial diversity and clear an established *C. difficile* infection in mice (Lawley *et al*., 2012). This approach was further validated in humans when a stool substitute preparation, containing just 33 species of bacteria isolated from a healthy donor, was used to

restore normal bowel patterns in two patients suffering from recurrent CDI (Petrof *et al*., 2013), providing an attractive alternative to standard faecal transplant therapy.

1.2. The bacterial cell wall

While toxin-mediated pathogenicity has been extensively studied in *C. difficile*, and its contribution to CDAD has been well characterised, relatively little is known about the early stages of infection, critical in the establishment of the pathogen's niche. Successful colonisation of the human gut is largely dependent on the interactions that occur at the host-pathogen interface, typically mediated by surface-exposed, cell wall-associated virulence factors, facilitating adhesion, micro-colony formation and evasion of the host's immune responses. This is why increasingly more attention is now being paid to the *C. difficile* cell wall and its surface structures, as key factors in CDI pathogenesis.

The cell wall is of central importance in bacterial physiology, providing protection from stresses, determining the cell shape and forming an interface for communication with the environment. In pathogenic bacteria it can also play a key role during the course of infection, facilitating invasion, immune evasion, and acting as a platform for anchoring virulence factors such as adhesins and toxins (reviewed in Silhavy *et al*., 2010). The cell walls of Gram-positive and Gram-negative bacteria can be clearly distinguished by their thickness and the presence or absence of an outer membrane. Yet the chemical structure of their primary component, the peptidoglycan layer, is largely conserved (Vollmer, 2008), consisting of linear chains of alternating N-acetylglucosamine (NAG) and N-acetylmuramic acid (NAM) residues, cross-linked by peptides attached to the lactate residue of NAM (Liu and Gotschlich, 1967, Wheat and Ghuysen, 1971, Young, 1966). While this architecture is preserved in *C. difficile*, a recent study by Peltier *et al*. found that 96% of NAG residues within the *C. difficile* peptidoglycan are de-acetylated, accounting for its resistance to lysozyme. In addition to peptidoglycan, the Gram-positive cell wall can contain secondary cell wall polymers such as peptidoglycan-bound wall teichoic and teichuronic acids (WTA) and membrane-

bound lipoteichoic acids (LTA) (Coley *et al*., 1975, Hancock and Baddiley, 1976, Lambert *et al*., 1977). These can make up between 10 – 60% of the cell wall structure and play an important role in maintaining cell wall integrity, attaching the peptidoglycan layer to the membrane and anchoring additional structures that provide important functional properties to the surface of the cell (reviewed in Schaffer and Messner, 2005, Weidenmaier and Peschel, 2008).

1.2.1. The *C. difficile* S-layer

The most prominent cell wall-associated surface structures in prokaryotes are surface layers (S-layers), formed by one or more glycoproteins, that self-assemble into a two-dimensional crystalline array covering the entire surface of the cell (Sleytr and Messner, 1983). These are ubiquitous among both Gram-positive and Gram-negative bacteria (Sleytr and Beveridge, 1999) as well as Archaea (Albers and Meyer, 2011), and have been extensively studied in numerous species since their initial discovery in the 1950's. S-layer proteins are believed to be anchored to the cell surface through non-covalent interactions with cell surface structures, most commonly with LPS in Gram-negative bacteria and with cell wall polysaccharides in Gram-positive bacteria. To date, two conserved Gram-positive S-layer anchoring modules have been identified, utilizing either the S-layer homology (SLH) domain, typically found in *Bacillus* species, or the cell wall-binding (CWB2) domain, more common among Clostridia (Mesnage *et al*., 2000, Fagan *et al*., 2011). S-layer biogenesis consumes considerable metabolic resources and therefore must confer a significant advantage to the cell. It is thus not surprising that, as a major structure of the cell, a variety of functions have been proposed for the S-layer, acting as a scaffold for enzyme display, forming a permeability barrier, and playing important roles in host-pathogen interactions (Fagan and Fairweather, 2014).

To date, the best studied examples of S-layers in Gram-positive bacteria are those found in *Bacillus anthracis* and *C. difficile*. In the latter, the S-layer is composed primarily of the major cell wall protein, SlpA (Calabi *et al*., 2001). Following SecA2-mediated export (Fagan and Fairweather, 2011)

SlpA undergoes post-translational cleavage by a specific, surface layer-associated cysteine protease Cwp84 (Kirby *et al*., 2009), forming two proteins: the high and low molecular weight S-layer proteins (HMW SLP and LMW SLP). Together these form a non-covalent, heterodimeric complex that assembles into a two-dimensional array completely surrounding the bacterial cell (Fagan *et al*., 2009), most likely in a Ca^{2+}-dependent manner (Takumi *et al*., 1992) (Figure 1.4A). Both proteins are highly variable across different strains of *C. difficile*, show little cross-reactivity and often produce different band patterns when separated *via* SDS-PAGE (Calabi and Fairweather, 2002, McCoubrey and Poxton, 2001). In addition to HMW SLP and LMW SLP, *C. difficile* encodes an 'arsenal' of minor SLP homologues forming a family of cell wall proteins (CWPs), scattered throughout the *C. difficile* S-layer. Each member of this family contains a conserved CWB2 motif (Pfam 04122) and many contain additional domains that may specify a functional property (Figure 1.4B) (Emerson and Fairweather, 2009). As is the case with the major SLPs, many CWPs show significant sequence diversity (Reynolds *et al*., 2011). Transcriptomic and proteomic studies have shown several of these proteins to be expressed *in vitro* (Emerson *et al*., 2008, Wright *et al*., 2005) while CWP-specific antibodies found in the serum of CDAD patients suggest that at least some of the CWPs are also expressed *in vivo* during infection being recognised by the host's immune system (Wright *et al*., 2008). A number of CWPs have now been characterised. The cysteine protease Cwp84 has been shown to be involved in SlpA processing while its paralog Cwp13 appears to have a role in Cwp84 processing, although it is not essential for its activity (de la Riva *et al.*, 2011, Janoir *et al.*, 2007, Kirby *et al*., 2009). Cwp66 has been shown to be expressed on the cell surface, and has been implicated in adhesion to the epithelial lining of the gut as antibodies raised against recombinant Cwp66 were shown to inhibit adhesion of *C. difficile* to a mammalian cell line (Waligora *et al*., 2001). This was further confirmed in the mouse model of CDI using a Cwp66 knock-out strain (Dr Zoë Seager, unpublished results). The largest member of the CWP family, CwpV, was shown to be surface expressed in a phase-variable manner (Emerson *et al*., 2009), and to be post-translational cleaved *via* enzyme-independent intramolecular autoproteolysis into two fragments, forming a stable, non-covalently associated

complex (Dembek *et al*., 2011, Reynolds *et al*., 2011). The protein has been implicated in cell aggregation as its overexpression results in severe cell clumping (Emerson *et al*., 2009). Finally, the highly conserved, immunodominant protein Cwp2 has attracted a lot of attention from vaccinologists and has been recently implicated in flagellar motility (Dr Aaron Dale, unpublished

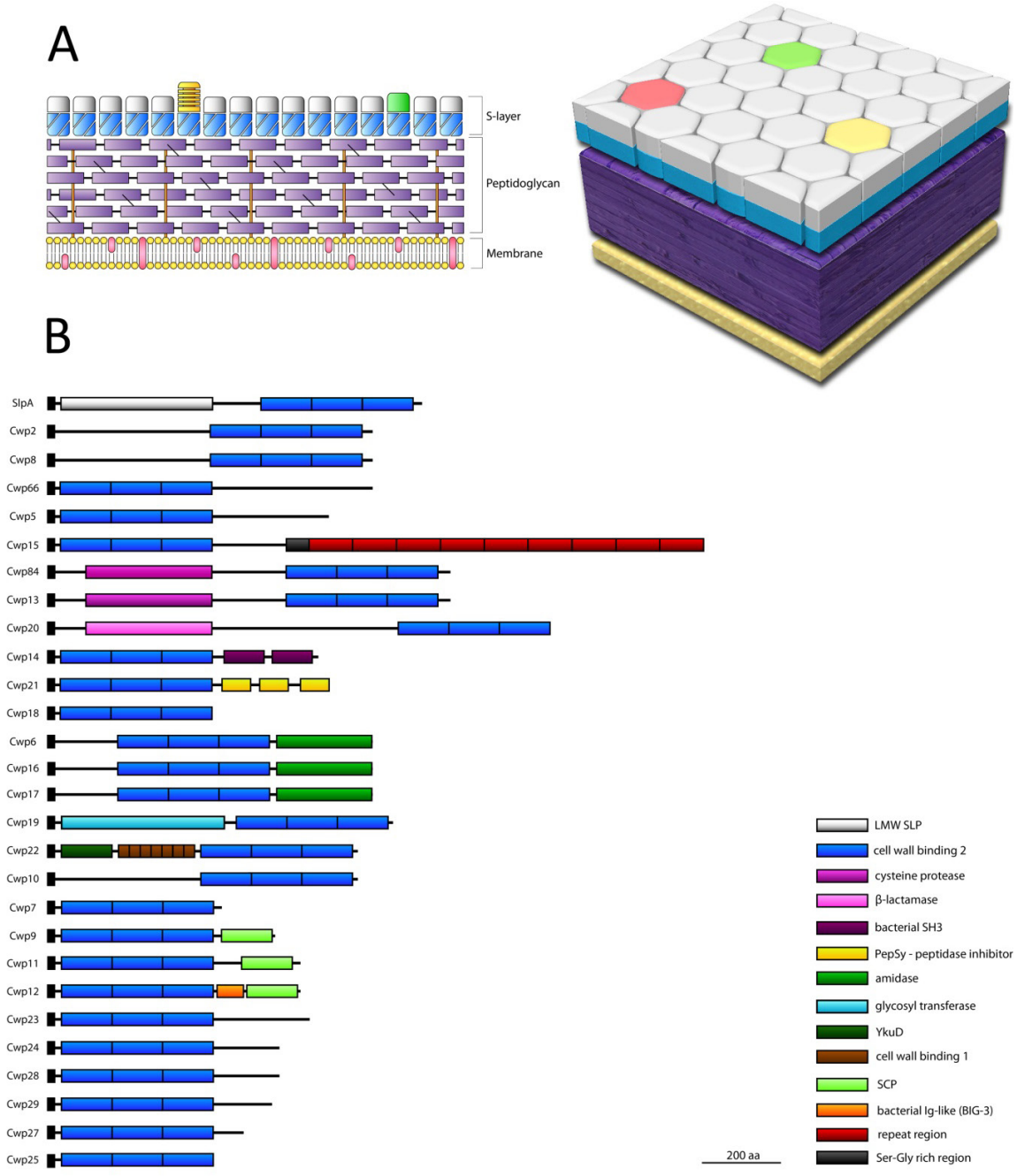

Figure 1.4. The *C. difficile* cell wall and S-layer. **(A)** Schematic cross section through the *C. difficile* cell wall and the S-layer structure. The major S-layer proteins HMW SLP and LMW SLP form heterodimeric complexes (white-blue) that self-assemble into a hexagonal crystalline array on the surface of the cell wall peptidoglycan (purple). Minor cell wall proteins scattered throughout the S-layer are indicated as hexagons of varying colours. **(B)** *C. difficile* CWP family. Each protein contains 3 putative cell wall binding motifs (blue: Pfam 04122) and many contain a unique domain that specifies the proteins function. Adapted from Fagan and Fairweather (2014).

1.3. Role of endospores in *C. difficile* infection

Many bacterial species, including important human pathogens belonging to the *Bacillus* and *Clostridium* genera, have evolved to form specialised, differentiated cells known as endospores (henceforth referred to as spores for simplicity) as a means of surviving in unfavourable conditions, non-conducive for vegetative growth. Due to their robust characteristics, spores are resistant to extreme chemical and physical insult and provide the mechanism by which sporeformers can evade the potentially fatal consequences of exposure to heat, oxygen, alcohol, and certain disinfectants (reviewed in Setlow, 2006, Setlow, 2007). This makes spores extremely difficult to eradicate, allowing them to persist in the environment for extended periods of time. As a consequence, spores produced by pathogenic bacteria are now widely recognised as the primary infectious agent in diseases such as anthrax, tetanus, botulism and CDAD (Deakin *et al*., 2012, Wells and Wilkins, 1996, LaForce *et al*., 1969).

The importance of spores in CDI has been highlighted in a number of recent studies. *C. difficile* spores can be frequently found in hospital settings, mostly in rooms of patients suffering from CDI (Dubberke *et al*., 2007), leading to infection or re-infection of individuals through inadvertent ingestion of contaminated material (Gerding *et al*., 2008, Riggs *et al*., 2007). Once in the anaerobic environment of the gut, spores germinate to form toxin-producing vegetative cells and, in susceptible individuals, diarrhoeal disease. *C. difficile* spores have been shown to be highly infectious in animal models with as few as seven spores per cm^2 cage floor area deemed sufficient to establish a persistent infection among exposed, antibiotic-treated mice (Lawley *et al*., 2009b). Interestingly, non-infectious mice asymptomatically colonised with *C. difficile* treated with antibiotics enter a highly contagious 'supershedder' state whereby large numbers of spores are shed in faeces, infecting non-colonised, cohabiting mice (Lawley *et al*., 2009a). Furthermore, disruption of *spo0A*, the master response regulator initially identified in *Bacillus subtilis* as essential in sporulation (Olmedo *et al.*, 1990), results in mutants that are not only defective in sporulation (Underwood *et*

al., 2009), but also unable to persist in mice and transmit between animals, suggesting an essential role of sporulation in infection, transmission and recurrence of *C. difficile* (Deakin *et al*., 2012).

1.3.1. Mechanism of sporulation

The process of sporulation has been the subject of continuous microbiological investigation since the seminal 19th century reports of Robert Koch (Koch, 1876) and Ferdinand Cohn (Cohn, 1877). Its basic principle is based on an ancient bacterial cell differentiation programme of temporally and spatially-controlled gene expression that is largely conserved among *Baciliales* and *Clostridiales* (Figure 1.5) (reviewed in Paredes *et al*., 2005). The most widely studied spore-forming organism is *B. subtilis*, and the molecular mechanisms that underpin its sporulation have been extensively studied, becoming a useful paradigm for spore research carried out in other systems (reviewed in Sonenshein, 2000).

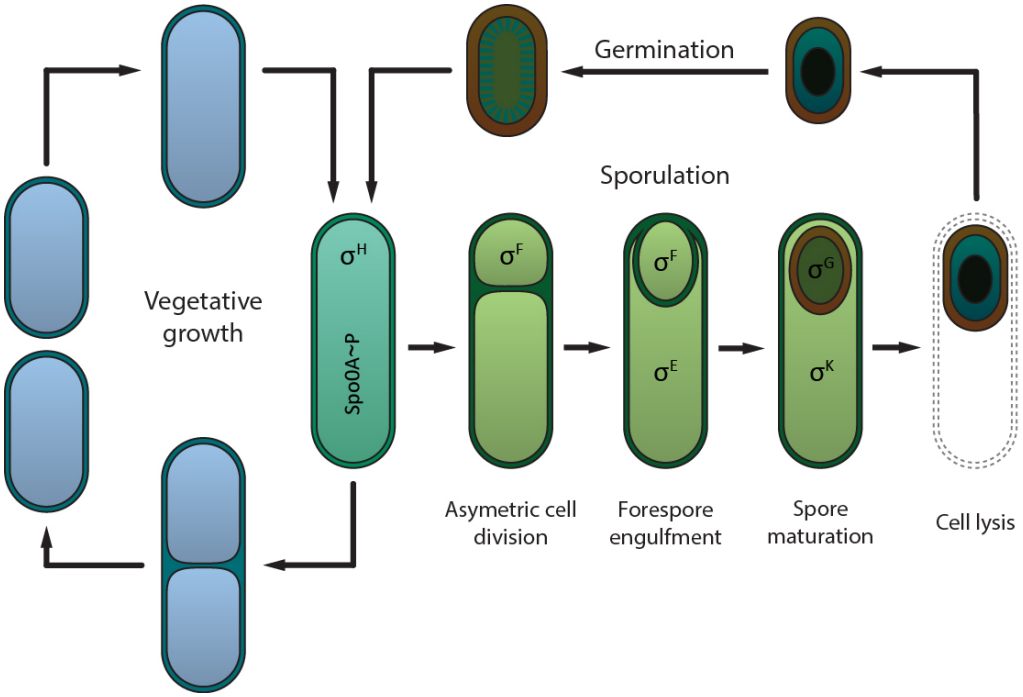

Figure 1.5. Schematic representation of *B. subtilis* life cycle. When stressed, *B. subtilis* exits vegetative growth and triggers asymmetric cell division. Two compartments are formed, the smaller forespore and the larger mother cell compartment which eventually engulfs the former so that a 'cell-within-a-cell' structure is formed. Gene expression is spatially and temporarily controlled by a cascade of sporulation specific RNA polymerase sigma factors: σ^F and σ^G in the forespore and σ^E and σ^K in the mother cell compartment. Following maturation, the endospore is released into the environment where it can persist for extended periods of time without loss of viability. Under conditions favourable for growth, the spore initiates germination, followed by outgrowth of a fully developed vegetative cell. Adapted from Errington (2003).

1.3.1.1. Entry into sporulation

Initiation of sporulation is governed by phosphorylation of Spo0A, a transcriptional factor that plays a central role in phenotypic differentiation and adaptation to changing environmental conditions. The *spo0A* gene itself is expressed from two different promoters: Pv which is active throughout vegetative growth and Ps, a sporulation-specific promoter activated by the RNA polymerase sigma factor σ^H, the product of s*po0H* (Siranosian and Grossman, 1994). Both the level of Spo0A phosphorylation and its abundance can affect the physiological outcome of its activation, which can result in biofilm formation and cannibalism when Spo0A is phosphorylated at low levels (Gonzalez-Pastor *et al*., 2003, Hamon and Lazazzera, 2001) or spore formation when Spo0A is phosphorylated at higher levels (Fujita and Losick, 2005).

Spo0A phosphorylation in *B. subtilis* is facilitated by a complex phosphorelay (Burbulys *et al*., 1991) comprised of several sensor kinases (KinA-E) that respond to external signals by autophosphorylating and subsequently transferring phosphate either directly to Spo0A or *via* intermediary proteins Spo0F and Spo0B (Jiang *et al*., 2000). Kinase activity is antagonised by a number of regulatory factors that add an additional level of regulation, protecting the cell from premature sporulation. These include KipI (Wang *et al*., 1997) and Sda (Burkholder *et al*., 2001), both of which bind KinA, the major kinase involved in initiation of sporulation, preventing its autophosphorylation, as well as a family of protein-aspartate phosphatases (RapA, RapB, RapE and RapH) that dephosphorylate Spo0F thus reducing the level of Spo0A~P (Figure 1.6) (Perego *et al*., 1994).

A number of environmental and cell cycle-related signals have been shown to induce sporulation, either by acting upon elements of the phosphorelay or by independent signal transduction pathways. One such stimulus is nutrient limitation (Schaeffer *et al*., 1965) and the corresponding drop in intracellular GTP concentration, the primary indicator of nutrient availability. It has been suggested that a number of GTP-binding proteins such as CodY, a global repressor of stationary phase genes, loose their ability to repress target genes as the intracellular GTP levels

drop, thus allowing for initiation of sporulation (Handke *et al*., 2008, Ratnayake-Lecamwasam *et al*., 2001). Culture density has also been shown to affect spore formation *via* a mechanism involving *phrA, phrC* and *phrE.* Proteins encoded by these genes are exported out of the cell and cleaved into pentapeptides that accumulate in the culture supernatant during growth, inhibiting the activity of their respective Rap phosphatases and allowing for initiation of sporulation when the culture density reaches a certain threshold (Pottathil and Lazazzera, 2003). Finally, the state of chromosomal DNA is an important factor in committing to sporulation and a number of proteins that monitor DNA replication and chromosome integrity are known to prevent spore formation under conditions that could compromise DNA replication. These include DisA, a cyclic diadenosine monophosphate (c-di-AMP) synthase that couples chromosome integrity with progression of sporulation (Bejerano-Sagie *et al*., 2006) and the previously mentioned Sda protein which inhibits sporulation while the cell contains actively replicating chromosomes (Burkholder *et al*., 2001). A corresponding mechanism regulating chromosome replication during sporulation involves the sporulation-specific SirA protein that prevents new rounds of replication during sporulation (Figure 1.6) (Rahn-Lee *et al*., 2009, Wagner *et al*., 2009).

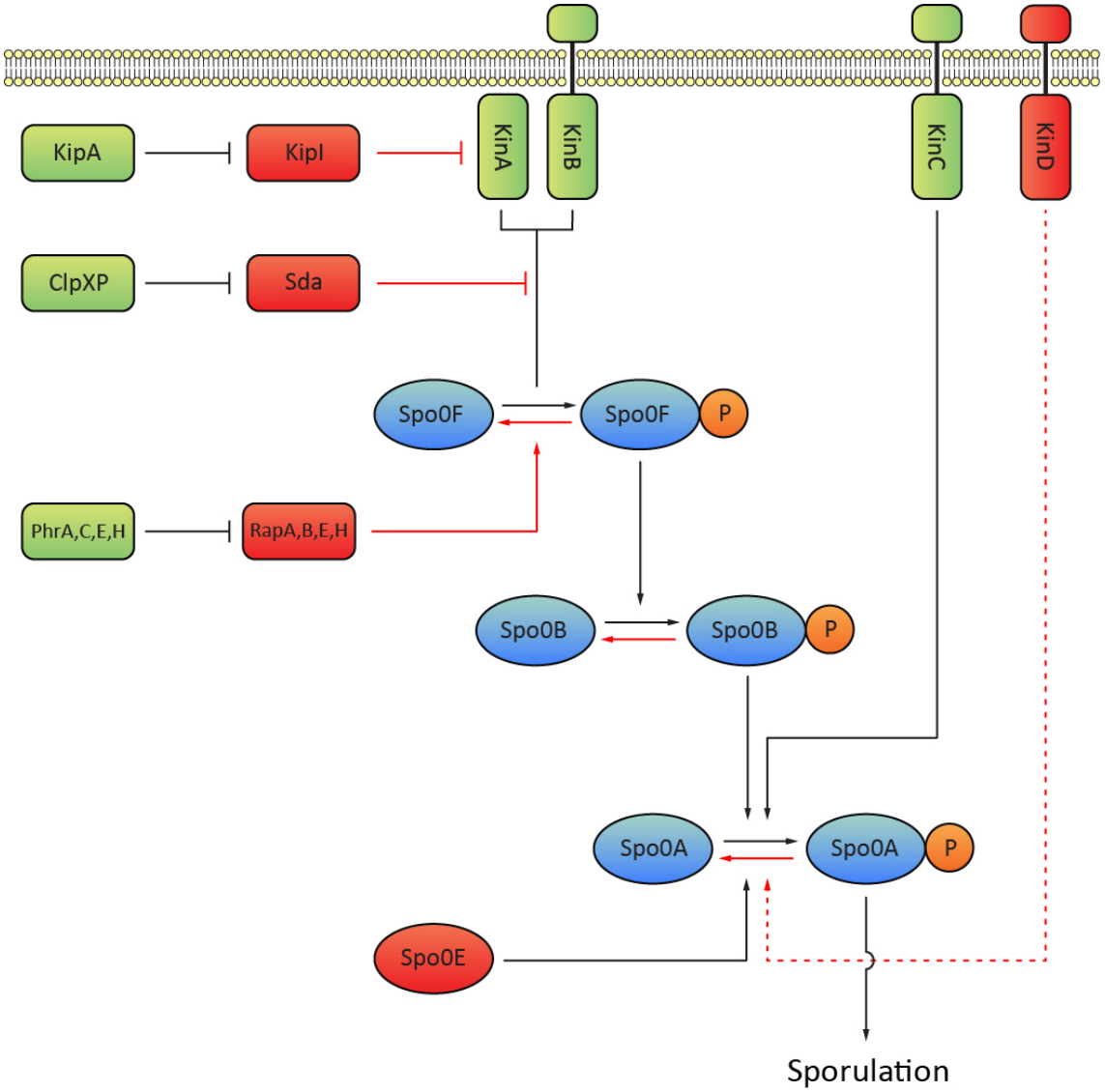

Figure 1.6. Entry into sporulation in *B. subtilis*. Phosphorylation of Spo0A is controlled by a phosphorelay comprised of several kinases and a number of intermediaries. Interactions that work against Spo0A phosphorylation are presented in red while those that stimulate Spo0A phosphorylation are presented in green. The phosphorelay is initiated when KinA and KinB respond to external signals by autophosphorylating and subsequently transferring phosphate to Spo0F. Spo0F phosphorylates Spo0B, which passes phosphate onto Spo0A. A third kinase, KinC, bypasses the phosphorelay and acts directly on Spo0A. A number of phosphatases and kinase inhibitors act at various steps in the pathway to directly antagonize Spo0A phosphorylation. These inhibitors are subject to their own regulation. KinD has been shown to inhibit Spo0A phosphorylation, although the exact mechanism has not been described. Adapted from Higgins and Dworkin (2012).

1.3.1.2. Asymmetric cell division

Once phosphorylated, Spo0A acts to repress *abrB*, a negative regulator of stationary phase genes, some of which are required for sporulation (Perego *et al*., 1988), and activates transcription from the *spoIIA, spoIIE* and *spoIIG* loci which encode key developmental regulators. This triggers asymmetric cell division leading to the formation of two cell compartments, the smaller forespore and the larger mother cell compartment. During this process the nucleoid is remodelled into a filament of chromatin that spans the length of the cell, attached to the cell pole through the action of RecA (Ben-Yehuda *et al*., 2003), while elements of the cell cytoskeleton, including the essential tubulin homologues FtsZ are re-localized to sites near the cell pole *via* a σ^H mediated mechanism. As the cell septum expands, only the origin-proximal one-third of a chromosome is present in the forespore. The remainder is then transported through the septum by the DNA translocase SpoIIIE (Wu and Errington, 1994). Soon after the division, distinct programmes of gene expression are initiated, driven by cell compartment-specific action of a series of RNA polymerase sigma subunits, σ^F in the forespore and σ^E in the mother cell, replaced by σ^G and σ^K respectively during the later stages of sporulation. However, events that follow do not occur in isolation as inter-cellular communication between the forespore and the mother cell is maintained throughout sporulation. Activation of σ^F in the forespore is necessary for the expression of SpoIIR, a secreted protein that crosses into the space between the septal membranes and mediates processing of the σ^E precursor into its active form. Later on, σ^E is required for σ^G activation in the forespore, which, in turn, leads to σ^K activation in the mother cell (reviewed in Hilbert and Piggot, 2004). In order to explain this cross-talk, the 'feeding tube' model has been proposed in which the signalling between the mother cell and the forespore is facilitated by a channel linking the two compartments (Meisner *et al*., 2008). This channel is formed primarily by two proteins: SpoIIQ and SpoIIIAH. The former localizes to the septum in the forespore membrane (Rubio and Pogliano, 2004, Rodrigues *et al*., 2013, Fredlund *et al*., 2013) where it interacts with the mother cell proteins encoded by the *spoIIIA* locus, several of which show homology to type III and type IV secretion systems (Camp and Losick,

2008). One of these, SpoIIIAH, directly interacts with SpoIIQ (Doan *et al*., 2005, Blaylock *et al*., 2004) forming a channel that spans the inter-membrane space ensuring communication between the two compartments of the sporulating cell (Meisner *et al*., 2008, Doan *et al*., 2009, Camp and Losick, 2009).

1.3.1.3. Engulfment

Following asymmetric cell division and DNA translocation, the membrane of the mother cell continues to develop, eventually engulfing the forespore so that a 'cell-within-a-cell' structure is formed. Once initiated, the process is irreversible, committing the cell to sporulation even if nutrient levels are restored (Dworkin and Losick, 2005). Three partially redundant mechanisms of engulfment have been proposed. The first involves the so-called ‘DPM machine’, an enzyme complex owing its name to three peptidoglycan hydrolases located within the outer forespore membrane: SpoIID, SpoIIP and SpoIIM (Chastanet and Losick, 2007). These act at the junction of the septum and the cell wall, hydrolysing peptidoglycan located between the two membranes and moving the mother cell membrane around the forespore. The DPM machine is tracked by sites of active peptidoglycan synthesis, which form the second mechanisms, providing the motive force for membrane movement until the mother cell membrane fuses at the cell pole releasing the forespore into the cytosol (Meyer *et al*., 2010). The third and final mechanism that facilitates membrane movement during engulfment involves the previously mentioned SpoIIQ and SpoIIIAH. These track the mother cell membrane as it moves around the forespore, irreversibly driving engulfment *via* a ratchet-like mechanisms (Broder and Pogliano, 2006). While being partially redundant, it remains unclear whether the three mechanisms overlap spatially and temporally or participate in distinct stages of engulfment (Figure 1.7).

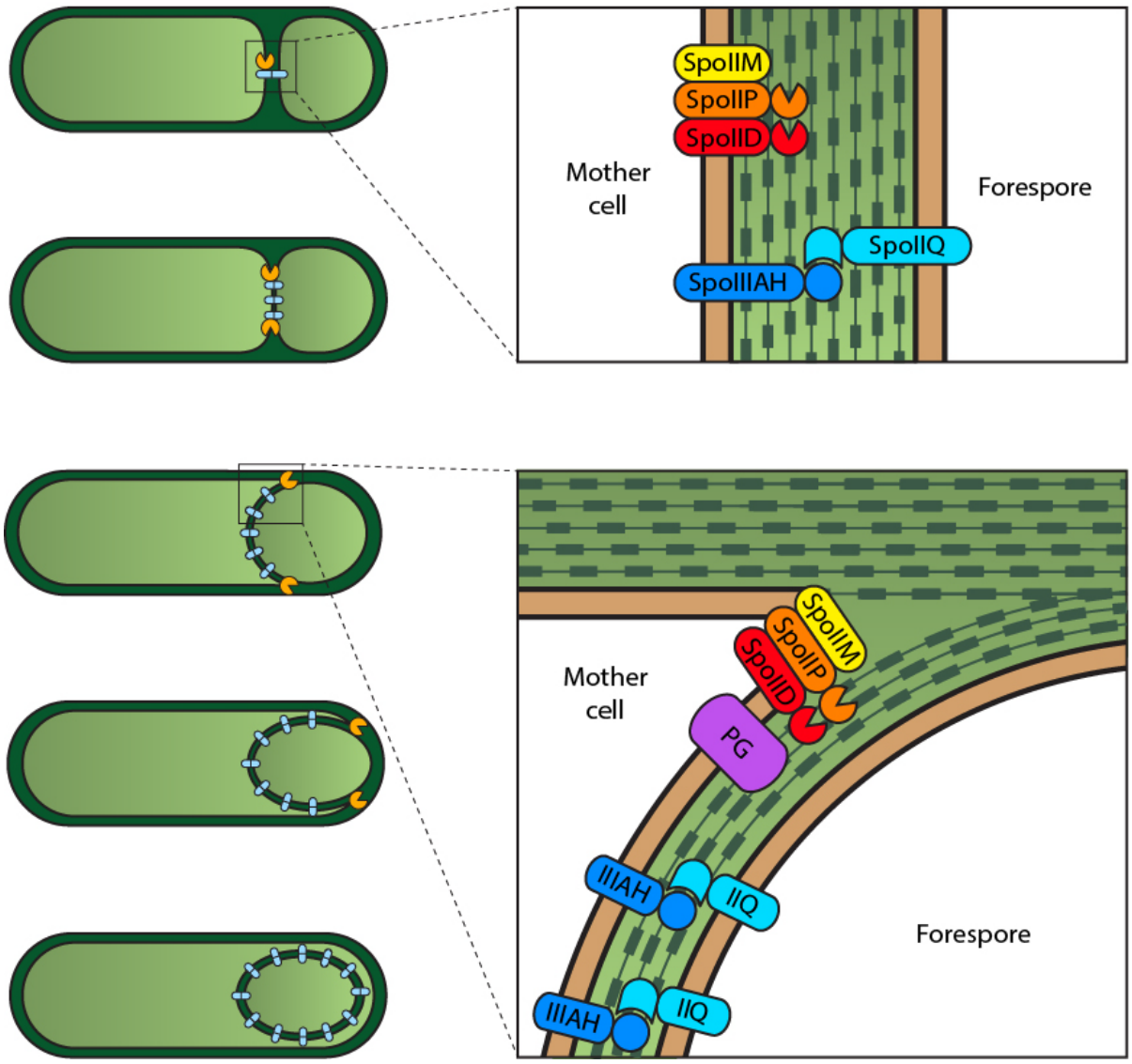

Figure 1.7. Mechanism of engulfment. Three partially redundant molecular mechanisms are responsible for the membrane movement that occurs during engulfment. Firstly, the 'DMP' machine (orange) is responsible for membrane migration by hydrolyzing the peptidoglycan between the inner and outer membranes, thereby moving the outer membrane around the forespore. Secondly, the SpoIIQ-SpoIIIAH zipper (blue) acts as a ratchet to irreversibly drive engulfment. Finally, peptidoglycan synthesis (purple) of the germ cell wall provides a motive force for membrane movement during early engulfment as well as the final step of forespore detachment. Adapted from Sogaard-Andersen (2013).

1.3.1.4. Spore morphogenesis

On completion of forespore engulfment, σ^F and σ^E activity falls, while two new subunits become active, σ^G in the forespore and σ^K in the mother cell compartment. This compartmentalisation of gene expression is coupled to spore morphogenesis as the sequential activation of these four sporulation-specific sigma factors governs assembly of the three principal layers that comprise the spore: the core compartment which contains the chromosome, and two protective layers of different properties: the cortex peptidoglycan and the proteinaceous coat (Figure 1.8).

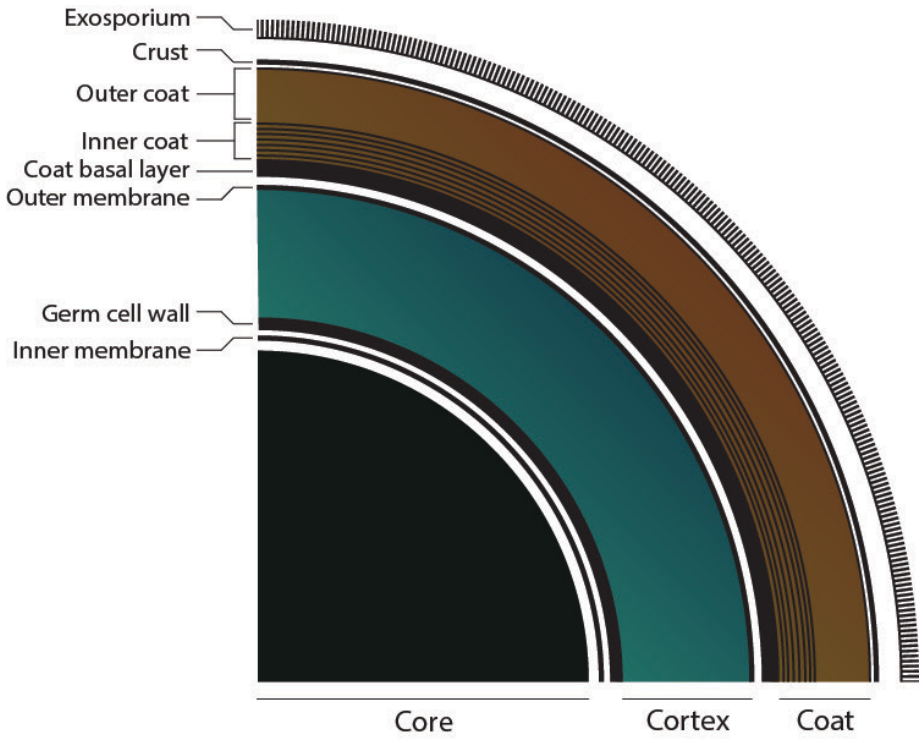

Figure 1.8. Spore ultrastructure. The innermost layer, the core, contains genomic DNA, RNA, densely packed ribosomes and enzymes critical in re-establishment of cell metabolism following a phase of dormancy. The low water content of the core, its high levels of Ca^{2+}-DPA and the saturation of DNA with SASPs contribute to the resistance properties of the spore, particularly against high temperatures and UV irradiation. Surrounding the core is a significantly compressed inner membrane, in which the lipids are largely immobile. This membrane has low permeability to small molecules, which is likely to protect the spore core from DNA damaging chemicals. Surrounding the inner membrane is the primordial cell wall, and the cortex composed of modified peptidoglycan containing muramic-δ-lactam (MAL). The MAL residues appear to be the recognition element for spore cortex-lytic enzymes (SCLEs), which hydrolyze the cortex but not the cell wall during spore germination. The cortex is surrounded by the outer membrane, which in turn is surrounded by the proteinaceous coat, composed of approx. 80 spore-specific proteins, protecting the spore from reactive chemicals and lytic enzymes. Four major layers of the coat can be distinguished: The amorphic basal layer, the lamellar inner coat, the electron-dense outer coat and the crust. In some species, the coat is the outermost layer of the spore. In others, including *C. difficile*, an additional glycoprotein layer called the exosporium is loosely attached to the coat. Adapted from McKenney *et al*. (2013).

1.3.1.4.1. Spore core

Following engulfment, the forespore protoplast undergoes a number of modifications in order to protect the genetic material stored within. This leads to the formation of the core, the innermost layer of the spore containing genomic DNA, ribosomes, tRNA and most of the spore enzymes, the minimal set of components required to re-establish metabolism following a phase of dormancy. During this process the water content of the forespore drops to 25-50% of dry weight as most of the water is replaced with pyridine-2,6-dicarboxylic acid [dipicolinic acid (DPA)] (Murrell, 1967). DPA is produced in the mother cell and then transported into the forespore compartment where it forms a 1:1 chelate with divalent cations, predominantly Ca^{2+} (Daniel and Errington, 1993). The high content of Ca^{2+}-DPA within the spore (20% dry weight) contributes to DNA resistance to dry and wet heat, desiccation and hydrogen peroxide (reviewed in Setlow, 2006). The core components that gives DNA the most protection however are α/β-type small acid-soluble proteins (SASP), expressed in the forespore compartment from monocistronic genes in a σ^G-dependent manner. SASPs make up 5-10% of total core protein and saturate the bacterial chromosome, changing its topology (Nicholson *et al*., 1990) and protecting it from DNA-damaging agents such as wet and dry heat, UV radiation, desiccation and genotoxic chemicals including nitrous acid, hydrogen peroxide and formaldehyde (reviewed in Setlow, 2007). Finally, surrounding the core is a significantly compressed inner membrane, in which the lipids are largely immobile (Cowan *et al*., 2004). This membrane has low permeability to small molecules, which is likely to protect the spore core from DNA damaging chemicals (Setlow, 2006).

1.3.1.4.2. Spore cortex

Following the completion of engulfment, the forespore protoplast is surrounded by two membranes of opposite polarity: the inner and outer membrane. Two types of peptidoglycans are then layered between the two membranes. The surface of the inner spore membrane is the site of assembly of a thin layer of peptidoglycan called the primordial germ cell wall, similar in

composition to the vegetative cell wall that serves as the initial wall of the newly formed vegetative cell following spore germination (Tipper and Linnett, 1976). The outer forespore membrane is the site of assembly of a second, thicker, and chemically distinct layer of peptidoglycan called the spore cortex, which is essential for the maintenance of protoplast dehydration and spore mineralization, both key factors in spore resistance to wet and dry heat (Lewis *et al*., 1960), and the corresponding metabolic dormancy. In contrast to vegetative cell peptidoglycan, where each NAM residue carries a peptide side chain, approximately half of the NAM residues in the cortex peptidoglycan carry no side chains and instead are cyclized to form muramic-δ-lactam (MAL) (Warth and Strominger, 1969, Warth and Strominger, 1972) (Figure 1.9). These lactam residues are distributed regularly, alternating with NAM residues within the glycan strands, and are thought to act as the recognition element for cortex-lytic enzymes (CLEs), which hydrolyze the cortex but not the cell wall during spore germination (Makino and Moriyama, 2002). In *B. subtilis*, formation of MAL residues in catalysed by an N-acetylmnoramoyl-L-alanine amidase encoded by *cwlD* and its disruption results in spores with a severe germination defect (Popham *et al*., 1996, Sekiguchi *et al*., 1995). In addition to MAL formation, 25% of NAM residues only carry a single L-alanine. The peptides on the remaining NAM residues are cross-linked at a frequency of 13–19% (Popham *et al*., 1996, Warth and Strominger, 1969, Warth and Strominger, 1972). The outer membrane of the spore surrounds the cortex, and although this membrane might not act as a permeability barrier in the dormant spore, it is essential for spore formation.

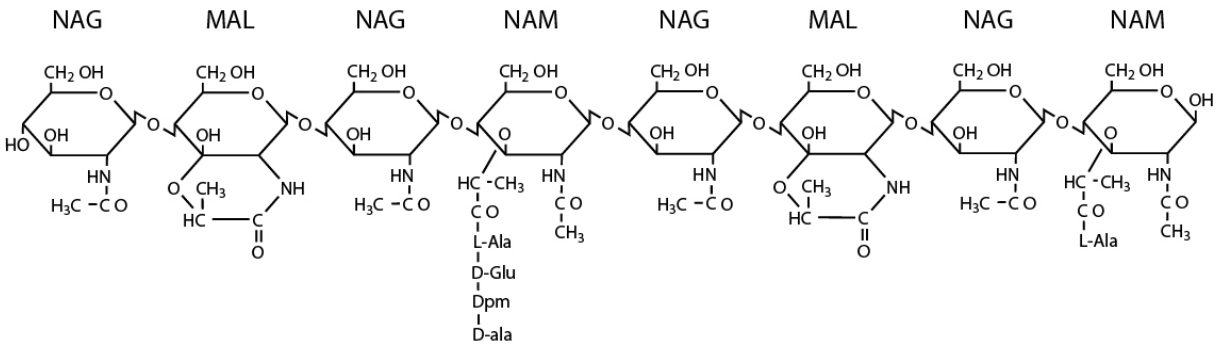

Figure 1.9. Structure of *B. subtilis* cortex spore peptidoglycan. Approx. 50% of N-acetylmuramic acid (NAM) residues are cyclized to form muramic-δ-lactam (MAL). The glycan chains are cross-linked *via* the peptide side chains on N-acetylglucosamine (NAG) residues. Adapted from Popham *et al*. (1996).

1.3.1.4.3. Spore coat

The cortex peptidoglycan is surrounded by a proteinaceous coat comprising of an amorphic basal layer, a lamellar inner coat and an electron-dense, striated outer coat (reviewed in McKenney *et al*., 2013). Recently, a fourth layer called the crust has been identified in *Bacillus subtilis* (McKenney *et al*., 2010). The spore coat consists of approx. 80 proteins synthesized in the mother cell compartment and then targeted to the outer surface of the forespore. The protein composition of the spore coat differs significantly between species. Analysis of existing genome sequences suggest that only half of the known *B. subtilis* coat proteins have recognizable orthologues in other *Bacillus* species. In *Clostridium* species, conservation is even more limited (Henriques and Moran, 2007, Permpoonpattana *et al*., 2011). Considering that the spore surface represents the interface between spores and the environment, diversity in coat composition may have a crucial role in defining the ecological niches of spore-forming bacteria.

The primary function of the spore coat is to protect the bacterial genome from environmental stresses, both passively, by forming a barrier that blocks access to the spore core, and actively, through the action of enzymes contained within the coat layers. It provides protection from oxidizing agents, detoxifying them before they reach sensitive targets in the spore inner layers. One of the coat components involved in this is CotA, a copper-dependent laccase involved in protection against hydrogen peroxide (Riesenman and Nicholson, 2000). Interestingly, CotA is also thought to enhance the spores' resistance to UV radiation by generating a pigment structurally similar to melanin (Hullo *et al*., 2001, Riesenman and Nicholson, 2000). The spores resistance to lysozyme and other peptidoglycan-hydrolysing enzymes is thought to be mediated by CotE, conferring protection form predation by a variety of bacteriovores including as the protozoan *Tetrahymena thermophila* and the nematode *Caenorhabditis elegans* (Klobutcher *et al*., 2006, Laaberki and Dworkin, 2008). While the exact molecular mechanism of this protection is unknown it has been proposed that the coat may have an important role in limiting access of peptidoglycan hydrolases to the peptidoglycan-containing cortex. Finally, the coat also plays an important role in modulating spore responses to

germinants such as sugars, amino acids, peptidoglycan fragments and ions. While this effect is primarily passive, acting as a molecular sieve that allows small molecule germinants to reach their respective receptors and preventing larger molecules such as lysozyme from entry, active mechanism involving enzymes immobilized within the spore coat have also been proposed. These include alanine racemase which has been shown to be important in preventing premature germination in *B. anthracis* (Chesnokova *et al*., 2009) and peptidoglycan hydrolases CwlJ and SleL, both essential in cortex degradation during germination (Chirakkal *et al*., 2002).

Coat assembly is a highly dynamic process, precisely coordinated with spore development, and is governed by a set of key morphogenetic proteins: SafA, CotE and SpoIVA. Each of these interacts with a subset of coat polypeptides forming three independent modules: the SafA-dependent protein sub-network involved in inner coat assembly, the CotE-dependent protein sub-network involved in outer coat assembly and a third module consisting of proteins that are independent of both SafA and CotE, and interact with SpoIVA, the primary component of the coat basal layer. A fourth module, controlled by CotX, CotY and CotZ has been recently identified and implicated in crust assembly (McKenney *et al*., 2010). During the first phase of coat morphogenesis, SafA, CotE, SpoIVA and CotX/Y/X are involved in targeting spore coat proteins to their respective layers in a σ^E-dependent manner, forming the so-called scaffold cap on the mother cell proximal pole of the newly formed forespore. The cap is then extended through successive waves of a σ^E and a σ^K-dependent gene expression in the encasement phase of coat assembly to form a full spherical shell. During the process of assembly, coat proteins undergo extensive modifications including, proteolysis, cross-linking and glycosylation all of which play an important role in forming the functional characteristics of the coat (reviewed in McKenney *et al*., 2013).

1.3.1.4.4. The exosporium

In *B. subtilis*, the coat is the outermost layer of the spore. In others, including *C. difficile*, an additional glycoprotein layer called the exosporium is loosely attached to the coat. The structure and composition of the exosporium is highly diverse and can vary significantly between species and even strains within a species. It is also highly dynamic, being smooth in the dormant state but developing numerous filamentous projections that attach to the host tissue during germination (Panessa-Warren *et al*., 2007). The exosporium may confer resistance to chemical and enzymatic treatments, and provides a hydrophobic surface that enhances the spore's adhesive properties. It also contains several enzymes with roles in spore germination, at least some of which localize to specific regions of the structure. The exosporium is also the first point of contact of the spore with cells of the immune system and as such forms an important interface in host-pathogen interactions. To date, the best studied exosporium is that of *B. anthracis,* consisting of a paracrystalline basal layer covered by a hair-like nap. The filaments of the hair-like nap appear to be formed mainly by a single collagen-like protein called BclA. This immunodominant protein has been show to affect spore germination, interaction with extracellular matrix proteins and host immune responses and thus plays an important role in *B. anthracis* pathogenesis. Three homologues of BclA have been identified in *C. difficile* 630 genome, designated BclA1, BclA2 and BclA3 and are likely candidates for the main components of the *C. difficile* exosporium (Henriques and Moran, 2007).

1.3.2. Germination and outgrowth

Spore germination is defined as the irreversible loss of spore-specific properties allowing the bacterium to resume vegetative growth following a phase of dormancy. In *Bacillus*, it is typically initiated by one or more members of the GerA family of germination receptors (GRs) encoded by the homologous tricistronic *gerA, gerB* and *gerK* operons, expressed in the forespore late in sporulation. All GRs are most likely membrane proteins, and at least some of them (GerAA, GerAC, GerA) are localized in the spore's inner membrane (Hudson *et al*., 2001). They are synthesized in relatively

small amounts with only tens of molecules per spore for individual GRs (Paidhungat and Setlow, 2001). According to the simplest model, each GR is composed of three proteins encoded by its cognate operon homolog. However, the topology of these proteins in the membrane, the stoichiometry of proteins in the receptor, and the possible physical interaction between different germinant receptors and with additional proteins is not clear (reviewed in Setlow, 2003).

All GRs monitor the spore's environment for specific signals (germinants) indicating favourable growth conditions. A wide range of germinants have been identified and include nutrients (amino acids, carbohydrates, purine nucleosides) as well as other, non-nutrient chemical and physical agents: lysozyme, salts, high pressure, cationic surfactants, peptidoglycan fragments and Ca^{2+}-DPA, although the latter are most likely non-physiological. While mutant *B. subtilis* spores lacking all germinant receptors do not germinate with nutrients (Paidhungat and Setlow, 2000) they do exhibit a slow constant rate of spontaneous germination, the mechanism of which is not understood. These 'receptorless' spores do, however, germinate normally with non-nutrient germinants (Paidhungat and Setlow, 2000, Setlow *et al*., 2003).

Upon binding of germinants, GRs initiate a series of irreversible biophysical events that cannot be stopped even after the removal of stimulus, although the mechanism of commitment remains unknown. Firstly, monovalent cations (H^+, Na^+ and K^+) and Zn^{2+} are released from the spore core, elevating its pH from approx. 6.5 to 7.7. This is essential for spore metabolism as it ensures optimal conditions for enzyme activity in later stages of germination. Secondly, a large depot of DPA is released together with its associated divalent cations, predominantly Ca^{2+}. Both steps are facilitated by one or more ion/DPA channels within the spore inner membrane (Paidhungat *et al*., 2001). Simultaneously, DPA is replaced by water resulting in an increase in core hydration and lowering the spore's resistance to wet heat. This is followed by hydrolysis of cortex PG by germination-specific SCLEs. In *B. subtilis* two enzymes, CwlJ and SleB, play redundant roles in the degradation of the spore's peptidoglycan cortex during germination (Chirakkal *et al*., 2002) and both require MAL residues for PG cleavage. Degradation of the PG cortex is essential for completion of

spore germination as it removes a physical constraint to spore core expansion, and allows further water uptake into the core to the levels found in vegetative cells. Full core hydration then enables protein mobility, enzyme activity and initiation of spore outgrowth (reviewed in Setlow, 2003).

Once the constraints of spore outer layers are lifted, the cell enters a period of longitudinal growth, accompanied by re-establishment of cell metabolism during which DNA, RNA and protein synthesis resume. This period is termed outgrowth and is often not distinguished in literature from the more general term: germination. Although the two processes normally form a continuum, outgrowth is distinguished by its sensitivity to inhibitors of macromolecular synthesis and strictly depends on the completion of germination.

Most of the pioneering work on cell metabolism during sporulation, germination and outgrowth was done in *Bacillus spp.* in a series of biochemical studies conducted by Arthur Kornberg and colleagues and published over a period of four years in the late 60's and early 70's. This combined effort comprising twenty-three research papers covers everything from nucleic acid and protein synthesis to energy metabolism and patterns of enzymatic activity, summarising the state of knowledge on the subject at that time. While it is beyond the scope of this thesis to report on each of those finding, the most important aspects of cell metabolism during outgrowth are listed below. Macromolecular synthesis, essential for the re-establishment of biochemical pathways, nutrient uptake, and replication, can only be initiated upon the production of ATP. In the first stage of outgrowth, ATP is generated through conversion of 3-phosphoglyceric acid stored in the spore core. Only later does the outgrowing spore switch to the use of extracellular nutrients. The enzymes required for energy metabolism are previously formed and found present in the dormant spore (Setlow and Kornberg, 1970b, Singh and Setlow, 1979). Phosphate metabolism is highly active in germination. Inorganic phosphate (P_i) is generated from both endogenous and exogenous sources and is incorporated into RNA, glucose-6P, fructose diphosphate, ATP and L-α-glycerophosphate (Nelson and Kornberg, 1970). The level of fatty acids and phospholipids increases during germination and outgrowth, most likely reflecting the necessity of rebuilding the membrane during cell

expansion. The newly produced fatty acids are predominantly branch-chained pentadecanoates and their distribution, by the time vegetative cell development is complete, resembles that observed in an exponentially growing culture (Scandella and Kornberg, 1969). RNA synthesis is underway early on in germination. During the first 10 min it can proceed in the absence of exogenous nutrients at the expense of previously existing RNA. Salvage pathways for bases, nucleosides, and nucleotides are operative during this period and utilize enzymes which are previously formed in the dormant spore (Setlow and Kornberg, 1970a). Biosynthesis of purines and pyrimidines *de novo* begins approximately 15 to 20 min after the onset of germination. The increase in nucleotide pools sustains an increase in the rate of RNA synthesis (Setlow and Kornberg, 1970a). Chromosomal replication is initiated after approximately 30 min (Garrick-Silversmith and Torriani, 1973). Protein synthesis in the outgrowing spore is dependent on *de novo* transcription and is initiated in the first minutes of germination (Setlow, 1975, Setlow and Primus, 1975). Distinct patterns of protein production have been revealed, suggesting the existence of an ordered process (Hirano *et al*., 1991, Huang *et al*., 2004). Amino acids generated by proteolysis are sufficient for synthesis of proteins required early on in germination, however exogenous carbon and energy sources must be supplied (Setlow and Kornberg, 1970a).

1.3.3. Comparison of sporulation and germination in *Clostridiales* and *Baciliales*

Sporulation is an ancient bacterial cell differentiation programme that has emerged some 2.5 billion years ago at the base of the Firmicutes phylum and is largely conserved among *Clostridiales* and *Baciliales*, particularly with regard to the key regulatory components: Spo0A and the sporulation-specific sigma factors (reviewed in Paredes *et al*., 2005). However, recent studies have highlighted several notable differences in the sporulation programmes of *Bacillus* and *Clostridium* species. While both Spo0A and σ^H are present and required for sporulation in *C. difficile* and other Clostridia (Saujet *et al*., 2011, Underwood *et al*., 2009), the complex phosphorelay that

modulates Spo0A activity in *B. subtilis* is replaced with a simple two-component system, as phosphorylation of Spo0A is mediated directly by Spo0A-assocaited kinases (Paredes *et al*., 2005, Steiner *et al*., 2011). Furthermore, studies carried out in *C. perfringens* and *C. acetobutilicum* have shown than in contrast to *B. subtilis*, σ^E and σ^F are active prior to asymmetric cell division. This is also true for σ^K, which *in B. subtilis* controls late stages of morphogenesis in the mother cell. In *C. difficile*, the main periods of activity of the four cell type-specific sigma factors are more conserved when compared to the *B. subtilis* model, with σ^F and σ^E controlling early stages of development and σ^G and σ^K governing late developmental events. However, the temporal segregation between the activities of the early and late-stage sigma factors is less stringent and the cross-talk between the forespore and the mother cell seems to be weaker, as the activity of σ^E is partially independent of σ^F, and activation of σ^G and σ^K does not require σ^E and σ^G, respectively (Pereira *et al*., 2013, Saujet *et al*., 2013). The *C. difficile* σ^E, σ^F, σ^G and σ^K regulons have now been identified (Saujet *et al*., 2013), each containing key representatives of the homologous regulons previously identified in *B. subtilis* (de Hoon *et al*., 2010). Containing 228 genes, this core set of *C. difficile* sporulation genes corresponds to about half the number of genes under the control of cell type-specific sigma factors of *B. subtilis* (Steil *et al*., 2005). While this could be attributed to the experimental design of the study in question, it could also be a reflection of the more ancestral mechanism of sporulation proposed for Clostridia (Galperin *et al*., 2012, Paredes *et al*., 2005).

Similarly, while many of the components of the germination machinery are conserved between spore forming members of the *Bacillales* and *Clostridiales* orders, recent studies have revealed significant differences both in the proteins and in the signal transduction pathways involved (Figure 1.10) (reviewed in Paredes-Sabja *et al*., 2010). Bioinformatic analysis of *C. difficile* genome has failed to reveal genes encoding known GR subunits (Sebaihia *et al*., 2007, Sebaihia *et al*., 2006) even though a number of such genes were identified in other Clostridia. Furthermore, while the *C. difficile* 630 spore proteome has recently been identified (Lawley *et al*., 2009b), little homology has been shown between *C. difficile* spore proteins and those found in other Clostridia

and Bacilli. Possibly, *C. difficile* GRs are too divergent from those of other sporulating bacteria. Alternatively, *C. difficile* may use a different set of proteins as GRs.

It is well established that bile salts: cholate, taurocholate, glycocholate and deoxycholate stimulate *C. difficile* spore germination (Wilson *et al.*, 1982, Wilson, 1983), while more recent studies revealed that glycine and histidine act as a co-germinants with these cholate derivatives (Sorg and Sonenshein, 2008, Wheeldon *et al*., 2011, Wheeldon *et al*., 2008). Even though neither of these compounds has been previously described as a germinant for spores of *Bacillus* or *Clostridium* species, supporting the notion of a novel mode of germinant recognition, kinetic studies have suggested that there are distinct germination receptors for taurocholate and glycine in *C. difficile* (Ramirez *et al*., 2010). Furthermore, chenodeoxycholate, another bile salt, has been shown to inhibit *C. difficile* spore germination (Sorg and Sonenshein, 2009), although a recent study has pointed to substantial diversity among different clinical isolates in their response to bile salts (Heeg *et al*., 2012). This adds a new level of regulation to the model of *C. difficile* colonisation of the gut. While chenodeoxycholate and taurocholate have been shown to have antagonistic effects, spores of *C. difficile* are suggested to have a higher affinity for chenodeoxycholate than for taurocholate (Sorg and Sonenshein, 2010). Therefore, in equal concentrations both compounds may compete for binding to putative *C. difficile* GRs and germination may be inhibited. However, as the rate of absorption of chenodeoxycholate by the colon is ten times that of cholate (Mekhjian *et al*., 1979), spores reaching the large intestine encounter a higher concentration of cholate derivatives, such as taurocholate. This suggests that germination may be inhibited until *C. difficile* spores reach the anaerobic environment of the large bowel, where conditions are suitable for vegetative cell growth. Furthermore, in a normal, healthy host, the colonic microflora dehydroxylates chenodeoxycholate to lithocholate, also an inhibitor of germination. In an antibiotic-treated host, chenodeoxycholate is not dehydroxylated and is absorbed by the colonic epithelium at a rate 10 times higher than that of cholate (Mekhjian *et al*., 1979). Thus, in an antibiotic-treated individual, the ratio of cholate to chenodeoxycholate derivatives would favour germination. This generated the hypothesis that the

metabolism of bile salts by the normal gut flora is one mechanism by which it can protect against *C. difficile* infection, and experiments with antibiotic-treated and untreated mice cecal extracts support this hypothesis (Giel *et al*., 2010).

While the chemical signals that promote the initiation of germination in *C. difficile* have been well characterised over the years, it was not until 2013 that the first germination receptor has been described in the form of CspC, a germination-specific, subtilisin-like serine protease responsible for triggering germination upon stimulation with bile salts (Francis *et al*., 2013). In *C. perfringens,* the Csp family of proteins (CspA, CspB and CspC) has been previously implicated in germination as being responsible for cleaving the cortex hydrolase precursor pro-SleC to an active form (Shimamoto *et al*., 2001) thus initiating cortex degradation. While all three proteins contain an active catalytic triad, only CspB has been shown to be essential in germination (Paredes-Sabja *et al*., 2009), although the signals that stimulate this proteolysis have not been elucidated. In *C. difficile*, the *cspA* and *cspB* coding sequences are fused, and only CspB contains an active catalytic triad necessary to activate SleC, suggesting that it might play a similar role to that observed in *C. perfringens*. Indeed, a recent study by Adams *et al*. (2013) has shown that CspBA undergoes auto-processing to generate CspB, which can cleave the cortex hydrolase precursor pro-SleC to an active form. It has also been suggested that the stimulus required for activation of CspB might come from CspC which changes its conformation upon binding of bile salts (Francis *et al*., 2013).

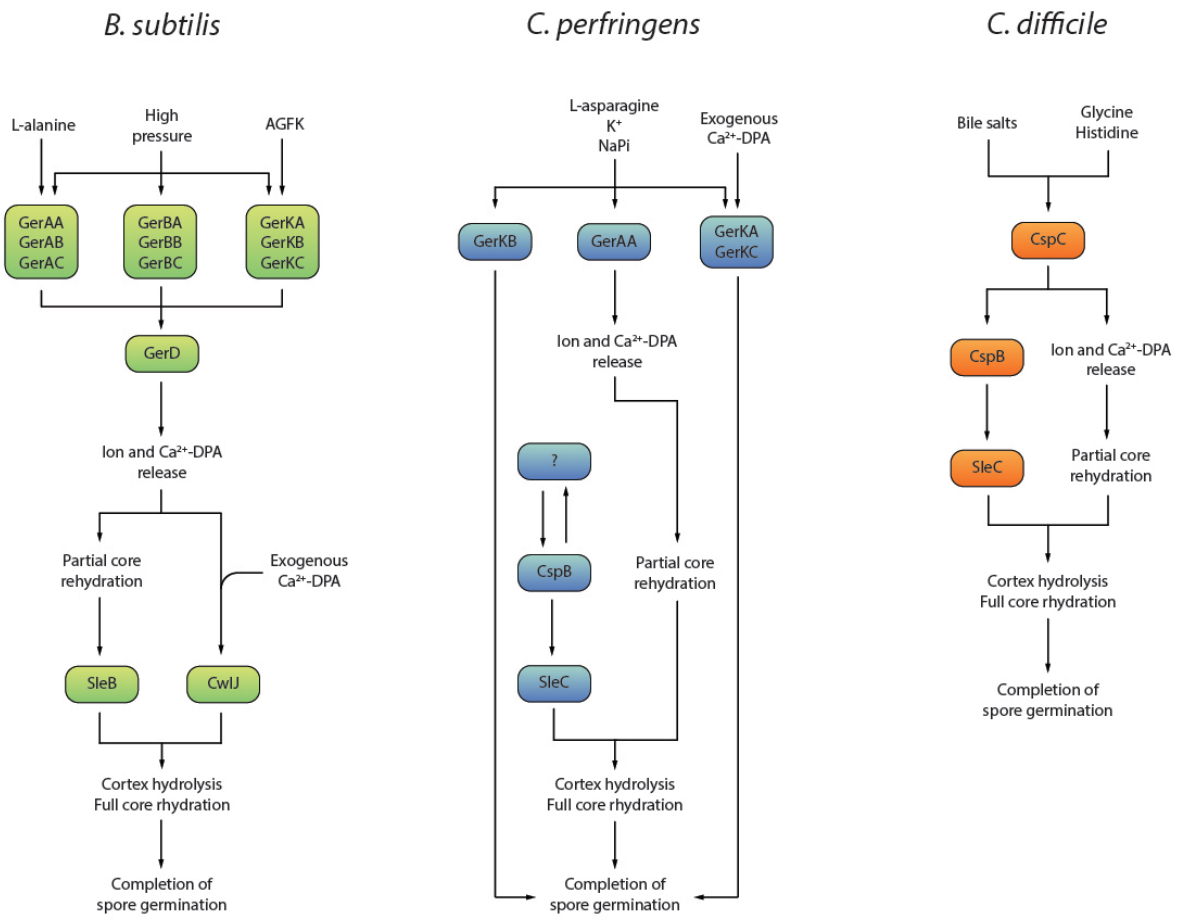

Figure 1.10. Tentative models of germination signalling pathways in *B. subtilis, C. perfringens* and *C. difficile*. In *B. subtilis*, spore germination is triggered by L-alanine, which acts through the GerA receptor, and a mixture of L-asparagine, fructose, glucose and KCl (AGFK) acting through the GerB and GerK receptors. High hydrostatic pressures (HHPs) of 200–400 MPa also trigger germination through the GerA, GerB and GerK receptors. The germination signals from the GRs are transduced and amplified, possibly *via* GerD, and lead to ion and Ca^{2+}-DPA release, which in turn activates CwlJ. The resulting changes in cortex structure activate SleB. These two redundant CLEs degrade the PG cortex, allowing completion of germination and initiation of spore outgrowth. In *C. perfringens*, germinants such as L-asparagine and KCl or the co-germinants NaPi and sodium ions act primarily through the GerKA–GerKC receptor proteins, while GerKB and GerAA, play auxiliary roles. Exogenous Ca^{2+}–DPA does not trigger *C. perfringens* spore germination through a CLE, but acts through GerKA–GerKC, In the absence of a GerD homolog, germinant–GR binding is presumed to directly trigger Ca^{+2}–DPA release, allowing partial core hydration and perhaps some cortex deformation. However, Ca^{2+}–DPA release has no role in activation of the *C. perfringens* CLE, SleC. Instead, the serine protease, CspB, is activated through an unknown mechanism, and cleaves and activates pro-SleC. Mature SleC then hydrolyzes the PG cortex, allowing entry into spore outgrowth, and the action of SleC and thus of CspB increase rates of DPA release. *In C. difficile* germination is triggered by bile salt and the co germinants glycine and histidine, acting upon CspC. This results in Ca^{+2}–DPA release and partial core rehydration as well as CspB mediated activation of SleC, the major CLE present in *C. difficile,* allowing completion of germination and initiation of spore outgrowth. Adapted from Parades-Sabja *et al*. (2010).

1.4. Overview of genetic tools for studying *C. difficile*

The rapid increase in prevalence and severity of *C. difficile* infections seen since 2001 has attracted attention from the scientific community, driving the development of new diagnostics, treatments and prevention regimes. Despite its importance in human disease, progress in understanding the molecular basis of *C. difficile* pathogenicity has been slow, hindered by the scarcity of established methods suitable for studying CDI, particularly with regard to genetic studies. While the organism has been genetically tractable since 2006, when the complete genome sequence of *C. difficile* strain 630 was published (Sebaihia *et al*., 2006), the genetic tools necessary to exploit this information have been lacking. Recent advancements in the field and the introduction of new methods for both forward and reverse genetic studies have helped overcome these issues, bridging the gap between *C. difficile* research and that carried out in better-characterised organisms.

1.4.1. Clostridial vector systems

The first attempts at delivering DNA into *C. difficile* were based on conjugative transposons such as Tn*916* that may be conjugated from *B. subtilis* donors using a filter mating technique (Mullany *et al*., 1991). While this method has been successfully used to transfer heterologous DNA through co-integration of a replication-deficient plasmid, the relatively low transfer frequency (10^{-8} per donor) combined with preferential integration into a single site within the recipient's genome drastically limit its usability (Mullany *et al*., 1994). Further advances in the field came with the use of *E. coli* – *C. difficile* shuttle vectors for the episomal expression of native or exogeneous genes. These were largely based on pMTL960 plasmids developed by Purdy *et al.* (2002) which utilised the Gram-positive replicon from the *C. difficile* native plasmid pCD6, the *E. coli* origin of replication ColE1 and the conjugative transfer origin *oriT* allowing for efficient conjugation into *C. difficile* from *E. coli* donor strains. The *catP* gene from *C. perfringens* encoding resistance to chloramphenicol (in *E. coli)* and thaimphenicol (in *C. difficile*) was included as a selectable marker. This has been further refined with the introduction of the pMTL8000 modular vector family, in which both Gram-positive and

Gram-negative replicons as well as the selection markers can be swapped, allowing for higher flexibility in experimental design (Heap *et al*., 2009). Over the years a number of variations of the original system have been developed. Native, well-characterised *C. difficile* promoters such as the *cwp2* promoter have been successfully used to express or over-express *C. difficile* genes in expression studies. These included the study of the *C. difficile* cell wall protein CwpV (Dembek *et al*., 2011, Emerson *et al*., 2009, Reynolds *et al*., 2011), and the cell wall-associated cysteine protease Cwp84 (de la Riva *et al*., 2011). More recently, an inducible promoter system has been developed by introducing a tetracycline inducible promoter from *Staphylococcus aureus* into pMTL960 (Fagan and Fairweather, 2011). The system has been successfully used to express genes in a controlled, dose-dependent manner as well as in knock-down studies, to temporarily disrupt the expression of a particular gene using antisense RNA (Fagan and Fairweather, 2011). Finally, a variant of the inducible promoter plasmid lacking a transcriptional terminator directly downstream of the tetracycline repressor gene *tetR,* has been shown to be segregationally-unstable due to transcriptional read-through from the inducible promoter. Upon induction, the plasmid is rapidly lost from the population and can thus be used as a conditional replicon, the first conditional replicon for use in *C. difficile* (Dr Robert Fagan, unpublished results).

1.4.2. Genomic mutations in *C. difficile*

1.4.2.1. ClosTron insertional mutagenesis

The introduction of ClosTron technology in 2007 (Heap *et al*., 2007) was an important milestone in Clostridial research allowing for the creation of genetically stable mutants by targeted disruption of selected genes within the genome. The system makes use of group II introns, genetic elements widespread in both eukaryotic and bacterial genomes that insert into specific DNA target sites by a unique mechanism in which the intron RNA reverse splices directly into double-stranded DNA and is then reverse transcribed by the intron-encoded reverse transcriptase. The rules that govern group II intron mobility were first characterised by Mohr *et al*. (2000) who elucidated the

mechanism of replication of a group II intron found in the *ltrB* gene of *Lactococcus lactis*, and demonstrated that by changing the intron sequence, its target specificity could be altered to allow for disruption of almost any gene of interest. It was also noted that the intron-encoded protein (IEP) that confers intron mobility can be provided *in trans* without affecting its function, preventing further mobility after the desired insertion has been achieved. In order to facilitate rapid selection of genetically stable mutants, re-targeted introns were equipped with retrotransposition-activated markers (RAM) carrying a nested group I intron (Zhong *et al*., 2003). Upon transcription, the group I intron is spliced out and the complete group II intron carrying a functional selection marker is integrated into the desired site within the genome, disrupting gene expression (Figure 1.11). The system has been further refined in 2010 (Heap *et al*., 2010) becoming the gold standard in genetic manipulation of *C. difficile*, successfully used in a wide range of studies (de la Riva *et al*., 2011, Deakin *et al*., 2012, Emerson *et al*., 2009, Kirby *et al*., 2009, Reynolds *et al*., 2011).

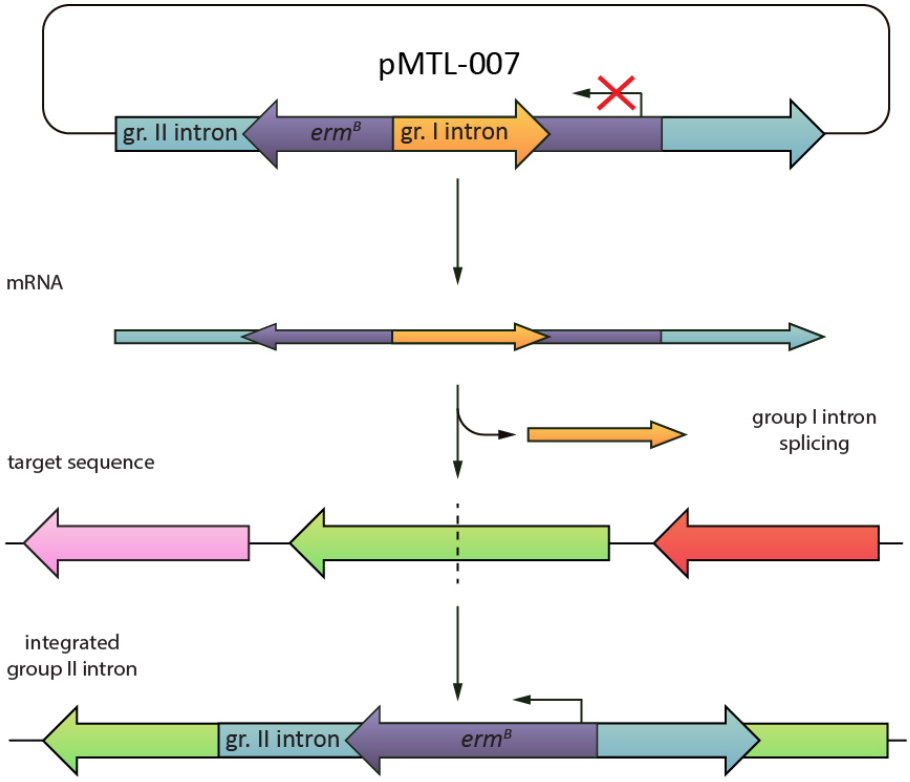

Figure 1.11. Schematic representation of ClosTron insertional mutagenesis. pMTL007-based plasmid carrying a retargeted group II intron is conjugated into *C. difficile*. Following transcription, the group I intron disrupting *erm*^{R} undergoes splicing and the active group II intron integrates into the target site within a gene, disrupting its expression. ClosTron mutants are selected through erythromycin resistance.

1.4.2.2. Homologous recombination techniques

While the ClosTron system provides a fast, reliable and reproducible method for targeted disruption of genes, insertional mutagenesis does impose certain limitations. Polar effects are common as insertion of the group II intron can disrupt the expression of neighbouring genes. Multiple insertions, while rare, have been reported necessitating the use of time consuming screening techniques. While double mutants have been successfully created by introducing a second selectable marker (Kuehne *et al*., 2010), the limited availability of such markers makes creating multiple gene deletions difficult. Finally, as *in situ* complementation of a disrupted gene is not possible, plasmid-based *in trans* complementation has to be used, often resulting in unwanted gene dosage effects.

In order to overcome these problems and to allow for more refined genetic manipulations required for robust functional analyses, methods involving homologous recombination were investigated. Early attempts at creating unmarked mutations within the *C. difficile* genome involved single crossovers that were largely unstable, often reverting to wild-type (O'Connor *et al*., 2006). At this early stage, all attempts to generate stable double crossover were unsuccessful. It was not until 2012 that this became possible with the introduction of two independent methods for homologous recombination in *C. difficile*.

The first method utilises *codA* from *E. coli* which encodes for cytosine deaminase (EC 3.5.4.1), an enzyme that converts the innocuous 5-fluorocytosine (FC) into toxic 5-fluorouracil (FU). A plasmid carrying the *cod*A gene and a mutated allele containing 500 bp-long upstream and downstream homology regions is transferred into *C. difficile* through conjugation. Single crossover mutants carrying the entire plasmid are selected for using *catP*-mediated thiamphenicol resistance and are further confirmed by PCR. Isolated mutants are then plated onto minimal medium supplemented with FC, to select for the rare, double crossover event resulting in excision of the plasmid backbone carrying *codA* and replacement of the original allele with the plasmid-encoded copy. Standard PCR techniques are used to differentiate between allele exchange and reversion to wild-type. As a proof-

of-principle this system has been successfully used in *C. difficile* R20291 to correct point mutations in *tcdC* and to study their role in regulation of toxin production (Cartman *et al*., 2012).

The second system was developed in parallel as a method for introducing heterologous DNA fragments of any size or complexity into the *C. difficile* genome without the need for a counter-selection marker and is based on the native *pyrE* gene involved in uracil biosynthesis. Strains carrying a functioning copy of *pyrE* can grow in the absence of uracil but are sensitive to 5-fluoroorotic acid (FOA). This is exploited to select for double crossover events that allow for integration of DNA fragments directly downstream of the *pyrE*. Briefly, homology regions of varying lengths are used to target the plasmid-encoded DNA cargo to the *pyrE* locus such that a single cross-over event, which does not interrupt the gene, occurs first. These thiamphenicol resistant, FOA-sensitive clones are then plated onto minimal medium supplemented with FOA to select for double crossover events. Upon excision of the plasmid backbone the *pyrE* allele is replaced with a truncated copy, rendering the cells sensitive to thiamphenicol and resistant to FOA. This defective *pyrE* allele can be returned to WT by homologous recombination, selected for by growth in the absence of uracil. In an elegant study by Heap *et al*., (2012) this method, dubbed Allele-Coupled Exchange (ACE), was successfully used to deliver a 40 kb fragment of lambda DNA into the chromosome of *C. acetobutilicum* using a multi-step approach. The system was further exploited by Ng *et al*. (2013) who used *pyrE* mutants to deliver DNA anywhere in the genome by integrating constructs carrying the DNA cargo alongside a functional *pyrE* allele. The resulting mutants were then returned to uracil prototrophy as described above or simultaneously complemented by introducing a WT copy of the disrupted gene under the control of a native or heterogeneous promoter directly downstream of the *pyrE* allele (Figure 1.12). Both systems are now considered the gold standard for precise genetic manipulation of *C. difficile* and have contributed greatly towards understanding this, once genetically intractable, organisms.

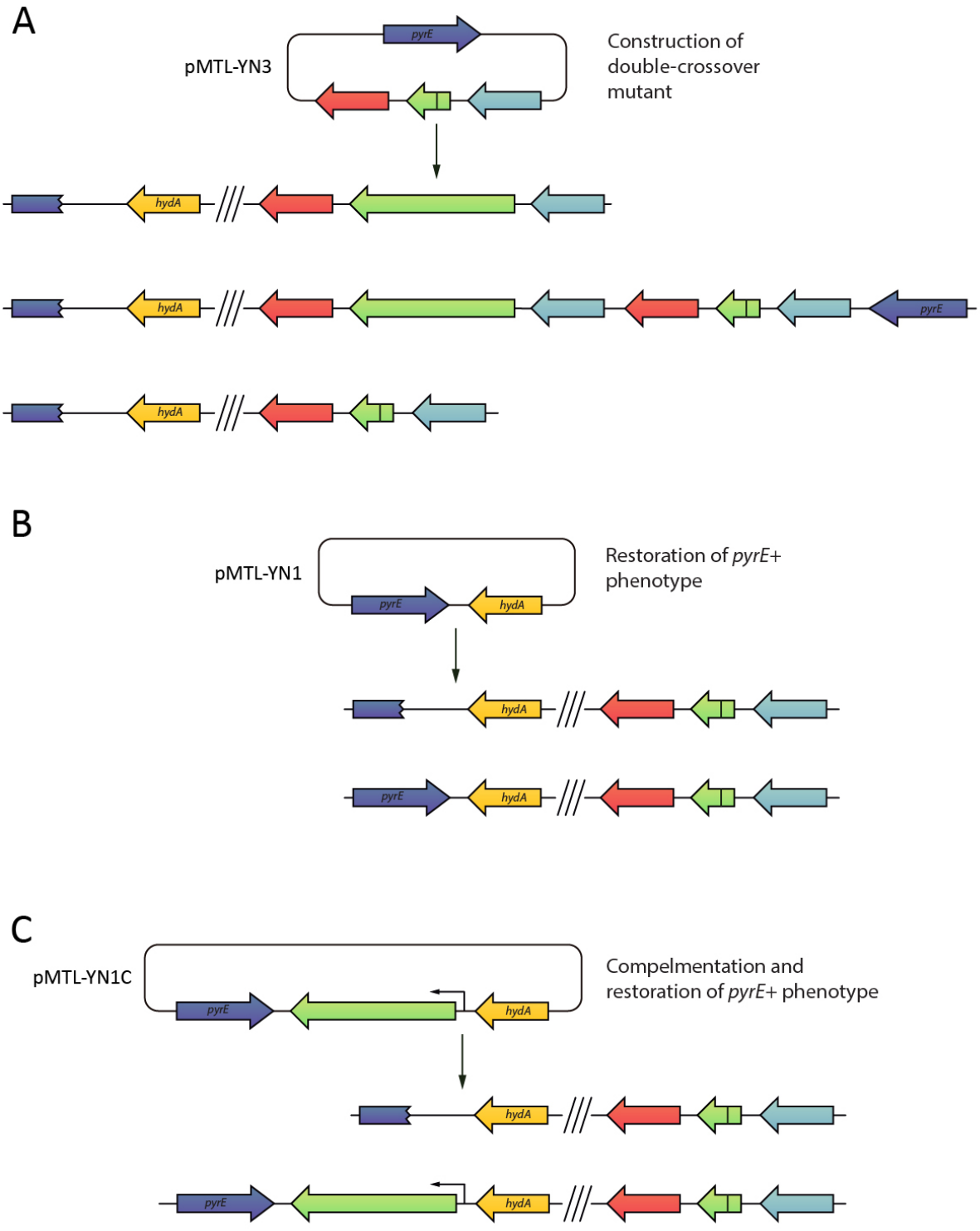

Figure 1.12. Schematic representation of Allele Coupled Exchange (ACE) mutagenesis. (A) A pMTL-YN3-based plasmid carrying a mutated allele of the targeted gene (green) together with upstream and downstream homology regions (teal and red) as well as a WT copy of *pyrE* (dark blue) is conjugated into Δ*pyrE* background. Single cross-over mutants are selected through plasmid-encoded thiamphenicol resistance. These are then plated onto minimal medium supplemented with FOA to select for double cross-over events. **(B)** Mutants are restored to uracil prototrophy by introduction of a WT *pyr*E allele *via* homologous recombination, **(C)** and can be complemented by concomitant introduction of the WT allele of the targeted gene between the *pyr E* and *hydA* loci.

1.4.2.3. Transposon mutagenesis and sequencing

Since their discovery in the 1950s (McClintock, 1950), transposons have become a valuable component of the 'molecular toolbox', allowing for the precise manipulation of genes in virtually any genetically tractable organisms. Originally identified as factors controlling gene expression in maize, these mobile genetic elements have since been found in every kingdom of life, playing important roles in the evolution of speciation and antibiotic resistance in microorganisms (reviewed in Kidwell and Lisch, 2001, Alekshun and Levy, 2007). Their remarkable characteristics have been exploited in molecular biology, primarily in the creation of random mutant libraries *via* insertional mutagenesis, allowing for large-scale analyses of gene function. Such studies have benefited greatly from the recent advances in microbial genome sequencing, which have enabled researchers to directly link an observed phenotype to a particular genotype. With the advent of high-throughput sequencing and the introduction of signature-tagged mutagenesis methodologies (Hensel *et al*., 1995) it is now possible to sequence comprehensive libraries of mutants simultaneously, thus allowing for genome-wide, genotype-phenotype analyses. These have already led to the identification of thousands of virulence genes in a number of clinically-relevant bacteria, including *Salmonella enterica* subsp. *enterica* serovar Typhimurium (Hensel *et al*., 1995), *Staphylococcus aureus* (Mei *et al*., 1997), *Vibrio cholerae* (Chiang and Mekalanos, 1998), *Streptococcus agalactiae* (Jones *et al*., 2000), *Listeria monocytogenes* (Autret *et al*., 2001) and *Streptococcus pneumoniae* (Polissi *et al*., 1998). Further advancements in the field and the introduction of massively parallel sequencing (MPS) have led to the development of transposon sequencing methods in which a comprehensive mutant library, containing insertions in all but the essential genes is passaged under permissive or non-permissive conditions in order to determine the minimal set of genes necessary for survival (reviewed in Barquist *et al*., 2013). In these methods, genomic DNA extracted from the entire mutant pool is either sheered or digested into small fragments which are ligated to adapter DNA. Primers specific to the transposon inverted repeats and the adapter, are then used to PCR-amplify across the insertion junction and the resulting PCR

products are sequenced. The differences in the number of sequence reads for each junction can be then analysed to assess the fitness contribution of each gene under a particular set of conditions. One such method, dubbed transposon-directed insertion site sequencing (TraDIS) has recently been used in *S. typhi* to identify genes essential for growth in rich medium as well as those involved in tolerance to bile, a substance the pathogen encounters when colonizing the gall bladder (Langridge *et al*., 2009).

To date, the undeniable success of transposon mutagenesis has not been translated into *C. difficile* research. While *in vitro* transposon mutagenesis systems have been successfully used in the closely related *C. perfringens* (Vidal *et al*., 2009, Lanckriet *et al*., 2009), their reliance on transformation as a way of introducing DNA into the cell, makes them unsuitable for use in *C. difficile*. An alternative approach was introduced by Cartman *et al*. (2010) who attempted to generate random libraries of *C. difficile* mutants *in vivo*, by introducing *mariner*-based transposons *via* segregationally unstable, 'pseudo-suicide' vectors (Cartman and Minton, 2010). The *mariner*-transposable element *Himar1* has been previously shown to insert randomly into TA target sites in genomes of many bacterial species *via* a cut-and-paste mechanism mediated by the *Himar1* transposase (Lampe *et al*., 1996, Lampe *et al*., 1998), a useful characteristic considering the low GC-content found in the *C. difficile* genome. While the experiment provided good evidence that a *mariner*-based transposon could be an effective tool for generating random mutants in *C. difficile*, and a number of stable mutants carrying single insertions were identified, the lack of a well-defined conditional replicon meant that the system provided little control over the transposition event and was not suitable for the creation of large scale libraries.

1.5. Project aims

Sporulation and germination play a pivotal role in CDI transmission, allowing the otherwise strictly anaerobic organism to survive outside of the host and being responsible for recurrence of disease when therapy is stopped. While the molecular basis of sporulation and germination has been extensively studied in *B. subtilis,* and more recently in other clostridia, our current understanding of these events in *C. difficile* remains rudimentary at best. A detailed understanding of the mechanisms behind sporulation and germination could have direct implications in infection control and the development of new therapeutics.

Two complementary approaches were taken in order to provide a more complete image of sporulation and germination in *C. difficile*. Firstly, a transcriptomic analysis of temporal gene expression patterns during germination was performed to illustrate how the germinating cell re-establishes its metabolism following a phase of dormancy. Secondly, transposon mutagenesis combined with next-generation sequencing was used to identify genes essential in sporulation and/or germination. These results could be validated thanks to the recent development of robust systems for genetic manipulation of Clostridia, facilitating a more in-depth characterisation of genes of interest.

The major aims for this project were:

I. To perform a genome-wide analysis of sporulation and germination in C. difficile

II. To identify sporulation and germination core gene set

III. To characterise selected genes and identify their role in sporulation and/or germination

Chapter II

Materials and Methods

2.1. Bacterial strains and growth conditions

Plated cultures of *C. difficile* strains were routinely grown on blood agar base II (Oxoid) supplemented with 7% horse blood (TCS Biosciences), brain-heart infusion (BHI) agar (Oxoid), BHIS agar (BHI agar supplemented with 0.1% L-cysteine and 5 mg/ml yeast extract (Bacto)) or *Clostridium difficile* Defined Medium (CDMM) (Karasawa *et al*., 1995).

Table 2.1. Composition of *Clostridium difficile* Defined Medium.

	Stock concentration [mg/ml]	**Final concentration [mg/ml]**
Amino acids (5x)		
Casamino acids	50	10
L-Tryptophan	2.5	0.5
L-Cysteine	2.5	0.5
Salts (10X)		
Na_2HPO_4	50	5
$NaHCO_3$	50	5
KH_2PO_4	9	0.9
NaCl	9	0.9
Glucose (20X)		
D-Glucose	200	10
Trace salts (50X)		
$(NH_4)_2SO_4$	2.0	0.04
$CaCl_2 \cdot 2H_2O$	1.3	0.026
$MgCl_2 \cdot 6H_2O$	1.0	0.02
$MnCl_2 \cdot 4H_2O$	0.5	0.01
$CoCl_2 \cdot 6H_2O$	0.05	0.001
Iron (100X)		
$FeSO_4 \cdot 7H_2O$	0.4	0.004
Vitamins		
D-Biotin (1000X)	1	0.001
Calcium-D-panthothenate (1000X)	1	0.001
Pyridoxine (1000X)	1	0.001

Liquid cultures were grown in BHI broth (Oxoid), BHIS broth or TY broth (3% tryptose, 2% yeast extract (Bacto)). All cultures were supplemented where appropriate with antibiotics: thiamphenicol (15 µg/ml), cycloserine (250 µg/ml) or erythromycin (5 µg/ml). Unless stated otherwise, liquid cultures were grown statically overnight (O/N) in an anaerobic cabinet (Don Whitley Scientific), at 37°C, in an atmosphere of 10% CO_2, 10% H_2 and 80% N_2. All media were pre-reduced in the anaerobic cabinet before inoculation.

Plated cultures of *E. coli* strains were routinely grown on LB agar (VWR). Liquid cultures were grown in LB broth (VWR). For inducible protein expression, strains were grown in Overnight Express Instant TB medium (Merck) supplemented with 1% (v/v) glycerol. All media were supplemented where appropriate with antibiotics: kanamycin (50 µg/ml) or chloramphenicol (15 µg/ml). *E. coli* NovaBlue (Merck) or NEB5α (NEB) were used as the recipient strains in all cloning procedures. *E. coli* CA434 was used as the donor strain for conjugation of plasmids into *C. difficile. E. coli* Rosetta (Novagen) and BL21(*DE3)* were used as expression strains for protein production. Unless stated otherwise, cultures were grown O/N with agitation (225 rpm) at 37°C.

All strains were stored at -80°C in 20% glycerol. A detailed list of strains used and created throughout this project is provided in Appendix A, Table A1.

2.2. Production of chemically-competent *E. coli* CA434

An O/N culture of *E. coli* CA434 in LB broth was sub-cultured 1:100 and grown to exponential phase [optical density at 600nm (OD_{600}) 0.4 – 0.6]. The culture was harvested by centrifugation (10 min at 3,400 x g at 4°C), resuspended in 5 ml of ice-cold 100 mM $CaCl_2$ and incubated on ice for 15 min. Cells were harvested as above, resuspended in 1 ml ice-cold $CaCl_2$ with 15% (v/v) glycerol and incubated on ice for 2h before aliquoting and freezing at -80°C. All steps except centrifugation were carried out at 4°C.

2.3. *C. difficile* sporulation and spore purification

C. difficile sporulation was induced as described previously (Permpoonpattana *et al*., 2011). Briefly, 10 ml of TGY broth (3% tryptic soy broth; 2% glucose; 1% yeast extract; 0.1% L-cysteine) was inoculated with a single colony of *C. difficile* grown on BHIS agar. Following O/N static incubation, bacteria were sub-cultured 1:10 in sporulation medium (SM) broth (9% Bacto peptone, 0.5% proteose peptone, 0.15% Tris base, 0.1% ammonium sulphate), grown to OD_{600} of 0.6 and 200 µl aliquots were spread out on SM agar plates. The number of plates used depended on the required yield and ranged from 6 to 48 plates. After 7 days of anaerobic incubation at 37°C, spores were harvested in 2ml of ice-cold sterile water per plate.

Crude spore suspensions were washed five times with 1 ml of ice-cold sterile water and vortexed for 10 min in between washes. Pellets from four plates were pooled, re-suspended in 500 µl of 20% HistoDenz (Sigma) and layered over 1 ml of 50% HistoDenz in a 1.5 ml tube. Tubes were centrifuged at 14,000 x g for 15 min. The spore pellet was recovered and washed three times with ice-cold sterile water to remove residual HistoDenz. Spore purity was assessed *via* phase contrast microscopy. Spore yields in individual preparations were estimated by counting colony-forming units (CFU) on BHI agar plates supplemented with 0.1% sodium taurocholate (Tch). Purified spores were stored in water at 4°C until further analysis.

2.4. DNA manipulation

2.4.1. Genomic DNA extraction

C. difficile genomic DNA (gDNA) was isolated *via* phenol:chloroform extraction as described previously (Wren *et al*., 1987). 10 ml O/N cultures were harvested by centrifugation (10 min at 5,000 x g). Bacterial pellets were resuspended in 2 ml lysis buffer (200mM NaCl, 50mM EDTA, 20mM Tris-HCl pH 8.0) supplemented with 2mg/ml lysozyme and incubated at 37°C for 1 h. The resulting suspension was treated with 0.5 mg/ml pronase (1 h at 37°C), 2% N-lauroylsarcosine (1 h at 55°) and 0.1 mg/ml RNase (1 h at 37°C). Following lysis, gDNA was extracted twice with

phenol:chloroform:isoamyl alcohol (25:24:1) and twice with chloroform:isoamyl alcohol in 15 ml phase lock gel (PLG) tubes (VWR), followed by O/N precipitation with 2.5 volumes of absolute EtOH at -20°C. gDNA pellets were re-suspended in nuclease-free water do a desired volume. gDNA quantity and quality was assessed on a NanoDrop instrument (Thermo Scientific) by measuring total concentration as well as A_{260}/A_{280} and A_{260}/A_{230} ratios. gDNA integrity was assessed *via* standard agarose gel electrophoresis.

2.4.2. Chelex DNA preparations

DNA preparations for routine colony screening were extracted using 5% (w/v) Chelex 100 resin (Bio-Rad) in nuclease-free water. Single colonies were suspended in 100 µl 5% Chelex, boiled for 10 min at 100°C and pelleted at 10,000 x g for 1 min. Supernatants containing DNA were transferred to a fresh tube for further analysis.

2.4.3. Plasmid DNA extraction

Plasmid DNA was extracted from *E. coli* using the QIAprep spin kit (Qiagen) according to manufacturer's protocols. Briefly, 5 ml O/N cultures were centrifuged (10 min at 5,000 x g) and the resulting pellets were re-suspended in 250 µl of buffer P1. An equal volume of buffer P2 was added, the sample was mixed gently and incubated for 5 min. 350 µl of buffer N3 was added, the sample was mixed once more and centrifuged at 10,000 x g for 10 min. The supernatant was applied to a QIAprep column and centrifuged at 10,000 x g for 1 min. The column was washed with 700 µl of buffer PE. Residual buffer was removed by centrifuging a second time at 10,000 x g for 1 min. DNA was eluted by adding 30-50 µl of nuclease-free water, incubating for 1 min at room temperature (RT) and centrifuging at 10,000 x g for 1 min. A complete list of plasmids used or created throughout this study is provided in Appendix A, Table A2. Plasmid maps are provided in Appendix A, Figure A1.

2.4.4. Polymerase chain reaction (PCR)

Routine screening PCR and colony PCR were carried out using *Taq* polymerase (Sigma) according to manufacturer's guidelines in a total volume of 20 µl (1x PCR buffer, 2.5 mM $MgCl_2$, 0.2 mM dNTPs, 0.1 µM forward and reverse primers, 0.2 U *Taq*). Initial denaturation was at 94°C for 3 min followed by thirty cycles of denaturation at 94°C for 30 s, annealing at 1°C below primers T_m for 1 min and extension at 72°C for 1 min per kb. A final extension at 72°C for 10 min was included to ensure completion of DNA synthesis.

Reactions requiring higher stringency (amplification of gDNA fragments for cloning purposes and inverse PCR) were carried out using KOD Hot Start polymerase (Merck) according to manufacturer's guidelines in a total volume of 50 µl (1x PCR buffer, 1 mM $MgSO_4$, 0.2 mM dNTPs, 0.3 µM forward and reverse primers, 0.02 U KOD). Initial denaturation was at 95°C for 2 min followed by thirty cycles of denaturation at 95°C for 20 s, annealing at 1°C below primers T_m for 30 s and extension at 72°C for 15 s per kb. A final extension at 72°C for 10 min was included to ensure completion of DNA synthesis. All reactions were carried out using a G-Storm GS2 thermal cycler. Primers used throughout this study were synthesised by either Euorfins or Sigma-Aldrich and are listed in Appendix A, Table A3.

2.4.5. Purification of PCR reactions

PCR-amplified DNA fragments were purified using the QIAquick PCR purification kit according to manufacturer's guidelines.

2.4.6. Restriction endonuclease digestion of DNA

All restriction endonuclease digest were carried out using enzymes provided by New England Biolabs (NEB) according to manufacturer's guidelines. Unless stated otherwise, PCR products and plasmid DNA were digested at 37°C for 1h while gDNA was digested O/N.

2.4.7. Agarose gel electrophoresis

Agarose gels were prepared by melting 0.6 - 3% (w/v) agarose powder (Invitrogen) in 1 x TAE (40mM TrisAcetate, 2mM Na_2EDTA pH 8.3) in a microwave oven. When sufficiently cool, 1/10,000 volume SybrSafe DNA stain was added and the gel was cast on a horizontal perspex plate. When fully set, gels were placed in a tank containing 1 x TAE. DNA samples were mixed with 0.25 volumes DNA loading buffer and then loaded into the gel wells. Electrophoresis was performed at approximately 10V/cm. DNA was visualised on a UV transilluminator at 312 nm, and images recorded on an InGenius gel documentation system (Syngene).

2.4.8. Extraction of DNA from agarose gels

DNA was extracted from agarose gels using the QIAquick Gel Extraction kit according to manufacturer's guidelines. Briefly, bands were excised using a scalpel, weighed and mixed with 3 volumes of buffer QG (100 µg ~ 100 µl). Following 10 min incubation at 50°C 1 volume of isopropanol was added and the resulting samples were applied onto a QIAquick column and centrifuged at 10,000 x g for 1 min. The column was washed with 500 µl of buffer QG and 750 µl of buffer PE (10,000 x g for 1 min). DNA was eluted by adding 30-50 µl of nuclease-free water, incubating for 1 min at RT and centrifuging at 10,000 x g for 1 min.

2.4.9. DNA Ligation

Ligation reactions were carried out for 15 min at RT using QuickStick ligase (Bioline) according to manufacturer's guidelines in a total volume of 20 µl (50 ng of DNA in nuclease-free water, 5 µl 4x Quick Stick ligase buffer, 1 µl QuickStick ligase). For routine cloning a 3:1 insert:vector molar ratio was used. Blunt-ended products obtained *via* inverse PCR, were phosphorylated using T4 polynucleotide kinase (NEB; 30 min at 37°C) prior to ligation.

2.4.10. Transformation

25 µl aliquots of chemically competent *E. coli* cells were transformed with 1 µl of ligation reaction and incubated on ice (5 min for NEB5α, Top10 and NovaBlue cells; 30 min for CA434 cells). Following a 30 s heat-shock at 42°C cells were incubated on ice for 2 min, resuspended in 125 µl of sterile S.O.C. medium, incubated for 1 h at 37°C with agitation and plated onto LB agar supplemented with the appropriate antibiotic.

2.4.11. DNA sequencing

Routine Sanger sequencing was carried out by GATC Biotech (Konstanz, Germany) on previously purified plasmid DNA or PCR-amplified DNA fragments. Sequencing primers were provided at 10 pmol/µl or synthesised directly by GATC.

2.4.12. *E. coli – C. difficile* conjugation

pMTL960-based shuttle plasmids were transformed into *E. coli* CA434 and conjugated into *C. difficile* as described previously (Purdy *et al*., 2002). Briefly, 1 ml of O/N *E. coli* culture (donor) was spun down (1 min at 3,000 x g), washed gently with sterile phosphate-buffered saline (PBS) and mixed with 200 µl of O/N *C. difficile* culture (recipient). The resulting mixture was spotted onto non-selective BHIS agar and incubated anaerobically for 8h. The resulting growth was resuspended in 1 ml of sterile PBS and spread out onto BHIS agar supplemented with thiamphenicol (15 µg/ml) to select for pMTL960-based plasmids and cycloserine (250 µg/ml) to counterselect against *E. coli*.

2.4.13. ClosTron insertional mutagenesis

All *C. difficile* ClosTron mutants were generated in *C. difficile* 630Δ*erm* (Hussain *et al*., 2005) by insertion of a bacterial group II intron containing a retrotransposition-activated marker (RAM) conferring erythromycin resistance (Zhong *et al*., 2003) using the ClosTron clostridial gene knockout system (Heap *et al*., 2007). 45bp intron target sites were identified within the respective genes using

the Perutka algorith (http://www.clostron.com). Plasmids were synthesised (DNA 2.0) and transferred into *C. difficile* 630Δ*erm* by conjugation from previously transformed *E. coli* CA434. Transconjugants were restreaked twice onto Brazier's agar (BioConnections) supplemented with thiamphenicol (15 μg/ml), cefoxitin (8 μg/ml) and cycloserine (250 μg/ml). Potential Ll.ltrB insertions were selected by plating bacteria on Brazier's agar supplemented with erythromycin (5 μg/ml). Putative mutants were screened by colony PCR using (i) primers specific for genes of interest flanking the intron insertion site, (ii) gene specific primers in combination with a primer internal to the group II intron (iii) and RAM specific primers flanking the group I intron.

2.4.14. Allele-Coupled Exchange (ACE) mutagenesis

ACE mutants were generated in *C. difficile* 630Δ*ermΔpyrE* as described by Ng *et al.* (2013). Briefly, mutated alleles carrying in-frame deletions were generated by cloning PCR-amplified 750 bp upstream and downstream homology regions into pMTL-YN3 using Gibson Assembly according to manufacturer's instructions. The resulting plasmids were conjugated into 630Δ*ermΔpyrE* as described above. Following two passages on BHIS agar supplemented with 5 μg/ml uracil, 15 μg/ml thiamphenicol and 250 μg/ml cycloserine, colonies that were noticeably larger (indicative of plasmid integration) were screened by colony PCR to identify single-crossover mutants using (i) primers flanking the upstream and downstream homology regions and (ii) one of these primers in conjunction with a plasmid-specific primer to amplify across the integration junction. Pure, single crossover mutants were streaked onto *C. difficile* minimal medium (CDMM) supplemented with 5 μg/ml uracil and 2 mg/ml 5-fluoroorotic acid (FOA) to select for plasmid excision. The isolated FOA-resistant colonies were screened by PCR. Double-crossover mutants in which the mutated allele was successfully integrated yielded products smaller than those seen in WT revertants.

In order to restore the *pyrE+* phenotype, plasmid pMTL-YN1 carrying the WT *pyrE* allele was conjugated into the isolated double-crossover mutants. The resulting colonies were restreaked onto non-supplemented CDMM agar to select for uracil prototrophy indicating successful allele exchange.

Restoration of the *pyrE* allele was further confirmed by colony PCR using primers flanking the *pyrE* locus followed by Sanger sequencing of the amplified product.

In order to complement the mutants, WT alleles including their Ribosome Binding Site (RBS) and a 200bp 5' non-coding region containing the putative promoter signals as identified by BPROM (SoftBerry) were cloned into pMTL-YN1C using SacI and BamHI sites. The resulting plasmids were conjugated into the isolated double-crossover mutants. Following 96h of incubation individual transconjugantes were re-streaked onto non-supplemented CDMM agar to select for uracil prototrophy indicating successful allele exchange and the introduction of the WT allele immediately downstream of the concomitantly restored *pyrE* locus. Complementation was confirmed by colony PCR using primers flanking the *pyrE* locus followed by Sanger sequencing of the amplified product.

2.4.15. Southern blotting

5 µg gDNA was digested O/N with 20u AseI in a total volume of 30 µl and then separated O/N on a 1% agarose gel at 20V. The gel was incubated in denaturing buffer (1.5 M NaCl; 0.5 M NaOH) for 45 min, rinsed briefly with water, incubated in neutralising buffer (1.5 M NaCl; 1 M Tris-HCl, pH 7.4) for 45 min and rinsed once more. The capillary blotting stack was assembles as follows. Two gel-sized pieces of Whatman 3MM filter paper soaked in 20x SSC buffer (3 M NaCl; 300mM sodium citrate, pH 7.0) were placed on a plastic support tray immersed in 20x SSC buffer, followed by the gel, a gel-sized piece of Biodyne B nylon membrane and two pieces of Whatman 3MM filter paper soaked in 20x SSC buffer. A 5 cm stack of tissue paper was placed on top of the filter paper and weighed down. The stack was left to transfer O/N. The following day the transfer stack was disassembled, the membrane was allowed to dry and was then cross-linked in a UV Stratalinker (Strategene). The membrane was rolled into a glass hybridization bottle and immersed in 10 ml pre-warmed hybridization solution containing the probe, a PCR product complementary to the ClosTron group II intron labelled using the AlkPhos Direct Labelling and Detection System (Pierce) according to manufacturer's instructions. Hybridization was carried out O/N at in a hybridization oven at 55°C

with rotation. The following day, the membrane was washed twice with wash buffer 1 (2 M urea; 0.1% SDS; 150mM NaCl; 0.2% blocking reagent; 1 mM $MgCl_2$; 50 mM Na_2HPO_4) (10 min at 55°C) and twice with wash buffer 2 (100 mM NaCl, 2 mM $MgCl_2$; 500 mM Tris base) (10 min at RT). The membrane was developed by adding 5 ml 1x CDP-Star detection reagent (Roche) and incubating for 5 min at RT prior to imaging on a LAS 4000 imager (Fuji).

2.5. RNA manipulation

2.5.1. Total RNA extraction

RNA was extracted using the FastRNA Pro Blue Kit (MP Biosciences) according to manufacturer's guidelines. Briefly, 10 ml vegetative cell cultures or 5 ml cultures containing 5 x 10^9 endospores (OD_{600} 10) at various stages of germination were mixed with 2 volumes of RNA Protect (Qiagen) and incubated for 5 min at RT. Samples were centrifuged (10 min at 5,000 x g at 4°C), resuspended in 1 ml of RNA Pro solution and transferred to a lysing matrix tube containing 0.1 mm silica beads. Tubes were processed in a FastPrep-24 instrument (MP Biosciences) (45 s at 6.5 m/s). For vegetative cells, 1 cycle was used. For spores, 3 cycles were used with 2 min of cooling on ice between cycles. The efficiency of spore rupture was evaluated *via* phase contrast microscopy as well as by plating spore samples prior to and post processing onto BHIS agar supplemented with 0.1% Tch. Following disruption, samples were centrifuged to remove spore debris and silica beads from suspension (16,000 x g; 10 min; 4°C). Approx. 700 µl of liquid was transferred to an RNase-free tube and incubated at RT for 5 min. 300 µl of chloroform was added. The sample was vortexed for 10s and centrifuged (16,000 x g; 15 min; 4°C) to separate the phases. The aqueous phase was transferred to a fresh tube containing 200 µl of 95% EtOH and placed on ice. The mixture was transferred to a spin column assembly (SV Total RNA isolation system; Promega) and centrifuged (1 min at 16,000 x g). Columns were washed twice with 600 µl and 250 µl of RNA wash solution. RNA was eluted in 45 µl of RNase-free water. DNase treatment was carried out using the Turbo DNase kit

(Ambion) according to manufacturer's protocol. The enzymatic reaction was cleaned-up using the RNeasy Mini Kit (Qiagen).

2.5.2. RNA quality control

RNA purity and quantity was determined by nanodrop UV spectroscopy. RNA integrity was confirmed on a RNA 6000 nano lab-Chip using a Bioanalyzer 2100 instrument (Agilent). Samples were stored at -80°C until further analysis.

2.6. Expression and purification of recombinant proteins

2.6.1. Growth and induction

5 ml starter cultures of *E. coli* Rosetta strains carrying expression plasmids based on pET28a were used to inoculate 100 ml of Overnight Express Instant TB medium (Merck). Cultures were grown for approx. 24 h at 37°C with agitation (225 rpm). Cells were harvested (5,000 x g; 10 min; 4°C) and frozen at -80°C.

2.6.2. Inclusion body purification

Frozen pellets were resuspended in 10 ml of Tris-buffered saline (TBS) pH 7.2 supplemented with 5 µg of lysozyme and 400 µg of DNase I. Suspensions were lysed on a French press (3 cycles at 1,500 psi) and spun down (25,000 x g; 10 min; 4°C) to separate the soluble and insoluble fractions. Pellets were washed in TBS containing 10% BugBuster (Novagen) until the supernatant was clear.

2.6.3. On-column protein refolding

Isolated inclusion bodies were resolubilized in buffer A1 (20 mM Tris-HCl pH 7.7; 500 mM NaCl; 8 M urea) and incubated O/N on a rotating wheel at 4°C. The following day, the supernatant was harvested and applied onto a His-Trap FF column (GE Healthcare). Proteins of interest were

purified on an ACTA Prime (GE Healthcare) by sequential washes in buffer A2 (20 mM Tris-HCl pH 7.7; 500 mM NaCl; 0.1% Triton-X-100), buffer A3 (20 mM Tris-HCl pH 7.7; 150 mM NaCl; 5 mM ß-cyclodextrin), buffer A4 (20 mM Tris-HCl pH 7.7; 150 mM NaCl; 20 mM imidazole) and eluted in buffer B (20 mM Tris-HCl pH 7; 150 mM NaCl; 250 mM imidazole).

2.6.4. Dialysis of purified proteins

Following purification, fractions containing the desired protein were pooled and injected into a Slide-A-Lyzer Dialysis Cassette (Thermo Scientific). Cassettes were allowed to equilibrate in 2 litres pre-chilled buffer (10mM Tris-HCl pH 7.7; 150 mM NaCl) for 6h. Three buffer changes were performed. The resulting samples were concentrated if needed on an Amicon Centrifugal Spin Filter (Millipore) with an appropriate MWCO and analysed *via* SDS-PAGE to assess purity and stability.

2.6.5. BCA assay

Protein concentration was determined using a BCA assay kit (Pierce) according to manufacturer's guidelines. Briefly, BSA standards of known concentrations and purified protein samples were diluted in HBS. Reagents A and B were mixed in a 50:1 ratio, with 180 µl reagent added to 20 µl sample in a 96 well plate. The reaction was incubated at 37°C for 30 minutes and the absorbance read at 595 nm using a Benchmark microplate reader (Bio-Rad). Sample concentration was estimated form the BSA standard curve.

2.7. Protein characterisation assays

2.7.1. S-layer extraction

S-layer extracts were prepared using low pH glycine incubation as described by Wright *et al.* (2005). Briefly, 50 ml overnight cultures of *C. difficile* (OD_{600} 1) were harvested by centrifugation (5,000 x g; 10 min; 4°C). Pellets were washed once with 5 ml sterile PBS, centrifuged as above, resuspended in 0.5 ml of 0.2 M glycine–HCl pH 2.2 and incubated at RT with rotation for 30 min.

Preparations were then centrifuged at 10,000 x g rpm for 15 min at 4 °C. Supernatants were recovered and pH adjusted to pH 6 – 8 with 2 M Tris-HCl. The volume ratios were altered accordingly, depending on the starting volume and optical density of overnight culture.

2.7.2. TCA protein precipitation

C. difficile culture supernatants were harvested by centrifugation (4,000 x g; 10 min; 4°C). Trichloroacetic acid (TCA) was added to a final concentration of 10%. Samples were vortexed briefly, incubated on ice for 30 min and precipitated twice with ice-cold 90% acetone. Protein pellets were incubated at 50°C for 5 min to evaporate any residual liquid and re-suspended to OD_{600} 20 in PBS.

2.7.3. Membrane fractionation

C. difficile was grown O/N, harvested by centrifugation (5,000 x g; 10 min; 4°C) and frozen down at -80°C. Frozen bacterial pellets were re-suspended in PBS containing 1.4 mg/ml lysozyme and 0.12 µg/ml DNaseI to an OD_{600} of 20 and incubated at 37°C for 1 h. Membranes were harvested by centrifugation at 25,000 x g for 10 min at 4°C. The supernatant, containing the soluble cytoplasmic proteins, was removed and mixed with an equal volume of 2 x Laemmli sample buffer (4% SDS, 20% glycerol, 10% 2-mercaptoethanol, 0.004% bromphenol blue, 0.125M Tris-HCl, pH 6.8). The harvested membranes were washed twice with 500 µl PBS, re-suspended in PBS and solubilised with 1% SDS to a final equivalent OD_{600} of 20 and mixed with an equal volume of 2 x Laemmli sample buffer.

2.7.4. Protein cross-linking

200 ml of exponentially growing *C. difficile* cultures was pelleted (5,000 x g; 10 min), washed with 10 ml of PBS and re-suspended in 10 ml PBS containing 0.1% - 1% formaldehyde. The cross-linking reaction was carried out at 37°C for 10 – 60 min and was then quenched by adding 2 ml of 1 M glycine and incubating for 10 min at RT. Cultures were pelleted (5,000 x g; 10 min), freeze-

thawed thrice and re-suspended in 5 mL 1× SMM buffer [0.5 M sucrose; 20 mM $MgCl_2$; 20 mM morpholineethanesulfonic acid (Mes), pH 6.5] supplemented with lysozyme (1.4 mg/ml), amidase (3 µg/ml) and protease inhibitor mixture (1 tablet of cOmplete Mini, EDTA-free (Roche) per 10 ml of buffer). Following 1 h of incubation at 37°C, cultures were pelleted and resuspended in 5 ml buffer H (200 mM NaCl; 1 mM DTT; 100 nM $MgCl_2$; 100 nM $CaCl_2$; 20 mM Hepes, pH 8) supplemented with 5 µg/ml DNase I (Sigma) and 10 µg/ml pre-boiled RNase (Roche). Following 1 h of incubation on ice, the insoluble fraction was pelleted (16,000 x g; 30 min; 4°C) and re-suspended in 2 ml CoIP lysis buffer (50 mM Tris-HCl; pH 7.4, 150 mM NaCl; 1 mM EDTA; 1% (v/v) Triton X-100) and incubated for 30 min on ice. The membrane suspension was cleared of insoluble cell debris *via* centrifugation (16,000 x g; 10 min; 4°C), mixed with 80 µl of anti-FLAG M2 affinity gel (Sigma), pre-equilibrated by in CoIP wash buffer (50 mM Tris-HCl; pH 7.4, 150 mM NaCl; 1 mM EDTA) and incubated O/N at 4°C with agitation. The following day, the samples were applied to a 5 ml gravity flow column (Bio-Rad) and washed thrice with 1 ml CoIP lysis buffer. Flag-tagged protein was eluted with 200 µl FLAG elution buffer (CoIP wash buffer containing 3x FLAG peptide at 150 µg/ml). Residual protein was eluted by washing the column twice with 200 µl CoIP wash buffer. The resulting protein sample was concentrated on an Amicon Ultra Centrifugal Filter Unit (10,000 kDa MWCO) to a volume of 40 µl according to manufacturer's instructions. Concentrated samples were split evenly into two samples, and each sample was mixed with 20 µl 2× Laemmli sample buffer containing 5% (v/v) β-mercaptoethanol. One sample was heated at 90°C for 1 h to break the cross-links, while the other sample was stored on ice. Samples were separated by SDS-PAGE as described below.

2.7.5. SDS-PAGE and Coomassie staining

Protein samples were analysed by electrophoresis under denaturing conditions using polyacrylamide gels in the presence of SDS. 0.75 mm gels were prepared using an acrylamide:bisacrylamide ratio of 29:1 according to standard protocols. Gel percentage was adjusted depending on the size of analysed proteins. Samples were mixed with an equal volume of 2x

Laemmli sample buffer and boiled for 5 min before loading onto the gel. Electrophoresis was carried out in a vertical Mini Protean II apparatus (Bio-Rad) at constant voltage (200 V), until the dye front reached the bottom of the gel. Proteins were stained with Coomassie Blue R-250 (1 h at RT), followed by destaining overnight (40% methanol (v/v), 10% acetic acid (v/v) overnight. Gels were scanned using an Epson Perfection V750 Pro scanner running SilverFast software.

2.7.6. Semi-dry transfer

Following SDS-PAGE, proteins were transferred onto PVDF membranes by semi-dry transfer. The transfer stack was assembled as follows. Two pieces of Whatman 3MM filter paper soaked in Anode buffer I (300 mM Tris-HCl in 10% methanol, pH 10.4), followed by one piece of filter paper soaked in Anode buffer II (25 mM Tris-HCl in 10% methanol, pH 9.4), followed by PVDF membrane wet with methanol, washed with water and soaked in Anode buffer II, followed by the gel soaked in Cathode buffer 40 mM glycine; 25 mM Tris-HCl in 10% Methanol, pH 9.4) followed by three pieces of filter paper soaked in Cathode buffer. Transfer was carried out for 15 min at a constant voltage of 15V. Following transfer, membranes were stained (0.1% Ponceau S (w/v) in 5% acetic acid) to visualise the molecular weight marker, destained in water and dried.

2.7.7. Western blotting

Following protein transfer, membranes were incubated with primary antibodies in 3% skimmed milk in PBS for 1h at RT. After washing the membrane with PBS, HRP-conjugated secondary antibodies were applied in 3% milk in PBS and incubated as above. The membranes were washed with PBS once more and developed using SuperSignal West Pico chemiluminescence substrate. Signal was detected using a Las 4000 imager (Fuji). A complete list of primary and secondary antibodies used throughout this study is provided in Appendix A, Table A4.

2.7.8. Peptide mass fingerprinting

Peptide mass fingerprinting was carried out in its entirety by Dr Len Packman at the Protein and Nucleic Acid Chemistry Facility, University of Cambridge. Following destaining, gels were fixed in 10% MeOH. Gel bands were excised and treated as follows (30 min per step at 20^{o}C in 200 µl 100 mM ammonium bicarbonate/50% acetonitrile). Firstly, samples were reduced with 5 mM tris(2-carboxyethyl)phosphine. Secondly, samples were alkylated by addition of iodoacetamide (25 mM final concentration). Finally, excess liquid was removed and the bands were washed. Gel pieces were dried *in vacuo* for 10min and 25 µl 100 mM ammonium bicarbonate containing 10 µg/ml modified trypsin (Promega). Digestion was carried out for 17h at 32^{o}C. Peptides were recovered and desalted using µC18 ZipTip (MIllipore) and eluted to a MALDI target plate using 2 µl alpha-cyano-4-hydroxycinnamic acid matrix (Sigma) in 50% acetonitrile, 0.1% trifluoroacetic acid. Peptide mass was determined using a MALDI micro MX mass spectrometer (Waters) in reflectron mode and analysed with Masslynx software. Database searches of the mass fingerprint data were performed using Mascot (http://www.matrixscience.com). For tandem MS/MS analysis, desalted peptides in 70% MeOH, 0.2% formic acid were delivered to a ThermoFinnigan LCQ Classic ion-trap mass spectrometer using a static nanospray needle (Thermo Proxeon). Peptide masses of interest were manually selected for fragmentation using manufacturer-recommended settings. Fragment ions were matched to possible sequence interpretations using MS-Product and/or MS-Tag (http://prospector.ucsf.edu/).

2.8. Microscopy

2.8.1. Phase contrast and immunofluorescence microscopy

1 ml of sample was centrifuged at 5,000 x g for 10 min at 4°C, washed with 1 ml of PBS and fixed with 0.5 ml 3.7% formaldehyde in PBS for 15 min at RT. Following fixation, samples were washed with PBS, incubated in 0.5 ml 20mM NH_4Cl for 15 min, washed with PBS once more and

dried onto glass slides. For immunofluorescence microscopy, samples were incubated with primary antibodies (1:20 dilution) in 10% donkey serum for 45 min, rinsed with PBS and incubated with secondary antibodies (1:200 dilution) in 10% donkey serum for another 45 min in the dark. Following a final rinse with PBS, slides were mounted in 3 µl of ProLong Gold Anti-fade reagent (Invitrogen). DNA staining was carried out by adding Hoechst 33258 dye to the mounting medium to a final concentration of 20µg/ml. Images were captured using an Eclipse E600 microscope (Nikon) with a 100x oil immersion lens and a Retiga-400R Charge Coupled Device (Q-Imaging).

2.8.2. Transmission electron microscopy (TEM)

Transmission electron microscopy was done in collaboration with Dr David Goulding (Sanger Institute). Pelleted spores were re-suspended in a freshly prepared primary fixative containing 2% paraformaldehyde and 2% glutaraldehyde in 0.1 M sodium cacodylate buffer (pH 7.4) with added magnesium and calcium chloride at 0.1% and 0.05%, respectively, at RT for 10 min before transfer to an ice bath for the remainder of 2 h. The spores were pelleted again at 5,000 x g and were rinsed three times, for 10 min each time, in sodium cacodylate buffer with added chlorides on ice. Secondary fixation with 1% osmium tetroxide in sodium cacodylate buffer only was carried out at RT for 1 h. All subsequent steps were performed at RT. Spores were rinsed three times in cacodylate buffer over 30 min and were mordanted with 1% tannic acid for 30 min, followed by a rinse with 1% sodium sulfate for 10 min. The samples were dehydrated through an ethanol series of 20%, 30% (staining *en bloc* with 2% uranyl acetate at this stage), 50%, 70%, 90%, and 95% for 20 min at each stage and then were subjected to 100% ethanol three times (for 20 min each time). This step and all subsequent steps were carried out on a rotator to aid infiltration through the spore coat. Ethanol was exchanged for propylene oxide (PO) twice, for 15 min each time, followed by a 1:1 mixture of PO and Epon resin for at least 1 h and undiluted Epon (with a few drops of PO) overnight. The spores were embedded in a flat molded tray with fresh resin and were cured in an oven at 65°C for 24 h. Sections (thickness, 40 nm) were cut on a Leica UCT ultramicrotome, contrasted with uranyl

acetate and lead citrate, and imaged on a 120-kV FEI Spirit BioTWIN transmission electron microscope using an F415 Tietz charge-coupled device camera.

2.9. Microarray analysis

2.9.1. Microarray design

The microarray was constructed by determining all unique genes from the predicted coding sequences of *C. difficile* strains 630, QCD-32g58, 196, R20291 plasmid pCD630. Multiple optimal hybridisation 60-mer oligonucleotide sequences were designed (Oxford Gene Technologies), from which a minimal non-redundant subset of oligonucleotides were selected with a target coverage of three 60-mers per gene. Arrays were manufactured on the Inkjet *in situ* synthesized platform (Agilent) using the 8x15k format.

2.9.2. RNA labelling

5 µg of RNA in 21 µl of nuclease-free water was incubated with 5 µl of random primers for 3 min at 95°C and chilled on ice for 5 min. 24 µl of reaction mixture (10 µl 5x First Strand Buffer; 5 µl 10x dNTPs; 5 µl DTT; 2.5 µl Super Script II (Invitrogen); 1.5 µl Cy3) was added. Samples were incubated for 10 min at 25°C and for 90 min at 42°C and then cleaned-up using the PCR Purification MiniElute Kit (Qiagen) according to manufacturer's guidelines.

2.9.3. DNA labelling

1 µg of gDNA in 26 µl of nuclease-free water was incubated with 5 µl of random primers for 3 min at 95°C and chilled on ice for 5 min. 19 µl of reaction mixture (10 µl 5x buffer, 5 µl 10x dNTPs, 1.5 µl Exo-Klenow, 1.5 µl Cy5) was added. Samples were incubated for 2h at 37°C and then cleaned-up using the PCR Purification MiniElute Kit (Qiagen) according to manufacturer's guidelines.

2.9.4. Hybridization, washing and scanning

9 µl of Cy3-labled cDNA and Cy5-labled gDNA were mixed with 4.5 µl of 10x Blocking Agent and 22.5 µl of Hybridization buffer and incubated for 3 min at 95°C and for 30 min at 37°C. Samples were then applied to a *C. difficile* OGT array CDv2.0.1 (BµG@S) and incubated for 24h in a hybridization oven set to 65°C. The microarray slide was washed for 5 min in wash buffer 1, 1 min in wash buffer 2 pre-heated to 37°C, fixed in acetonitrile for 1 min and dried in Stabilization and Drying Solution for 30 s. Microarrays were scanned using an Agilent G2565CA Scanner.

2.9.5. Data analysis

Microarray data extraction was performed using ImaGene software (BioDiscovery), and further processed using MAVI Pro software (MWG Biotech). Normalization and statistical analysis were performed using GeneSpring v7.3.1 software (Agilent Technologies). Gene specific data was derived from average intensity of between 1 and 5 oligonucleotide reporters. Gene values below 0.01 were set to 0.01. Each gene's measured intensity was divided by its control channel value in each sample; if the control channel was below 10 then 10 was used instead. If the control channel and the signal channel were both below 10 then no data was reported. Each measurement was divided by the 50th percentile of all measurements in that sample. Replicate timepoints were normalized to the 180 minute time point: each measurement for each gene was divided by the median of that gene's measurements in the corresponding control samples. Following the initial experiment covering eight time points (0', 15', 30', 45', 60', 90', 120' and 180'), two additional biological replicates were carried out for time points 30', 60', 90' and 180'. Each time point was independently tested versus 180 min using 1-way ANOVA using Benjamini-Hochberg multiple testing correction and p=0.01 or 0.05.

2.9.6. Accession numbers

The array design (CDv2.0.1) is deposited in BmG@Sbase (Accession No. A-BUGS-49; http://bugs.sgul.ac.uk/A-BUGS-49) and ArrayExpress (Accession No. A-BUGS-49). Fully annotated microarray data have been deposited in BmG@Sbase (accession number E-BUGS-145; http://bugs.sgul.ac.uk/E-BUGS-145) and also ArrayExpress (accession number E-BUGS-145).

2.10. Transposon mutagenesis and TraDIS

2.10.1. Plasmid construction

Plasmid pRPF215 used to create a transposon mutant library in *C. difficile* was designed and constructed in its entirety by Dr Robert Fagan. Briefly, codon-optimised *Himar1* hyperactive C9 transposase (Lampe *et al*., 1999) was cloned into pRPF177, a plasmid carrying the inducible Ptet promoter but lacking a transcriptional terminator directly downstream of *tetR* gene. The *Mariner*-based transposon was generated by PCR amplifying the *ermB* gene from pMTL82254 and adding a transcriptional terminator and the transposon inverted terminal repeats (ITRs) in successive PCR reactions. The resulting DNA fragment was cloned downstream of the transposase giving pRPF215.

2.10.2. Library construction

Plasmid pRPF215 was conjugated into *C. difficile* 630Δ*erm* as described above. Pure transconjugant colonies were used to inoculate 5 ml O/N cultures in TY broth supplemented with 15 µg/ml thiamphenicol. These were sub-cultured the following morning, grown to OD 0.3 and spread out on pre-reduced BHIS agar supplemented with 5 µg/ml erythromycin and 100 ng/ml anhydrotetracycline (ATc) to allow for *Himar1*-mediated transposition (150 square Petri dishes [120mm x 120mm] were used). Following O/N incubation colonies were scraped of in TY broth and the resulting culture (input library) was used to inoculate 20 ml nutrient-rich TYG broth supplemented with 5 µg/ml erythromycin and 100 ng/ml ATc. The following day the resulting culture was sub-cultured 1:10 in 20 ml SM broth supplemented with 5 µg/ml erythromycin and 100 ng/ml

ATc, grown to OD 0.6 and spread out on SM agar plates to induce sporulation. Spores were harvested and purified as described above (spore library) and incubated O/N in BHIS broth supplemented with 0.5% Tch to allow for spore germination and outgrowth (germinated library).

2.10.3. Transposon-Directed Insertion Site Sequencing (TraDIS)

TraDIS was carried out at the Wellcome Trust Sanger Institute. Briefly, genomic DNA was extracted from the three and fragmented to an average size of 300bp using Covaris Focused-Ultrasonicator. Illumina sequencing adapters were ligated, according to the manufactures instructions and purified using Ampure XP beads. Fragments containing the transposon were PCR enriched using transposon and adapter-specific primers to enrich for transposon containing fragments. The PCR products were purified before being quantified by qPCR. Single end sequencing was performed on the enriched fragments using an Illumina Hiseq 2500 sequencer.

2.10.4. Data analysis

TraDIS data analysis was carried out in its entirety by Dr. Christine Boinett and Dr. Amy Cain at the Wellcome Trust Sanger Institute as described in Myho *et al*. (in press). Briefly, approx. two million reads per samples were generated. Illumina FASQ files containing 50 bp reads were parsed for 100% identity to the transposon. The tags were stripped from the resulting reads and mapped back onto their corresponding references using SMALT-0.7.2 and the precise insertion site of the transposon was determined.

2.11. Phenotypic assays

2.11.1. Sporulation efficiency assay

C. difficile O/N cultures were sub-cultured to OD_{600} 0.1 in fresh, pre-reduced medium, allowed to reach logarithmic growth phase (OD ~ 0.6) and sub-cultured once more to OD_{600} 0.1. These were then used to inoculate 10 ml of fresh, pre-reduced medium in order to synchronise the

culture and minimise the amount of spores carried over from the initial culture. Upon reaching stationary phase (T_0) 0.5 ml samples were taken, 10-fold serial dilutions were prepared and spotted in triplicate onto BHIS agar + 0.1% Tch (total counts). For spore counts, samples were incubated at 70°C for 30 min, prior to dilution. Colonies were enumerated after 24h of incubation at 37°C under anaerobic conditions. In addition, in order to differentiate between germination and sporulation defects the entire experiment was monitored *via* phase-contrast microscopy.

2.11.2. Spore chemical resistance assay

Purified *C. difficile* spores were re-suspended in 5 ml of sterile water, 70% EtOH, lysozyme solution (250 µg/ml), 1% Virkon or 1% ParaSafe to OD_{600} 0.1. At given time points 0.5 ml samples were taken, centrifuged at 10,000 x g for 1 min, washed with 1 ml of sterile water and re-suspended in 0.5 ml of sterile water. 10-fold serial dilutions were prepared and 20 µl drops were spotted in triplicate onto BHIS agar + 0.1% Tch. Colonies were enumerated after 24h of incubation at 37°C under anaerobic conditions.

2.11.3. Spore thermal resistance assay

Purified *C. difficile* spores were re-suspended in 1 ml of sterile water to OD_{600} 0.1 and incubated at 60°C, 70°C or 80°C for 24h. At given time points, 10-fold serial dilutions were prepared and 20 µl drops were spotted in triplicate onto BHIS agar + 0.1% Tch. Colonies were enumerated after 24h of incubation at 37°C under anaerobic conditions.

2.11.4. Germination dynamics assay

Purified *C. difficile* spores were re-suspended in 10 ml of BHIS + 0.5% Tch to OD_{600} 1. The gradual drop in OD_{600} due to Ca^{2+}-DPA release was monitored over time and expressed as relative OD_{600} (OD_{600} t_x/OD_{600} t_0). In addition, for each time point 0.5 ml samples were taken, 10-fold serial dilutions were prepared and spotted in triplicate onto BHIS agar + 0.1% Tch (total counts). For spore

counts, samples were incubated at 70°C for 30 min, prior to dilution. Colonies were enumerated after 24h of incubation at 37°C under anaerobic conditions. The germination process was additionally monitored *via* phase contrast and fluorescence microscopy as described in paragraph 8.1.

2.11.5. Swimming motility assay

Swimming motility was assessed by inoculating a plate of 0.3% BHIS agar with 1 µl of O/N culture. Growth was monitored over 96 h. The non-motile *C. difficile* 630 Δ*erm fliC::erm* strain was used as a negative control.

2.11.6. Capsule staining

O/N cultures of *C. difficile* were mixed 1:1 with 1% (w/v) aqueous Congo Red and dried onto a poly-L-lysine-coated glass slide. Slides were flooded with modified Maneval Solution (3.0 g of ferric chloride; 5% (v/v) acetic acid; 3.9 ml of phenol; 95 ml of distilled water) and incubated for 5 min at RT. Excess liquid was blotted, slides were gently washed with water, dried, mounted in water and imaged as described in paragraph 8.1.

2.12. Bioinformatics

Routine operations on DNA and protein sequences including sequence visualisation, sequence alignment, sequencing result analysis, *in silico* cloning and creation of plasmid maps were carried out using Geneious 5.6.5 (Biomatters). Protein parameters including molecular weight and isoelectric point calculation as well as prediction of hydrophobic regions and secondary structure were done using tools from the ExPASy website (http://www.expasy.ch/tools). Signal peptide predictions were done using SignalP (http://www.cbs.dtu.dk/services/SignalP/) or LipoP (http://www.cbs.dtu.dk/services/LipoP/). Bacterial promoter regions were predicted using Softberry BPROM (http://www.softberry.com). Primers for Gibson Assembly vectors were designed using

NEBuilder (http://nebuilder.neb.com/). TraDIS plots were viewed using Artemis (http://www.sanger.ac.uk/resources/software/artemis/).

Chapter III

Characterisation of *C. difficile* 630 sporulation and germination dynamics

3.1. Introduction

It is well established that sporulation efficiency can vary greatly depending on the choice of growth medium (Errington, 1993). While the mechanism of *B. subtilis* sporulation has been well characterised over the years and the optimal conditions for spore development have been described (Schaffer *et al*, 1965), a molecular description of the sporulation mechanisms of *C. difficile* has been lacking and the precise conditions for optimal *C. difficile* sporulation remain to be elucidated. As a consequence, even though reproducible methods for preparing *B. subtilis* spores and measuring sporulation efficiency have been known for a number of years, there have been few published examples of using these methods to study sporulation in *C. difficile* and the ones that have been published vary significantly from study to study in the methodologies used (reviewed in Burns and Minton, 2011). To date, brain-heart infusion (BHI) has been the most commonly used medium for inducing *C. difficile* sporulation, used neat or supplemented with 0.1% L-cysteine and 0.5% yeast extract (BHIS) (Sorg and Sonenshein, 2008, Sorg and Sonenshein, 2009, Sorg and Sonenshein, 2010, Burns *et al*., 2010b, Burns *et al*., 2010a, Underwood *et al*., 2009). In other studies, trypticase peptone sporulation medium (SM) more commonly known as Wilson's broth has been suggested as an optimal medium for inducing *C. difficile* sporulation (Lawley *et al*., 2009, Wilson, 1983, Wilson *et al*., 1982, Deakin *et al*., 2012, Pereira *et al*., 2013). Germination has also been extensively studied in *B. subtilis* and the signals known to stimulate germination of *B. subtilis* spores have been well described (reviewed in Setlow, 2003). Yet, at the onset of this study, only the bile salt taurocholate together with glycine have been strongly linked to stimulating germination of *C. difficile* spores, improving spore recovery on solid media (Wilson *et al*, 1982; Wilson, 1983).

In the first part of this chapter I set out to establish a platform for studying sporulation in *C. difficile* and the phenotypic analysis of sporulation-deficient mutants. A number of *C. difficile* sporulation methods have been tested and the corresponding sporulation efficiency has been assessed in order to establish the optimal conditions for large scale spore production. Spore purification methods have been optimised to facilitate the rapid removal of cell debris and vegetative cells from sporulated cultures and the properties of the resulting spore preparation have been analysed. Finally, in the second part of this chapter the optimal germination conditions for *C. difficile* spores have been assessed in preparation for transcriptional analysis of temporal gene expression patterns during germination and outgrowth. Some of the results presented here have been published in Dembek *et al*. (2013) and are referenced accordingly.

3.2. Results

3.2.1. Identification of conditions suitable for efficient *C. difficile* sporulation

As part of preliminary work leading up to studying germination in *C. difficile*, an efficient method for producing large quantities of spores had to be developed. To this end, previously existing sporulation protocols were refined and optimized to ensure reproducible results and the highest possible yields. *C. difficile* 630 (*tcdA+*, *tcdB+;* PCR ribotype 012) a virulent, multidrug-resistant, epidemic strain was chosen for our analysis as its full genome sequence has been published (Sebaihia *et al*., 2006) and its culture under laboratory conditions has been well defined.

Sporulation was induced through nutrient starvation in BHI broth, BHIS broth or SM broth and its efficiency was assessed over a period of 5 days by measuring the number of colony forming units (CFU) on agar plates after incubation at 70°C for 30 min. The rationale for this approach is that only spores will survive heat treatment and the colonies recovered on plates are therefore representative of spores within the population. By comparing the number of spore CFUs to the number of total CFUs obtained from samples that were not heat-treated, one can assess the dynamics of sporulation and its efficiency. In addition, at each time point, spore formation was

monitored *via* phase contrast microscopy. As O/N cultures of *C. difficile* may contain varying amounts of spores, in order to minimise potential spore carry-over and the resulting bias in spore counts, starter cultures were sub-cultured twice and grown to stationary phase (t0) prior to starting the experiment.

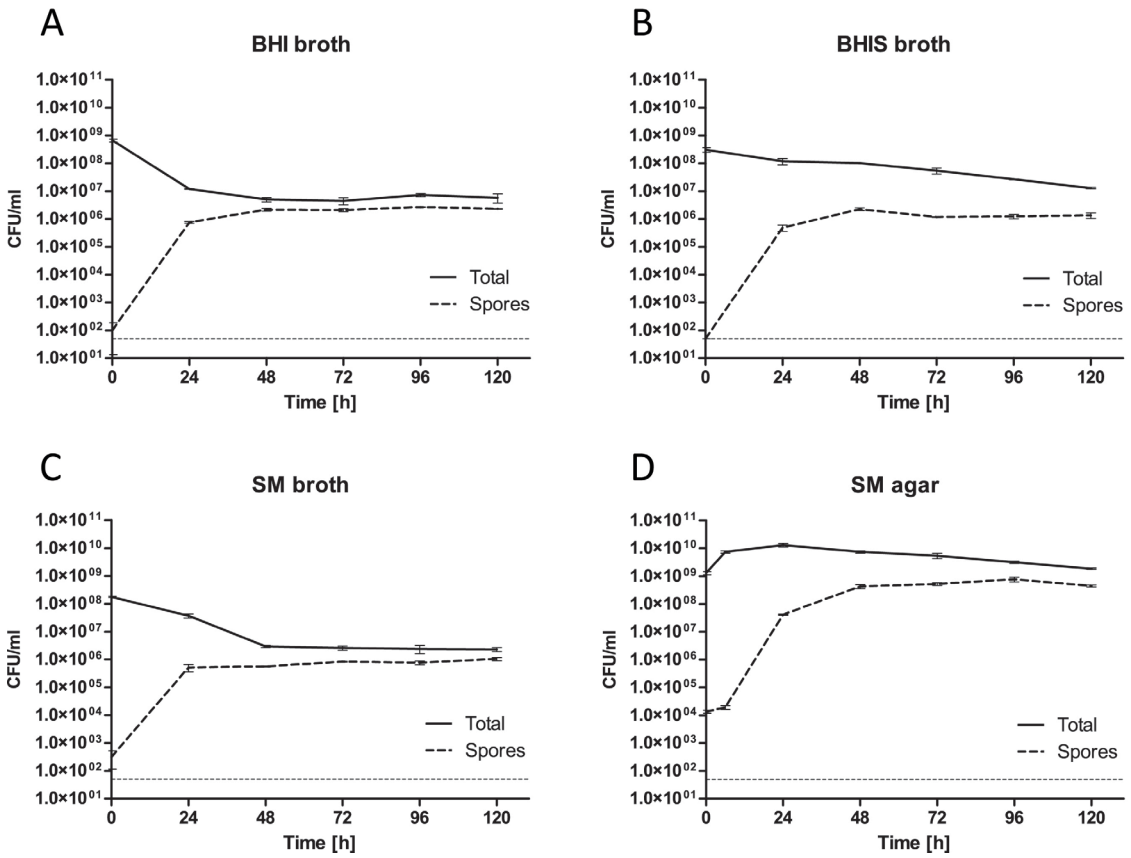

Figure 3.1. *C. difficile* 630 sporulation efficiency in liquid media and on solid media. O/N cultures of *C. difficile* 630 were sub-cultured to OD 0.01 in **(A)** BHI broth, **(B)** BHIS broth, **(C)** SM broth, grown to exponential phase and sub-cultured once more in order to prevent spore carry-over. At given time points, 10-fold serial dilutions were prepared and spotted in triplicate onto BHIS agar supplemented with 0.1% Tch. Colonies were enumerated following 24h of incubation in an anaerobic cabinet. For spore counts, samples were heat-treated at 70°C for 30 min before diluting. **(D)** O/N cultures of *C. difficile* 630 were sub-cultured in SM broth, grown to exponential phase and plated onto SM agar plates. At given time points, growth from each plate was scraped off in 1 ml of sterile PBS, 10-fold serial dilutions were prepared and spotted in triplicate onto BHIS agar supplemented with 0.1% Tch. Colonies were enumerated following 24h of incubation in an anaerobic cabinet and expressed as CFU/ml of initial SM broth culture at t_0. Data represented as means ± SD from three biological replicates. Limit of detection is marked with a horizontal dotted line.

As shown in Figure 3.1, no heat-resistant CFUs could be detected at the onset of the experiment (t0). This number grew to approx. 5 x 10^5 CFU/ml within the first 24h. Irrespective of the medium used, maximum spore yields were detected within 48h and remained relatively constant reaching a maximum of 2.68 x 10^6 CFU/ml in BHI, 2.25 x 10^6 CFU/ml in BHIS and 1.05 x 10^6 CFU/ml in SM (Figure 3.1A, 3.1B and 3.1C). This corresponds to a sporulation efficiency of 0.4%, 0.73% and 1.66% for BHI, BHIS and SM respectively, expressed as max spore CFU recorded throughout the experiment/total CFU at t0.

Phase contrast microscopy of the sporulating liquid cultures revealed that while the typical morphological stages of spore formation could be observed throughout the experiment, a vast majority of cells lysed within 24 hours from initiation of sporulation (t0) (Figure 3.2). This suggests that only a subset of the initial population would eventually undergo sporulation, possibly explaining the relatively low sporulation efficiency described above. Furthermore, even though a vast majority of the population sporulated within 24-48h from initiation, the process was highly asynchronous as single, sporulating cells could be seen even five days into the experiment. This underlines the heterogeneity of bacterial population in regards to sporulation, a phenomenon previously reported in *B. subtilis* (Chung and Stephanopoulos, 1995, Grossman, 1995, Veening *et al*., 2005).

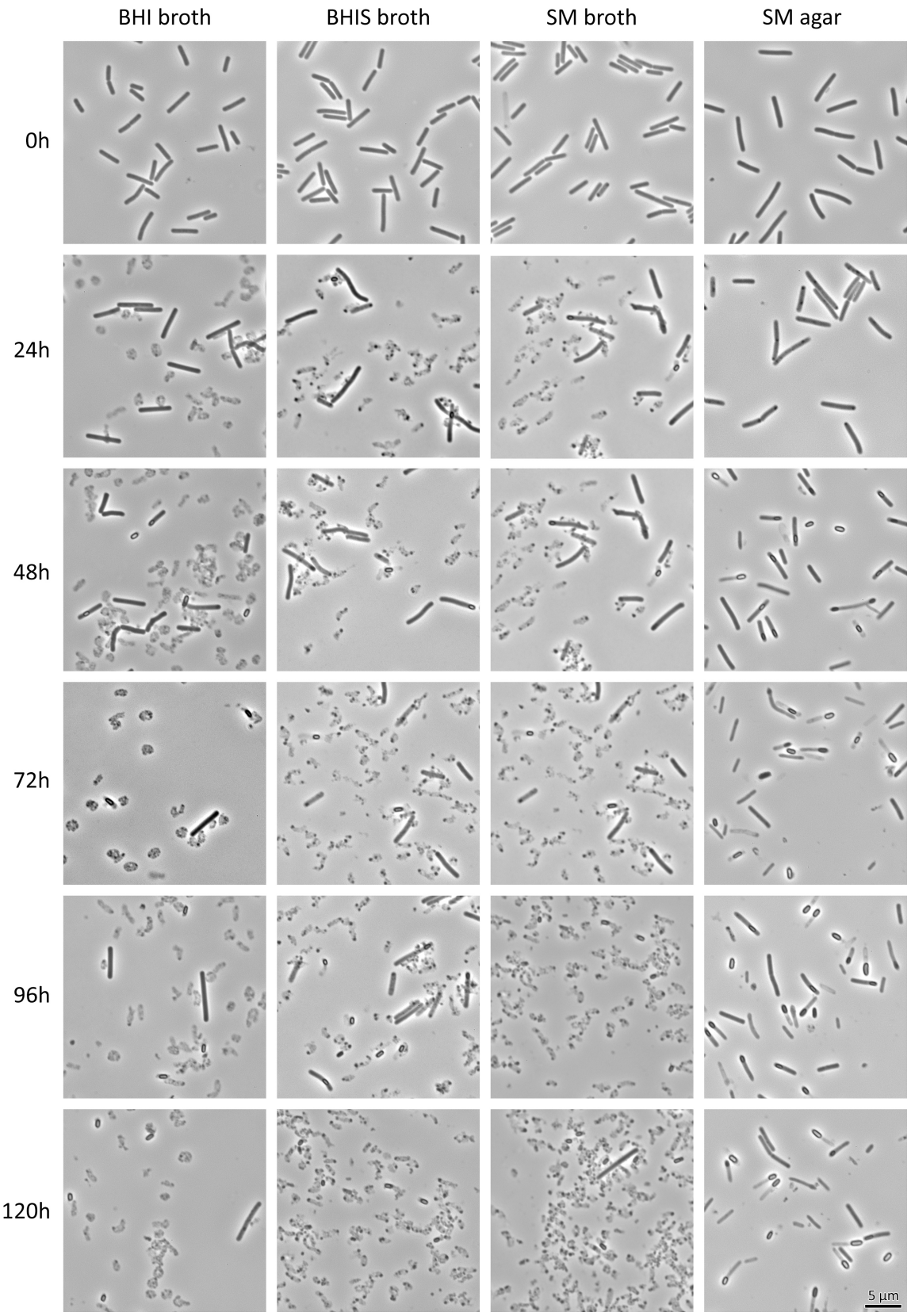

Figure 3.2. Phase contrast microscopy of sporulating *C. difficile* 630. Sporulating cultures were harvested at given time points, fixed with 3.7% formaldehyde and dried onto glass slides. Significant cell lysis can be observed in BHI broth, BHIS broth and SM broth but not SM agar. Fully developed, phase-bright spores are visible in all cultures. Microscopy data representative of three biological replicates. Scale bar provided.

In order to overcome the low sporulation efficiency observed in liquid media, a combination of nutrient starvation and desiccation on solid medium was employed (Permpoonpattana *et al*., 2011, Putnam *et al*., 2013). In this method, starter cultures grown in nutrient medium (TGY broth) are sub-cultured into minimal medium (SM broth), allowed to reach exponential growth phase, plated onto SM agar and incubated for 5-7 days. At given time points, the growth from each plate was re-suspended in sterile PBS and the number of total and heat-resistant spore CFUs was measured and expressed as CFU/ml of initial SM broth culture at t_0. As previously, maximum spore yields were observed within 48h and reached 7.76 x 10^8 CFU/ml corresponding to a sporulation efficiency of 59.38%, a 2-log increase when compared to results obtained in liquid culture (Figure 3.1D). Importantly, when compared to sporulating liquid cultures, significantly less lysis was observed. SM agar was therefore used in subsequent experiments as the optimal method for producing *C. difficile* spores.

3.2.2. Spore purification

Transcriptional analysis of germination would require spore preparations of the highest purity, free of vegetative cells and residual cell debris as these could interfere with downstream analysis. To this end, a protocol for purifying spores had to be developed. While a number of such methods have been published (Lawley *et al*., 2009, Permpoonpattana *et al*., 2011), most involve the use of detergents, lysozyme and sonication in order to separate spores from cell debris. Such harsh treatment could potentially disrupt the outer layers of the spore and in result affect its ability to germinate. Therefore a more gentle protocol based on density gradient centrifugation was adapted. The purity of the resulting spore suspension was confirmed using phase contrast microscopy, revealing mature, phase-bright spores, free of vegetative cells and cell debris (Figure 3.3A and 3.3B). Transmission Electron Microscopy (TEM) analysis of the purified spores revealed the typical spore ultrastructure observed in other Gram-positive sporeformers, with concentric layers corresponding to the inner core surrounded by a primordial germ cell wall, a thick cortex and an electron-dense

proteinacious coat (Figure 3.3C and 3.3D). A closer examination revealed further details of this layer, including laminations resembling the striated outer coat of *Bacillus* spores. An additional, fragmented layer, most probably corresponding to the exosporium could also be observed, loosely associated with the spore coat, consistant with previous observations of *C. difficile* spores (Permpoonpattana *et al*., 2011).

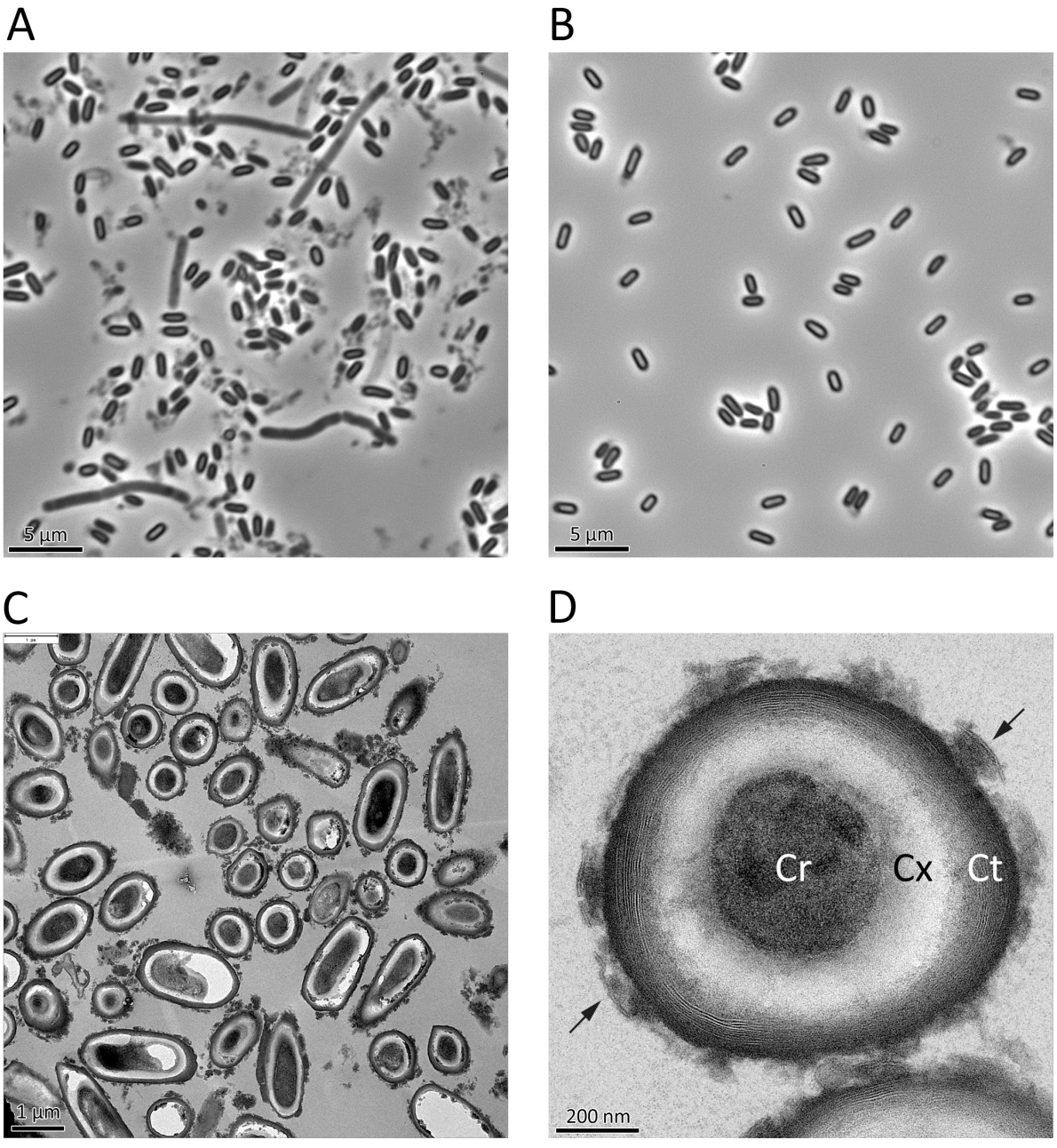

Figure 3.3. Phase contrast and TEM images of *C. difficile* 630 endospores. (A) Crude spore preparation contaminated with vegetative cells and cell debris**. (B)** Spore preparation after purification containing phase-bright endospores, free of contaminants **(C and D)** TEM images of spore ultrasections. Concentric layers corresponding to the spore core (Cr), cortex (Cx) and coat (Ct) can be observed. Arrows indicate fragments of putative exosporium basal layer loosely associated with the outer coat. Scale bars provided.

3.2.3. Characterisation of spore resistance to environmental stresses

Due to their multi-layered structure, spores are resistant to most chemical and physical insult including extremes of temperature and pH, high pressure, irradiation, desiccation, enzyme action as well as a variety of noxious chemicals (reviewed in Setlow, 2006). In order to confirm that the purification process has not detrimentally affected the integrity of the spore, heat and chemical resistance was assessed. Previous studies have shown that *C. difficile* spores are able to survive incubation at 60-80°C for 10-30 min without loss of viability (Burns *et al*., 2010a). Indeed, when incubated at temperatures below 80°C, no significant changes in spore viability were observed up to 24 hours into the experiment. In contrast, spores incubated at 80°C showed a gradual decrease in viability with a 2-log decrease at 4 hours, 4-log decrease at 8h and complete loss of viability at 24h into the experiment (Figure 3.4A). As expected, neither ethanol nor lysozyme treatment had any noticeable effect on spore viability. Interestingly, Virkon, an oxidant-based, multi-purpose disinfectant used in hospitals, laboratories and nursing homes was only marginally effective in killing *C. difficile* spores, with a 2-log decrease in spore viability 2 hours into the experiment. In contrast, PERAsafe® (0.2% paracetic acid) originally developed as a safer alternative to 2% activated glutaraldehyde, with documented activity against spores, showed the highest efficiency in spore killing out of all the chemicals tested, as no viable spores could be detected 90 min after exposure (Figure 3.4B). Taken together these results show that (i) purified spores show the same level of thermal and chemical resistance as indicated previously in literature and that (ii) Virkon does not show sufficient sporicidal activity to be used against *C. difficile* spores as reported previously by Dawson *et al*. (2011).

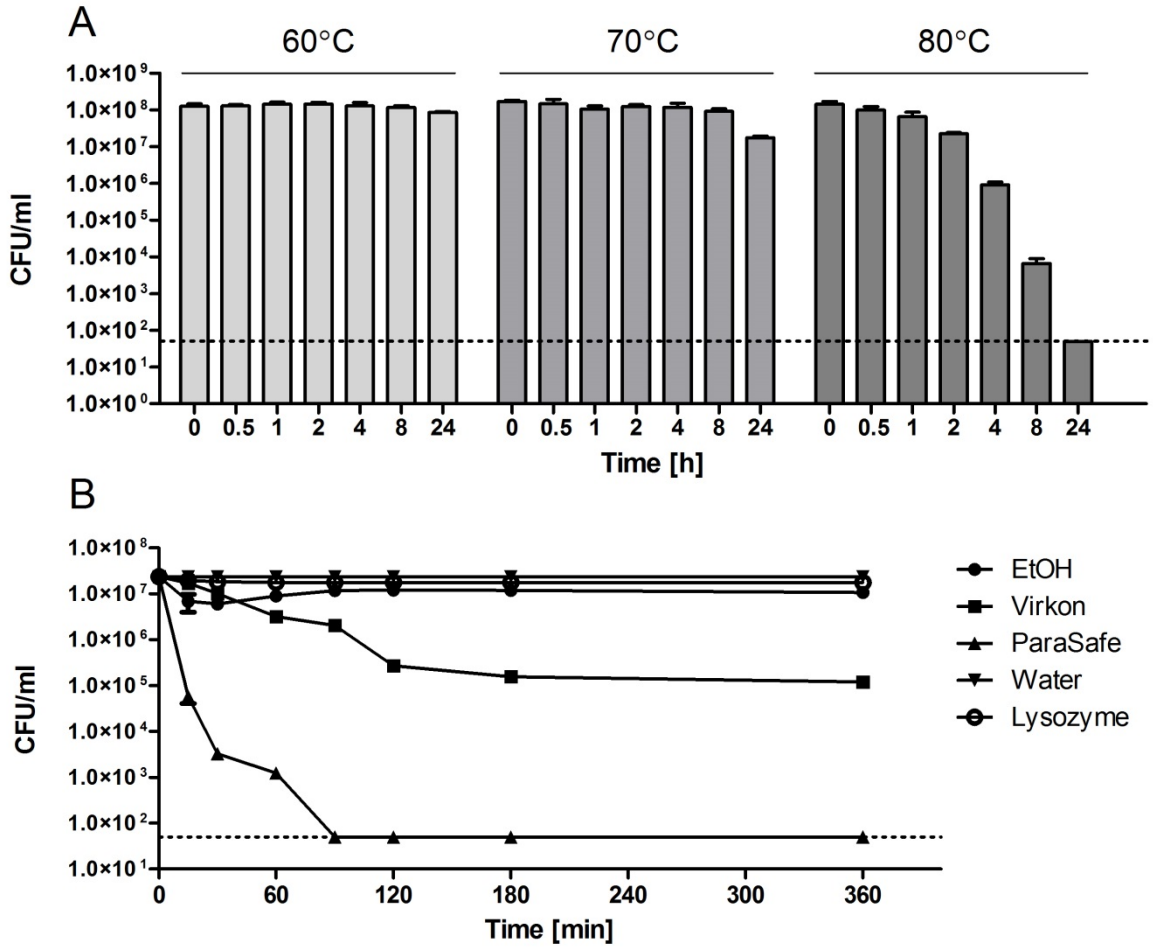

Figure 3.4. *C. difficile* 630 spore thermal and chemical resistance. Purified spores (1 x 10^8) were resuspended in 1ml sterile water and **(A)** incubated for 24 hours at 60°C, 70°C or 80°C, **(B)** resuspended in 1ml sterile water, 70% EtOH, lysozyme in PBS (250µg/ml), 1% Virkon or 1% PERASafe™. The viability of heat treated or chemically treated spores was assessed at given time points by measuring spore CFUs following plating of 10-fold serial dilution in triplicate onto BHIS agar supplemented with 0.1% Tch. Data represented as means ± SD from thre technical replicates. Limit of detection indicated as a horizontal dashed line.

3.2.4. Characterisation of spore germination dynamics

In order to carry out a transcriptional analysis of the temporal gene expression during germination, it was first necessary to gain more insight into the dynamics of the process. To this end, the time required for germination, the morphological changes that accompany it and the optimal conditions for germination were analysed. Spore germination is typically measured as a drop in optical density (OD) of a spore suspension, resulting from an alteration to the spore's optical properties, that occurs with the release of dipicolinic acid (DPA) from the spore core (Setlow, 2003). This is then followed by an increase in $OD_{600,}$ correlated with outgrowth and cell division as the cells re-enters vegetative growth. OD_{600} measurement of liquid cultures containing germinating *C. difficile* 630 spores, combined with total/spore CFU counts and phase-contrast microscopy revealed that >99.9999% of the spore population undergoes germination when grown in nutrient medium (BHIS) supplemented with the germinant, sodium taurocholate (Tch) as indicated by a rapid decrease in OD_{600} (approx. 50% of initial value within 5 minutes of induction) and a 5-log drop in the number of recovered spore CFUs (Figure 3.5A and 3.5C). Importantly, basing on phase contrast and fluorescence microscopy analysis, spore germination in nutrient medium supplemented with an excess of Tch (0.5%) was largely synchronous and appeared to be complete within 180 min from induction. This would be critical in subsequent transcriptomic analysis of gene expression during germination as it ensured that the population was in the same phase of germination. No significant difference in germination was observed between cultures incubated in the presence of 0.1%, 0.5% and 1% of Tch (data not shown).

Microscopic analysis revealed that immediately upon induction of germination, the dormant spores lost their phase-bright appearance and increased in volume, presumably due to Ca^{2+}-DPA release and subsequent rehydration of the spore core, resulting in increased susceptibility to Hoechst 33258 DNA staining (0 - 30 min). This was followed by hydrolysis of cortex peptidoglycan, breakdown of the outer spore layers on one of the cell poles and shedding of the empty coat 'shell' during outgrowth (45-60 min). Upon removal of these 'physical constraints', germinating cells

entered a phase of longitudinal growth, coinciding with DNA replication, and followed by symmetric cell division (60-180 min) (Figure 3.6A and 3.6B). In contrast, spores grown in medium devoid of the germinant failed to germinate, as no changes in OD_{600}, spore CFU count or spore morphology could be observed throughout the 6h incubation period (Figure 3.5A and 3.5D; Figure 3.6D). Interestingly, no germination was observed when liquid cultures were incubated aerobically, presumably due to the inhibitory presence of oxygen. Even though a decrease in OD_{600} and spore CFUs was observed immediately after induction with Tch, and the spores lost their phase-bright appearance (indicative of Ca^{2+}-DPA release and core rehydration), becoming susceptible to DNA staining, progression to outgrowth was not observed. These compromised spores were eventually killed, as indicated by the gradual drop in total CFUs (Figure 3.5A and 3.5C; Figure 3.6C). This is consistent with recent findings (Nerandzic and Donskey, 2010) and suggests that oxygen is a negative regulator of *C. difficile* endospore germination acting downstream of any signalling events that induce germination.

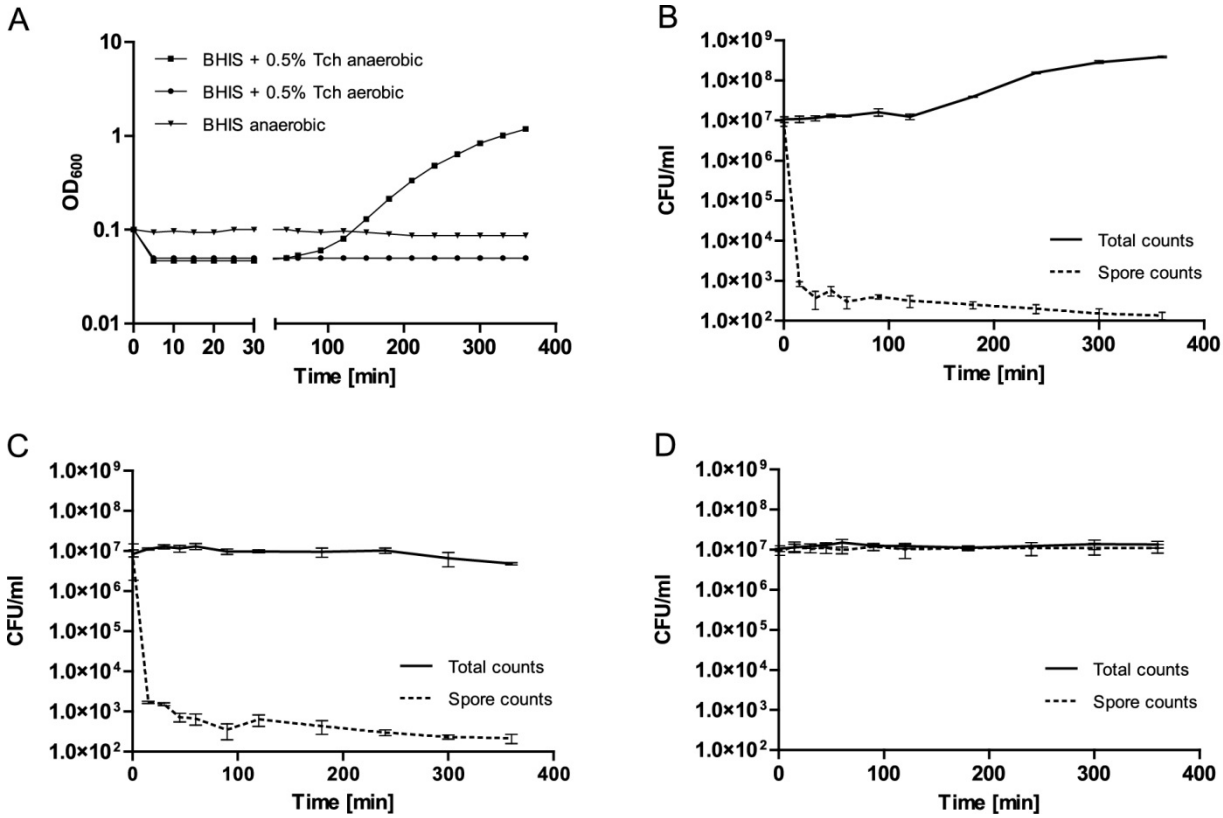

Figure 3.5. Growth characteristics during spore germination and outgrowth. Purified *C. difficile* 630 spores were resuspended in BHIS ± 0.5% sodium taurocholate (Tch) to an OD_{600} of 0.1 and incubated either aerobically or anaerobically for 6 h at 37°C. Growth was monitored *via* OD_{600} measurements and total/spore CFU counts. **(A)** *C. difficile* 630 germination dynamics growth curve. Spores incubated in the presence of 0.5% Tch showed a rapid decrease in OD_{600} immediately after re-suspension, in both aerobic and anaerobic conditions. No decrease in OD_{600} was observed for spores incubated in the absence of Tch. **(B)** CFU counts for spores germinated anaerobically in BHIS + 0.5% Tch. **(C)** CFU counts for spores germinated aerobically in BHIS + 0.5% Tch. **(D)** CFU counts for spores germinated anaerobically in BHIS. Data reported as mean ± SD from three biological replicates. Previously published in Dembek *et al*. (2013).

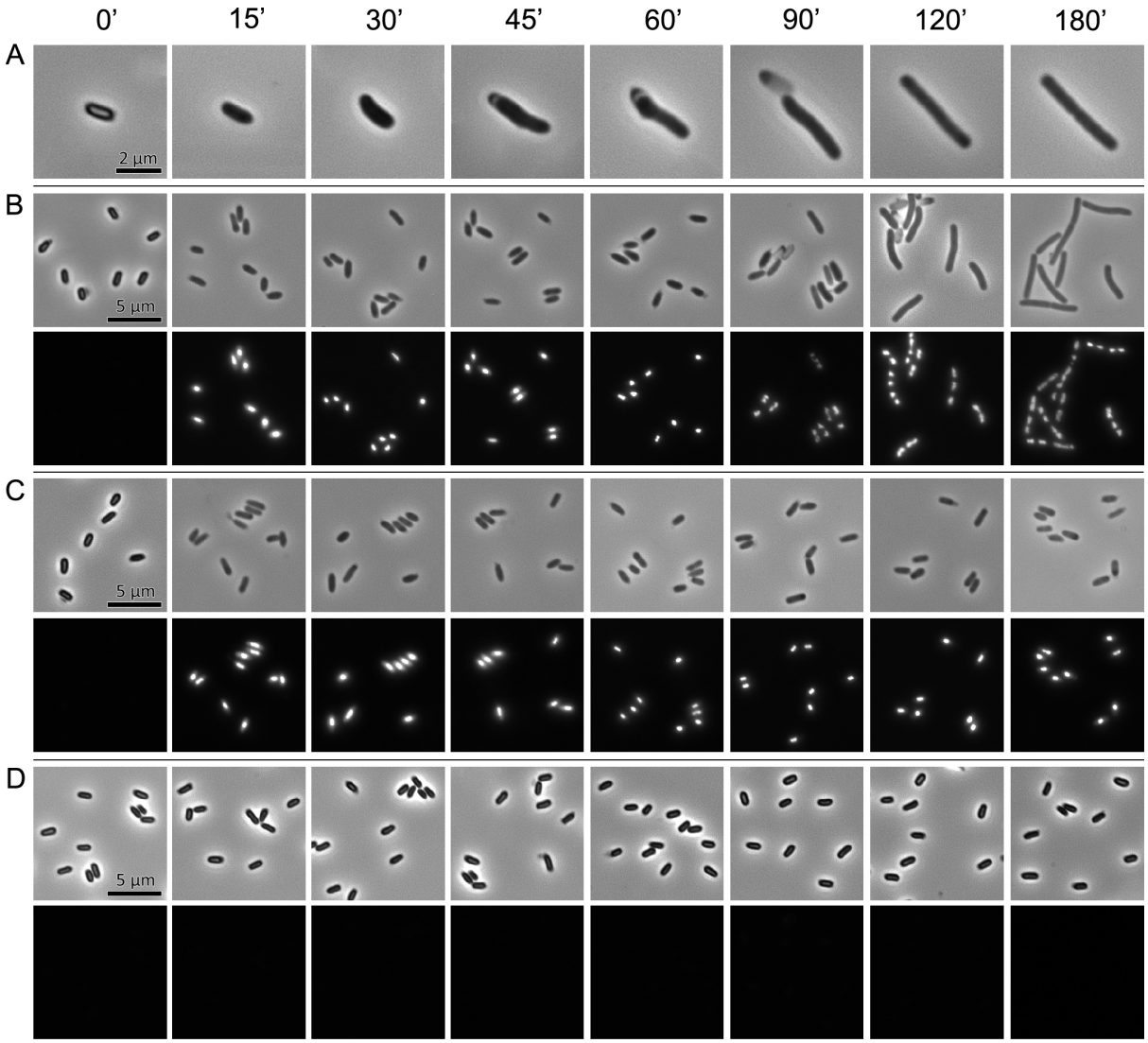

Figure 3.6. Morphological changes during spore germination and outgrowth. Purified *C. difficile* 630 spores were re-suspended in BHIS ± 0.5% sodium taurocholate (Tch) to an OD_{600} of 0.1 and incubated either aerobically or anaerobically for 6 h at 37°C. At given time points, samples were fixed with 3.7% formaldehyde and analysed using phase contrast microscopy and fluorescence microscopy following DNA staining with Hoechst 33258. **(A)** and **(B)** Spores germinated anaerobically in BHIS +0.5% Tch. Upon induction of germination, dormant spores lose their phase-bright appearance and become susceptible to DNA staining. This is followed by a gradual increase in volume and shedding of spore outer layers which remain visible as empty ‘shells’. Once the physical constraints of the outer spore layers are removed, the spore enters a phase of longitudinal growth coinciding with DNA replication followed by symmetric cell division. **(C)** Spores germinated aerobically in BHIS +0.5% Tch. Following induction of germination, spores lose their phase-bright appearance and become susceptible to DNA staining but fail to progress to outgrowth. **(D)** Spores germinated anaerobically in BHIS. No changes in spore appearance and no DNA staining could be observed. Previously published in Dembek *et al*. (2013).

3.3. Discussion

While our understanding of sporulation and germination in the model organism *B. subtilis* is well grounded in years of research, studies aimed at understanding the molecular basis of sporulation and germination in *C. difficile* have been lagging behind, primarily due to the difficulties in culturing the pathogen, the lack of established methodologies and the scarcity of genetic tools necessary for studying the intricacies of *C. difficile* physiology. Here, an attempt was made to create a platform for the analysis of sporulation and germination in *C. difficile*, and the phenotypic characterisation of mutants with sporulation and/or germination defects.

One of the primary goals was to establish a reproducible method for sporulating *C. difficile*. Considering the low sporulation efficiency in liquid culture and the significant cell lysis observed irrespective of the medium used, neither of the sporulation methods described to date seems to be optimal for efficient sporulation of *C. difficile* strains. While gradual desiccation on solid media increases spore yields and makes sporulation more homogeneous, sporulation efficiency is still significantly lower that than that seen in *B. subtilis*, suggesting that further optimisation of sporulation methods is necessary. Density gradient centrifugation proved to be a viable alternative to more complex methods of spore purification that require the use of detergents, enzymes and sonication, yielding spore suspensions free of noticeable contaminants. Importantly, an in-depth analysis of the purified spores revealed that their general characteristics including spore ultrastructure and their resistance to heat, chemicals and lysozyme were no different than those described for *B. subtilis* spores.

Analysis of germination dynamics confirmed that *C. difficile* spores respond to the bile salt sodium taurocholate (Tch) as the primary germinant and that anaerobic conditions are essential for the completion but not initiation of germination as spores stimulated with Tch in the presence of oxygen did lose their phase-bright appearance but failed to progress through the remaining stages of germination. This is intriguing as in *B. subtilis*, once induced, spores are committed to continue through germination even if the germinant is removed (Yi and Setlow, 2010). The dynamics of the

germination process were significantly different than those previously described for the closely related *C. botulinum* (Broussolle *et al*., 2002) and *C. sporogenes* (Bassi *et al*., 2013) where initiation of germination was found to be a much slower process. Importantly, basing on phase contrast and fluorescence microscopy analysis, spore germination in nutrient medium supplemented with an excess of Tch was largely synchronous and appeared to be complete within 180 min from induction. This is somewhat surprising as germination in *Bacillus* species, as well as the more closely related *C. perfringens* and *C. botulinum* has been shown to be highly heterogeneous (Ghosh and Setlow, 2009, Ghosh and Setlow, 2010, Stringer *et al*., 2005, Wang *et al*., 2011), with a sub-population of spores failing to germinate immediately upon exposure to germinants. This phenomenon of 'superdormancy' has been correlated with a low level of specific germination receptors in individual spores (Ghosh *et al*., 2012) and is thought to be an example of 'bet hedging', ensuring the survival of a given population in a rapidly changing environment. Under the conditions tested 99.9999% of the *C. difficile* 630 spore population germinated synchronously. This might be a reflection of the unique germination mechanism present in *C. difficile* and/or the fact that the human gut is a relatively stable environment eliminating the need for super-dormancy.

Taken together, results presented in this chapter have provided further insight into the physiology of sporulation and germination in *C. difficile*, laying down the groundwork for the transcriptional analysis of the temporal gene expression patterns during germination and an in-depth characterisation of sporulation and germination deficient mutants presented in subsequent chapters of this thesis.

Chapter IV

Transcriptional analysis of temporal gene expression in germinating *C. difficile* 630 endospores

4.1. Introduction

Determination of the complete *C. difficile* genome sequence (Sebaihia *et al*., 2006) was a turning point in *C. difficile* research, paving the way for comprehensive genetic analysis of the pathogen's physiology. The first studies of Clostridial gene expression using microarray platforms (Alsaker and Papoutsakis, 2005, Jones *et al*., 2008, Tomas *et al*., 2003) were instrumental in the characterisation of the cell cycle, particularly in the context of sporulation. While transcriptomic analysis of gene expression during germination has been carried in *B. subtilis (*Keijser *et al.,* 2007*)* and more recently *C. novyi-NT* (Bettegowda *et al*., 2006) and *C. sporogenes (*Bassi *et al.,* 2013*)*, no such studies have been attempted in *C. difficile.*

To address this issue, in this chapter I describe the use of genome-wide transcriptome analysis to explore the physiological, morphological, and transcriptional changes that occur during three continuous steps of *C. difficile* 630 *in vitro* life cycle: spore dormancy, germination and outgrowth of vegetative cells, trying to elucidate some of the metabolic changes that occur during the transformation of a dormant spore into an actively growing vegetative cell. Results presented in this chapter have been published in Dembek *et al.* (2013) and are referenced accordingly.

4.2. Results

4.2.1. Optimisation of RNA extraction

RNA quality is of paramount importance in any transcriptional analysis of gene expression. While a number of well-defined RNA extraction methods are available, allowing researchers to choose the most suitable protocol for a particular application, working with spores entails a new set

of challenges. This is largely due to their robust characteristics and the resulting difficulties in disrupting the protective layers of the spore, necessitating the use of extremely harsh lysis conditions which can jeopardise RNA quality. It was therefore critical to develop a method for extracting RNA that would not only be able to penetrate the spore outer layers and provide high recovery rates, but would also ensure that the integrity of RNA was maintained. A number of methods were tested. Mechanical disruption with silica beads followed by acid phenol-based extraction was shown to give the highest quality RNA, reproducibly yielding between 2 and 10 µg of total RNA per 10^8 spores. The amount of extracted RNA coincided with the status of the spore, increasing gradually as the spores went from dormancy, through germination to outgrowth (Figure 4.1A). This could be explained by the increasing susceptibility of the spore envelope to lysis during germination and/or the initiation of RNA synthesis (Setlow, 2003). All RNA preparations were of high purity and integrity as indicated by a 260/280nm absorption ratio in the range of 2.05 to 2.18 and Bioanalyzer electropherograms showing sharp peaks suggesting little RNA degradation (Figure 4.1B and 4.1C). Interestingly, distinct differences in the ribosomal RNA (rRNA) profiles of spores and vegetative cells were observed. In addition to the 16S and 23S rRNA species, two smaller rRNA species were identified in dormant spores, represented by small peaks on Bioanalyzer spectra (Figure 4.1C). These could only be discerned in dormant spores and reduced in intensity as germination progressed. A similar phenomenon has been previously reported in *Bacillus* (Keijser *et al*., 2007) as well as the more closely related *Clostridium novyi* (Bettegowda *et al*., 2006) and *Clostridium sporogenes* (Bassi *et al*., 2013), although its significance remains to be elucidated. One could argue that these smaller species might represent rRNA fragments or be indicative of RNA maturation within the germinating spore (Bleyman and Woese, 1968).

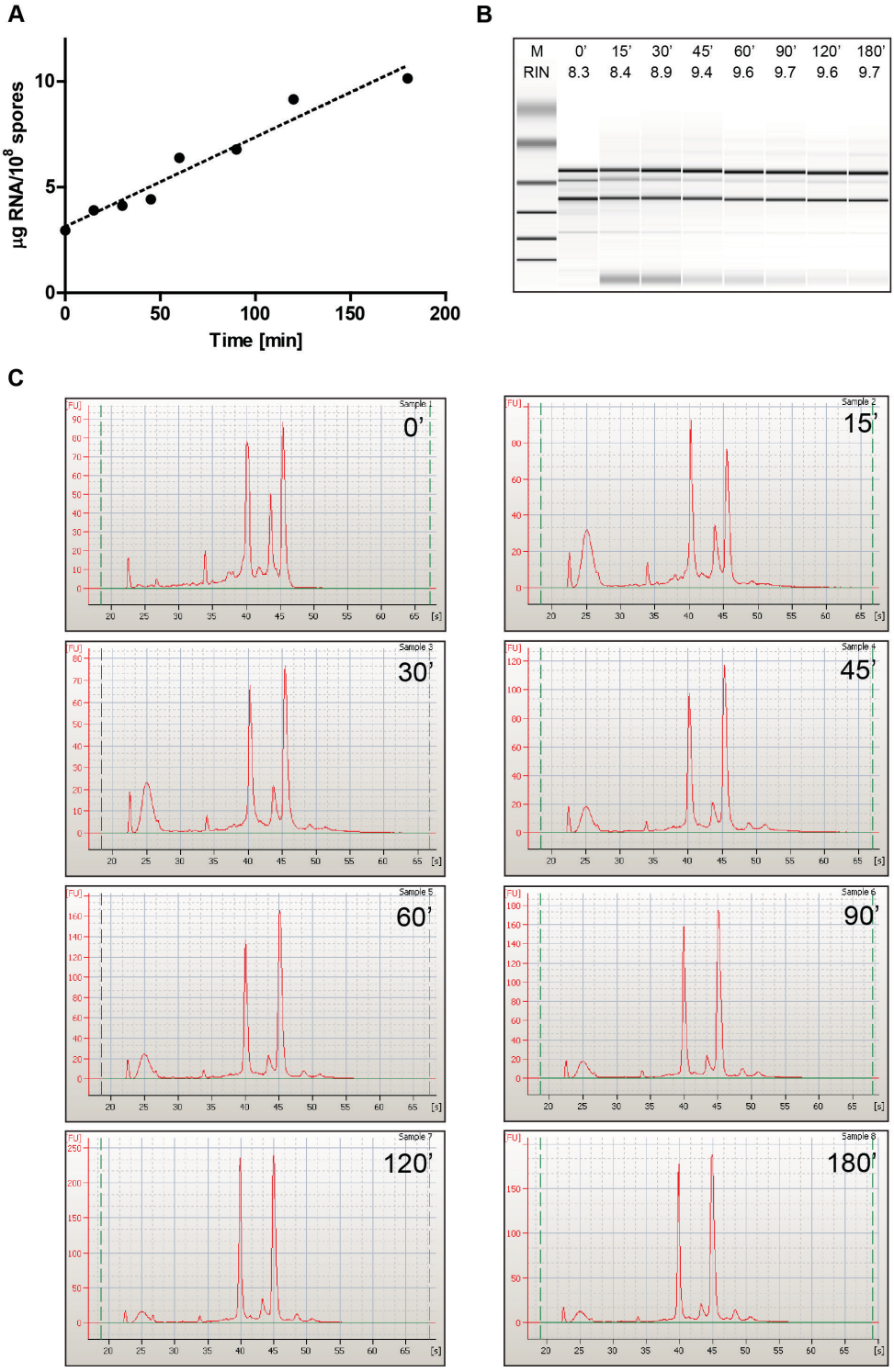

Figure 4.1. RNA extraction and quality control. (A) Gradual increase in RNA recovery observed during spore germination. **(B)** Bioanalyzer pseudogel with RNA integrity number (RIN) values **(C)** Bioanalyzer electropherograms showing two distinct peaks corresponding to 16S and 23S rRNA. In addition, two smaller rRNA species were identified in dormant spores and in early germination, represented by small peaks on Bioanalyzer spectra. 5S rRNA peak visible at retention time 23 seconds. Previously published in Dembek *et al.* (2013).

4.2.2. Microarray analysis

4.2.2.1. Experimental design and general observations

Total RNA samples extracted from germinating spores at eight time points representing dormancy (0 min), germination (15, 30, 45, 60 min) and outgrowth (90, 120, 180 min) were analysed by competitive RNA/DNA hybridisations using the CDv2.0.1 microarray designed and manufactured by the Bacterial Microarray Group at St. George's (BμG@S). The microarray experiment itself, including sample preparation, hybridisation and scanning was carried out at the London School of Hygiene and Tropical Medicine (LSHTM) in collaboration with Dr. Richard Stabler and Prof. Brendan Wren.

Gene expression was found to be highly dynamic during germination and outgrowth, involving a large part of the genome. Relatively few transcripts were identified in dormant spores (see below), consistent with their metabolically dormant state. In contrast, a significant up-regulation of gene expression was observed immediately after induction of germination, peaking at 30 min (Figure 4.2). Two time points were chosen for further investigation: 30 min, when all spores are actively germinating, and 180 min post germination, when normal vegetative growth has commenced. In total, 263 genes were up-regulated and 248 genes down-regulated at 30 min when compared to the 180 min time point ($p \leq 0.01$). The magnitude of change of the statistically up-regulated genes ranged from 1.3-fold to 80-fold, and that of down-regulated genes ranged from 1.3- to 100-fold (Figure 4.2). Fully annotated microarray data have been deposited in BμG@Sbase (accession number E-BUGS-145; http://bugs.sgul.ac.uk/E-BUGS-145) and also ArrayExpress (accession number E-BUGS-145). In addition, lists of up- and down-regulated genes ($p \leq 0.01$) with a minimum of 2-fold change in expression are included in Appendix B, Table B1 and B2 respectively.

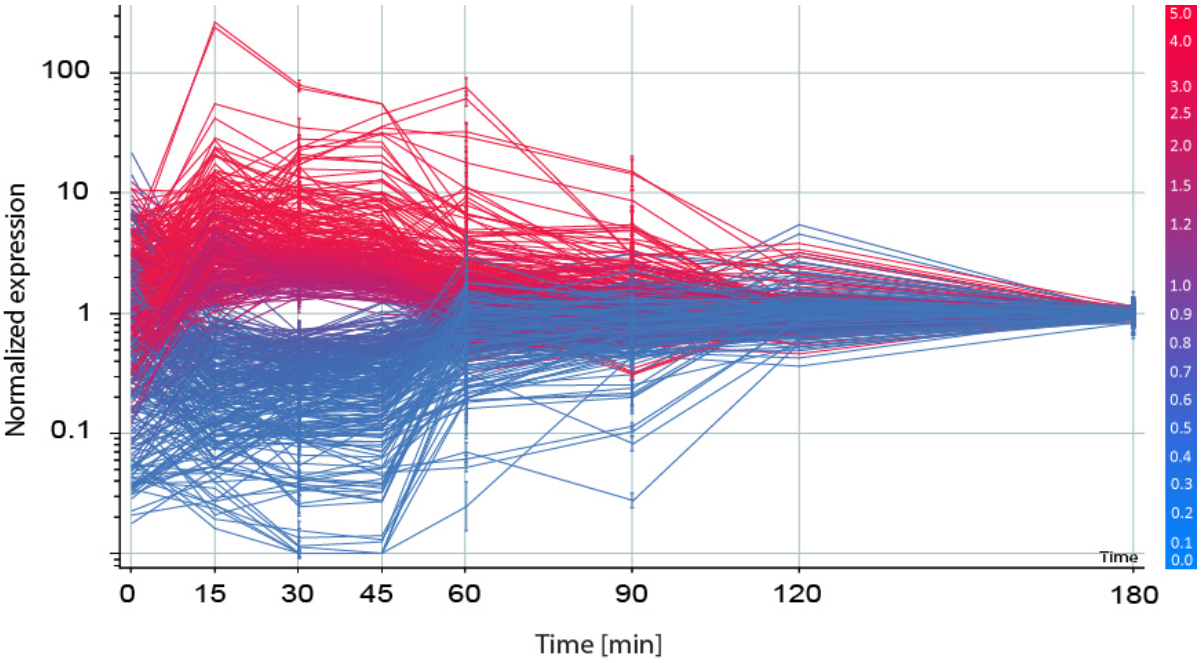

Figure 4.2. **All genes differentially expressed during germination**. Microarray gene expression data represented as normalised intensity with respect to control conditions. 511 genes were found to be differentially regulated at 30 min into germination when compared to a vegetative cell (180 min). Data represented as means ± SD from three biological replicates. Analysed using 1-way ANOVA with Benjamini-Hochberg false discovery rate (FDR) correction ($p \leq 0.01$). Previously published in Dembek *et al.* (2013).

4.2.2.2. Microarray validation

Array-based experiments are prone to artifacts which can be introduced at any stage of the procedure. Large datasets generated through measurements of gene expression profiles using microarray technology can thus be difficult to interpret and always require validation. Under most circumstances this has to be done on a gene-to-gene basis, as *in silico* confirmation is often not possible due to lack of previously published results. In order to validate the microarray data obtained in this study, semi-quantitative RT-PCR was used to confirm the temporal expression pattern for a number of selected genes showing a wide range of distinct expression profiles. These included genes encoding cell wall binding proteins: Cwp7 and Cwp10, the two toxins TcdA and TcdB and a putative membrane protein. In all cases, the expression profiles obtained matched those seen throughout the microarray experiment (Figure 4.3).

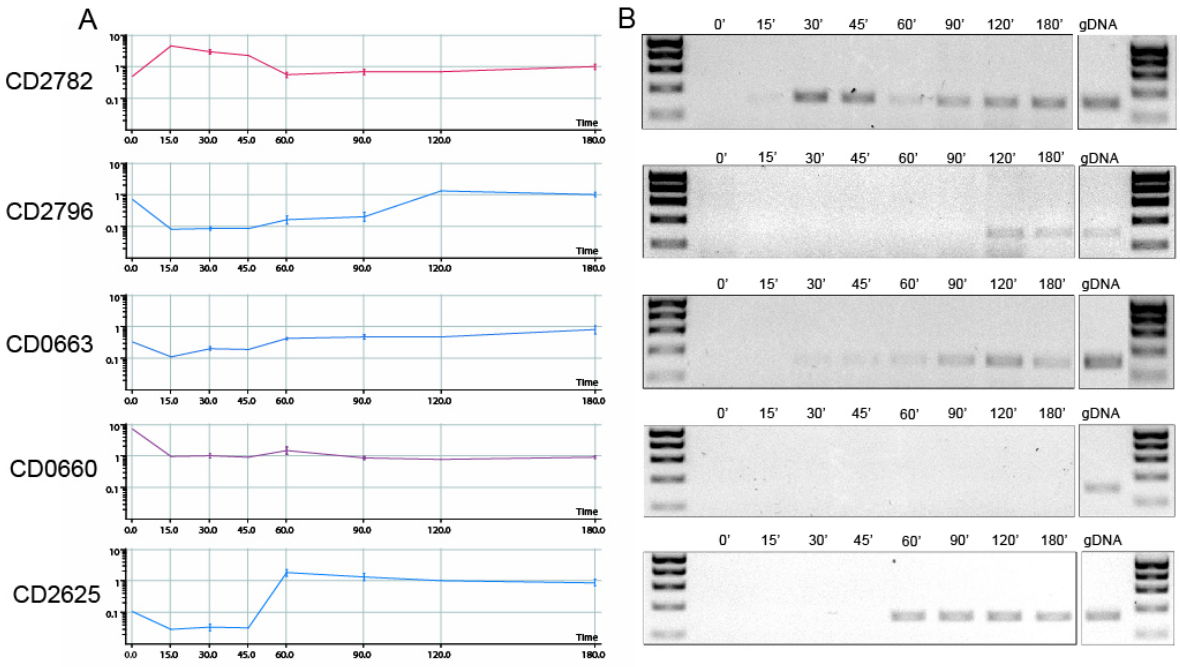

Figure 4.3. RT-PCR validation of microarray results. cDNA was prepared from total RNA using reverse transcription. Primers internal to five selected genes were used to amplify fragments of 150 bp: (CD2782 - cell wall binding protein, CD2796 - cell wall binding protein, CD0663 - toxin A, CD0660 - toxin B, CD2625 - putative membrane protein). *C. difficile* 630 gDNA was used as a positive control reaction. 25 reaction cycles were carried out to ensure non-saturating conditions. **(A)** microarray expression profiles (normalised to 180 minutes), **(B)** agarose gel electrophoresis of the PCR-amplified DNA fragments. Previously published in Dembek *et al.* (2013).

4.2.2.3. Spore transcripts

Despite early research hinting at the presence of mRNA in spores (Chambon *et al*., 1968, Jeng and Doi, 1974), until recently it has been generally assumed that dormant spores do not contain functional RNA transcripts. This view has now changed as studies conducted in *B. subtilis* (Keijser *et al*., 2007), *C. novyi-NT* (Bettegowda *et al*., 2006) and *C. sporogenes* (Bassi *et al*., 2013) have all shown that mRNA is abundant in spores and that its composition differs from that observed in vegetative cells. A number of explanations for this phenomenon have been suggested. Spore transcripts might represent mRNA that has been entrapped in the forespore during the late phases of sporulation and is later degraded to act as a reservoir of nucleotides during germination. Indeed, six out of fifteen most abundant spore transcripts identified in this study represented late-sporulation genes such as those encoding a putative spore coat protein (CD0213), small acid-soluble proteins A and B (CD2688 and CD3249 respectively) and a stage IV sporulation protein (CD0783), while the second most abundant transcript encoded a putative Mn-dependent superoxide dismutase (CD1631), an orthologue of SodA found in *B. subtilis*, involved in oxidative cross-linking of spore coat proteins during the late stages of spore morphogenesis (Henriques *et al*., 1998, Permpoonpattana *et al*., 2011). Alternative explanations argue that transcripts might be stored to equip the spore with proteins that will become necessary during the transformation into a vegetative cell, such as those involved in metabolism, protein synthesis and secretion, transport, detoxification etc. One such group of transcripts present at relatively high levels in dormant spores were those involved in redox reactions, including an NADH oxidase (CD2540), an NADH-dependent flavin oxidoreductase (CD2709) as well as two putative oxidoreductase complexes with ferrodoxin activity (CD2197-CD2199A and CD2427-CD2429A). The inclusion of such a large number of redox genes within the spore transcriptome is intriguing, particularly in the light of the anaerobic life cycle of *C. difficile*. While *C. difficile* spores are resistant to ambient oxygen concentrations, even short exposure to oxygen can kill vegetative cells. It would thus be tempting to speculate that at least a subset of these genes might play a role in detoxification by scavenging reactive oxygen species (ROS).

Finally, consistent with previous reports (Bettegowda *et al*., 2006), we found that a large proportion of spore transcripts encode proteins of unknown function (nine out of top fifteen hits). This not only underlines the difference in mRNA composition between spores and vegetative cells but also the need for more research into the spore transcriptome of major spore-forming bacteria. A list of the top 50 spore transcripts found in this study is included in Appendix B, Table B3.

4.2.2.4. Functional analysis

Many gene clusters encoding enzyme complexes or biochemical pathways and identified as differentially expressed during germination appeared to be co-ordinately regulated. In order to dissect these interactions and obtain a more precise image of the metabolic changes that accompany germination and outgrowth, a functional analysis of the microarray data was performed. To this end the Kyoto Encyclopedia of Genes and Genomes (KEGG) database was used to identify differentially regulated genes and organise them according to metabolic pathways they take part in. Selected examples have been listed below and summarised in Table 4.1. Where appropriate, genes that marginally failed the stringent statistical cut-off ($0.01 \leq p \leq 0.05$) are also mentioned.

Functional group	Up-regulated	Down-regulated
Two-component systems	26	5
ABC-transporters	71	34
Phosphotransferase system	11	30
Ribosomal proteins	12	1
Transcriptional regulators	45	24
Flagellum and chemotaxis	0	34
Type IV pili	0	7
Peptidoglycan biosynthesis	9	1
Secondary cell wall polymers	12	0

Table 4.1. Numbers of genes differentially regulated during germination. The total number of genes within specific functional groups up-regulated or down-regulated at 30 min into germination was determined using microarray analysis ($p \leq 0.05$). Previously published in Dembek *et al.* (2013).

4.2.2.4.1. Two-component signal transduction systems

Two-component regulatory systems serve as a basic stimulus-response coupling mechanism to allow organisms to sense and respond to changes in many different environmental conditions. They typically consist of a membrane-bound histidine kinase that senses a specific environmental stimulus and a corresponding response regulator that mediates the cellular response, mostly through differential expression of target genes (reviewed in Stock *et al*., 2000). *C. difficile* 630 has fifty-one two-component sensor histidine kinases and fifty-four response regulators. Nine kinase genes and seventeen response regulator genes were up-regulated in germinating spores. Only five genes (three kinases and two response regulators) were down-regulated (Figure 4.4).[more about how spores sense the environment]

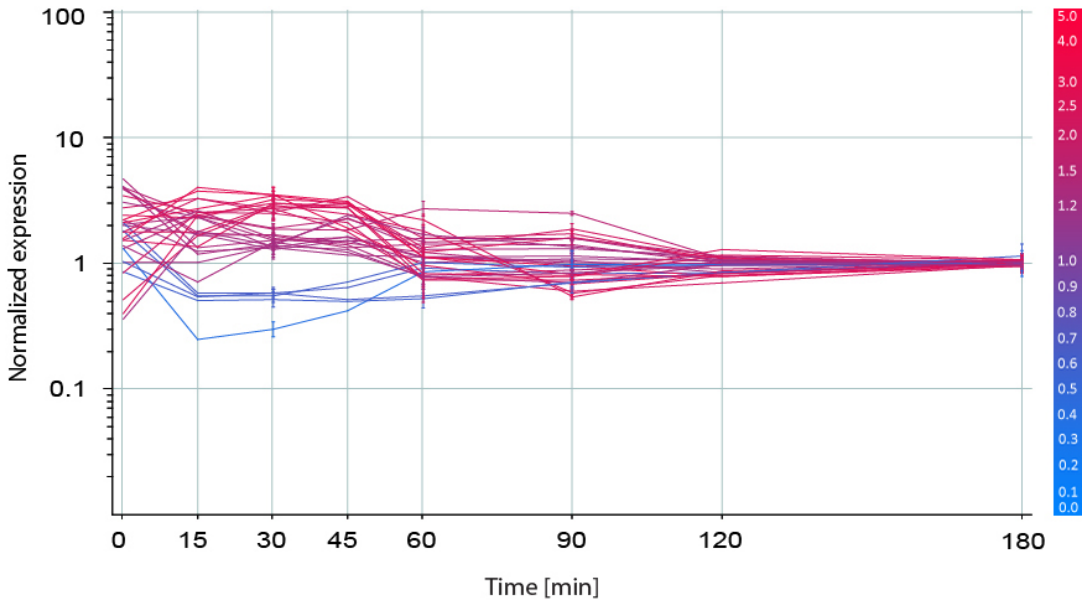

Figure 4.4. **Two-component signal transduction system genes differentially regulated during germination.** 26 genes were up-regulated regulated while 5 genes were down-regulated at 30 min into germination when compared to a vegetative cell (180 min). Gene expression data represented as normalised intensity with respect to control conditions, as means ± SD from three biological replicated. Analysed using 1-way ANOVA with Benjamini-Hochberg false discovery rate (FDR) correction($p \leq 0.05$). Previously published in Dembek *et al.* (2013).

4.2.2.4.2. Transport of metabolites and sugars

Re-establishment of cell metabolism in a germinating spore requires a large supply of metabolites and cofactors. Consistent with this requirement, 100 out of 229 ABC-transporter genes contained within the *C. difficile* 630 genome were found to be differentially regulated during germination. A majority of these (71 genes) were up-regulated during germination when compared to the vegetative state, including the *appABC* operon (peptide/nickel ABC-transporter), the entire *potABCD* locus (spermine/putrescine ABC-transporter), and the *ssuABC* operon (sulfonate/nitrate/taurine ABC-transporter). Other ABC-transporters that had at least one significantly up-regulated gene included maltose/maltodextrin ABC-transporter (9.5-fold), lactose/L-arabinose ABC-transporter (13.6-fold) and iron complex ABC-transporter (2.6-fold). In contrast, two ABC-transporter complexes involved in cobalt and nickel transport and encoded by the *cbiMNOQ* operon were down-regulated (Figure 4.5A).

The PTS system is a complex phosphate translocation mechanism involved in the transport of sugars such as glucose, mannose and mannitol. As such it plays a key role in cell metabolism driving glycolysis. Unlike ABC-transporters, sugar transport was largely inactive during germination with the entire branch of the system responsible for glucose trafficking significantly down-regulated (from 1.9- to 23.8-fold) in germinating spores when compared to vegetative cells, including members of the *pstG-ABC* operon. In contrast, a number of genes involved in fructose and lactose metabolism were up-regulated in germinating spores. These included CD2270 (putative 1-phosphofructokinase; 79.8-fold), *fruABC* (fructose-specific phosphotransferase; 75.2-fold) and CD1806 (putative fructokinase; 2.8-fold) (Figure 4.5B). While this could simply reflect the composition of the culture medium, it could also indicate the preference for fructose as the main carbon source in early germination.

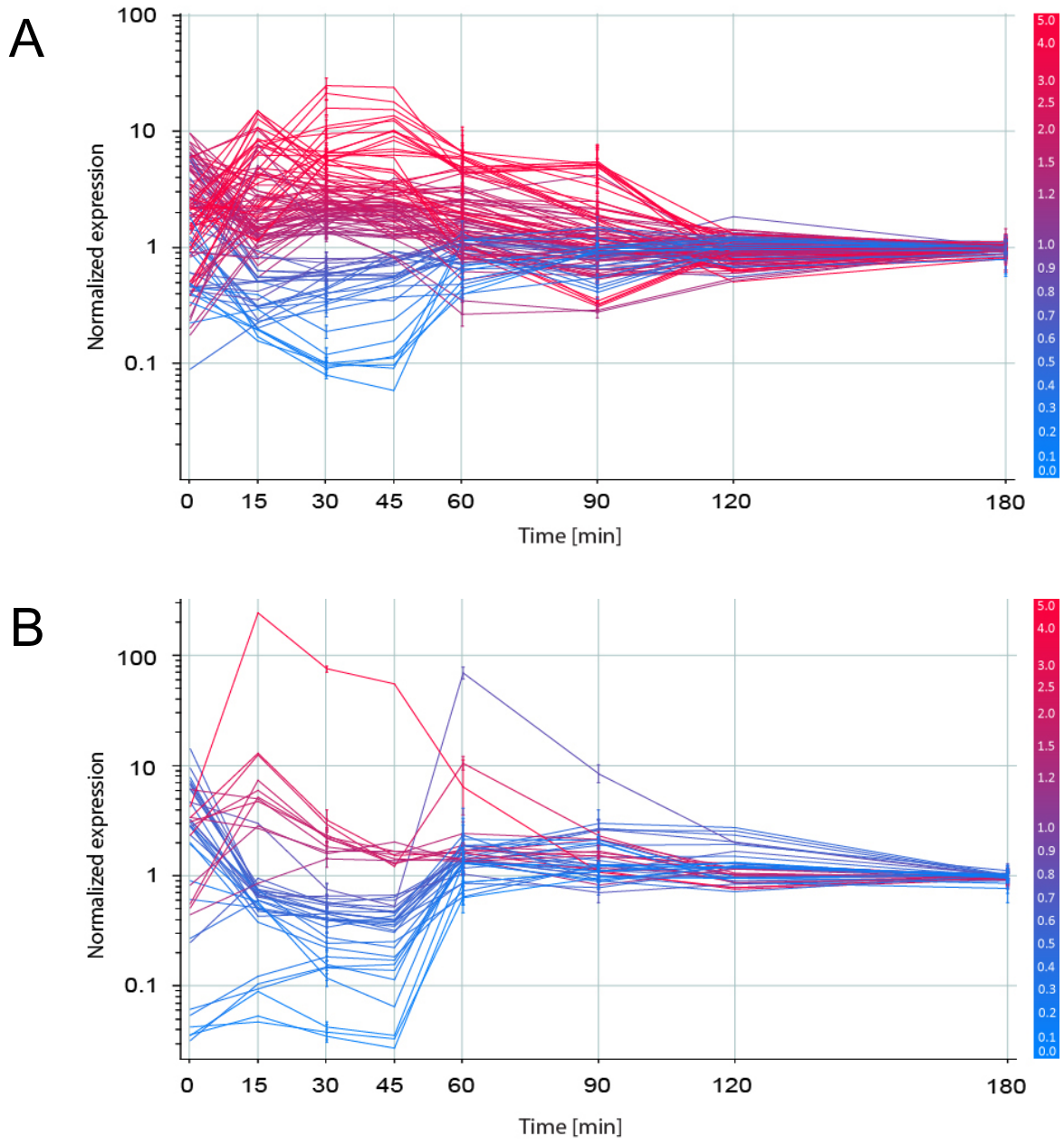

Figure 4.5. **Genes involved in transport and metabolism of sugars differentially regulated during germination. (A)** 71 genes encoding ABC-transporters were up-regulated while 29 were down-regulated at 30 min into germination when compared to a vegetative cell (180 min). **(B)** 13 genes involved in the PTS system were up-regulated while 30 were down-regulated at 30 min into germination when compared to a vegetative cell (180 min). Gene expression data represented as normalised intensity with respect to control conditions, as means ± SD from three biological replicated. Analysed using 1-way ANOVA with Benjamini-Hochberg false discovery rate (FDR) correction ($p \leq 0.05$). Previously published in Dembek *et al.* (2013).

4.2.2.4.3. Ribosomal proteins and transcriptional regulators

Exit from dormancy requires the bacterium to rebuild most of the structures found in a vegetative cell, necessitating large amounts of protein synthesis. It is not surprising then that a significant up-regulation of genes involved in transport, coincided with up-regulation of transcription and translation. In general, all genes encoding ribosomal proteins were up-regulated during germination. These included three genes encoding 30S subunit proteins and eight genes encoding 50S subunit proteins (Figure 4.6A). Similarly, genes encoding DNA-directed RNA polymerase were up-regulated, although only the genes encoding the β and β' subunits of the polymerase had a *p* value ≤ 0.05. Furthermore, sixty-eight genes encoding transcriptional regulators were up-regulated (from 1.3- to 10.9-fold) while twenty-four genes were down-regulated (from 1.3- to 21.2-fold) in germinating spores (Figure 4.6B). These included members of the *gntR, tetR araC, marR, merR, rpiR, copR, deoR* and *lysR* gene families. On the whole, genes encoding tRNA synthetases were down regulated in germinating spores when compared to a vegetative cell. Similarly, enzymes involved in amino acid metabolism were largely down-regulated during germination, possibly reflecting the preferential catabolism of endogenous nutrients as a means for obtaining the necessary 'building blocks' for protein synthesis in early germination.

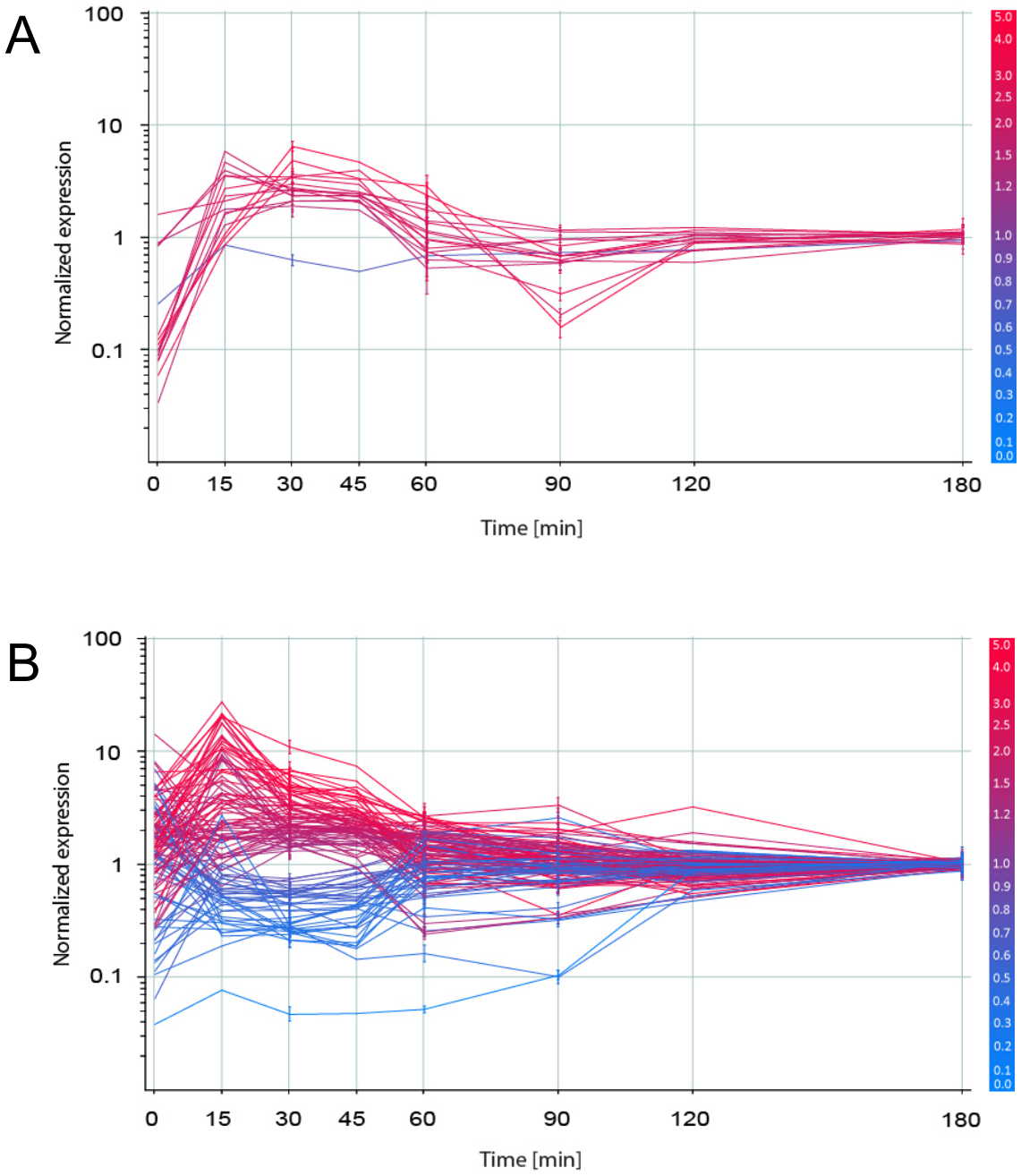

Figure 4.6. Ribosomal proteins and transcriptional regulators differentially regulated during germination. (A) 12 genes encoding ribosomal proteins were up-regulated while one was down-regulated at 30 min into germination when compared to a vegetative cell (180 min). **(B)** 68 genes encoding transcriptional regulators were up-regulated while 24 were down-regulated at 30 min into germination when compared to a vegetative cell (180 min). Gene expression data represented as normalised intensity with respect to control conditions, as means ± SD from three biological replicated. Analysed using 1-way ANOVA with Benjamini-Hochberg false discovery rate (FDR) correction ($p \leq 0.05$). Previously published in Dembek *et al.* (2013).

4.2.2.4.4. Secretion and cell wall components

The Sec machinery provides a major pathway of protein translocation from the cytosol across the cytoplasmic membrane in bacteria (Mori and Ito, 2001). A number of components of the *sec* secretory pathway can be identified in *C. difficile 630* including *secA1, secA2, secE and secY* (Fagan and Fairweather, 2011). In general, all genes within the *secAYEG* operon were up-regulated in germinating spores, although only *secA2* (3.4-fold) and *secE* (3.8-fold) significantly so. The lipoprotein signal-peptidase *lspA* was also up-regulated (2.6-fold) as was the signal recognition particle encoded by *ffh* (4.16-fold) and prolipoprotein diacylglyceryl transferase encoded by *lgt* (3-fold).

The *C. difficile* flagellar assembly is encoded by thirty-five genes located within a single cluster. A vast majority of flagellar genes were inactive in germinating spores when compared to vegetative cells. In addition, five genes encoding components of the bacterial chemotaxis machinery including *motA, motB, cheY, cheD* and *cheW* were also found to be down-regulated in germinating spores (Table 4.2; Figure 4.7A) as were seven genes within two gene clusters encoding type IV pilus proteins (Table 4.3; Figure 4.7B). As cell motility is typically initiated upon nutrient deprivation in stationary phase, the overall inactivity of genes involved in motility during germination is in accordance with expectations, in that flagellar genes are dormant during germination and are transcribed in vegetative cells.

Table 4.2. Type IV pili genes differentially expressed during germination

Systematic name	Gene product	*p*-value	Fold change
CD3295	putative type IV pilus-assembly protein	0.0211	+1.3
CD3504	putative type IV prepilin leader peptidase	0.00385	-2.4
CD3505	putative type IV pilus retraction protein	0.0186	-2.5
CD3507	putative type IV pilin	0.00579	-2.5
CD3508	putative type IV pilin	0.0141	-2.3
CD3509	putative type IV pilus assembly protein	0.0191	-2.3
CD3511	type IV pilus assembly protein	0.0245	-3.4
CD3512	type IV pilus assembly protein	0.0091	-2.9

Table 4.3. Flagellar assembly genes differentially expressed during germination

Systematic name	Gene product	*p*-value	Fold change
CD0228	flagellar motor switch protein	0.0248	-1.9
CD0230	putative flagellar biosynthesis protein	0.0151	-3.7
CD0231	putative flagellar hook-associated protein	0.0204	-3.6
CD0232	flagellar hook-associated protein	0.0167	-5.0
CD0235	flagellar protein FliS	0.0106	-3.7
CD0236	flagellar protein	0.0161	-4.0
CD0237	flagellar cap protein	0.0165	-3.1
CD0239	flagellin subunit	0.0282	-2.0
CD0246	flagellar basal-body rod protein	0.0271	-3.1
CD0247	flagellar hook-basal body complex protein	0.0117	-3.8
CD0248	flagellar M-ring protein	0.0177	-3.9
CD0249	flagellar motor switch protein	0.0187	-4.8
CD0250	flagellar assembly protein	0.0115	-5.6
CD0251	flagellum-specific ATP synthase	0.0139	-5.7
CD0252	flagellar protein	0.0172	-6.1
CD0253	putative flagellar hook-length control protein	0.0177	-5.7
CD0255	flagellar hook protein	0.00833	-6.0
CD0255A	putative flagellar protein	0.0154	-6.2
CD0256	chemotaxis protein	0.0164	-6.4
CD0257	chemotaxis protein	0.0236	-6.0
CD0258	flagellar basal body-associated protein	0.00927	-5.3
CD0259	putative flagellar protein	0.0297	-4.9
CD0260	flagellar biosynthetic protein	0.0394	-4.4
CD0261	flagellar export protein	0.0393	-4.9
CD0262	flagellar export protein	0.0364	-5.4
CD0263	flagellar export protein	0.0232	-5.5
CD0265	flagellar number regulator	0.0284	-6.3
CD0268	flagellar basal-body rod protein FlgG	0.0078	-6.6
CD0269	putative flagellar basal-body rod protein	0.00932	-6.5
CD0270	putative flagellar motor switch protein	0.00953	-6.7
CD0271	putative flagellar motor switch protein	0.0475	-4.6
CD0533	chemotaxis protein	0.017	-1.8
CD0535	chemotaxis protein	0.0329	-1.9
CD0540	chemotaxis protein	0.0257	-1.6

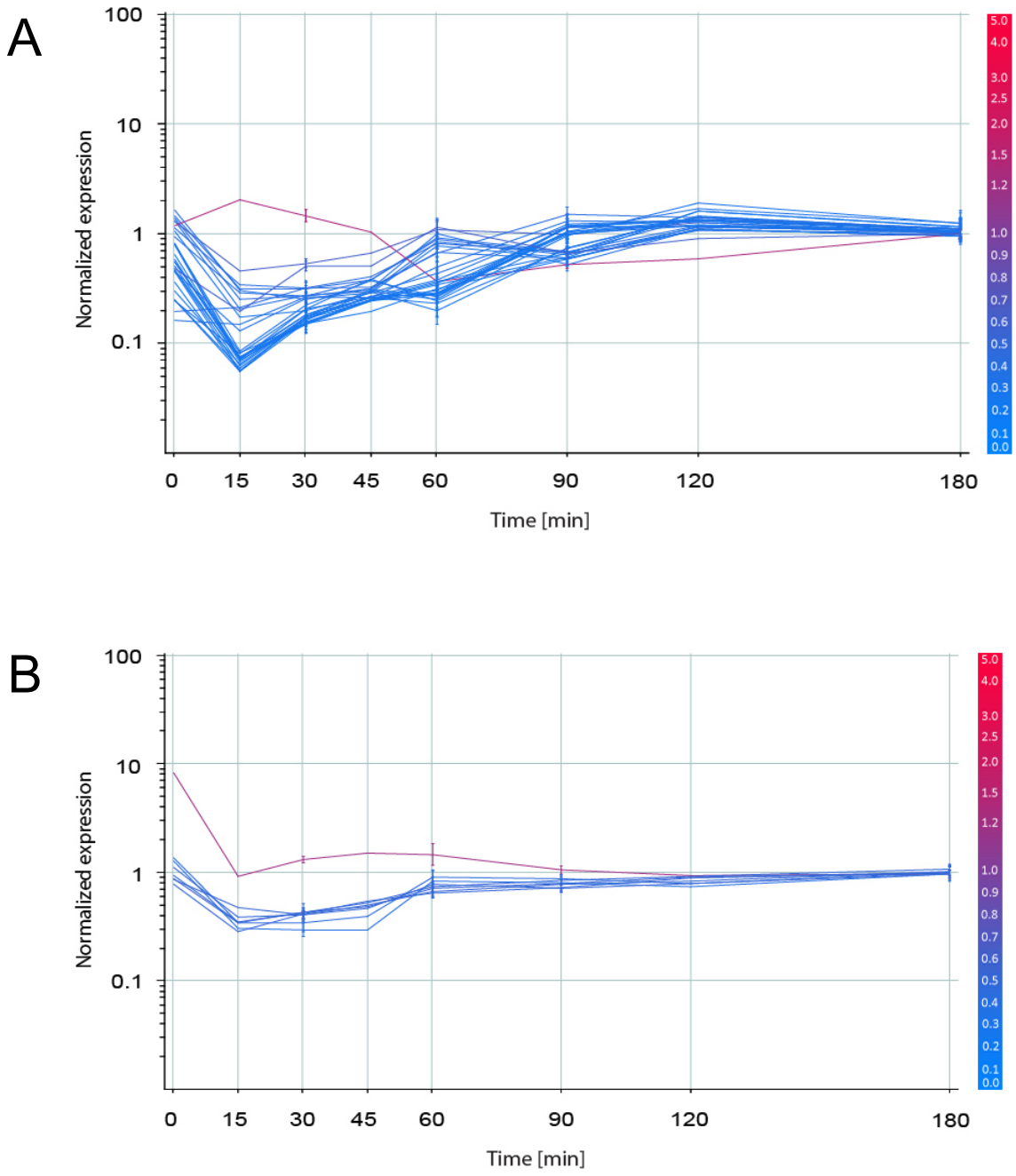

Figure 4.7. Flagellar assembly and type IV pili genes differentially regulated during germination. (A) 29 genes encoding flagellar proteins were down-regulated at 30 min into germination when compared to a vegetative cell (180 min). **(B)** One gene encoding type IV pili were up-regulated while one was down-regulated at 30 min into germination when compared to a vegetative cell (180 min). Gene expression data represented as normalised intensity with respect to control conditions, as means ± SD from three biological replicated. Analysed using 1-way ANOVA with Benjamini-Hochberg false discovery rate (FDR) correction ($p \leq 0.05$). Previously published in Dembek *et al.* (2013).

As a hallmark of cell expansion during germination and outgrowth, genes involved in cell wall biosynthesis were found to be significantly up-regulated in germinating spores. Peptidoglycan is produced from N-acetylglucosamine (NAG) and N-acetylemuramic acid (NAM) in a series of reactions involving incorporation of D-glutamine and D-alanyl-D-alanine. Genes encoding the enzymatic components of this pathway are largely located within the *mur-mra* cluster. Ten enzymes involved in peptidoglycan biosynthesis were up-regulated in germinating spores, including *ddl* (D-Ala D-Ala ligase B; 7.3-fold) *glnA* (glutamine synthase; 2.6-fold) and *murF* (UDP-MurNAc-pentapeptide synthase; 2.4-fold) as well as other members of the *mur-mra* cluster: *murGDE* and *mraYW* (Table 4.4; Figure 4.8).

Table 4.4. Peptidoglycan biosynthesis genes differentially expressed during germination.

Systematic name	Gene product	*p*-value	Fold change
CD0784	putative N-acetylmuramoyl-L-alanine amidase	0.0195	+2.0
CD1343	glutamine synthetase	0.0081	+2.6
CD1408	D-alanine--D-alanine ligase B	0.00843	+7.3
CD2651	UDP-N-acetylglucosamine--N-acetylmuramyl-(penta peptide) pyrophosphoryl-undecaprenol N-acetylglucosamine transferase	0.022	+1.4
CD2653	UDP-N-acetylmuramoylalanine--D-glutamate ligase	0.0105	+1.5
CD2654	phospho-N-acetylmuramoyl-pentapeptide-transferase	0.0145	+1.7
CD2655	UDP-N-acetylmuramoyl-tripeptide--D-alanyl-D-alan ine ligase	0.00508	+2.4
CD2664	putative UDP-N-acetylmuramoylalanyl-D-glutamate--2,6-diaminopimelate ligase	0.0344	+2.4
CD3563	putative spore cortex-lytic enzyme	0.0245	+2.2
CD1898	putative phage-related cell wall hydrolase (endolysin)	0.0174	-6.1

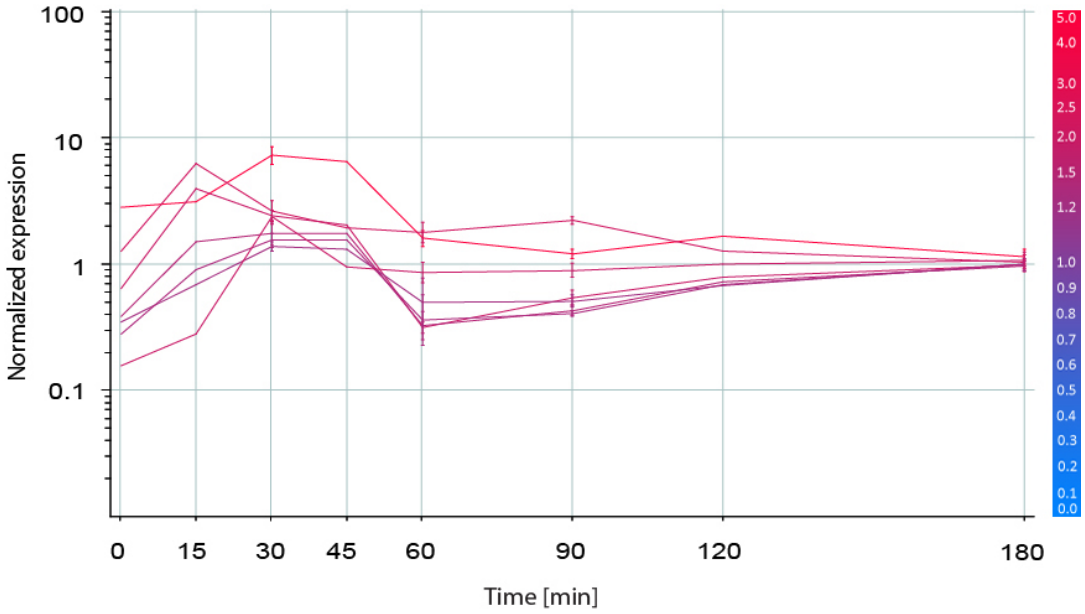

Figure 4.8. **Peptidoglycan biogenesis genes differentially regulated during germination.** 9 genes were up-regulated regulated at 30 min into germination when compared to a vegetative cell (180 min). Gene expression data represented as normalised intensity with respect to control conditions, as means ± SD from three biological replicated. Analysed using 1-way ANOVA with a $p \leq 0.05$ cut-off. Previously published in Dembek *et al.* (2013).

In addition to peptidoglycan, the Gram-positive cell wall can also contain secondary cell wall polymers (SCWP) such as teichoic, teichuronic acids and lipoteichoic acids which can make up between 10 and 60% of its structure. Although the genes specifying these components have not been identified in *C. difficile,* it might be relevant that a cluster of genes (CD2769-80) encoding glycosyltransferases and related enzymes was found to be significantly up-regulated in germinating spores (Table 4.5; Figure 4.9).

Table 4.5. SCWP biosynthesis genes differentially expressed during germination.

Systematic name	Gene product	*p*-value	Fold change
CD2769	capsular polysaccharide biosynthesis protein	0.0201	+2.9
CD2770	putative capsular polysaccharide biosynthesis glycosyl transferase	0.00656	+2.7
CD2771	putative UDP-glucose 6-dehydrogenase	0.00681	+2.4
CD2772	putative teichuronic acid biosynthesis glycosyl transferase	0.016	+2.2
CD2773	putative beta-glycosyltransferase	0.0115	+2.3
CD2774	putative teichuronic acid biosynthesis glycosyl transferase	0.019	+2.2
CD2775	putative minor teichoic acid biosynthesis protein	0.016	+2.3
CD2776	putative glycosyl transferase	0.0408	+2.4
CD2777	putative polysaccharide polymerase	0.0182	+2.5
CD2778	putative polysaccharide biosynthesis protein	0.0311	+2.5
CD2779	putative mannose-1-phosphate guanylyltransferase	0.0116	+2.2
CD2780	putative phosphomannomutase/phosphoglycerate mutase	0.00636	+2.7

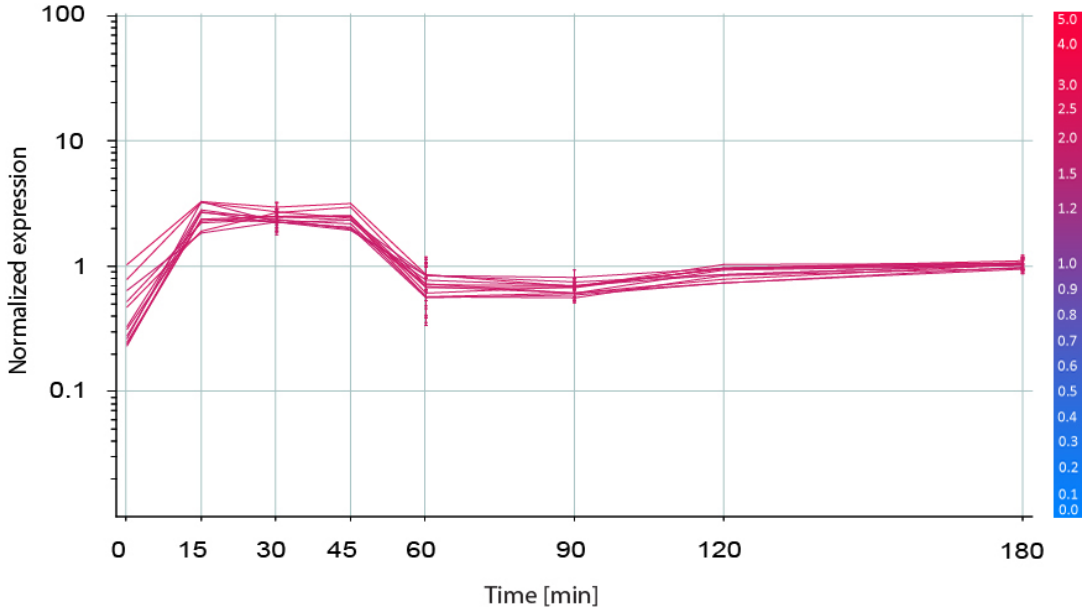

Figure 4.9. **Secondary Cell Wall Polymer biogenesis genes differentially regulated during germination.** 12 genes were up-regulated regulated at 30 min into germination when compared to a vegetative cell (180 min). Gene expression data represented as normalised intensity with respect to control conditions, as means ± SD from three biological replicated. Analysed using 1-way ANOVA with a $p \leq 0.05$ cut-off. Previously published in Dembek *et al.* (2013).

4.2.2.4.5. Toxins

Of central importance in *C. difficile* is the pathogenicity locus (PaLoc) containing five genes encoding two large clostridial toxins: TcdA and TcdB as well as their regulators (*tcdC, tcdR*) and export machinery (*tcdE*) (Voth and Ballard, 2005). Both toxin A and B are represented by multiple probes on the microarray. *tcdA* was down-regulated during germination when compared to the vegetative cell. No transcripts for *tcdB* could be detected in either state, consistent with the observation that toxins are expressed in stationary phase.

4.3. Discussion

The aim of the work presented in this chapter was to provide a genome-wide overview of the temporal gene expression patterns found during germination and outgrowth of *C. difficile* spores. Particular attention was paid to the events that follow initiation of germination and are critical in the transformation of a metabolically dormant spore into an actively growing vegetative cell. Using this approach, around 14% of the genome (511 genes out of 3679) was found to be differentially regulated during germination when compared to the vegetative cell and a number of functional groups of genes appeared to be co-regulated.

The germinating spore requires a large supply of metabolites and cofactors to facilitate re-establishment of cell metabolism. Indeed, a number of genes involved in transport were found to be differentially regulated. ABC-transporters were one such group with 34 significantly up-regulated in germinating spores. A few of these were particularly interesting, including the spermidine/putrescine transporter involved in polyamine trafficking which in turn play a crucial role in DNA replication, cell division and stress response (Pegg and McCann, 1982, Tabor and Tabor, 1984). Interestingly, polyamines have previously been implicated in the shift from a quiescent to a proliferating state in bacterial spores (Setlow, 1974), fungal spores (reviewed in Stevens and Winther, 1979) and plants (Mirza and Bagni, 1991). The sulfonate/nitrate/taurine ABC-transporter on the other hand is of particular interest as taurine conjugated with cholate yields taurocholate, the primary germinant for *C. difficile* spores. One could speculate that the up-regulation of this transporter might be a part of a positive feedback loop providing a constant supply of the germinant and the basis for commitment in germinating spores. In contrast, sugar transport was largely inactive during germination as the entire arm of the PTS system responsible for glucose trafficking was significantly down-regulated. Fructose transport on the other hand was highly up-regulated. In fact the gene encoding 1-phoshofructokinase (CD2270), a central enzyme in fructose catabolism catalysing the rate limiting, committed step in glycolysis, showed an 80-fold up-regulation when compared to vegetative cells, the highest values seen throughout this experiment. This could

indicate the preferential catabolism of fructose as opposed to glucose during the early stages of germination. Activation of transport coincided with a rapid up-regulation of transcription, translation and protein secretion pathways, all necessary in re-building of the basic structures of a vegetative cell as well as regulation of the re-established metabolism. Interestingly, amino acid biogenesis was largely inactive during early germination, possibly reflecting the preferential catabolism of endogenous nutrients as a means for obtaining the necessary 'building blocks' for protein synthesis. Genes involved in motility and chemotaxis were also down-regulated in germination when compared to a vegetative cell. The entire flagellar assembly was largely inactive as were the associated chemotaxis genes. Similarly, genes encoding type IV pili, responsible for twitching motility on *C. difficile* were also down-regulated. These observations are not surprising as cell motility is typically initiated upon nutrient deprivation in stationary growth. Finally, a number of genes involved in peptidoglycan biogenesis and SCWP biogenesis were also up-regulated, a hallmark of cell expansion during outgrowth.

One of the most intriguing aspects of this study was the RNA composition of the dormant spore, particularly with regards to the small rRNA species identified during RNA extraction as well as the abundance of mRNA transcripts and their potential function during the early stages of germination. One group of transcripts that were significantly overrepresented in the spore transcriptome were those encoding redox enzymes, possibly involved in detoxification by scavenging reactive oxygen species (ROS). Similar findings were previously reported by Bettegowda *et al*. (2006) in their microarray analysis of *C. novyi-NT* spores and it seems plausible that this is a common feature among anaerobic sporeformers.

While the microarray experiment presented here was informative regarding the metabolic changes that accompany germination, the limitations of the methodology used meant that the mechanisms that underpin spore germination could not be studied. This is largely due to the fact that factors involved in germination such as germination receptors and enzymes involved in cortex degradation are expressed in the late stages of sporulation and come pre-packed in the spore, ready

to act immediately upon stimulation. These issues are addressed in Chapter VI where recently developed methods are used in forward genetic studies to supplement the microarray data presented here and provide a more complete view of germination in *C. difficile*.

Chapter V

Characterisation of *C. difficile* cell wall protein Cwp7

5.1. Introduction

While the primary goal of the microarray analysis described in Chapter IV was to provide a genome-wide overview of the metabolic changes that accompany germination and outgrowth, the experiment was also a 'fishing exercise' intended to identify a subset of genes that could be followed-up in greater detail using standard genetic and biochemical approaches. This would not only provide 'proof-of-principle' for the entire experiment but would also give more mechanistic insight into how a metabolically dormant spore returns to vegetative growth.

Research carried out in the Fairweather lab is focused on understanding the structure and assembly of the *C. difficile* cell wall and its contribution to the establishment and maintenance of the colonized state during infection. Considering that a germinating spore needs to rebuild most of its structures before returning to vegetative growth, studying germination could provide useful insight into the events that contribute to cell wall biogenesis. Particular attention was therefore paid to genes implicated in the assembly of the cell wall and its surface layer. Three genes encoding previously uncharacterised S-layer proteins (*cwp7, cwp10 and cwp29)* showing interesting expression profiles in the microarray experiment were chosen for further *in vitro* analysis. Disrupting *cwp10* and *cwp29*, two genes significantly down-regulated in germination and highly active in vegetative cells, did not yield distinct phenotypes (data not shown). In contrast, knocking-out *cwp7*, the only CWP gene significantly up-regulated during germination, provided intriguing results which are detailed below.

In this chapter I describe the creation of a *cwp7* mutant using ClosTron insertional mutagenesis followed by an in-depth analysis of the effect *cwp7* disruption has on *C. difficile* physiology. These results are validated by direct comparison with a *cwp7* null mutant obtained using

the recently developed *pyrE*-based allele-coupled exchange system, highlighting some of the limitations of ClosTron mutagenesis. Finally, in an attempt to elucidate the function of Cwp7, protein-protein interactions are analysed and a potential molecular partner for Cwp7 is identified.

5.2. Results

5.2.1. General characteristics

The c*wp7* gene (CD2782) encodes a putative cell wall binding protein and is located within a ~52 kb genomic region containing a number of genes previously described as being involved in cell wall biogenesis and S-layer assembly (Figure 5.1A). Upstream of *cwp7* are 12 genes encoding members of the CWP gene family, including the major S-layer protein SlpA (Calabi *et al.*, 2001), the putative colonisation factor Cwp66 (Dr Zoe Seager, unpublished results), the cysteine protease involved in SlpA processing Cwp84 (de la Riva *et al.*, 2011; Janoir *et al.*, 2007; Kirby *et al.*, 2009) as well as Cwp2, a highly conserved protein recently implicated in flagellar motility (Dr Aaron Dale, unpublished results). Located between *cwp2* an*d slpA* is *secA2*, an accessory ATPase shown to be essential in energizing the translocation of at least two CWP substrates across the cell membrane *via* the canonical SecYEG translocase (Fagan and Fairweather, 2011). Located directly downstream of *cwp7* is *mviN,* a homolog of the *Salmonella typhimurium* mouse virulence factor identified as an essential gene implicated in peptidoglycan (PG) biogenesis in a number of organisms including *E. coli* and *Mycobacterium tuberculosis* (Gee *et al.*, 2012; Inoue *et al.*, 2008; Ruiz, 2008). Further downstream are 12 genes forming a putative secondary cell wall polymer (SCWP) biogenesis locus, all of which were found to be significantly up-regulated during germination in the microarray analysis described above.

With a predicted mass of 39.3 kDa, Cwp7 is one of the smallest members of the CWP family and displays the typical structural organisation seen in other proteins within this group, consisting of an N-terminal type I signal peptide followed by three repeats of the cell wall binding domain Pfam 04122 (Figure 5.1B). In contrast to most CWPs however, no functional domain has been identified in

Cwp7. Instead, a hydrophobic region spanning 21 amino acids followed by three charged residues (R_{344}, R_{347} and K_{351}) can be found on the C-terminus of the protein. Bioinformatic analysis of genome sequences from 12 *C. difficile* strains revealed that Cwp7 is highly conserved with a 99.3% pairwise identity (Figure 5.1C). However no homologue could be identified in other bacterial species, possibly due to the lack of a defined functional domain.

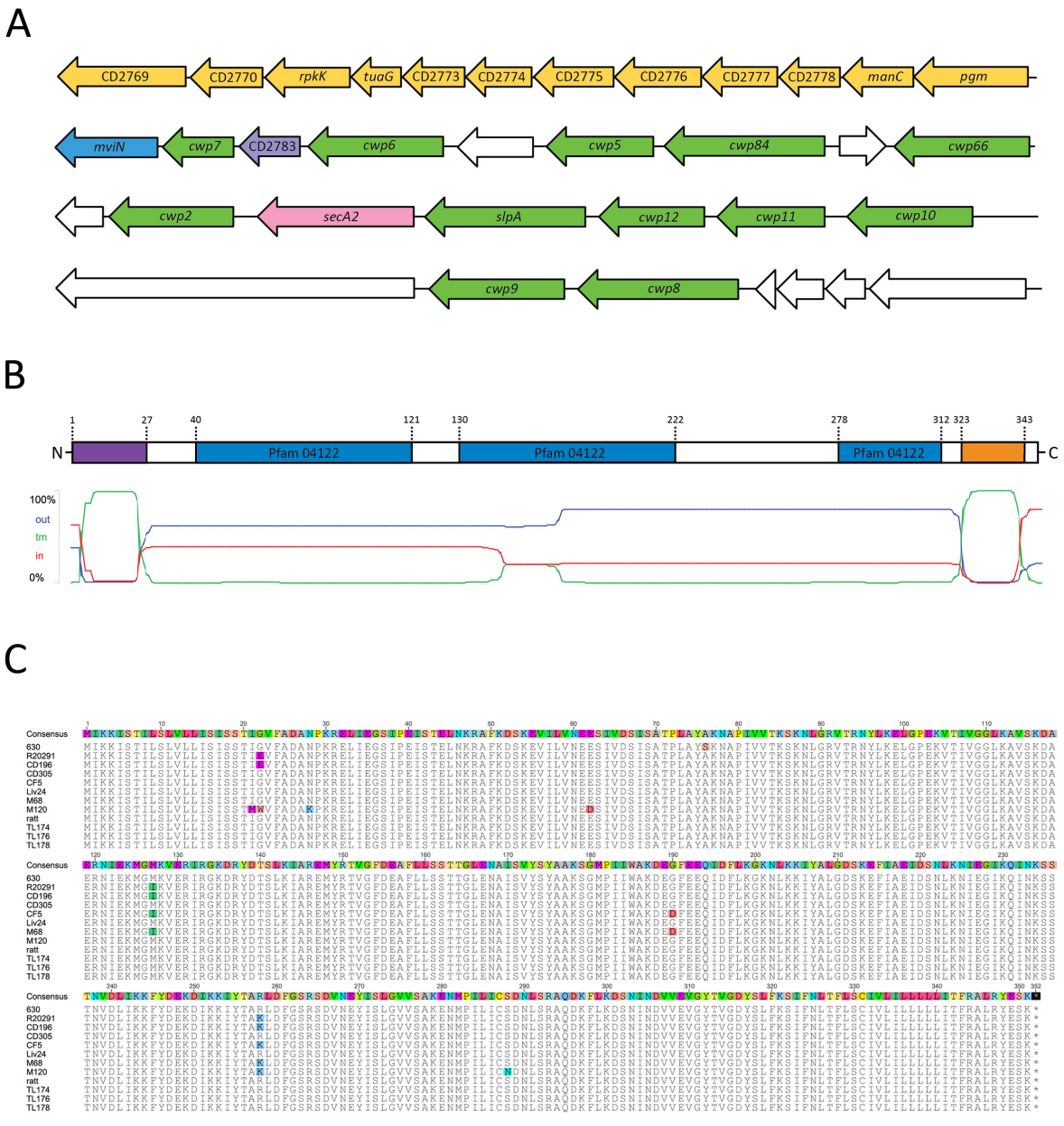

Figure 5.1. General characteristics *of C. difficile* cell wall protein Cwp7. (A) Genomic localisation of *cwp7*. Members of the CWP family are depicted in green, the putative SCWP biogenesis locus in yellow, *mviN* in blue, *secA2* in pink and CD2783, a putative glucosyltransferase, in purple. **(B)** Domain structure of Cwp7. The signal peptide is depicted in purple, Pfam 04122 cell wall binding domains in blue and a predicted transmembrane helix in orange. A prediction of transmembrane regions and the proteins orientation within the membrane is provided below. **(C)** Multiple alignment of Cwp7 protein sequences from 12 *C. difficile* strains showing 99.3% pairwise identity. Disagreements from consensus are highlighted. Created using ClustalW and BLOSUM 62 cost matrix.

5.2.2. RT-PCR analysis of *cwp7* expression patterns

In order to confirm *cwp7* expression and characterise its patterns, transcripts extracted from both germinating spores and vegetative cells were analysed *via* reverse transcriptase PCR (RT-PCR). Two distinct phases of gene expression could be observed. During germination, *cwp7* expression peaked at 30-45 min after induction, dropping off at 60 min. As cells progressed to outgrowth (90-180 min), *cwp7* expression raised, eventually levelling off and remaining constitutive throughout exponential growth. This level of gene expression was then maintained during stationary phase (Figure 5.2A and 5.2B).

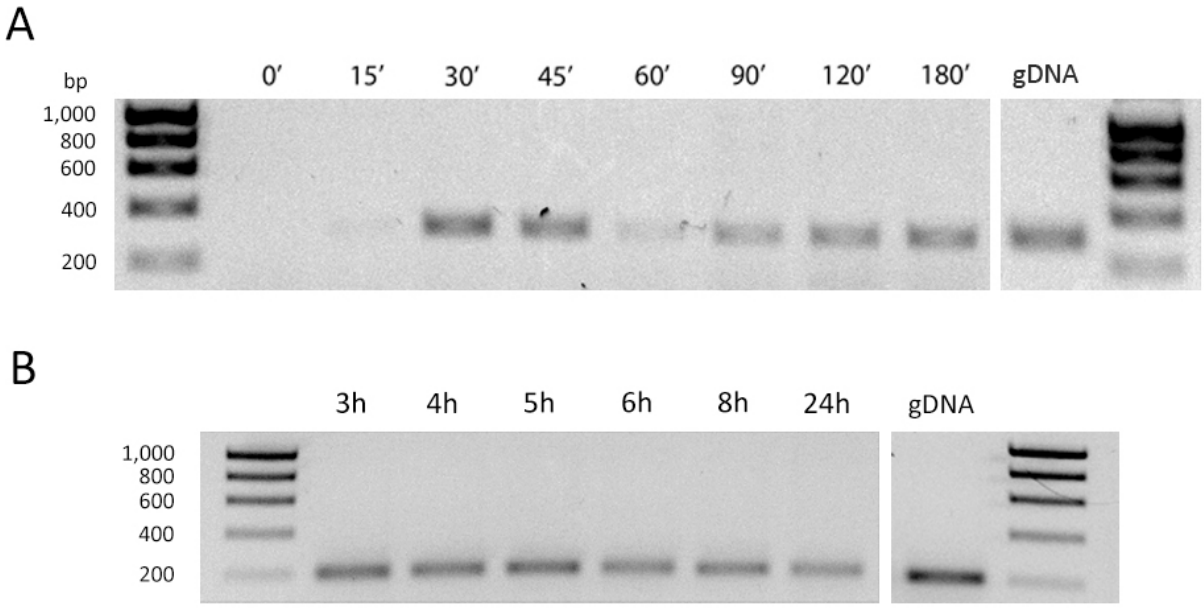

Figure 5.2. Reverse transcriptase PCR analysis of *cwp7* expression patterns. Total RNA extracted at given time points form **(A)** germinating spores, **(B)** vegetative cultures was reverse transcribed into cDNA and used in standard Taq PCR reactions using primers specific to *cwp7* [1671/1672]. 25 reaction cycles were used to ensure non-saturating conditions. RNA was checked for DNA contamination using standard 16S rRNA reactions. *C. difficile* 630Δ*erm* gDNA was used as a positive control. During germination, *cwp7* expression peaked at 30-45 min after induction, dropping off at 60 min. As cells progressed to outgrowth (90-180 min), *cwp7* expression raised, eventually levelling off and remaining constitutive throughout exponential growth. This level of gene expression was then maintained during stationary phase.

5.2.3. Disruption of *cwp7* expression through ClosTron insertional mutagenesis

In an attempt to elucidate the role of Cwp7 in *C. difficile* physiology, particularly in the context of sporulation, germination and cell wall biogenesis, ClosTron insertional mutagenesis was used to disrupt *cwp7* expression in *C. difficile* 630Δ*erm*, an erythromycin-sensitive derivative of *C. difficile* 630 obtained through serial passages of the parental strain (Hussain *et al.*, 2005). To this end, a pMTL007-based vector carrying a 344 bp *cwp7*-specific intron targeting region was synthesised (DNA2.0) and conjugated into 630Δ*erm* as described in Materials and Methods. Thiamphenicol-resistant transconjugants carrying the plasmid were re-streaked onto Brazier's agar plates supplemented with 5 μg/ml erythromycin to select for group II intron integration and activation of the erm^R cassette. Standard PCR techniques were used to screen potential mutants for correct integration and orientation of the group II intron (Figure 5.3A) and were followed by Southern blot analysis to exclude the possibility of multiple insertions (Figure 5.3B). The resulting mutant, *C. difficile* 630 Δ*erm cwp7::erm* (designated *cwp7*::CT) was then complemented with plasmid pMLD024 carrying the complete *cwp7* ORF under the control of a well characterised constitutive P_{cwp2} promoter (designated *cwp7*::CT [pCwp7]). The phenotypes of these two strains were analysed and compared to the isogenic wild-type (WT) strain.

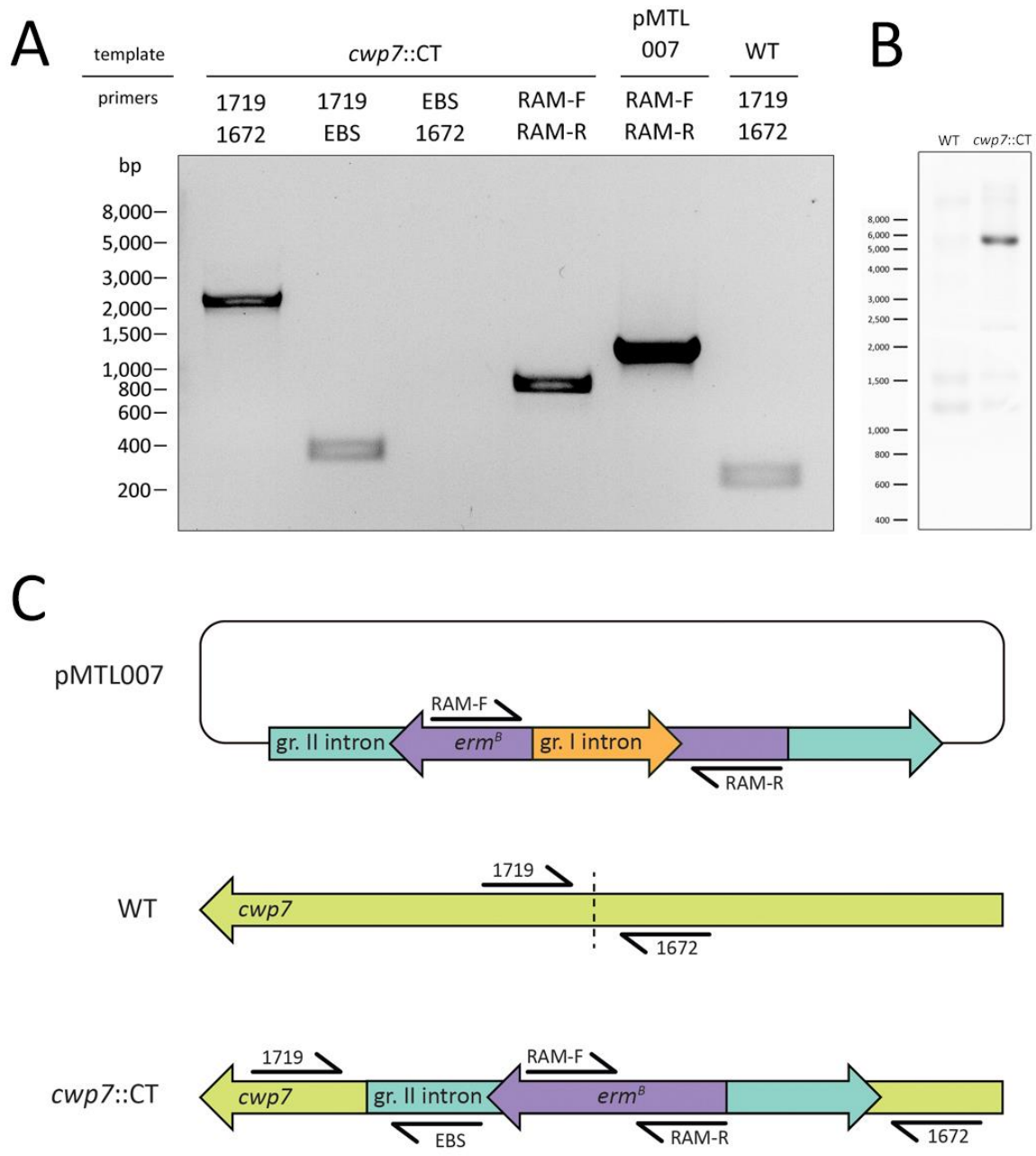

Figure 5.3. PCR screening of *cwp7* ClosTron mutant. (A) Genomic DNA extracted from a putative *cwp7* ClosTron mutant was subjected to PCR analysis using primers flanking the group II intron insertion site [1719/1672] to confirm intron integration, primers flanking the retroposition-activated marker (RAM) [RAM-F/RAM-R] to confirm the excision of the group I intron and an EBS universal primer to confirm the appropriate orientation of the group II intron within the *C. difficile* genome. pMTL007 and WT gDNA were used as templates in negative controls. **(B)** Southern blot analysis of *cwp7* ClosTron mutant. A single band corresponding to the predicted product size of 5,736 bp can be identified in *cwp7*::CT but not WT confirming a single insertion event. **(C)** Schematic representation of *cwp7* insertional mutagenesis. Primer binding sites and the intron insertion site (dashed line) are indicated.

5.2.4. Phenotypic analysis of *cwp7*::CT

5.2.4.1. Growth rate

In order to assess the effect *cwp7* disruption had on general strain fitness, growth rate in liquid culture was monitored. Disruption of *cwp7* expression resulted in a significant growth defect with an average 47% drop in growth rate observed throughout exponential phase. Endpoint culture density following O/N incubation was also significantly lower than WT. This was alleviated through plasmid-mediated *in trans* complementation, restoring the growth rate to WT levels (Figure 5.4A). Routine observations carried out during culture revealed that long-term viability of the mutant was significantly reduced as cultures inoculated with colonies that were left in the anaerobic cabinet for more than seven days often failed to grow or grew more slowly than corresponding WT and complemented cultures.

5.2.4.2. Colony and single cell morphology

Determining the morphology of a single colony growing on the surface of a plated culture can be an important tool in the description of microorganisms as any alterations to WT colony morphology are typically an early sign of phenotypic variation. The *cwp7* mutant formed small, smooth-edged, convex colonies as compared to the large, flat, rough-edged colonies of the isogenic WT strain. These typically took two days to grow following a re-streak, consistent with growth rate data described above, and shared a distinct mucoid appearance (Figure 5.4B). As with the growth defect, colony morphology was restored to WT upon complementation. Phase contrast microscopy of the analysed strains revealed significant changes in single cell morphology. In contrast to the straight bacilli of the WT strain, *cwp7*::CT cells were thinner, slightly curved and appeared to lack rigidity. Surprisingly, this phenotype was even more pronounced in the complemented mutant, in which a subset of cells showed a >180° bend (Figure 5.4B). The percentage of cells exhibiting this extreme curvature ranged from approx. 5% to 50% between different experiments and was found to depend largely on the growth phase, with exponentially growing cultures containing less curved cells

than those that reached stationary phase. Upon closer examination of non-immobilized cells, by changing the focal plane during imaging, these cells showed 'corkscrew' morphology as seen in helical bacterial species such as *Campylobacter jejuni* and *Helicobacter pylori* suggesting a severe alteration to the cell cytoskeleton. Over-expression of *cwp7* in the WT background did not result in a similar phenotype (data not shown), suggesting that the observed phenotype could be a result of a polar effect of *cwp7* disruption on downstream genes, most of which are predicted to be involved in cell wall biogenesis.

In an attempt to gain further insight into what effect *cwp7* disruption has on cell wall biogenesis and the general cell ultrastructure, TEM analysis was performed in collaboration with Dr Dave Goulding (Sanger Institute). While electron micrographs of the *cwp7* mutant and the complemented strain confirmed the disrupted single-cell morphology initially identified through phase-contrast microscopy, and layers corresponding to the cell membrane, cell wall peptidoglycan and the S-layer could be clearly discerned, no obvious differences in cell wall organisation were observed between *cwp7*::CT, *cwp7*::CT [pCwp7] and WT (Figure 5.5).

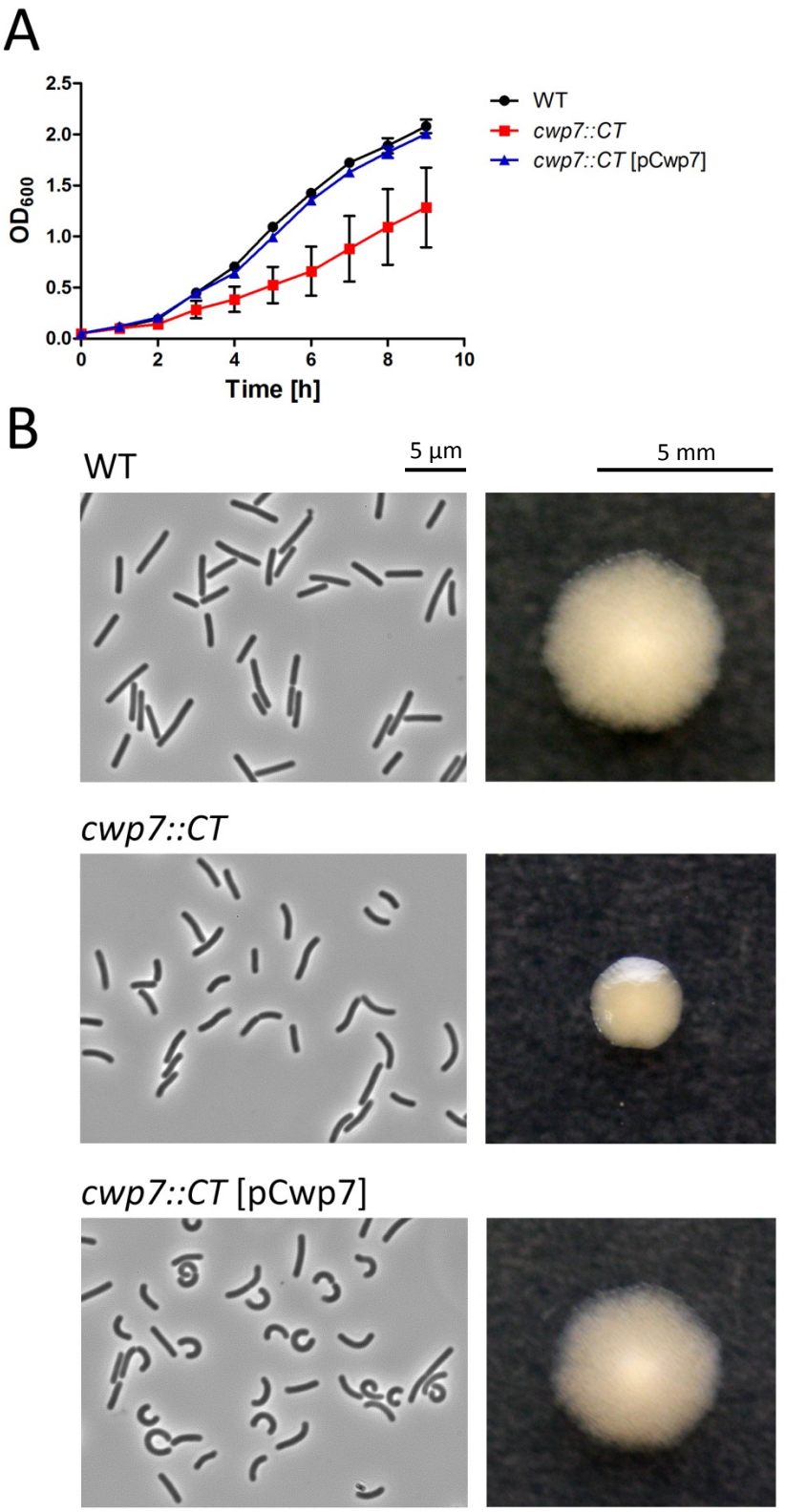

Figure 5.4. Characterisation of *cwp7* ClosTron mutant phenotype. (A) Growth curve indicating a severe defect in *cwp7*::CT growth rate when compared to WT and the complemented mutant. Data represented as mean ± SD from three biological replicates. **(B)** Phase contrast analysis of single cell morphology revealing slightly curved cells for the *cwp7* mutant when compared to the straight bacilli seen in WT. The mutant also displayed altered colony morphology, showing small, smooth, mucoid colonies as compared to the large, rough colonies seen in WT. Changes in the single cell morphology of the complemented mutant were even more severe, with a subset of cells being tightly curved. Colony morphology was not affected. Images representative of three biological replicates. Universal scale bar provided.

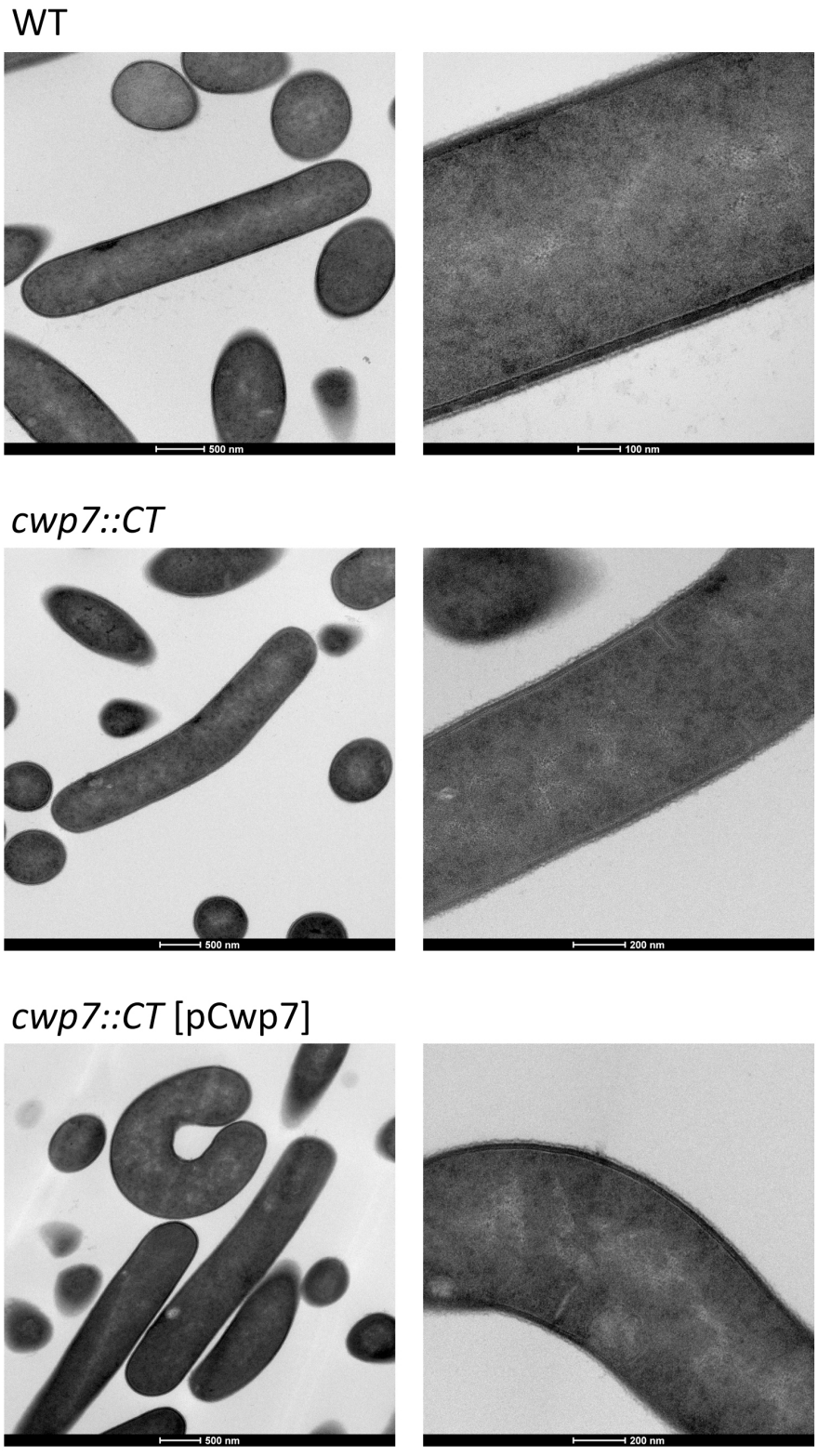

Figure 5.5. Transmission electron microscopy (TEM) examination of *cwp7* ClosTron mutant single cell morphology. Changes to single cell morphology previously identified for each of the analysed strains *via* phase-contrast microscopy are evident. Individual scale bars are indicated under each image.

5.2.4.3. Flagellar motility

The small colony morphology seen in *cwp7*::CT could indicate a possible defect in motility. To investigate this further, a swimming motility assay was performed. To this end 0.3% BHIS agar plates were inoculated with exponentially growing cultures and growth was monitored for 96h. *C. difficile* 630 Δ*erm fliC::erm* (designated *fliC*::CT), a non-motile strain obtained by disrupting the expression of the major flagellar protein FliC, was used as a negative control. No significant difference in swimming motility was observed between WT, *cwp7*::CT and *cwp7*::CT [pCwp7] suggesting that *cwp7* disruption has no effect on flagellar motility (Figure 5.6).

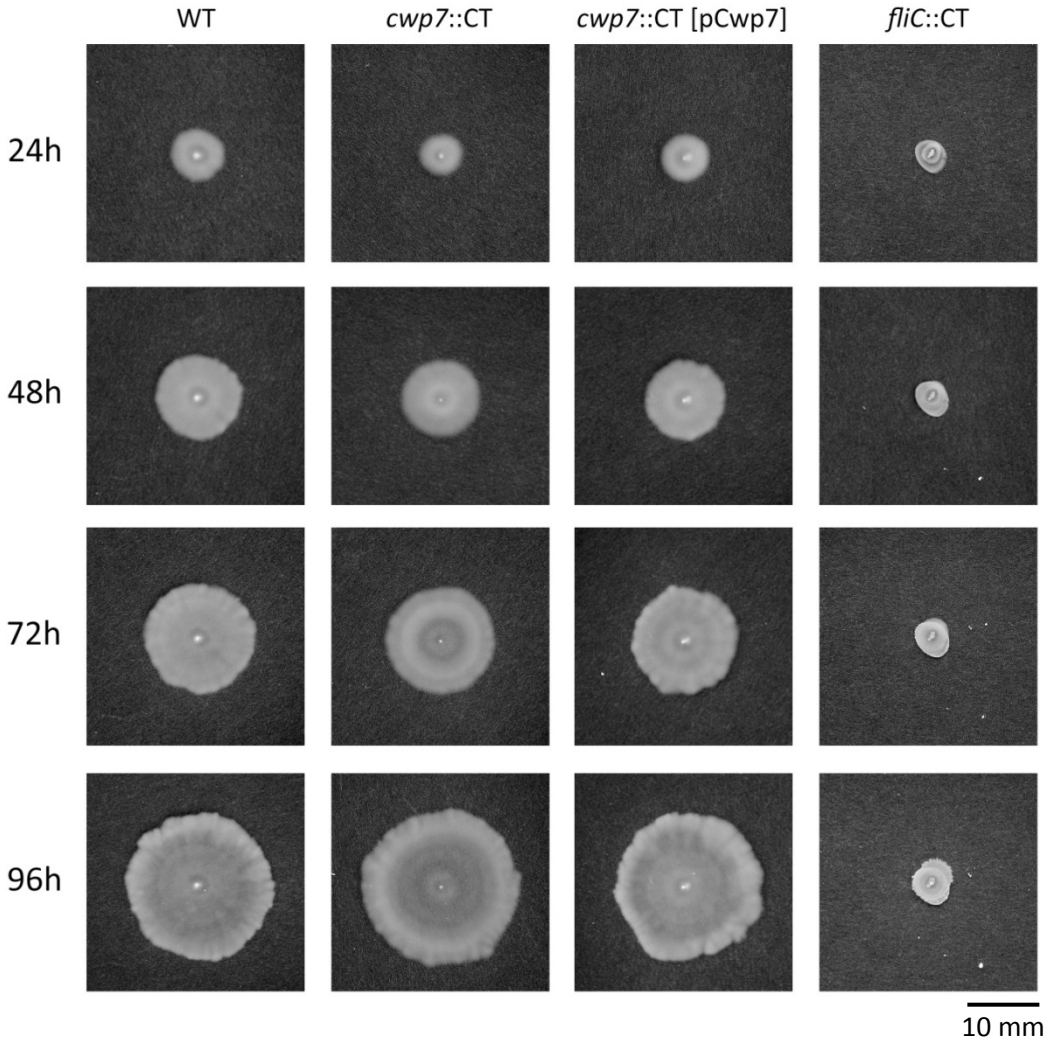

Figure 5.6. Assessment of *cwp7* ClosTron mutant swimming motility. Exponentially growing cultures were used to inoculate 0.3% BHIS agar plates. Growth was monitored over a period of 96h. The non-motile *fliC*::CT mutant was used as a negative control. No significant changes in motility were observed for *cwp7*::CT when compared to WT and the complemented mutant. Images representative of two biological replicates. Universal scale bar provided.

5.2.4.4. S-layer composition

It is well established that lateral interactions between the various CWPs comprising the S-layer are important in maintaining its integrity and that disruption of a single protein might have far reaching consequences for the entire structure. To further elucidate the effect *cwp7* disruption has on cell wall composition, S-layer extracts and culture supernatants were prepared and analysed *via* SDS-PAGE followed by Coomassie staining (Figure 5.7). Strikingly, while the composition of cell wall associated S-layer extracts did not seem to differ between the three strains, the *cwp7*::CT culture supernatant contained significantly more protein than WT and *cwp7*::CT [pCwp7]. This was further verified by probing the samples for S-layer proteins and CWPs using Western immunoblotting. While the amounts of the major S-layer proteins, HMW SLP and LMW SLP, were essentially equal in the S-layer extracts of all analysed strains, large amounts of the proteins were found to be present in the supernatant of the *cwp7* mutant. Interestingly, a band corresponding to unprocessed, full length SlpA was also identified indicating deficiencies in SlpA maturation. This coincided with shedding of Cwp84, a cysteine protease essential for SlpA cleavage. Both Cwp2 and Cwp66 were also found to be shed into the culture supernatant although only the later was depleted in the S-layer extract of *cwp7::*CT. While the amount of protein shed by *cwp7*::CT [pCwp7] was dramatically lower than the mutant, *in trans* complementation did not fully restore the WT phenotype.

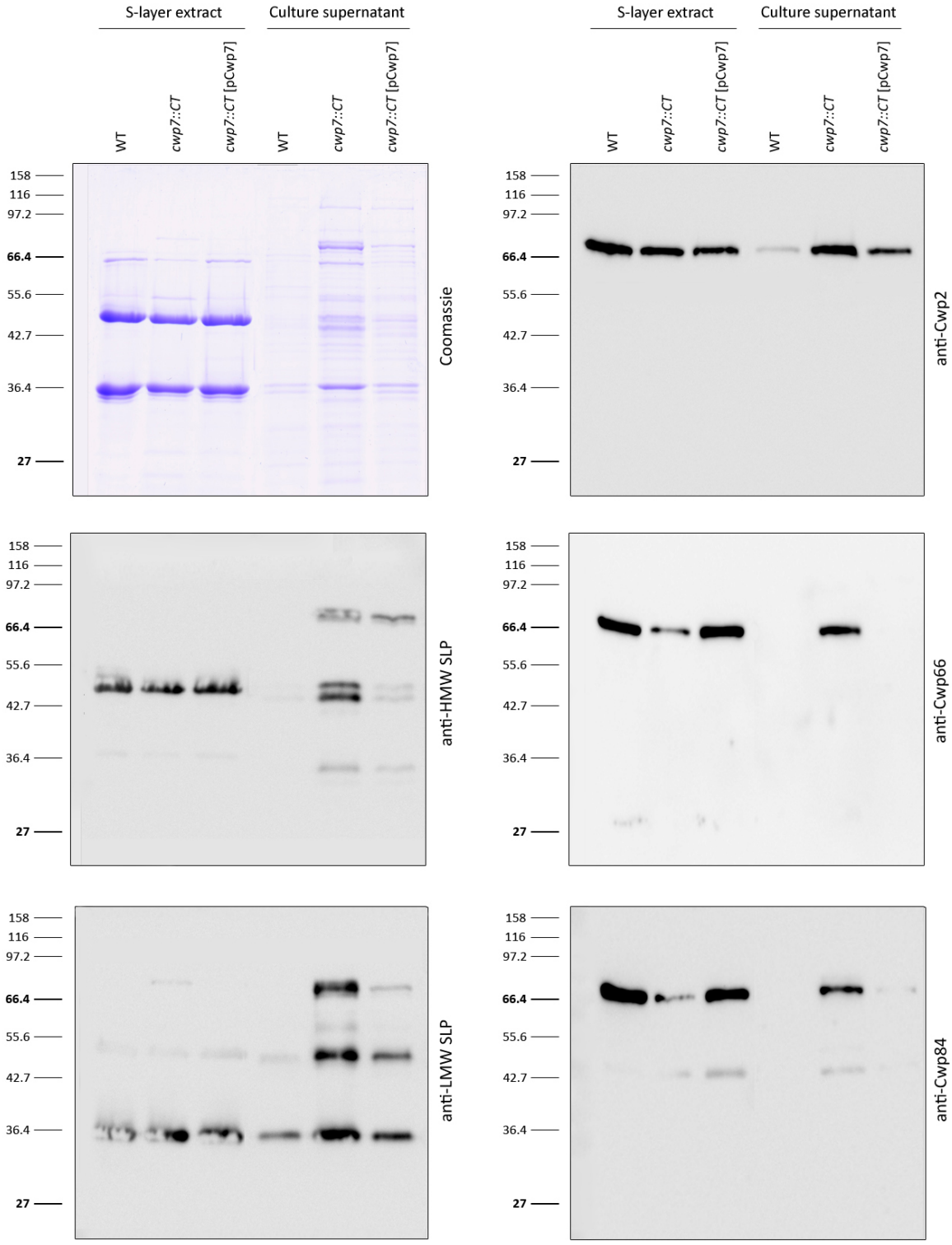

Figure 5.7. Examination of *cwp7* ClosTron mutant S-layer composition. S-layer extracts were prepared from O/N cultures using low pH glycine. Proteins shed into the supernatant were precipitated using trichloroacetic acid (TCA). All samples were separated using SDS-PAGE and probed for HMW-SLP, LMW-SLP, Cwp2, Cwp66 and Cwp84. Significant amount of all analysed proteins were found to be shed into the culture supernatant. Stark differences in S-layer composition were also observed, particularly with regard to Cwp66 and Cwp84. Phenotype was largely restored to WT upon complementation. Data representative of three biological replicates.

5.2.4.5. Sub-cellular localisation of Cwp7

Despite the high expression levels of *cwp7* seen in the microarray experiment and subsequently validated by RT-PCR, both during germination and vegetative growth, Cwp7 could not be detected in S-layer extracts separated on Coomassie stained gels. This suggested that Cwp7 might not localize to the S-layer. Taking into account that previous bioinformatic analysis using TMpred (http://www.ch.embnet.org/) revealed a 'high scoring', C-terminal transmembrane helix spanning 21 hydrophobic amino acids followed by three charged residues, it would seem likely that Cwp7 is a membrane protein. To investigate this, inverse PCR was used to delete the transmembrane helix in pMLD024 resulting in pMLD026 which was then conjugated into the *cwp7* ClosTron mutant. Crucially, the growth rate, colony and single cell morphology as well as S-layer composition of the resulting strain (designated *cwp7::CT* [pCwp7$_{trunc}$]) were largely identical to those observed in *cwp7*::CT (data not shown) indicating that the transmembrane helix is an essential functional part of the protein (data not shown).

To further elucidate the sub-cellular localisation of Cwp7, a Cwp7-specific antiserum was raised in mice. To this end, a fragment of *cwp7* lacking the N-terminal signal peptide and the C-terminal transmembrane helix was cloned into the pET28a expression vector yielding pMLD023 (pET28a-cwp7$_{26-323}$), which was then transformed into *E. coli* Rosetta competent cells. Cwp7 was over-expressed, purified form inclusion bodies *via* detergent-assisted on-column refolding and used to immunize mice. The resulting serum was subsequently used to probe membrane fractions prepared from WT, *cwp7*::CT, *cwp7*::CT [pCwp7] and *cwp7*::CT [pCwp7$_{trunc}$]. A band corresponding to a protein of approx. 39 kDa was detected in the membrane fractions from WT and *cwp7*::CT [pCwp7] but not *cwp7*::CT (Figure 5.8A). While a slightly smaller protein species was observed for the *cwp7* mutant complemented with a truncated copy of the gene, the intensity of the corresponding band was significantly lower than that seen in WT and *cwp7*::CT [pCwp7]. Taken together these results indicate that (i) unlike most members of the CWP family, Cwp7 is an integral membrane protein, (ii) the 21 amino acid C-terminal hydrophobic region is essential in anchoring Cwp7 to the cell

membrane and that (iii) the protein's location is essential in exerting its function within the cell as complementation with a truncated copy of the gene does not restore WT phenotype.

To obtain visual confirmation of Cwp7 membrane localisation and gain further insight into its spatial distribution within the cell, a number of localisation methods were tested. Unfortunately, while the Cwp7 anti-serum proved to be highly specific in immunoblotting experiments, attempts to use it for immunofluorescence purposes were unsuccessful, most likely due to the peptidoglycan layer forming a physical barrier preventing antibodies from binding to their target. Similarly, attempts at using immunogold labelling were also unsuccessful as no specific binding could be observed *via* TEM (data not shown). To overcome this problem, a number of fluorophores were tested in fusion with Cwp7, including the green-fluorescent LOV domain, the red-fluorescent SNAP-TMR-STAR and the red-fluorescent mCherry. The latter was found to be the most effective in *C. difficile* (data not shown). The *cwp7* ClosTron mutant complemented with a plasmid carrying *cwp7* C-terminally fused with codon-optimised mCherry (designated cwp7::CT [pCwp7$_{mCherry}$]) showed a distinct membrane stain (Figure 5.8B), although significant differences in signal level were observed between individual cells within the population, possibly a consequence of using the P$_{cwp2}$ promoter to drive *cwp7* expression. No signal was observed for WT cells (negative control).

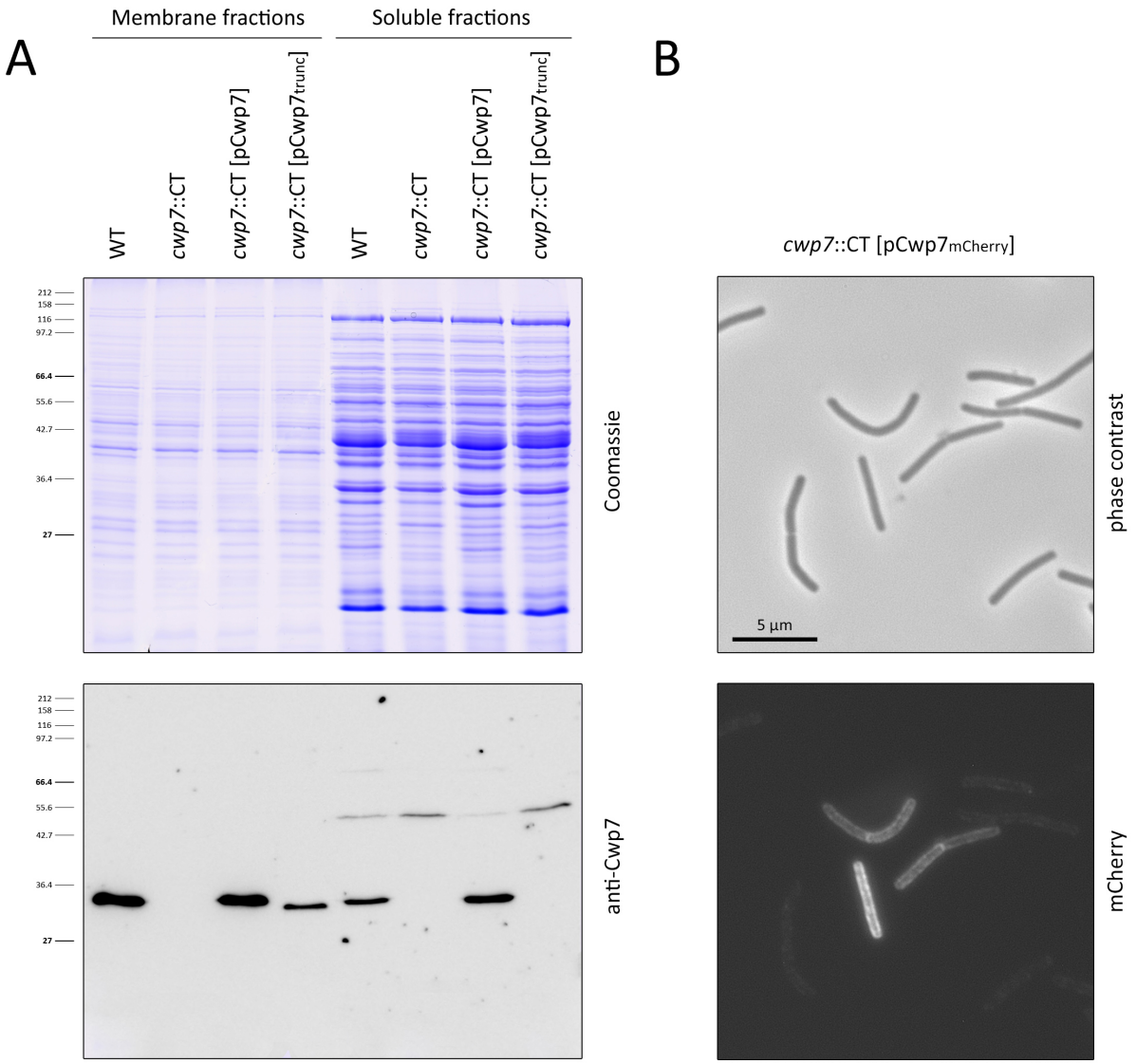

Figure 5.8. Investigation of Cwp7 sub-cellular localisation. (A) Membrane fractions and soluble fractions were separated *via* SDS-PAGE and probed for Cwp7 by Western blotting. Cwp7 could be detected in the membrane fractions from WT and *cwp7*::CT [pCwp7] but not *cwp7*::CT. Deletion of the C-terminal transmembrane helix resulted in a significantly decreased amount of Cwp7 within the membrane fraction. **(B)** Fluorescence microscopy of *cwp7*::CT complemented with Cwp7-mCherry fusion protein. Distinct membrane staining can be observed in a subset of cells.

5.2.4.6. Sporulation efficiency

Sporulation is a crucial part of *C. difficile* life cycle and requires considerable remodelling of the bacterial cell wall. It is thus conceivable that defects in cell wall organisation could have a detrimental impact on spore formation. In order to confirm whether *cwp7* disruption had any effect on *C. difficile* spore formation, sporulation efficiency was assessed. While previous experiments showed that spore formation on solid media is far more efficient and homogenous than when carried out in liquid culture, technical limitations render the method unsuitable for accurate quantification of spores, particularly when comparing multiple strains. Furthermore, while sporulation in SM broth was more efficient than in BHIS broth, the latter was found to provide far more reproducible results. BHIS broth was therefore used to assess sporulation efficiency of *cwp7*::CT mutant as described previously in Chapter 3. Strikingly, no spores could be detected for the *cwp7* ClosTron mutant throughout the duration of the experiment. This defect was alleviated through *in trans* complementation, restoring sporulation efficiency to WT levels (Figure 5.9A). As the read-out of the sporulation assay requires the strain to be both sporulation and germination-proficient, in order to differentiate between sporulation and germination defects the entire procedure was monitored using phase contrast microscopy. This confirmed that spores were not present in the *cwp7*::CT culture (Figure 5.9B). Interestingly, when compared to WT and *cwp7*::CT [pCwp7] strains, the *cwp7* mutant appeared to lyse more quickly, losing the structural integrity of the cells within 24h from the onset of the experiment. While cell lysis was also present in the other two strains, it was more gradual as intact cell sacculi could be detected even 72h into the experiment (Figure 5.9B).

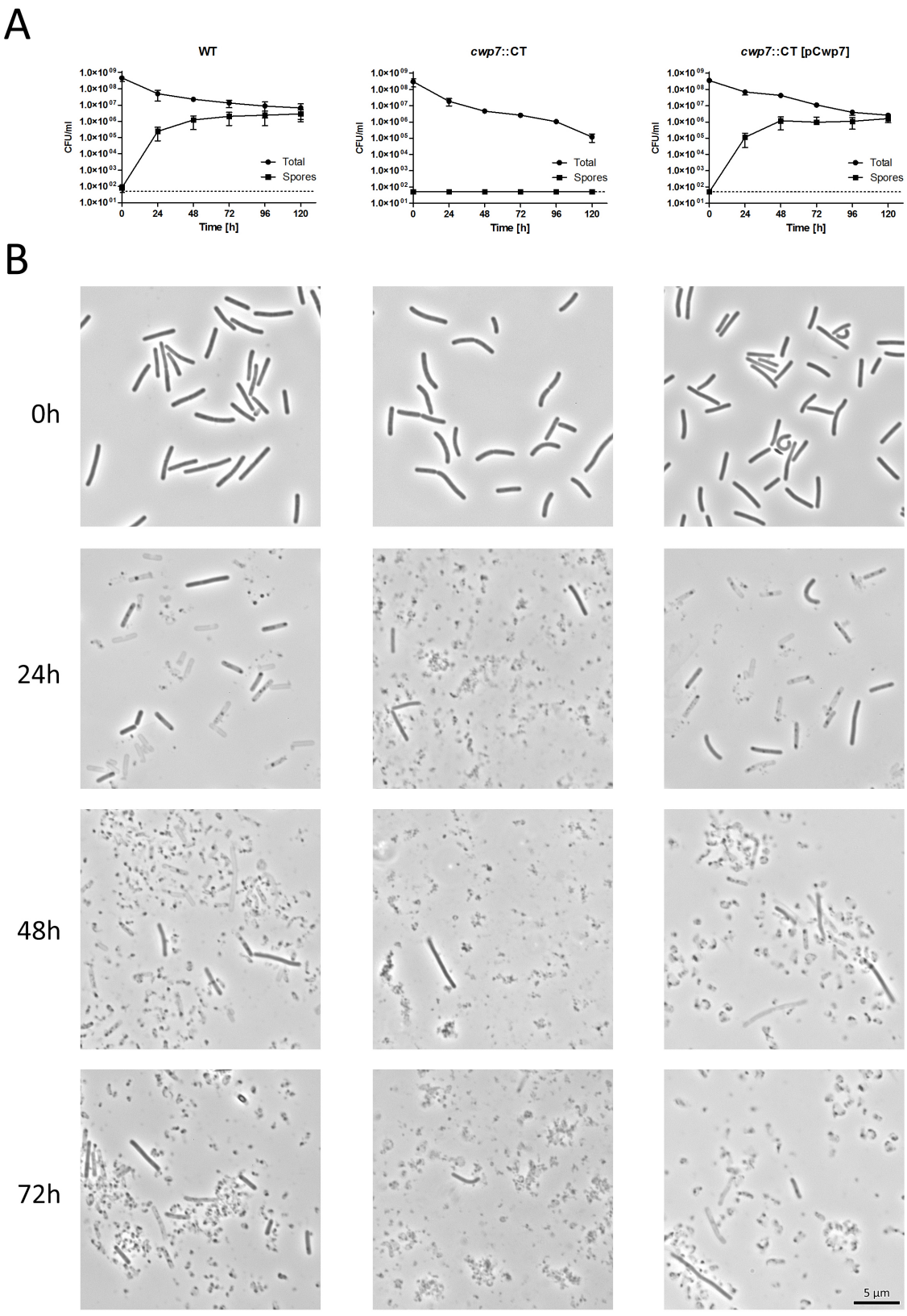

Figure 5.9. Assessment of *cwp7* ClosTron mutant sporulation efficiency. Sporulation was induced *via* nutrient starvation in BHIS broth and was assessed over a period of 5 days by **(A)** measuring total and spore CFUs and **(B)** monitoring spore formation using phase-contrast microscopy. No spore CFUs were identified in *cwp7*::CT throughout the duration of the experiment. Spore formation was restored to WT levels upon *in trans* complementation. While significant cell lysis was observed in all strains, this was more severe in *cwp7*::CT where a rapid loss of cell integrity was observed within 24h. Numerical data represented as means ± SD from three biological replicates. Limit of detection indicated as a horizontal dashed line. Microscopy data representative of two biological replicates. Scale bar provided.

To overcome the low sporulation efficiency in liquid culture and the relatively high limit of detection of the quantification methods used, an attempt was made to sporulate *cwp7*::CT on SM agar and purify the resulting spores. While not quantifiable, the purification process would allow for sample enrichment and thus, when sufficiently scaled-up, even relatively minute amounts of spores could be readily detected. Indeed, some spores were recovered from *cwp7*::CT cultures sporulated on solid media, although sporulation efficiency was significantly lower than that seen in WT and *cwp7*::CT [pCwp7]. Interestingly, upon phase-contrast analysis, the *cwp7*::CT spores demonstrated a propensity to form clumps containing large amounts of cell debris (Figure 5.10). These were resistant to mild detergents (0.01% Tween 20) thus preventing accurate quantification and their use in further experiments.

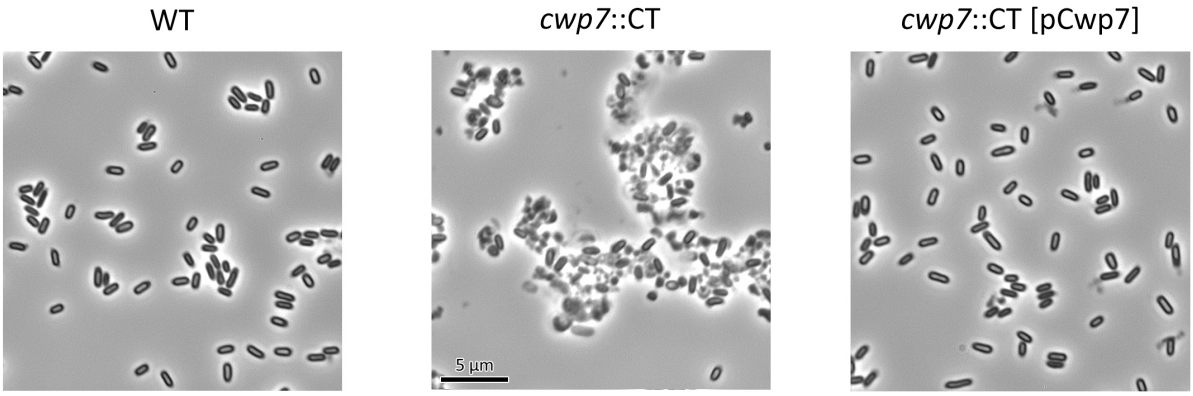

Figure 5.10. Phase-contrast microscopy examination of purified spores. Sporulation was carried out on solid media and spores were purified *via* density gradient centrifugation. Spores of the *cwp7* ClosTron mutant showed a propensity to form clumps contaminated with significant amount of cell debris. Spore yields were also significantly reduced. Scale bar provided.

5.2.5. Disruption of *cwp7* expression through Allele-Coupled Exchange (ACE)

Since its development in 2007, ClosTron insertional mutagenesis has quickly become the gold standard in genetic manipulation of *C. difficile*, providing a fast, reliable and reproducible method for targeted disruption of genes. While numerous studies successfully using this technique have now been published, the ClosTron system does have its limitations. Polar effects are common as insertion of the group II intron can disrupt the expression of neighbouring genes. Multiple insertions, while rare, have been reported necessitating the use of time consuming screening techniques. The limited availability of suitable selection markers makes creating multiple gene deletions difficult. Finally, as *in situ* complementation of a disrupted gene is not possible, plasmid-based *in trans* complementation has to be used, often resulting in unwanted gene dosage effects. Recently developed methods for creating non-marked mutations in *C. difficile* have helped overcome these problems. One such method, using *pyrE*-based allelic exchange allows the rapid insertion of heterologous DNA of any size or complexity into the genome. In order to exclude the possibility of polar effects in the phenotype seen for the *cwp7*::CT mutant, *pyrE*-based ACE was used to create a 660 bp in-frame deletion in *cwp7* as described by Ng *et al*. (2013). To this end, the mutated allele was created by amplifying 750bp-long homology regions flanking the deletion site and cloning them into pMTL-YN3 *via* Gibson assembly. The resulting plasmid, pMLD061 was then conjugated into *C. difficile* 630 Δ*erm* Δ*pyrE*, a strain auxotrophic for uracil and resistant to 5-fluoroorotic acid (FOA). Following two passages on BHIS agar supplemented with 5 µg/ml uracil, 15 µg/ml thiamphenicol and 250 µg/ml cycloserine, colonies that were noticeably larger (indicative of plasmid integration) were screened by colony PCR to identify single-crossover mutants using (i) primers 2308/2309 flanking the upstream and downstream homology regions and (ii) one of these primers in conjunction with a plasmid-specific primer 2369 to amplify across the integration junction (Figure 5.11A). Pure, single crossover mutants were streaked onto *C. difficile* minimal medium (CDMM) supplemented with 5 µg/ml uracil and 2 mg/ml FOA to select for plasmid excision. The isolated FOA-resistant colonies were screened by PCR using primers 2308/2309. Double-crossover mutants in which the mutated

allele was successfully integrated yielded products 660 bp smaller than those seen in WT revertants (Figure 5.11B).

In order to restore the *pyrE+* phenotype, plasmid pMTL-YN1 carrying the WT *pyrE* allele was conjugated into the isolated double-crossover mutant. The resulting colonies were re-streaked onto non-supplemented CDMM agar to select for uracil prototrophy indicating successful allele exchange (designated Δ*cwp7*). Restoration of the *pyrE* allele was confirmed by colony PCR using primers 2429/2430 flanking the *pyrE* locus (Figure 5.11B) followed by Sanger sequencing of the amplified product.

In order to complement the mutants, WT *cwp7* allele including the Ribosome Binding Site (RBS) was cloned into pMTL-YN1C using SacI and BamHI sites under the control of the constitutive P_{cwp2} promoter. The resulting plasmid (pMLD073) was conjugated into the isolated double-crossover mutant. Following 96h of incubation individual transconjugants were re-streaked onto non-supplemented CDMM agar to select for uracil prototrophy indicating successful allele exchange and the introduction of the WT *cwp7* allele immediately downstream of the concomitantly restored *pyrE* locus (designated Δ*cwp7* + *cwp7*). Complementation was confirmed by colony PCR using primers 2429/2430 flanking the *pyrE* locus followed by Sanger sequencing of the amplified product (Figure 5.11B).

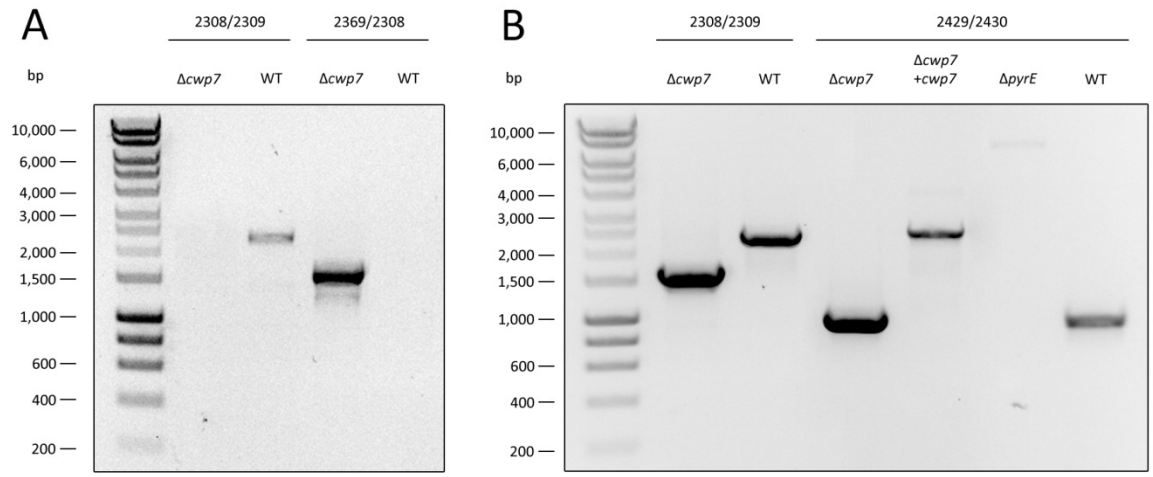

Figure 5.11. Disruption of *cwp7* expression using allele-coupled exchange (ACE). (A) PCR screening of single-crossover mutants using primers flanking the deletion site [2308/2309] and one of these primers in conjunction with a plasmid-specific primer 2369 to amplify across the integration junction. **(B)** PCR screening of *cwp7* ACE mutant following restoration of the *pyrE* locus and complementation. Primers [2429/2430] flank the disrupted *pyrE* locus used for complementation.

5.2.6. Comparison of *cwp7*::CT and Δ*cwp7* phenotypes

While the ACE *cwp7* mutant showed a growth defect similar to that seen in its ClosTron counterpart (approx. 46% drop in growth rate throughout exponential phase), both endpoint culture density and long term viability of the strain did not seem to be affected (Figure 5.12A). Importantly, both *cwp7*::CT and Δ*cwp7* had identical colony morphology and showed the same abnormalities in single cell structure, including a curved morphology. Interestingly, while the cells of the complemented ClosTron mutant showed exaggerated curvature, no such effect was seen in the complemented ACE mutant which shared the appearance of the WT strain, thus confirming that the extreme curvature seen in *cwp7*::CT [pCwp7] was not a direct effect of *cwp7* disruption but rather a consequence of polar effects exerted by the mutation in conjunction with over-expression of the WT allele (Figure 5.12B). S-layer composition was largely identical between the two mutants. As in the case of the ClosTron mutant, the supernatants from ACE mutant cultures contained significant amounts of partially degraded S-layer proteins including HMW-SLP, LMW-SLP, Cwp2, Cwp66 and Cwp84. Interestingly full length SlpA could not be detected indicating that disruption of SlpA processing observed in *cwp7*::CT could also be a result of a polar effect (Figure 5.13). While the sporulation efficiency of the Δ*cwp7* mutant was still lower than that recorded for WT and complemented mutant, it was significantly higher that seen for the ClosTron mutant in which no spores could be detected throughout the duration of the experiment (Figure 5.14A). This was further supported by purifying Δ*cwp7* spores from SM agar plates. In contrast to the ClosTron mutant, where significant clumping was observed, Δ*cwp7* spore preparations were no different than WT (Figure 5.14B), allowing for the measurement of germination dynamics. To this end purified spores of WT, Δ*cwp7* and Δ*cwp7* + *cwp7* were resuspended in BHIS broth + 0.5% Tch and the drop in OD corresponding to Ca^{2+}-DPA release was measured over time. No significant difference in germination dynamics were observed between the analysed strains (Figure 5.14C). Taken together these results indicate that at least part of the phenotypes seen for the ClosTron *cwp7* mutant could be attributed

to polar effects exerted on neighbouring genes and that non-marked mutations are a more suitable method for disrupting genes in *C. difficile*.

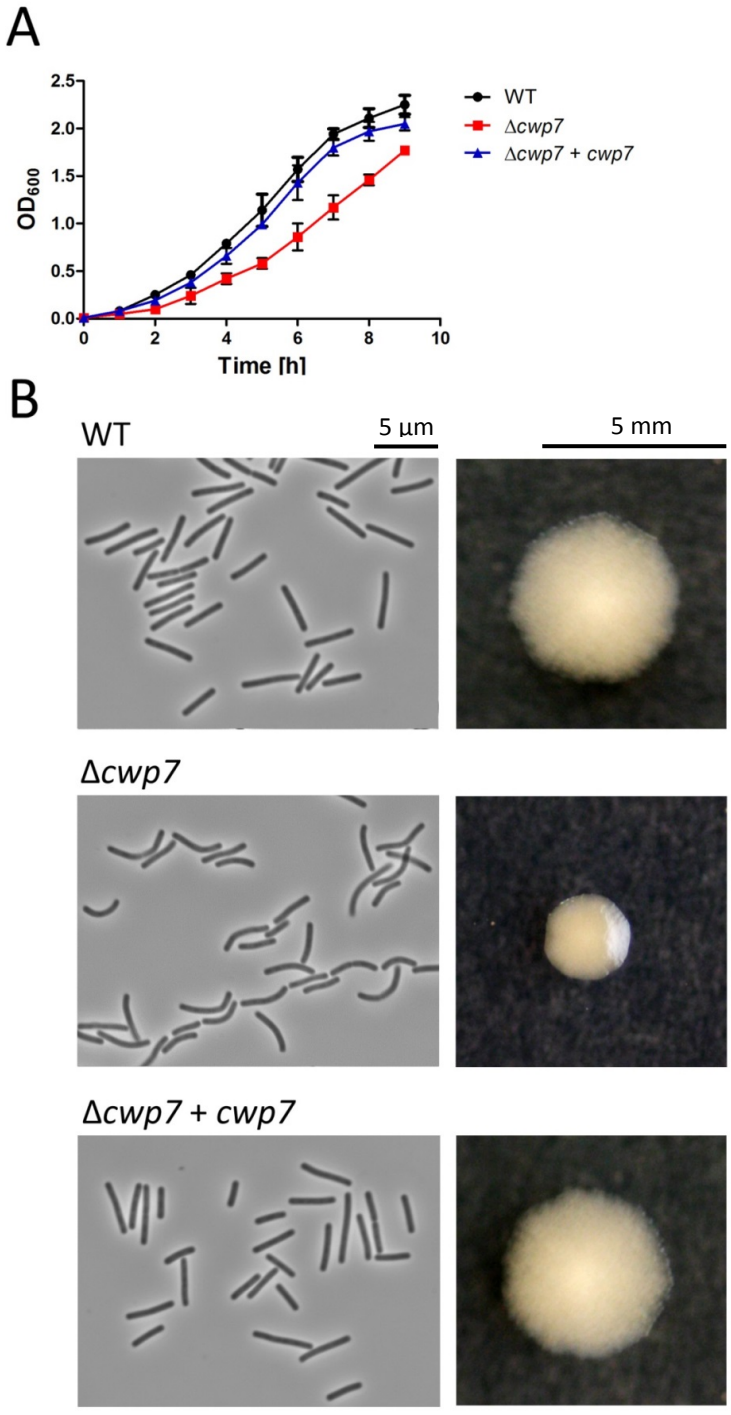

Figure 5.12. Characterisation of *cwp7* ACE mutant phenotype. (A) Growth curve indicating a severe defect in *cwp7*::CT growth rate when compared to WT and the complemented mutant. Data represented as mean ± SD from three biological replicates. **(B)** Phase contrast analysis of single cell morphology revealing slightly curved cells for the *cwp7* mutant when compared to the straight bacilli seen in WT. The mutant also displayed altered colony morphology, showing small, smooth, mucoid colonies as compared to the large, rough colonies seen in WT. No changes to single cell morphology or colony morphology were observed for the complemented mutant. Microscopy data representative of three biological replicates. Universal scale bar provided.

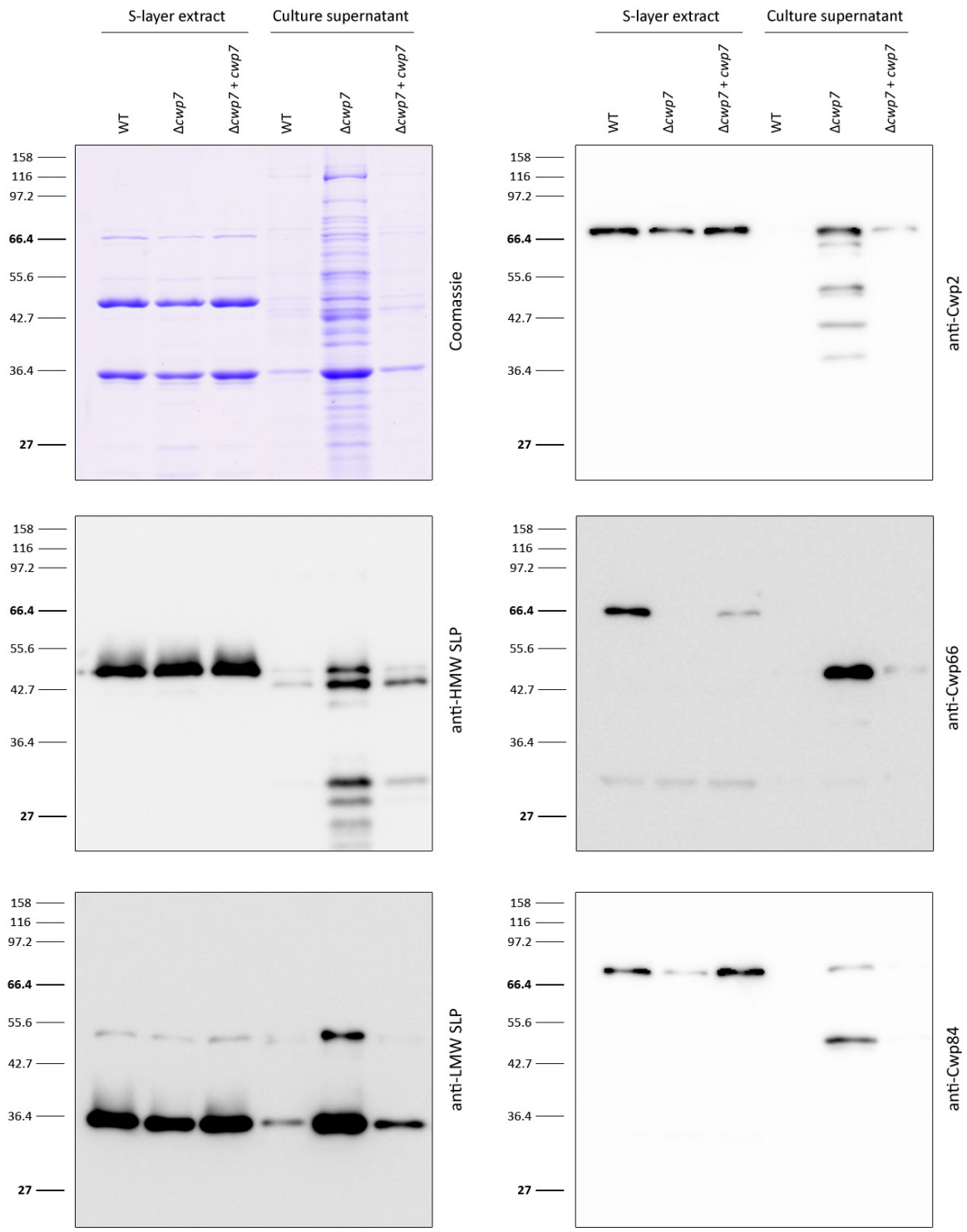

Figure 5.13. Examination of *cwp7* ACE mutant S-layer composition. S-layer extracts were prepared from O/N cultures using low pH glycine. Proteins shed into the supernatant were precipitated using trichloroacetic acid (TCA). All samples were separated using SDS-PAGE and probed for HMW-SLP, LMW-SLP, Cwp2, Cwp66 and Cwp84. Significant amount of all analysed proteins were found to be shed into the culture supernatant. Stark differences in S-layer composition were also observed, particularly with regard to Cwp66 and Cwp84.

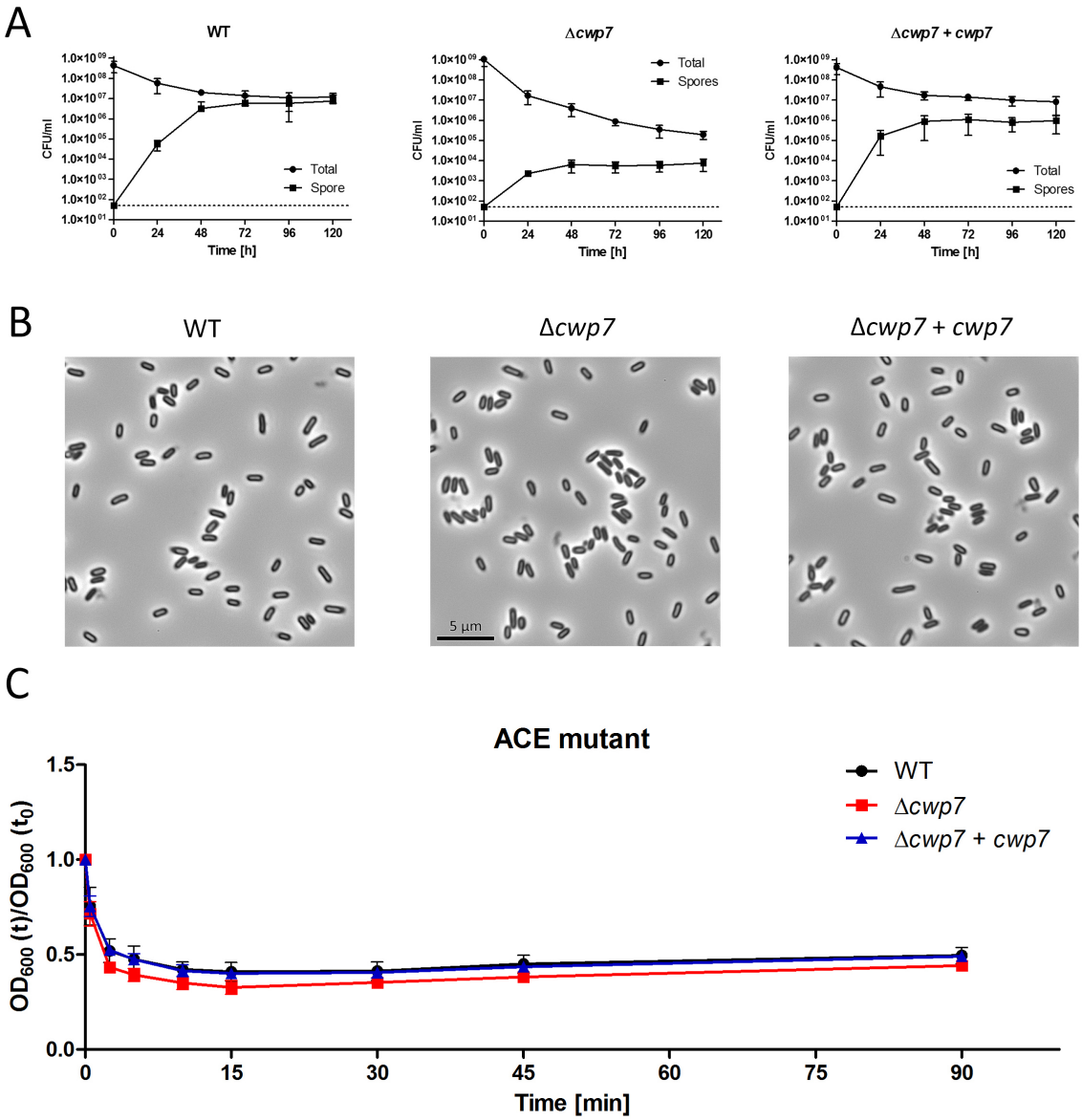

Figure 5.14. Characterisation of *cwp7* ACE mutant sporulation and germination dynamics. (A) Sporulation efficiency was assessed in BHIS broth over a period of 5 days by measuring total and spore CFUs. A significant sporulation defect was observed for Δcwp7 and was alleviated upon complementation. Data presented as means ± SD from three biological replicates. Limit of detection indicated as a horizontal dashed line **(B)** Phase-contrast microscopy analysis of purified spores. No significant difference was observed between WT, Δ*cwp7* and Δ*cwp7 + cwp7*. Scale bars provided. **(C)** Germination dynamics were assessed by measuring the drop in OD_{600} over a period of 90 min, concomitant with the release of Ca^{2+}-DPA. No significant differences in germination dynamics were observed between WT, Δ*cwp7* and Δ*cwp7* + *cwp7*. Data represented as means ± SD from three biological replicates.

5.2.7. Identification of Cwp7 molecular partners

While some proteins perform their functions independently, the vast majority interact with others forming complexes that exert a biological effect only when fully assembled. Characterizing protein-protein interactions is thus crucial in understanding protein functions. A number of methods for studying these interactions are now available, including yeast and bacterial two-hybrid systems, co-immunoprecipitation, cross-linking and pull-down assays allowing researchers to adapt their experiments depending on the strength of the interaction in question. Considering the effect *cwp7* disruption has on *C. difficile* physiology and the apparent lack of a functional domain within its predicted structure, it is likely that Cwp7 is part of a larger complex that requires additional proteins to function.

5.2.7.1. Optimisation of cross-linking conditions

To investigate the interactions between Cwp7 and its potential molecular partners, formaldehyde cross-linking, a well-established method for studying weak and transient interactions between proteins, was used. Due to its small size, formaldehyde can rapidly permeate cell walls and membranes, cross-linking proteins by adding a covalent methyl bridge between amine groups. As the optimal cross-linking conditions may vary significantly and need to be empirically verified on a case-by-case basis, a range of formaldehyde concentrations and exposure times were tested on *cwp7*::CT [pCwp7] (Figure 5.15A). Irrespective of the formaldehyde concentration used, exposure times of more than 30 min resulted in significant depletion of soluble protein in whole cell extracts from cross-linked cultures and caused an accumulation of large-scale, non-physiological protein agglomerates that could not be separated by SDS-PAGE as indicated by Coomassie staining of gel wells. Under the conditions tested a formaldehyde concentration of 0.5% and an exposure time of 15 min were deemed optimal.

5.2.7.2. Cwp7-FLAG cross-linking

In order to facilitate the pull-down of Cwp7 complexes from cross-linked samples, the protein was C-terminally FLAG-tagged by inverse PCR and the resulting plasmid (pMLD089) was conjugated into *cwp7*::CT as previously described, producing 630 Δ*erm cwp7::erm* [pRPF144-*cwp7*-FLAG] (designated *cwp7*::CT [pCwp7$_{FLAG}$]). Exponentially growing cultures of *cwp7*::CT [pCwp7$_{FLAG}$] and WT (negative control) were cross-linked and processed as described in Materials and Methods. Protein complexes containing FLAG-tagged Cwp7 were pulled-down, heat-treated to break the cross-links and analysed using SDS-PAGE and Western immunoblotting. As expected, a single band corresponding to the expected molecular weight of Cwp7-FLAG (40.3 kDa) was detected in *cwp7*::CT [pCwp7$_{FLAG}$] but not in WT samples. In the non-heated sample, an additional band corresponding to a protein species of approx. 85 kDa and reacting with both anti-Cwp7 and anti-FLAG antibodies was also detected. This band was absent in the heated sample, where it was replaced by a 45 kDa protein species (Figure 5.15B). In order to confirm the identify of the pulled-down proteins, MALDI peptide mass fingerprinting was carried out (Dr Len Packman, PNAC Facility, University of Cambridge). The ~40 kDa protein was identified as Cwp7, the ~45 kDa protein was identified as a putative lipoprotein (CD2701) while the ~85 kDa protein was identified as a complex of the two.

CD2701 encodes a previously uncharacterised putative lipoprotein with a predicted mass of 44.5 kDa. Microarray results confirmed that, as in the case of *cwp7*, CD2701 is significantly up-regulated during germination (2.1-fold change; p=0.0129). According to Pfam analysis the CD2701 product belongs to the DUF3798 family of bacterial lipoproteins that share a distant similarity to membrane-bound, ligand binding proteins. Bioinformatic analysis using the LipoP prediction server confirmed the presence of an N-terminal type II signal peptide followed by a cysteine residue at position 21 forming a canonical lipobox motif LTG/C (Juncker *et al.*, 2003). The protein was also found to be present in *C. difficile* 630 lipoproteome as identified my mass spectrometry (Tom Charlton, unpublished results). Interestingly, in 2011 a crystal structure of CD2701 was released by the Joint Centre for Structural Genomics, suggesting that it is a nutrient binding protein and that the

overall structure resembles the sugar binding domain of ABC transporters (http://www.jcsg.org/images/stim/3qi7-YP_001089212.1.html). Further genetic and biochemical analysis would be required to confirm and dissect the interaction between Cwp7 and CD2701 and to elucidate the role these two proteins exert on *C. difficile* physiology.

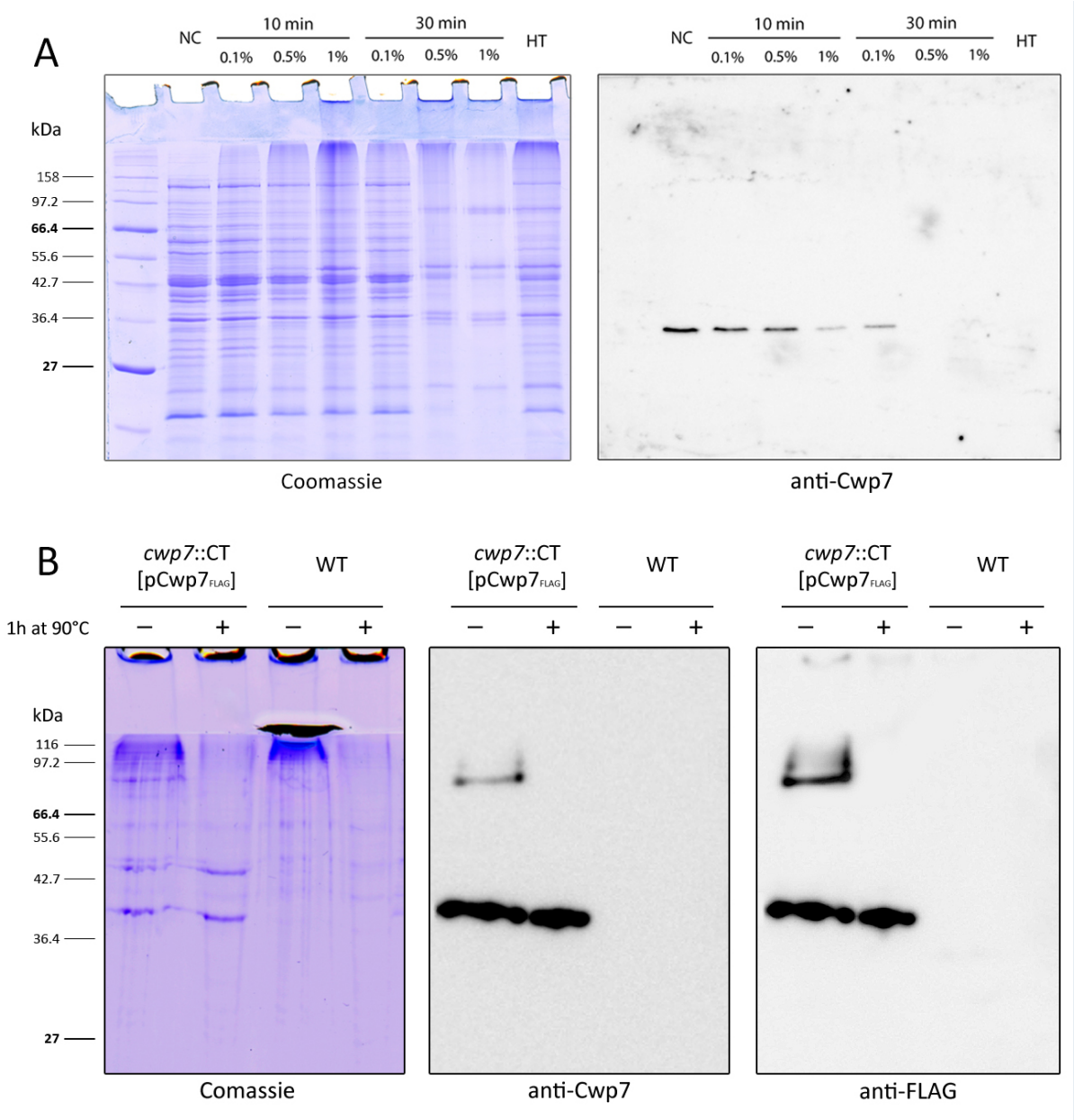

Figure 5.15 Investigation of Cwp7 protein-protein interactions. (A) Optimisation of formaldehyde cross-linking reaction conditions. O/N WT cultures were exposed to varying amount of formaldehyde for either 10 or 30 min. Membrane fractions were prepared, separated *via* SDS-PAE and probed for Cwp7 using Western blotting. The diminishing amount of Cwp7 detected indicates formation of protein complexes. (B) Identification of Cwp7 molecular partners. The *cwp7* ClosTron mutant complemented with a FLAG-tagged copy of the gene was cross-linked using formaldehyde. Protein complexes were pulled-down using affinity chromatography, separated via SDS-PAGE and probed for Cwp7 and FLAG-tag using Western blotting. A protein complex of approx. 85 kDa could be identified in cross-linked samples. Proteins of interest were identified using MALDI peptide mass fingerprinting.

5.3. Discussion

Considering its structure and the apparent lack of a predicted functional domain, Cwp7 does not seem to be a promising target for detailed analysis. Indeed, historically, priority has been given to CWPs harbouring defined functional domains and many of these have now been characterised, including the major S-layer protein SlpA, the putative colonisation factor Cwp66, the cysteine proteases Cwp84 and Cwp13, the phase-variable protein CwpV and the highly conserved cell wall protein Cwp2. Following up on results obtained through the microarray analysis described in Chapter IV, in which *cwp7* was found to be the only CWP gene with significantly up-regulated expression during germination, an attempt was made to further investigate this previously uncharacterised gene. The genomic localisation of *cwp7* is intriguing as it lies on the verge of two loci previously implicated in cell wall and S-layer biogenesis: a cluster of CWP-encoding genes and genes encoding accessory proteins necessary for their translocation across the cell membrane, located upstream, as well as a putative SCWP biogenesis locus located downstream, preceded by *mviN*, clearly involved in peptidoglycan synthesis in other organisms. Considering that within this ~52 kb region lie many genes that are known to be critical for cell wall and S-layer biogenesis, one could predict a similar role for *cwp7*.

Early RT-PCR validation experiments confirmed that *cwp7* expression peaks at 30 min into germination and remains at relatively high levels throughout exponential and stationary growth phases, pointing at the gene's importance in vegetative growth. This was further supported by disrupting *cwp7* expression in *C. difficile* 630Δ*erm* using ClosTron insertional mutagenesis, as the resulting mutant showed a severe growth defect and reduced long term viability. Intriguingly, the effects of *cwp7* disruption were not limited to a reduced growth rate. Phase-contrast microscopy analysis revealed significant changes in single cell morphology, suggesting defects in the general organisation of the cell wall. This was reflected in S-layer composition and stark deficiencies in S-layer assembly as significant amounts of CWPs were being shed into the culture supernatant during growth. Coincidently the large amount of protein shed could explain the mucoid colony phenotype

seen for the mutant strains. Since motility assays carried out in soft agar failed to identify any difference in swimming motility between the *cwp7* mutant and WT, the observed phenotype could be a result of highly viscous, proteinaceous extra-cellular matrix formed by degraded S-layer proteins 'gluing' the cells together. Most surprising was the fact that unlike all CWPs characterised so far and despite carrying the canonical Pfam 04122 cell wall-binding domains, Cwp7 does not localise to the cell wall but instead is anchored to the membrane *via* a 21 aa-long transmembrane helix. This forced us to rethink the dogma of S-layer assembly and consider the possibility that other, previously uncharacterised CWPs might also localise to the membrane and not the cell surface. Indeed upon closer inspection, following bioinformatic analysis of the proteins sequences, two additional members of the CWP family, Cwp18 and Cwp27 were identified as putative membrane proteins carrying predicted lipo-box motifs (Figure 5.16). While disruption of *cwp18* and *cwp27* expression *via* ClosTron did not result in any obvious phenotypes, further work would be necessary to explore the functioning of the somewhat controversial Gram-positive periplasmic space 'sandwiched' between the cell membrane and cell wall peptidoglycan, particularly since this is the most likely location for proteins involved in cell wall biogenesis.

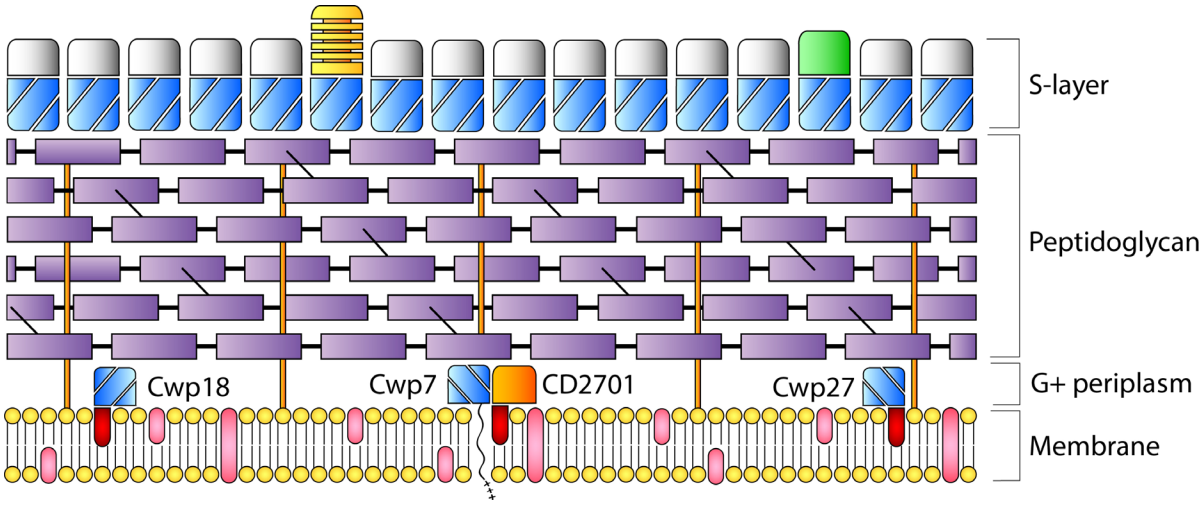

Figure 5.16. Schematic representation of *C. difficile* cell wall. A thick layer of peptidoglycan (purple) is anchored to the membrane through interweaving lipoteichoic acids and is covered by a two-dimensional, paracrystaline protein array forming the S-layer, composed of the major S-layer protein SlpA (white-blue) and minor CWPs scattered throughout. The putative Gram-positive periplasmic space is 'sandwiched' between the cell membrane and the peptidoglycan layer.

Since the initial suggestion of the gene's importance in the general physiology of *C. difficile* came from studying germination, we were keen to investigate whether *cwp7* disruption had any effect on spore formation and germination. While germination did not seem to be affected in the ACE mutant and could not be measured in the ClosTron mutant due to problems with purifying spores, a sporulation defect was observed in both the ClosTron and the ACE mutant, potentially explaining the reduced long term viability of *cwp7*::CT and the observed difficulties in culturing the mutant following prolonged incubation in the anaerobic cabinet. The severity of the observed sporulation defect was more pronounced in the ClosTron mutant, a likely consequence of using insertional mutagenesis and the inherent polar effects exerted on neighbouring genes. The limitations of ClosTron mutagenesis were further highlighted in direct comparison of the two mutants and although most phenotypes initially identified in *cwp7*::CT were also present in Δ*cwp7*, several differences were observed, particularly relating to *in trans* complementation and the resulting gene-dosage effects.

Considering the lack of a functional domain it is likely that Cwp7 forms a complex with additional proteins in order to exert its function. Indeed a molecular partner was identified in the form of CD2701, a previously uncharacterised lipoprotein, although its significance remains to be seen as the complete characterisation of the protein and its role within the complex lies outside of the scope of this study.

Taken together, these results illustrate the predictive power of genome-wide analysis in identifying targets that under different circumstances could have been overlooked due to the lack of features that are typically taken into account when choosing genes for further characterisation. Cwp7 is one such target. While our analysis does not give a definite answer as to the function of the protein, the severe phenotypes observed upon its disruption suggest a central role in cell wall maintenance. Further work would be necessary to elucidate the exact mechanism by which Cwp7 exerts its effect and the potential interactions with CD2701 and other components of the cell wall.

Chapter VI

Construction of a transposon mutant library in *C. difficile* 630Δ*erm*

6.1. Introduction

Understanding the genetic and molecular basis of *C. difficile* pathogenicity is a crucial step in the development of effective therapeutics. A number of methods for directed gene inactivation are now available including ClosTron insertional mutagenesis (Heap *et al*., 2010, Heap *et al*., 2007) and the recently developed allele-coupled exchange (Cartman *et al*., 2012, Heap *et al*., 2012, Ng *et al*., 2013), allowing for reverse genetic studies, in which the exact role of a gene, hypothesized to be important in a particular phenotype, can be elucidated experimentally. While certainly useful, reverse genetic studies are limited in that they are always based on pre-made assumptions regarding a particular gene's function. An alternative approach would be to use random mutant libraries in forward genetic studies aimed at identifying the genetic basis of a particular phenotype without making any assumptions about the genes involved. In other organisms, this is typically achieved through transposon-mediated mutagenesis creating random mutant pools that can be then screened to identify genes involved in a particular phenotype. While *in vitro* transposon mutagenesis systems have been successfully used in the closely related *C. perfringens* (Vidal *et al*., 2009, Lanckriet *et al*., 2009), they rely on being able to transform the recipient organisms. This makes them unsuitable for use in *C. difficile*, as at the time of writing this, DNA can be transferred into *C. difficile* only through conjugation. In 2010, an attempt was made to generate random libraries of *C. difficile* mutants *in vivo*, by introducing *mariner*-based transposons *via* segregationally unstable, 'pseudo-suicide' vectors (Cartman and Minton, 2010). The *mariner*-transposable element *Himar1* has been previously shown to insert randomly into TA target sites in genomes of many bacterial species *via* a 'cut-and-paste' mechanism mediated by the *Himar1* transposase (Lampe *et al*., 1996, Lampe *et al*., 1998), a useful characteristic considering the low GC-content found in the *C. difficile* genome. While the experiment provided good evidence that a *mariner*-based transposon could be an effective tool

for generating random mutants in *C. difficile*, and a number of stable mutants carrying single insertions were identified, the lack of a well-defined conditional replicon meant that the system provided little control over the transposition event and was not suitable for the creation of large scale libraries. Considering the recent advancements in high throughput sequencing methods, allowing researchers to simultaneously screen libraries comprising of as many as one million mutants in virtually any genetically tractable microorganism (reviewed in Barquist *et al*., 2013), a method for creating random libraries of transposon mutants could become a valuable tool in identifying genomic regions required for survival under a particular set of conditions.

In this chapter I describe the design and construction of the first comprehensive transposon mutant library in *Clostridium difficile* using a conditional plasmid recently developed in our group. This is followed by TraDIS analysis of three individual mutant libraries in order to identify genes involved in the process of sporulation and germination. These results are validated *in silico* by analysing genes previously known to be essential for vegetative growth or required for sporulation and/or germination, as well as *in vitro,* by targeted deletion of selected genes followed by in-depth analysis of the resulting phenotypes.

6.2. Results

6.2.1. Design of the *mariner* plasmid and construction of transposon mutant libraries

Plasmid pRPF215 used to create a comprehensive transposon mutant library in *C. difficile* was designed and constructed in its entirety by Dr Robert Fagan. Briefly, codon-optimised *Himar1* hyperactive C9 transposase (Lampe *et al*., 1999) was cloned into pRPF177, a plasmid carrying the inducible P_{tet} promoter but lacking a transcriptional terminator directly downstream of *tetR* (see Appendix A, Figure A1). As a consequence the plasmid is segregationally-unstable upon induction due to transcriptional read-through from the inducible promoter and is rapidly lost from the population as indicated by loss of thiamphenicol resistance shortly after induction with ATc (Dr Robert Fagan, unpublished results). The *mariner*-based transposon was generated by PCR amplifying the *ermB* gene from pMTL82254 and adding a transcriptional terminator and the transposon inverted terminal repeats (ITRs) in successive PCR reactions. The resulting DNA fragment was cloned downstream of the transposase giving pRPF215.

In order to identify genes involved in sporulation and/or germination, three mutant libraries were created by successively passaging a comprehensive mutant pool under selective conditions as described in Materials and Methods. Briefly, the input library was created by spreading out a culture of *C. difficile* 630Δ*erm* [pRPF215] onto BHIS agar supplemented with 15 µg/ml thiamphenicol to select for the plasmid, 5 µg/ml erythromycin to select for the transposon and 100 ng/ml anhydrotetracycline (ATc) to allow for *Himar1*-mediated transposition. Following O/N incubation, the resulting colonies were scraped off, thus forming a library of mutants carrying insertions in all but the essential genes. This culture was then sporulated on SM agar to produce the spore library. At this stage, all mutants carrying insertions in genes required for sporulation were lost from the mutant pool. Following purification, the spore library was germinated back into vegetative cells, losing all mutants carrying insertions in genes required for germination (Figure 6.1). Genomic DNA was extracted from all three libraries and submitted for TraDIS analysis.

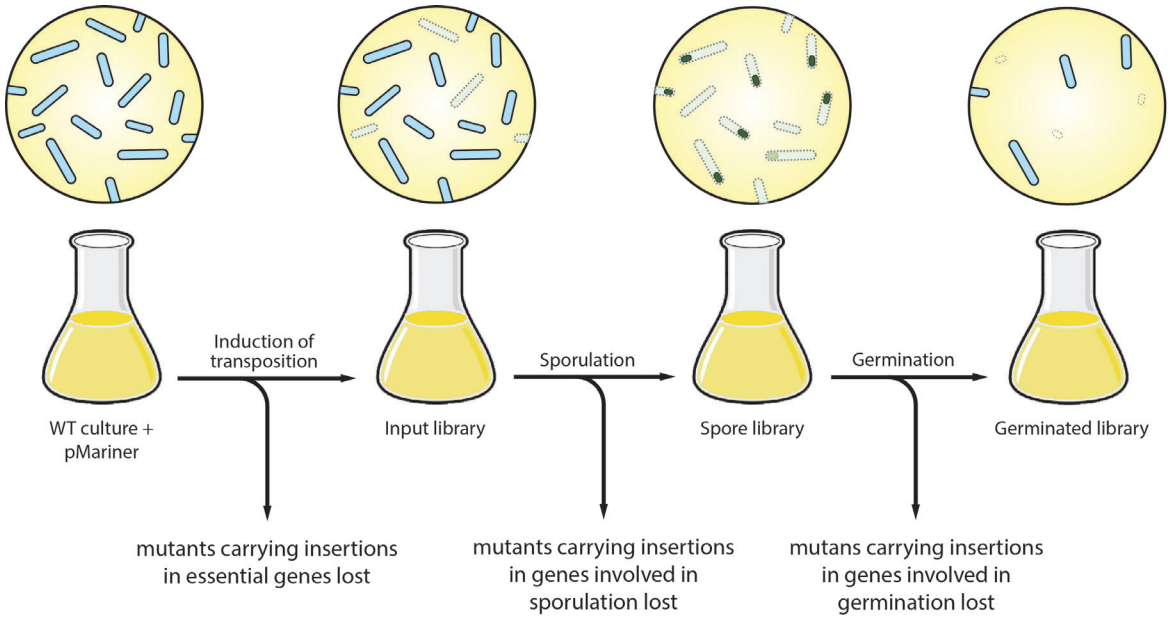

Figure 6.1. Construction of transposon mutant libraries in *C. difficile* 630Δ*erm*. Transconjugants carrying the pRPF215 plasmid were spread out on BHIS agar supplemented with 15 µg/ml thiamphenicol, 5 µg/ml erythromycin and 100 ng/ml ATc to allow for *Himar1*-mediated transposition. Following O/N incubation colonies were scraped of in TY broth and the resulting culture (input library) was used to inoculate 20 ml of nutrient-rich TYG broth supplemented with 5 µg/ml erythromycin and 100 ng/ml ATc. The following day the resulting culture was sub-cultured 1:10 in 20 ml SM broth supplemented with 5 µg/ml erythromycin and 100 ng/ml ATc, grown to OD 0.6 and spread out on SM agar plates to induce sporulation. Spores were harvested and purified as described in Materials and Methods to create the spore library. These were then incubated O/N in BHIS broth supplemented with 0.5% Tch to create the germinated library.

6.2.2. Transposon-Directed Insertion site Sequencing (TraDIS)

TraDIS analysis was carried out in its entirety by Dr Christine Boinett and Dr Amy Cain at the Wellcome Trust Sanger Institute using the HiSeq 2500 platform (Illumina). Sequencing reads were first filtered to only contain those that match the transposon exactly and then stripped of the transposon tag. These were mapped to the reference *C. difficile* 630Δ*erm* genome. In order to reduce signal to noise ratio, 10% of insertion sites at the 3' end were trimmed of as these may not alter the function of the encoded protein drastically. Complete lists of genes with significantly decreased numbers of insertions in the sporulation and germination libraries are included in Appendix B, Tables B1 and B2 respectively.

6.2.3. *In silico* validation of sequencing results

One of the most valuable applications of transposon-insertion site sequencing is the ability to identify genes important in a condition of interest, by comparing differences in the numbers of sequencing reads from input libraries (control) and output libraries that have been subject to passaging under a certain growth condition. Genes that either enhance or detract from survival and/or growth under the given conditions can thus be identified by a decreased or increased insertion frequency.

As a first step to validate the results obtained through TraDIS, genes that were either known to be essential in most bacteria or were previously identified in *C. difficile* as essential for growth were screened for the presence of transposon insertions. These included genes involved in initiation of DNA replication *dnaA, dnaB, dnaC* and *dnaD; gyrA* encoding the A subunit of type II topoisomerase*; murA* encoding UDP-N-acetylglucosamine 1-carboxyvinyltransferase, an enzyme involved in the early steps of peptidoglycan biosynthesis; *slpA* encoding the major S-layer protein and *secA2* encoding an accessory ATPase shown to be essential in energizing the translocation of SlpA across the cell membrane. In general, no insertions were identified in any of the genes in the input library (Figure 6.2). While a small number of insertions could be identified for some of the genes, particularly in the sporulation library, this was most likely a result of sequencing noise.

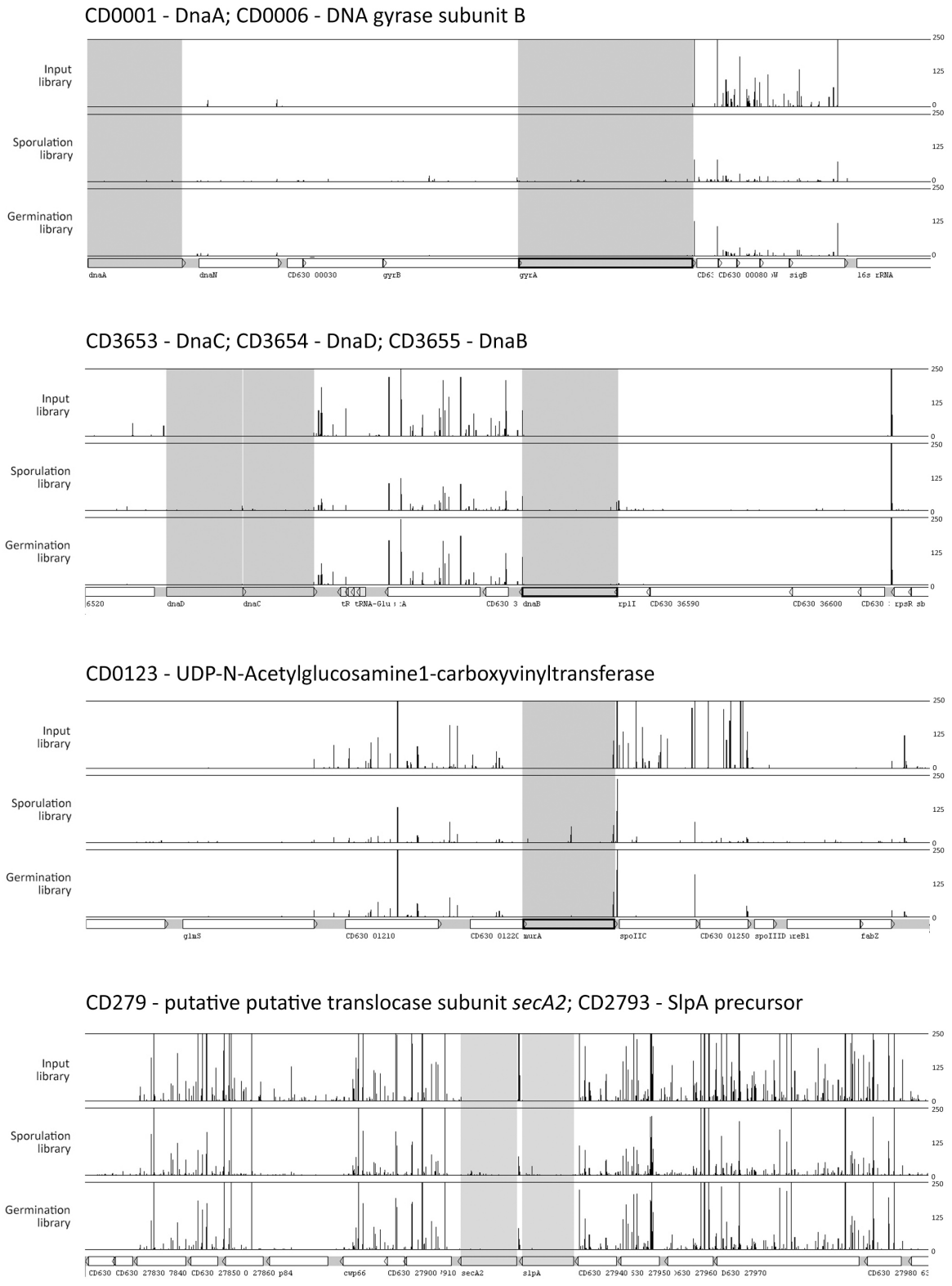

Figure 6.2. Analysis of transposon insertion sites for genes previously identified as essential for vegetative growth. Insertions identified in each of the mutant libraries *via* TraDIS were mapped to the *C. difficile* 630Δ*erm* genome and visualised using Artemis. Scale on the right-hand side of each graph indicates numbers of individual reads. Genomic regions corresponding to essential genes (greyed-out areas) were free of insertions in all the analysed libraries.

In order to verify whether the created libraries can be used to identify genes involved in sporulation and/or germination, genes previously implicated in these aspects of the *C. difficile* life cycle were screened, including *spo0A*, the master regulator of sporulation essential in spore formation but not in vegetative growth (Deakin *et al*., 2012). As expected, while a significant number of insertions could be identified in *spo0A* in the input library, no insertions were present in either the sporulation or the germination library (Figure 6.3). Similarly, genes previously identified as essential in germination such as *cspC* encoding the first germination receptor identified in *C. difficile* (Francis *et al*., 2013) *sleC* encoding the major cortex-lytixc enzyme (Burns *et al*., 2010, Paredes-Sabja *et al*., 2009) and *cspB* encoding a subtilisin-like serine protease essential for SleC activation (Adams *et al*., 2013) were found to lack insertions in both the sporulation and germination library, although few insertions were identified in the input library (Figure 6.3). This is puzzling as neither of these genes has been shown to be required for vegetative growth.

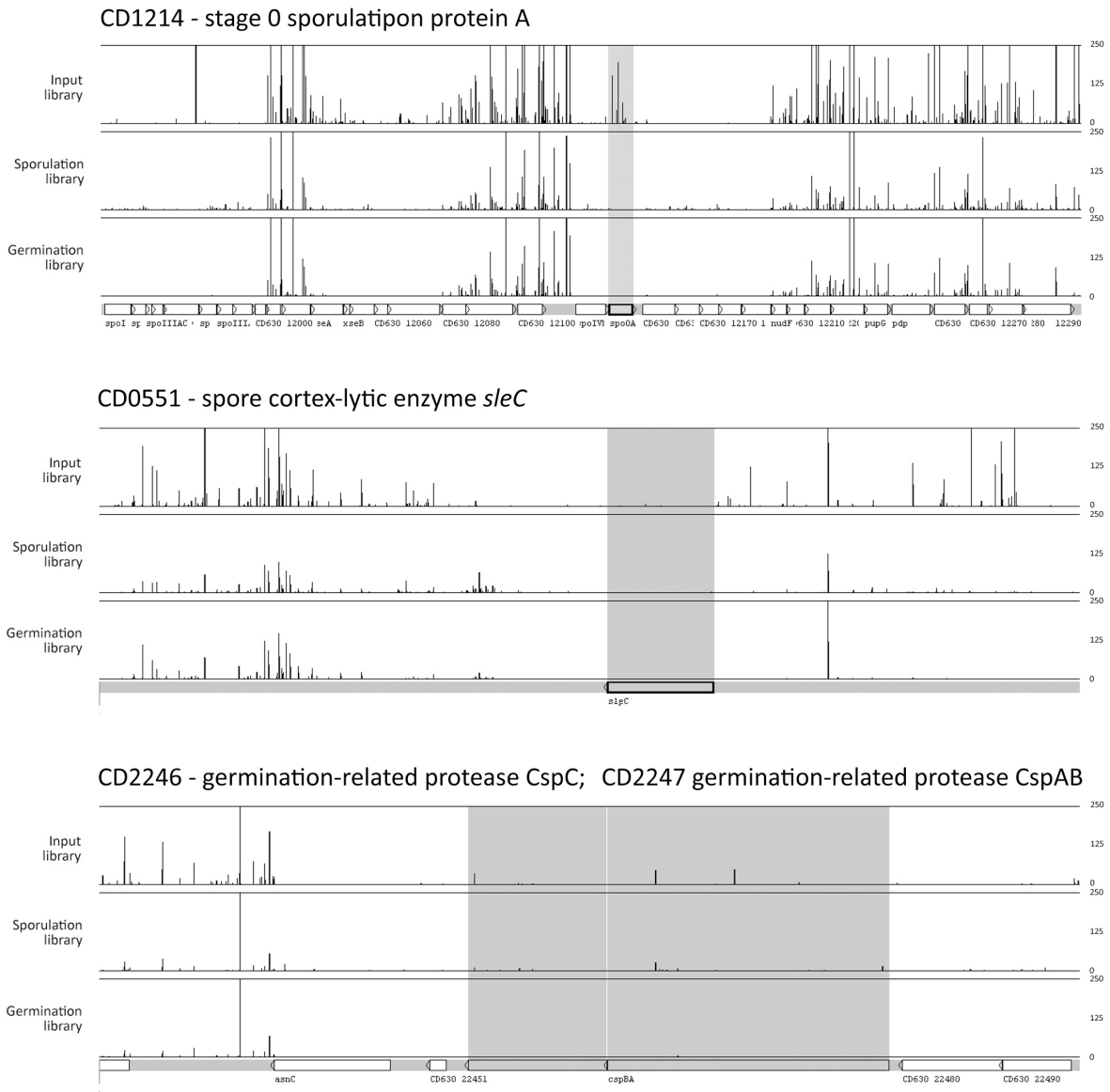

Figure 6.3. Analysis of transposon insertion sites for genes previously identified as involved in sporulation and germination. Insertions identified in each of the mutant libraries *via* TraDIS were mapped to the *C. difficile* 630Δ*erm* genome and visualised using Artemis. Scale on the right-hand side of each graph indicates numbers of individual reads. Genomic regions corresponding to genes involved in sporulation and/or germination (greyed-out areas) were free of insertions.

6.2.4. *In vitro* validation of sequencing results

Knowing that the basic principle of the experiment was validated I set out to identify genes that were not previously confirmed as sporulation/germination factors. To this end, non-essential genes exhibiting significantly decreased numbers of insertions in the sporulation and/or germination library were screened to identify potential targets for 'proof-of-principle' experiments. Insertion plots generated through Artemis were visually analysed and targets with clear differences between the vegetative and sporulation/germination phase were further dissected through BLAST and literature searches for homology with genes previously implicated in sporulation and/or germination in other organisms. The list of potential targets was narrowed down to four genes which are described below (Figure 6.4).

CD3494 encodes a putative spore protein belonging to the YabP superfamily (Pfam 07873), consisting of small proteins conserved in a wide range of bacteria and involved in spore coat assembly during the process of sporulation. The best studied member of this family is the σ^E-dependent, spore coat-associated protein YabP from *B. subtilis*. Using fusions to green fluoresecent protein (GFP), YabP-GFP from *Bacillus subtilis* was shown to assemble into two rings around the forespore before redistributing to form a shell around the developing spore (van Ooij *et al*., 2004). Disruption of *yabP* leads to a severe sporulation defect in late stages of spore morphogeneis as phase–contrast analysis of the sporulating mutant revealed phase-grey spores that failed to brighten upon maturation (Fawcett *et al*., 2000). The product of CD3494 shows 32.6% pairwise identity with YabP from *B. subtilis.*

CD0106 encodes a germination-specific N-acetylmuramoyl-L-alanineamidase, and a putative orthologue of *B. subtilis* CwlD required for muramic-δ-lactam formation during sporulation (Sekiguchi *et al*., 1995). This structural modification of peptidoglycan is found uniquely in the spore cortex and allows for substrate recognition by spore cortex-lytic enzymes (CLEs). While spores of a *B. subtilis cwlD* mutant are able to complete the earliest stages of germination, including the release of Ca^{2+}-DPA and partial spore core rehydration, cortex lysis and, therefore, spore outgrowth does not

occur (Sekiguchi *et al*., 1995, Moir, 2003, Popham *et al*., 1996). The product of CD0106 shows 37% pairwise identity with CwlD from *B. subtilis.*

CD3567 encodes a putative cell wall hydrolase that shows homology to peptidoglycan-binding proteins belonging to the LysM (Lysine Motif) family of enzymes involved in bacterial cell wall degradation (reviewed in Buist *et al*., 2008). Interestingly, LysM domains have previously been shown to play a role in spore development as tandem LysM domains from the *B. subtilis* coat protein YaaH fused to β-lactamase were sufficient to target the fusion protein to the surface of the developing spore (Kodama *et al*., 2000). YaaH is also predicted to be involved in L-alanine-dependant germination as its disruption results in a severe germination defect (Kodama *et al*., 1999). Further evidence came from studying SafA and SpoVID, two LysM-carrying, spore coat morphogenetic proteins also found in *B. subtilis*. SafA is initially targeted to the cortex-coat interface, possibly *via* its LysM domain, while in a second stage it forms a complex with SpoVID through direct protein-protein interaction. Both proteins promote attachment of the spore coat to the spore cortex and are likely to interact with additional coat components (Costa *et al*., 2006).

Finally, CD0125 encodes a putative cell wall endopeptidase and an orthologue of *B. subtilis* SpoIIQ, a σ^F-dependent, forespore-expressed membrane protein initially identified as required at a late stage of engulfment (Londono-Vallejo *et al*., 1997). SpoIIQ localizes to the septum in the forespore membrane (Rubio and Pogliano, 2004, Rodrigues *et al*., 2013, Fredlund *et al*., 2013) where it interacts with the mother cell proteins encoded by the *spoIIIA* locus, several of which show homology to type III and type IV secretion systems (Camp and Losick, 2008). One such protein, SpoIIIAH, directly interacts with SpoIIQ (Doan *et al*., 2005, Blaylock *et al*., 2004) forming a channel that spans the intermembrane space ensuring communication between the two compartments of the sporulating cell (Meisner *et al*., 2008, Doan *et al*., 2009, Camp and Losick, 2009). While being dispensable for engulfment (Sun *et al*., 2000), SpoIIQ-SpoIIIAH it is essential in maintaining forespore integrity and late forespore gene expression (Doan *et al*., 2005, Doan *et al*., 2009).

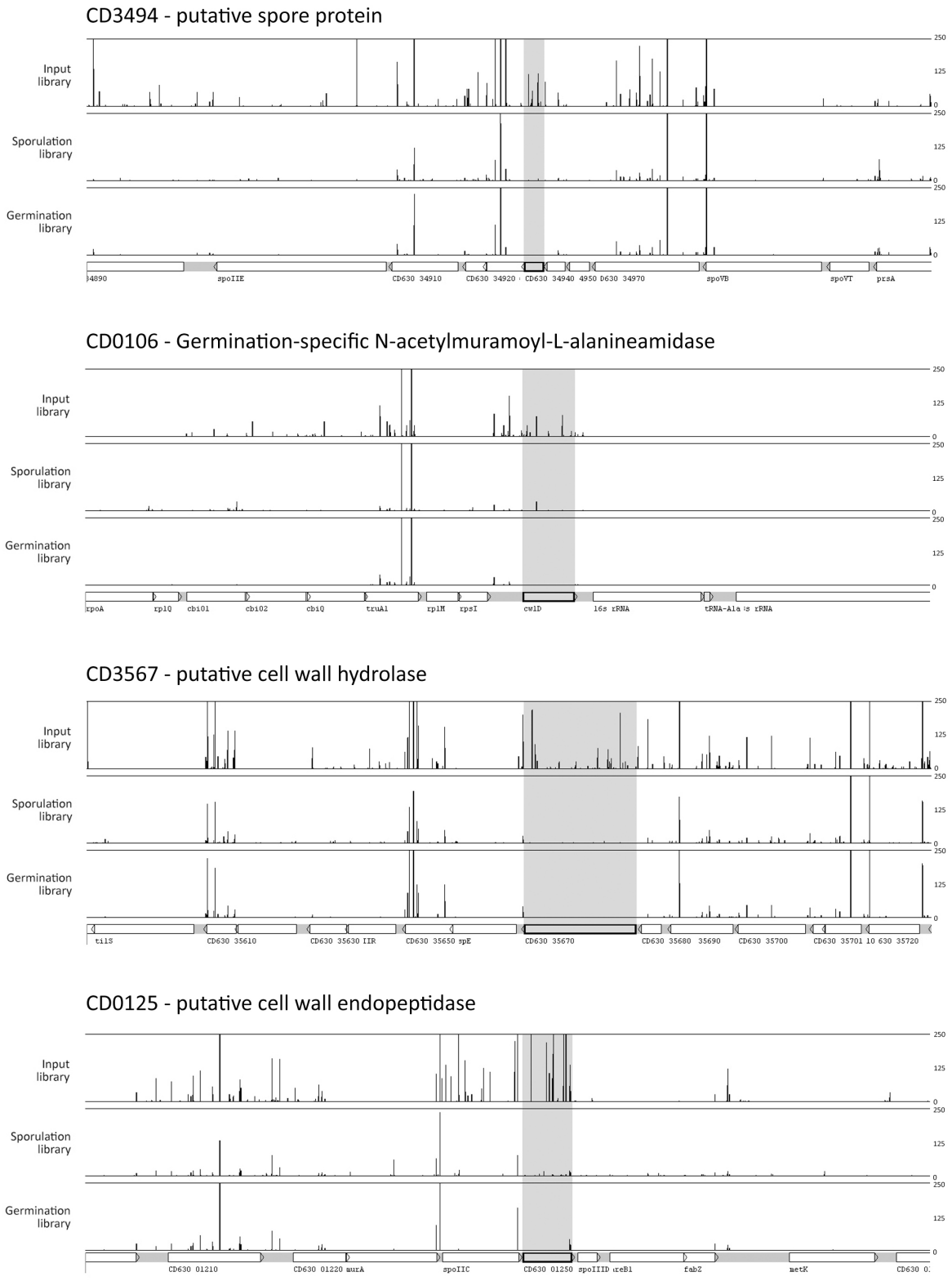

Figure 6.4. Analysis of transposon insertion sites for genes potentially involved in sporulation and germination. Insertions identified in each of the mutant libraries *via* TraDIS were mapped to the *C. difficile* 630Δ*erm* genome and visualised using Artemis. Scale on the right-hand side of each graph indicates numbers of individual reads. Genomic regions corresponding to genes involved in sporulation and/or germination (greyed-out areas) were free of insertions.

6.2.4.1. Mutant construction

The validation of hypotheses derived from transposon-insertion sequencing requires the construction of targeted deletions, as individual mutants cannot be recovered from libraries unless specialized protocols have been followed during library construction. To this end, null mutants were created in the four genes described above. The following strains were constructed: ΔCD3494 – 150 bp in-frame deletion covering aa 11 – 60 out of 85; ΔCD0106 – 390 bp in-frame deletion covering aa 21 – 150 out of 235; ΔCD3567 – 1,137 bp in-frame deletion covering aa 84 – 462 out of 517; ΔCD0125 – 462 bp in-frame deletion covering aa 42 – 195 out of 517. All mutants were generated using *pyrE*-based allele coupled exchange as described previously in Chapter 5. Briefly, mutated alleles were generated by cloning PCR-amplified upstream and downstream homology regions (750 bp for CD3494, 1,200 bp for CD0106, CD3567 and CD0125) into pMTL-YN3 using Gibson Assembly according to manufacturer's instructions. The resulting plasmids were conjugated into 630Δ*erm*Δ*pyrE* as described previously. Following two passages on BHIS agar supplemented with 5 μg/ml uracil, 15 μg/ml thiamphenicol and 250 μg/ml cycloserine, colonies that were noticeably larger (indicative of plasmid integration) were screened by colony PCR to identify single-crossover mutants using (i) primers flanking the upstream and downstream homology regions and (ii) one of these primers in conjunction with a plasmid-specific primer to amplify across the integration junction.

Pure, single crossover mutants were streaked onto *C. difficile* minimal medium (CDMM) supplemented with 5 μg/ml uracil and 2 mg/ml 5-fluoroorotic acid (FOA) to select for plasmid excision. The isolated FOA-resistant colonies were screened by PCR. Double-crossover mutants in which the mutated allele was successfully integrated yielded products smaller than those seen in WT revertants.

In order to restore the *pyrE+* phenotype, plasmid pMTL-YN1 carrying the WT *pyrE* allele was conjugated into the isolated double-crossover mutants. The resulting colonies were re-streaked onto non-supplemented CDMM agar to select for uracil prototrophy indicating successful allele

exchange. Successful restoration of the *pyrE* allele was confirmed by colony PCR using primers flanking the *pyrE* locus [2429/2430] (Figure 6.5) followed by Sanger sequencing of the amplified product.

In order to complement the mutants, WT alleles including the Ribosome Binding Site (RBS) and their native promoter signals identified *via* BPROM (Softberry) were cloned into pMTL-YN1C using Gibson assembly. The resulting plasmids were conjugated into the isolated double-crossover mutants. Following 96h of incubation individual transconjugants were re-streaked onto non-supplemented CDMM agar to select for uracil prototrophy indicating successful allele exchange and the introduction of the WT allele immediately downstream of the concomitantly restored *pyrE* locus. Complementation was confirmed by colony PCR using primers flanking the *pyrE* locus (Figure 6.5) followed by Sanger sequencing of the amplified product.

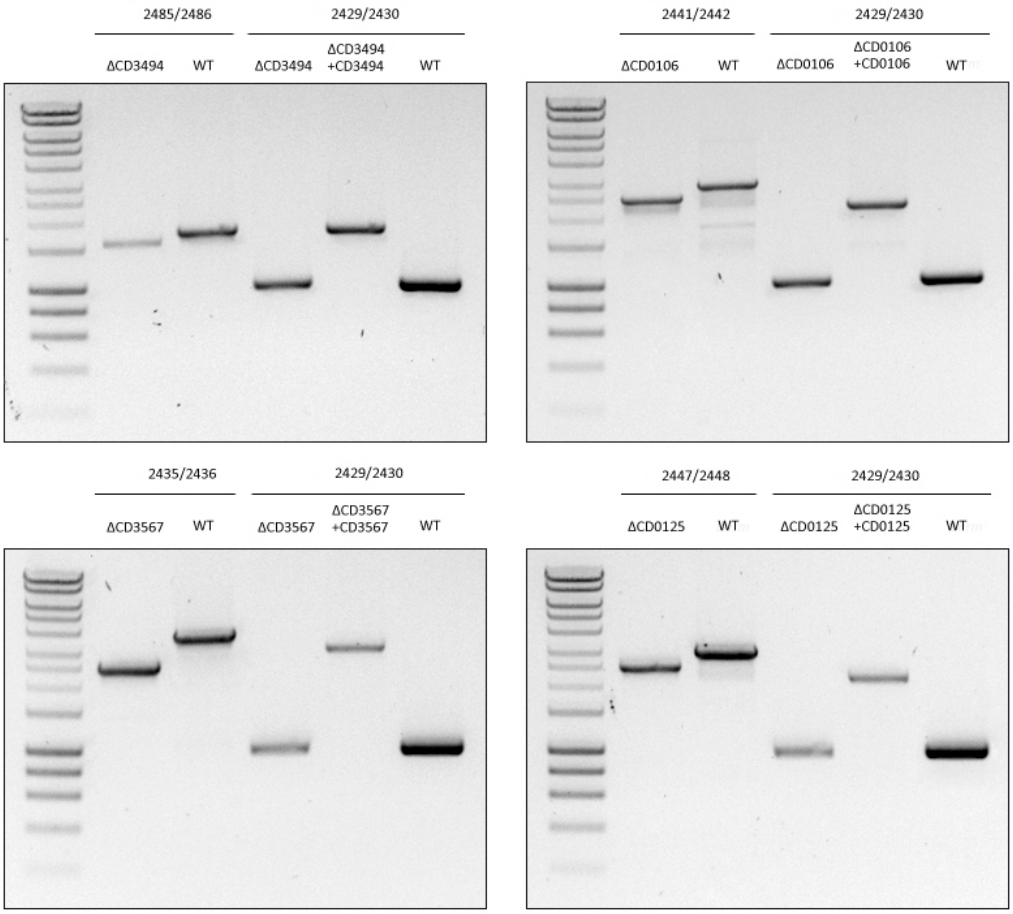

Figure 6.5. Disruption of CD3494, CD0106, CD3567 and CD0125 expression using allele-coupled exchange (ACE). PCR screening of ACE mutants following restoration of the *pyrE* locus and complementation using primers flanking the deletion sites (lanes 1 and 2) and primers flanking the disrupted *pyrE* locus used for complementation (lanes 3, 4 and 5).

6.2.4.2. Phenotypic analysis

6.2.4.2.1. General characteristics

In order to confirm that disruption of the analysed genes did not have any effect on the general fitness of the strains which could introduce bias into further analysis, growth rate in liquid culture was monitored. No significant changes in growth rate could be observed between WT, mutant and complemented strains (Figure 6.6). Similarly, no changes to colony morphology or single cell morphology were noted (data not shown).

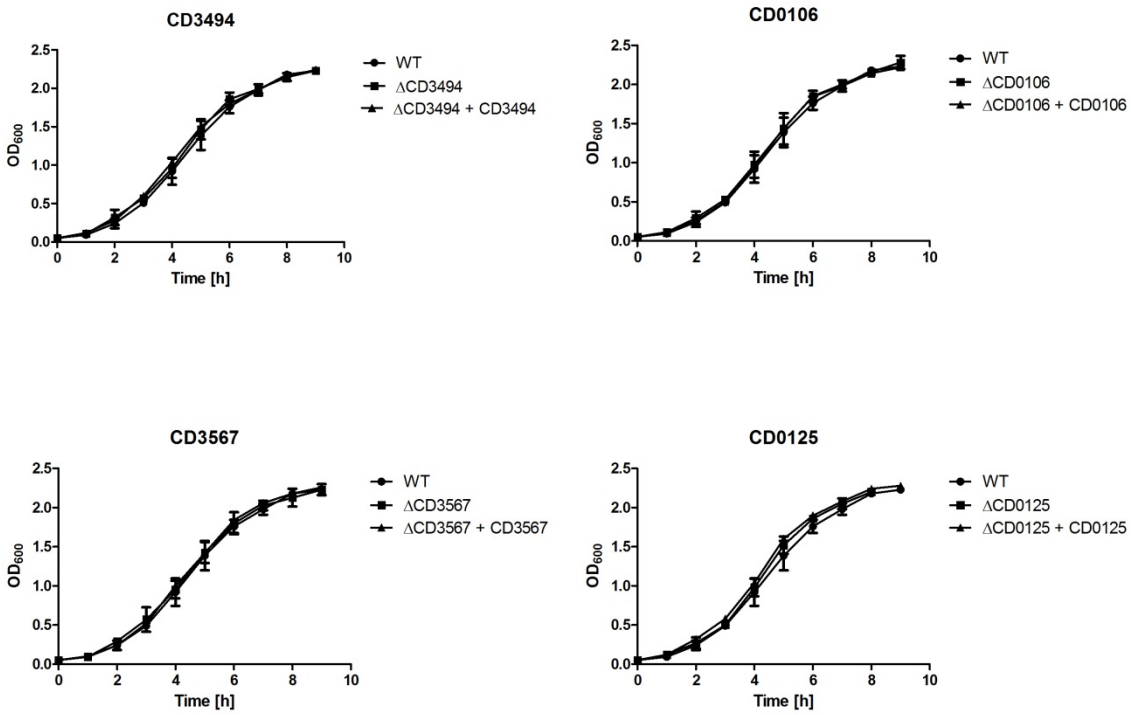

Figure 6.6 Characterisation of ΔCD3494, ΔCD0106, ΔCD3567, ΔCD0125 growth rate. O/N cultures in TY broth were sub-cultured to OD 0.05 and growth was monitored over a period of 9h by measuring OD_{600} at given time points. No significant differences in growth rate were observed between the WT, mutants and complemented strains. Data represented as means ± SD from two biological replicates.

6.2.4.2.2. Sporulation efficiency

Sporulation efficiency in liquid BHIS culture was measured as previously described in Chapter V. While no significant change in sporulation efficiency could be observed for ΔCD3494, all remaining mutants were characterised by significantly reduced spore CFU counts. The number of spore CFUs recovered for both ΔCD0106 and ΔCD0125 was on average 3-log lower than in WT or the complemented mutants. In addition a significant delay in spore formation was observed for ΔCD0106 as the first spore CFUs were detected after 48h as opposed to the 24h seen in WT, ΔCD3494 and ΔCD0125. The sporulation defect was even more pronounced in ΔCD3567 where no spore CFUs could be detected throughout the duration of the experiment (Figure 6.7). As CFUs were the primary read-out of this assay, only cells proficient in both sporulation and germination could be detected. Thus, in order to differentiate between sporulation and germination defects, phase-contrast and fluorescence microscopy were used to monitor spore formation. In support of the sporulation efficiency data, no obvious changes in sporulation were identified for ΔCD3494. Interestingly, even though spore CFU counts for ΔCD0106 were significantly lower than those seen in WT, microscopic analysis failed to identify any defects as mature, phase-bright spores were present in numbers similar to those seen in WT samples. This would suggest that the product of CD0106 is involved in germination and not sporulation, a notion supported by significant homology between CD0106 and *cwlD* found in *B. subtilis.* In accordance with the sporulation efficiency assay, both ΔCD3567 and ΔCD0125 showed a severe sporulation defect. While ΔCD3567 did form small, phase-dark spores that were eventually released following autolysis of the mother cell compartment, no spores could be identified for ΔCD0125, suggesting that sporulation was blocked at an early stage of development (Figure 6.8). Importantly, all phenotypes observed through this analysis were restored to WT upon complementation.

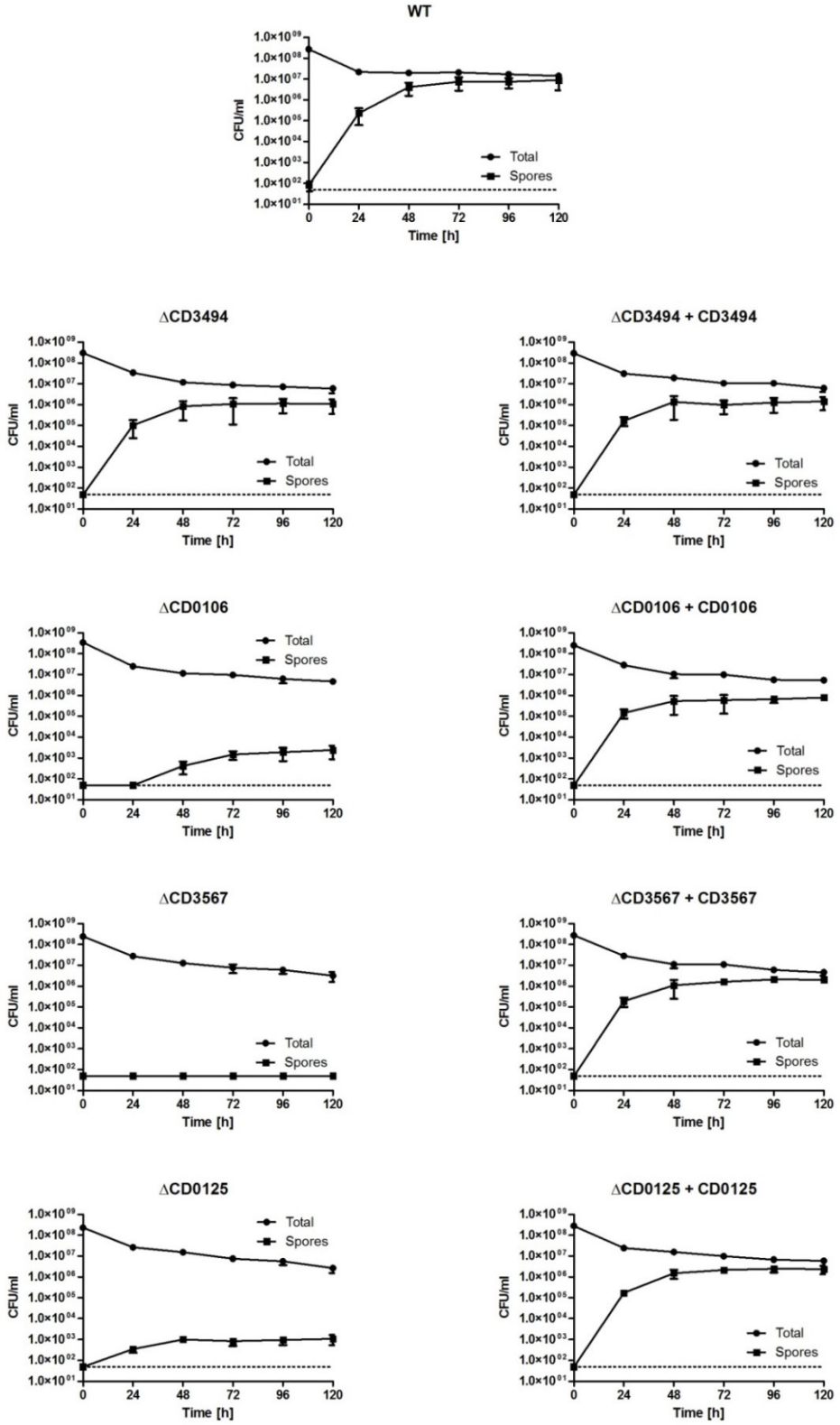

Figure 6.7. Assessment of CD3494, CD0106, CD3567 and CD0125 ACE mutant sporulation efficiency. Sporulation was induced *via* nutrient starvation in BHIS broth and was assessed over a period of 5 days by measuring total and spore CFUs. A severe defect in spore CFU recovery was identified in ΔCD0106, ΔCD3567 and ΔCD0125 throughout the duration of the experiment. In all cases spore CFU levels were restored to WT levels upon complementation. No significant changes in sporulation efficiency were observed for ΔCD3494. Data represented as means ± SD from two biological replicates, each consisting of three technical replicates. A *spo0A* mutant was included in each biological replicate as a sporulation-negative control but was omitted from analysis for reasons of clarity. Limit of detection indicated with a horizontal dashed line.

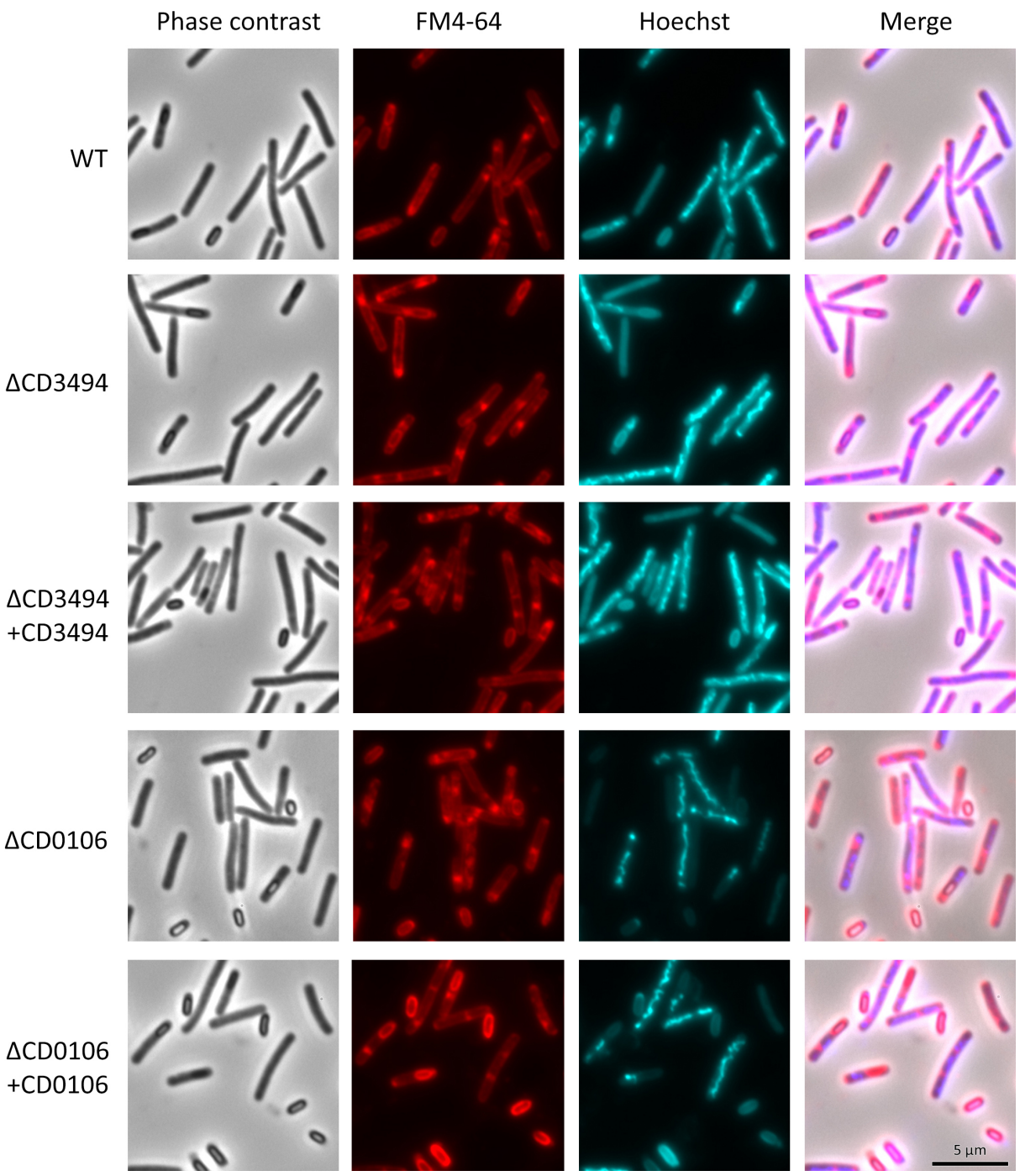
Phase contrast
FM4-64
Hoechst
Merge
WT
ΔCD3494
ΔCD3494
+CD3494
ΔCD0106
ΔCD0106
+CD0106
5 µm

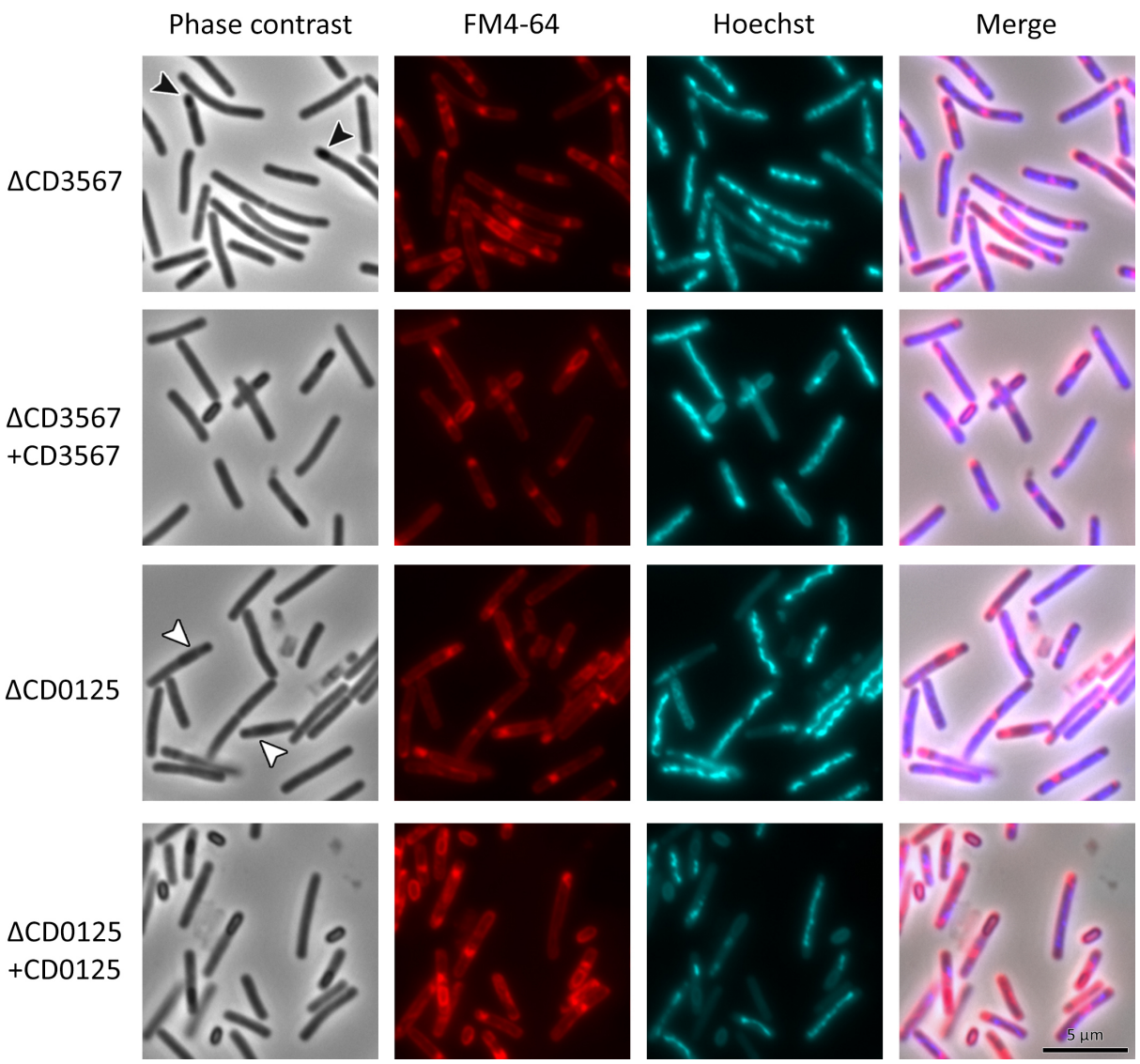

Figure 6.8. Phase contrast and fluorescence microscopy analysis of sporulation in ΔCD3494, ΔCD0106, ΔCD3567 and ΔCD0125. Cultures were sporulated on SM agar for 24h, harvested in PBS and stained with FM4-64 (membrane stain) and Hoechst 33258 (DNA stain). Severe sporulation defects were observed in ΔCD3567 and ΔCD0125 but not in ΔCD3494 and ΔCD0106. In ΔCD3567, small, phase-dark spores were identified (black arrows). These were eventually released into the culture medium following autolysis of the mother cell compartment but could not be isolated form the culture by density gradient centrifugation. In ΔCD0125, no spores were identified as sporulation was aborted at the forespore formation step (white arrows). Microscopy data representative of two biological replicates. Scale bars provided.

6.2.4.2.3. ΔCD0106 and ΔCD3494 germination dynamics

In order to confirm the germination defect observed in ΔCD0106, germination dynamics of purified spores were measured. ΔCD0106 spores re-suspended in BHIS supplemented with 0.5% Tch showed only a 4% drop in OD_{600} after 15 min of incubation as compared to a 54% drop seen in WT (Figure 6.9A). This was further supported by phase-contrast analysis of germinating spores, which revealed that ΔCD0106 spores remain phase-bright even after 180 min of incubation in the presence of the germinant, a period of time sufficient for completion of germination by germination-proficient strains (Figure 6.9B). As previously, WT phenotype was restored upon complementation. No germination defect was seen for ΔCD3494 (Figure 6.9A and 6.9B).

6.2.4.2.4. ΔCD3494 lysozyme resistance

Since CD3494 encodes a putative orthologue of the spore coat-associated protein YabP, and disruption of YabP has been shown to result in spore coat defects, the integrity of ΔCD3494 spore coat was assessed by testing the spore's resistance to lysozyme. To this end purified spores were re-suspended in PBS supplemented with 250 µg/ml lysozyme. At given time points serial dilutions were prepared, spread out on BHIS agar supplemented with 0.1% Tch and CFUs were enumerated following O/N incubation. No significant difference in resistance to lysozyme could be observed between WT, ΔCD3494 or ΔCD3494 + CD3494 (data not shown).

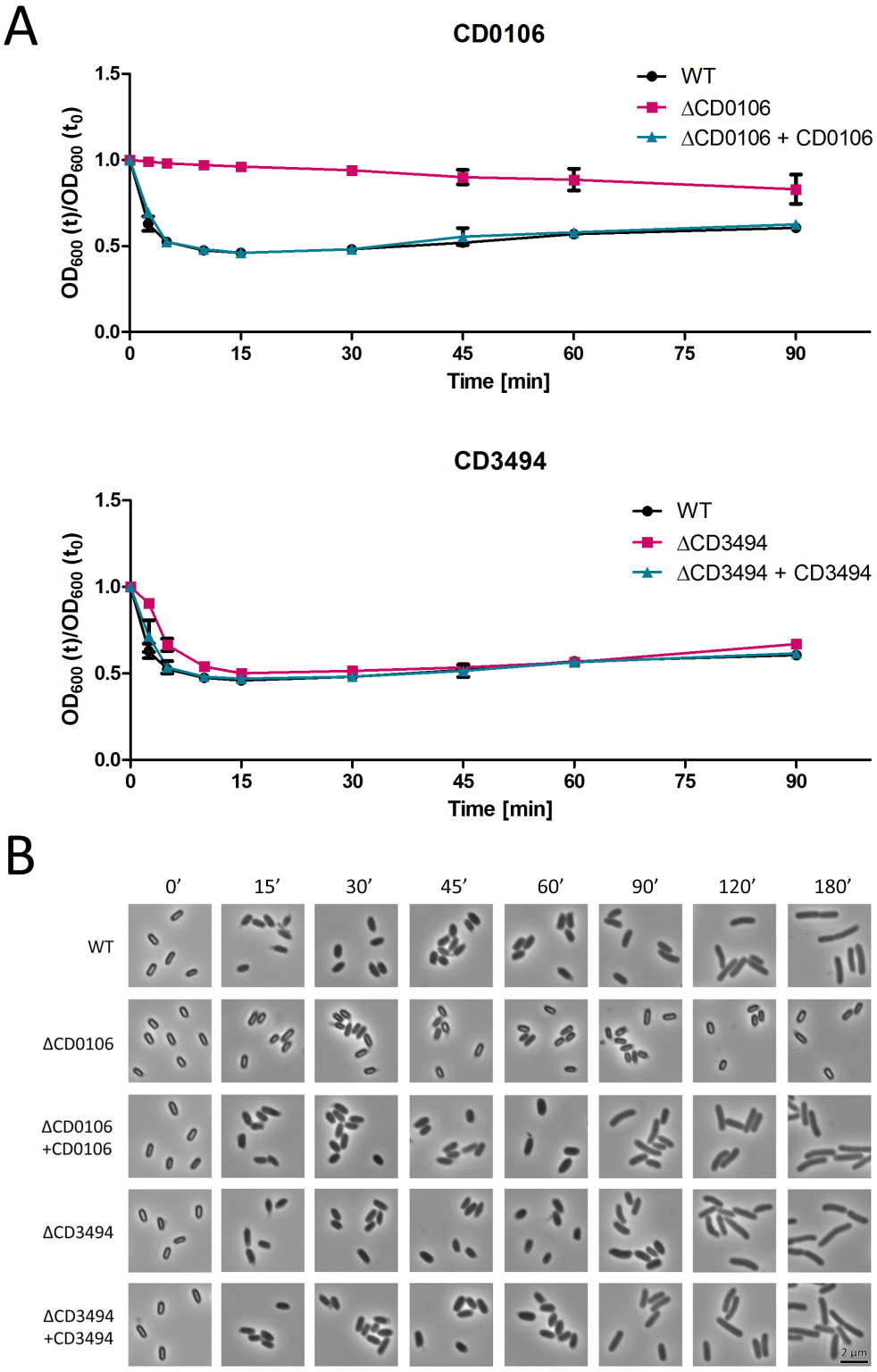

Figure 6.9. Characterisation of germination dynamics in ΔCD0106 and ΔCD3494. Purified spores were re-suspended in BHIS + 0.5% Tch and germination was monitored by **(A)** measuring the drop in OD_{600} concomitant with Ca^{2+}-DPA release and **(B)** phase-contrast microscopy on formaldehyde fixed samples. A severe germination defect was observed in ΔCD0106 as little Ca^{2+}-DPA release was observe when compared to WT and complemented strains and spores remained phase-bright throughout the duration of the experiment. Germination dynamics were restored to WT levels upon complementation. No significant changes in germination dynamics were observed for ΔCD3494. Numerical data presented as means ± SD from three biological replicates. Microscopy data representative of two biological replicates.

6.3. Discussion

As with many aspects of *C. difficile* research, forward genetic studies of *C. difficile* physiology have been hampered by the lack of suitable genetic tools and while transposon mutagenesis has been successfully used in closely related organisms, until now, similar methods have not been available for use in *C. difficile*. Taking advantage of a conditional replicon recently developed in our lab I set out to construct the first comprehensive mutant library in *C. difficile* and use it to identify genes involved in sporulation and germination using TraDIS.

*In silic*o validation of the sequencing results confirmed that our approach could be successfully used to identify genes that are essential for vegetative growth as well as those required for sporulation and/or germination. This was further supported by targeted disruption of selected genes followed by analysis of the resulting phenotypes. Out of the four genes analysed, both CD3567 and CD0125 were shown to be required in sporulation, albeit at different stages of the process.

Considering that the product of CD3567 belongs to the same protein family as YaaH, SafA and SpoVID found in *B. subtilis*, it seem likely that it is involved in spore coat morphogenesis. Indeed, while disruption of CD3567 did not prevent spore formation, the resulting spores were significantly smaller than ones observed in WT and were phase-dark. Interestingly, the aberrant spores formed by the CD3567 mutant failed to germinate. This again is consistent with disruption of the spore coat which under normal circumstances is responsible for efficient interaction of the spore with compounds that trigger germination (Driks, 1999, Henriques and Moran, 2000). As purification of these defective spores proved to be impossible, classical methods used to identify spore coat defects such as measuring lysozyme resistance could not be used. TEM imaging would be necessary to confirm potential changes in spore coat morphology.

While a small number of heat-resistant spores were detected for ΔCD0125 in the sporulation efficiency assay (3-log drop in spore CFUs when compared to WT), no spores could be visualised using phase-contrast microscopy, most likely due to the relatively high detection limit of this method. Instead, a significant number of cells that appeared to be arrested at forespore formation stage

could be observed. This phenotype is consistent with the predicted function of the CD0125 orthologue found in *B. subtilis*, *spoIIQ.* While deletion of *spoIIQ* causes a severe sporulation defect in *B. subtilis*, it does not block spore formation completely (Rodrigues *et al*., 2013). Furthermore, TEM analysis of Δ*spoIIQ* spores revealed that *spoIIQ* disruption causes the forespore to collapse and lose its integrity (Doan *et al*., 2009). This coincides with loss of metabolic potential (Camp and Losick, 2009). A detailed analysis of spore morphogenesis would be required to confirm whether similar phenotypes could be identified in the ΔCD0125 mutant.

The germination defect observed in the ΔCD0106 mutant (4-log drop in spore CFUs when compared to WT) is largely consistent with studies carried out in *B. subtilis*, where disruption of *cwlD* expression resulted in 4 to 8-log drop in spore CFUs recovered following heat-treatment (Popham *et al*., 1996, Sekiguchi *et al*., 1995). While Δ*cwlD* spores were able to carry out the first steps of germination and only a slight delay in Ca^{2+}-DPA release and loss of optical refractibility was observed (Sekiguchi *et al*., 1995), cortex hydrolysis did not occur thus blocking further steps of germination and outgrowth. In contrast, ΔCD0106 spores remained phase bright-throughout the duration of the experiment, suggesting that Ca^{2+}-DPA release did not occur. To some extent, this is consistent with work carried out in the more closely related *C. perfringens* where disruption of *sleC*, a cortex lytic enzyme involved in cortex PG degradation resulted in a severe germination defect, characterised by a significant decrease in the amount of Ca^{2+}-DPA released and the corresponding delay in loss of optical refractibility (Paredes-Sabja *et al*., 2009). These results were later recreated in *C. difficile* by disrupting a *sleC* homologue (CD0551) (Burns *et al*., 2010). Since the product of CD0106 is expected to be involved in the formation of muramyl-δ-lactam, a structural modification found in cortex PG essential for SleC function, one could expect that CD0106 disruption could exert a similar effect in *C. difficile.* Yet the severity of the germination defect observed in ΔCD0106 was higher than that seen upon *sleC* disruption in both *C. perfringens* and *C. difficile* suggesting that additional factors might be in play. While a detailed analysis of the ΔCD0106 germination characteristics lies outside the scope of this study, it would be useful to test whether the colony-forming efficiency of ΔCD0106 spores

was restored to WT levels after decoating and plating on BHIS agar supplemented with lysozyme as has been reported for *C. difficile* and *C. perfringens sleC* mutants (Burns *et al*., 2010, Paredes-Sabja *et al*., 2009).

Finally, disruption of CD3494, a putative spore protein belonging to the YabP superfamily did not result in any obvious phenotype. This is somewhat puzzling as the ΔCD3494 mutant was absent from both the sporulation and germination library while being present in the input library, suggesting that CD3494 is essential in sporulation. In fact, out of all the genes analysed, CD3494 showed the most significant decrease in transposon insertions when comparing the input library to the sporulation library ($p = 5.88 \times 10^{-37}$). It is important to note however, that 'essentiality' is always relative to growth conditions and has traditionally been determined in clonal populations. Since high-throughput transposon sequencing protocols contain a short period of competitive growth before DNA extraction, some mutants might be lost form the population due to competition from the remaining mutant pool (false positive). Conversely, as many otherwise essential genes tolerate insertions in their 3' coding region if this does not encode an essential domain, judging a gene purely by the presence of insertions can result in required genes being identified as non-essential (false negative). Determination of required genomic regions can thus be difficult and care should be taken when interpreting the results of high-throughput assays of gene requirements.

Despite these issues, 'proof-of-principle' experiments carried out in this study have provided good evidence that TraDIS analysis of random mutant libraries is a viable method for identifying genes required for sporulation and germination.

VII. General discussion

Despite the falling numbers of CDI cases reported in the UK in recent years, *C. difficile* remains a heavy burden on the healthcare system, causing disruptions in the functioning of hospitals and care homes, draining valuable resources, and resulting in significant morbidity and mortality (Dubberke and Olsen, 2012). In the United States alone, CDI develops in >500 000 patients, with up to 20 000 deaths per year and its economic impact cannot be underestimated as the yearly healthcare burden in both the United States and Europe has been estimated to be >$3 billion (Rupnik et al., 2009). While progress has been made in understanding the molecular basis of *C. difficile* pathogenicity, the majority of treatment methods currently available are aimed at reducing the bacterial load and preventing toxin-associated symptoms, rather than the onset of infection itself. Spores represent the principal infective stage within the *C. difficile* life cycle (Gerding et al., 2008, Riggs et al., 2007) but must germinate to allow for vegetative cell growth and toxin production, representing an attractive target for intervention. A detailed understanding of sporulation and germination could thus have direct applications for disease prevention in the healthcare environment, facilitating the development of new disinfection regimes, molecular diagnostics and targeted treatments such as vaccines or antibiotics. It has already been shown that germinants can be used in clinical settings to stimulate germination of *C. difficile* spores on contaminated surfaces (Nerandzic and Donskey, 2010, Nerandzic and Donskey, 2013). The resulting vegetative cells are extremely sensitive to stresses such as oxygen, traditional decontamination procedures and the gastric barrier and can therefore be easily killed. Conversely, chemical inhibition of spore germination could reduce the ability of *C. difficile* to colonise the gut and cause disease, becoming an effective tool in CDI prevention and infection control (Howerton et al., 2013).

Historically, *C. difficile* research has been lagging behind studies carried out in other Gram-positive sporeformers such as the model organism *B. subtilis* and the closely related *C. perfringens*, primarily due to difficulties in culturing the pathogen and the limited availability of suitable

methodology. However, recent advancements in the field precipitated by the introduction of new genetic tools have facilitated a more detailed understanding of *C. difficile* physiology. A number of key studies have recently been published, combining large scale genomic, transcriptomic and proteomic approaches with classic microbiology techniques to provide valuable insight into *C. difficile* sporulation, germination and spore morphology. The spore differentiation pathway has been described in great detail, highlighting some of the differences in the spatial and temporal programme of gene expression among *s*poreformers (Pereira et al., 2013). In a genome-wide analysis of cell type-specific gene transcription, Saujet *at al.* (2013) have used promoter mapping together with transcriptional analyses to define the *C. difficile* σ^F, σ^E, σ^G and σ^K regulons, identifying approx. 225 genes under the control of these sigma factors. Finally, by combining RNA sequencing with a detailed analysis of the spore proteome, Pettit *at al.* (2014) have dissected the Spo0A regulon, validating Spo0A as a positive regulator of novel sporulation genes as well as a number of virulence-associated factors and metabolic pathways.

Capitalizing on this wealth of new data as well as new genetic tools developed in the Fairweather lab and by other groups, this study aims to provide a genome-wide overview of sporulation and germination in *C. difficile*. In the final chapter of this thesis I discuss the main conclusions of my work in a broader, biological context, provide further perspectives for studying sporulation and germination in *C. difficile*, and attempt to address some of the questions raised throughout this thesis.

7.1. Sporulation and germination dynamics in *C. difficile*

While sporulation and germination in the model sporeformer *B. subtilis* has been characterised in great detail over the years, at the onset of this project, studies aimed at dissecting the molecular basis of sporulation and germination in *C. difficile* have been lacking, primarily due to difficulties in culturing the pathogen, inconsistencies in methodology and the scarcity of genetic tools necessary for studying the intricacies of *C. difficile* physiology. Here, as part of preliminary work

leading up to a more detailed analysis, we attempted to create a platform for studying sporulation and germination in *C. difficile*, and the phenotypic characterisation of mutants with sporulation and/or germination defects. To this end the optimal conditions for *C. difficile* sporulation have been assessed and the general characteristics of *C. difficile* spores have been analysed.

One of our primary goals was to develop a reproducible method for preparing *C. difficile* spores. In line with previous reports (Putnam *et al*., 2013, Pereira *et al*., 2013), sporulation in liquid culture was found to be extremely inefficient, irrespective of the medium used. This, combined with significant cell lysis observed throughout the experiment, suggests that neither of the sporulation methods described to date seems to be optimal for efficient sporulation of *C. difficile* strains. While gradual desiccation on solid media increased spore yields and made sporulation more homogeneous, sporulation efficiency was still significantly lower that than that seen in *B. subtilis*, suggesting that further optimisation of sporulation methods is necessary. Density gradient centrifugation proved to be a viable alternative to more complex methods of spore purification that require the use of detergents, enzymes and sonication, yielding spore suspensions free of noticeable contaminants. Importantly, an in-depth analysis of the purified spores revealed that their general characteristics including spore ultrastructure and their resistance to heat, chemicals and lysozyme were no different than those described for *B. subtilis* spores. This would be expected, considering that the basic 'blueprint' for endosporulation has evolved within the Firmicutes phylum some 2.5 billion years ago (Paredes *et al*., 2005).

While both spore morphology and the general programme of sporulation appeared to be conserved, several key differences were noticed during spore germination, particularly with regard to the dynamics of the process, its relative synchronicity and the potential role of anaerobic conditions in regulating progression into outgrowth. Analysis of germination dynamics confirmed that *C. difficile* spores respond to the bile salt sodium taurocholate (Tch) as the primary germinant. Interestingly, our experiments also highlighted the importance of maintaining anaerobic conditions during germination. While spores stimulated with Tch in the presence of ambient oxygen levels did

lose their phase-bright appearance, indicating initiation of germination, progression through the remaining stages of the process and eventually outgrowth did not occur. This suggests that oxygen affects signalling downstream of the germination receptor 'circuitry', an intriguing phenomenon, particularly in the light of the fact that in *B. subtilis*, once induced, spores are committed to continue through germination even if the germinant is removed (Yi and Setlow, 2010). While both the molecular basis of this 'fail-safe' mechanism and the fate of germination-arrested spores remain unclear, a means for monitoring ambient oxygen levels in the environment certainly makes sense in the light of the pathogens strictly anaerobic life cycle, as it would prevent premature germination under potentially harmful conditions.

Another intriguing finding of this study was that the dynamics of the germination process differed from those previously described in the closely related *C. botulinum* (Broussolle et al., 2002) and *C. sporogenes* (Bassi *et al*., 2013) where initiation of germination was found to be a much slower process. Importantly, germination was largely synchronous and appeared to be complete within three hours from induction. This is somewhat surprising, particularly when confronted with the heterogeneity of germination rate observed in *Bacillus* species, as well as the more closely related *C. perfringens* and *C. botulinum* (Ghosh and Setlow, 2009, Ghosh and Setlow, 2010, Stringer *et al*., 2005, Wang *et al*., 2011), in which a sub-population of spores fails to germinate upon induction. This kind of 'bet hedging' is often seen in nature, as it ensures the survival of given population in rapidly changing environments. One could argue that the relative homogeneity of the spore population observed under the conditions tested and the resulting synchronicity of germination is a reflection of the unique germination mechanism present in *C. difficile* and/or the fact that the human gut is a relatively stable environment eliminating the need for superdormancy.

7.2. Metabolic changes during germination

Work presented in Chapter IV, has demonstrated the application of microarray technology in providing a genome-wide overview of the temporal gene expression patterns during germination

and outgrowth of *C. difficile* spores, highlighting some of the metabolic changes that accompany these events. Particular attention was paid to genes expressed in the early stages of germination, which are thought to be critical in the transformation of a metabolically dormant spore into an actively growing vegetative cell. Using this approach, around 14% of the genome (511 genes out of 3679) was found to be differentially regulated during germination when compared to the vegetative cell and. Such high percentage of differentially regulated genes is not unusual and has been reported previously in microarray studies carried out in other sporeformers (Bassi *et al*., 2013, Bettegowda *et al*., 2006, Keijser *et al*., 2007), highlighting the severity of changes that the cell must undergo during sporulation. A functional profiling of the microarray results confirmed that many genes identified through our analysis were co-regulated. This was particularly true for genes involved in metabolite transport, transcription and translation as well as a number of biosynthetic pathways, including peptidoglycan and SCWP biogenesis, all necessary in re-building of the basic components of the cell and re-establishing of metabolism.

Potentially, one of the most intriguing aspects of this study was the RNA composition of the dormant spore, particularly with regards to the small rRNA species identified during RNA extraction as well as the abundance of mRNA transcripts and their potential function during the early stages of germination. One group of transcripts that were significantly overrepresented in the spore transcriptome were those encoding redox enzymes, possibly involved in detoxification by scavenging reactive oxygen species (ROS). Similar findings were previously reported by Bettegowda *at al*. (2006) in their microarray analysis of *C. novyi-NT* spores and it seems plausible that this is a common feature among anaerobic sporeformers.

7.3. Cwp7 and the cell wall

In order to further validate the microarray results presented in Chapter IV, several targets identified as differentially expressed during germination, were studied in more detail. These included the previously uncharacterised, putative cell wall proteins: Cwp10 and Cwp29, both of

which were shown to be highly expressed during vegetative growth, as well as Cwp7, the sole member of the CWP family to be up-regulated during germination. While no significant changes were observed upon disruption of either Cwp10 or Cwp29, insertional mutagenesis of Cwp7 resulted in a striking phenotype which suggested the genes involvement in cell wall biogenesis and/or maintenance. This was somewhat surprising considering the proteins structure and its apparent lack of a predicted functional domain. Nonetheless, judging by the data obtained thus far, as well as the genomic context of the gene in question, we felt that a detailed characterisation of the *cwp7* locus was warranted. The localisation of *cwp7* within the *C. difficile* genome was particularly intriguing as it lies on the verge of two loci previously implicated in cell wall and S-layer biogenesis: a cluster of genes encoding members of the CWP family and accessory proteins necessary for their translocation across the cell membrane, as well as a putative SCWP biogenesis locus, preceded by *mviN*, clearly involved in peptidoglycan synthesis in other organisms. Considering that within this ~52 kb region lie many genes previously identified as involved in cell wall and S-layer biogenesis, it was plausible that *cwp7* could play a similar role.

Indeed, upon disruption, phase contrast microscopy analysis revealed significant changes in single cell morphology, suggesting defects in the general organisation of the cell wall. This was reflected in S-layer composition and clear defects in S-layer assembly as significant amounts of CWPs were being shed into the culture supernatant during growth. The most surprising result of our analysis however, was the fact that unlike all CWPs characterised thus far and despite carrying the canonical cell wall-binding domains, Cwp7 does not localise to the cell wall but instead is anchored to the membrane. This forced us to rethink the current dogma of S-layer assembly and consider the possibility that other, previously uncharacterised CWPs might also localise to the membrane and not the cell surface.

While the initial suggestion of the gene's importance in the general physiology of *C. difficile* came from studying germination, we were unable to identify a germination defect in a *cwp7* mutant. However, a sporulation defect was observed, potentially explaining the reduced long term viability

and the observed difficulties in culturing the mutant following prolonged incubation in the anaerobic cabinet. The severity of the observed sporulation defect was more pronounced in the ClosTron mutant, a likely consequence of using insertional mutagenesis and the inherent polar effects exerted on neighbouring genes. The limitations of ClosTron mutagenesis were further highlighted in direct comparison of the two mutants and although most phenotypes initially identified in *cwp7*::CT were also present in Δ*cwp7*, several differences were observed, particularly relating to *in trans* complementation and the resulting gene-dosage effects.

While we were unable to identify a clear function for Cwp7, phenotypes observed upon its disruption point to a role in cell wall biogenesis and/or maintenance. The lack of a defined functional domain suggests that Cwp7 forms a complex with additional proteins in order to exert its function. Indeed, a molecular partner was identified in the form of CD2701, a previously uncharacterised lipoprotein. Interestingly, in Gram-negative organisms, some lipoproteins have been shown to interact with and stimulate peptidoglycan synthases, thus playing an important role in cell wall biogenesis (Paradis-Bleau *et al*., 2010, Typas *et al*., 2010). Considering that disruption of Cwp7 results in severe changes to cell shape, which is largely dictated by the cell wall, one could speculate that the protein is part of a membrane-anchored complex involved in regulating peptidoglycan biosynthesis. This opens up the prospect for further research into the Gram-positive periplasmic space, the protein complexes located within, and their role in cell wall synthesis.

7.4. Transposon mutagenesis and genome-wide analysis of sporulation and germination genes

As with many aspects of *C. difficile* research, forward genetic studies of *C. difficile* physiology have been hampered by the lack of suitable genetic tools and while transposon mutagenesis has been successfully used in closely related organisms, until now, similar methods have not been available for use in *C. difficile*. Taking advantage of a conditional replicon recently developed in our

lab we have constructed the first comprehensive mutant library in *C. difficile* and used next-generation sequencing to identify the core gene set required for sporulation and germination.

*In silic*o validation of the sequencing results confirmed that our approach could be successfully used to screen random mutant libraries for genes that are essential under a particular set of conditions. This was further supported in 'proof-of-principle' experiments where targeted disruption of selected genes was followed by a thorough analysis of the resulting phenotypes. Out of all genes tested at least three showed clear involvement in either sporulation or germination. One of these genes, CD3567, encoding a putative cell hydrolase has since been identified as a homologue of SpoVID, a major spore morphogenetic protein involved in tethering the proteinaceous spore coat to the spore cortex (Putnam *et al*., 2013).

Importantly, once generated, the mutant library can be used to determine gene requirement under any set of selective or permissive conditions. In support of this, in collaboration with Dr Robert Fagan and the Sanger Institute we are now exploring the use of this methodology in identifying the minimal set of genes required for establishment of the colonised state upon ingestion of spores using the mouse model of *C. difficile* infection developed ant the Sanger Institute (Lawley *et al*., 2009) which could have direct implications in developing effective intervention strategies aimed at preventing CDI rather than treating it.

7.5. Concluding remarks

We are now only beginning to understand the molecular basis of *C. difficile* physiology. However, considering the recent advancements in the field of Clostridial research and the range of genetic tools currently at our disposal the path is clear for more robust analysis of the key aspect of CDI. We believe that the data presented in this study, and the methods developed throughout, will provide a basis for further research aimed at elucidating some of the unanswered questions in *C. difficile* pathogenesis, particularly with regard to sporulation and germination, and the role of endospores in establishment of the colonised state.

VIII. References

ADAMS, C. M., ECKENROTH, B. E., PUTNAM, E. E., DOUBLIE, S. & SHEN, A. 2013. Structural and Functional Analysis of the CspB Protease Required for *Clostridium* Spore Germination. *PLoS Pathog,* 9**,** e1003165.

ALBERS, S. V. & MEYER, B. H. 2011. The archaeal cell envelope. *Nat Rev Microbiol,* 9**,** 414-26.

ALEKSHUN, M. N. & LEVY, S. B. 2007. Molecular mechanisms of antibacterial multidrug resistance. *Cell,* 128**,** 1037-50.

ALLO, M., SILVA, J., JR., FEKETY, R., RIFKIN, G. D. & WASKIN, H. 1979. Prevention of clindamycin-induced colitis in hamsters by *Clostridium sordellii* antitoxin. *Gastroenterology,* 76**,** 351-5.

ALSAKER, K. V. & PAPOUTSAKIS, E. T. 2005. Transcriptional program of early sporulation and stationary-phase events in *Clostridium acetobutylicum*. *J Bacteriol,* 187**,** 7103-18.

AUTRET, N., DUBAIL, I., TRIEU-CUOT, P., BERCHE, P. & CHARBIT, A. 2001. Identification of new genes involved in the virulence of *Listeria monocytogenes* by signature-tagged transposon mutagenesis. *Infect Immun,* 69**,** 2054-65.

BACCI, S., MOLBAK, K., KJELDSEN, M. K. & OLSEN, K. E. 2011. Binary toxin and death after *Clostridium difficile* infection. *Emerg Infect Dis,* 17**,** 976-82.

BARBUT, F., DECRE, D., LALANDE, V., BURGHOFFER, B., NOUSSAIR, L., GIGANDON, A., ESPINASSE, F., RASKINE, L., ROBERT, J., MANGEOL, A., BRANGER, C. & PETIT, J. C. 2005. Clinical features of *Clostridium difficile*-associated diarrhoea due to binary toxin (actin-specific ADP-ribosyltransferase)-producing strains. *J Med Microbiol,* 54**,** 181-5.

BARQUIST, L., BOINETT, C. J. & CAIN, A. K. 2013. Approaches to querying bacterial genomes with transposon-insertion sequencing. *RNA Biol,* 10**,** 1161-9.

BARTLETT, J. G., CHANG, T. W., GURWITH, M., GORBACH, S. L. & ONDERDONK, A. B. 1978a. Antibiotic-associated pseudomembranous colitis due to toxin-producing clostridia. *N Engl J Med,* 298**,** 531-4.

BARTLETT, J. G., CHANG, T. W., MOON, N. & ONDERDONK, A. B. 1978b. Antibiotic-induced lethal enterocolitis in hamsters: studies with eleven agents and evidence to support the pathogenic role of toxin-producing Clostridia. *Am J Vet Res,* 39**,** 1525-30.

BARTLETT, J. G. & GERDING, D. N. 2008. Clinical recognition and diagnosis of *Clostridium difficile* infection. *Clin Infect Dis,* 46 Suppl 1**,** S12-8.

BARTLETT, J. G., MOON, N., CHANG, T. W., TAYLOR, N. & ONDERDONK, A. B. 1978c. Role of *Clostridium difficile* in antibiotic-associated pseudomembranous colitis. *Gastroenterology,* 75**,** 778-82.

BASSI, D., CAPPA, F. & COCCONCELLI, P. S. 2013. Array-based transcriptional analysis of *Clostridium sporogenes* UC9000 during germination, cell outgrowth and vegetative life. *Food Microbiol,* 33**,** 11-23.

BEJERANO-SAGIE, M., OPPENHEIMER-SHAANAN, Y., BERLATZKY, I., ROUVINSKI, A., MEYEROVICH, M. & BEN-YEHUDA, S. 2006. A checkpoint protein that scans the chromosome for damage at the start of sporulation in *Bacillus subtilis*. *Cell,* 125**,** 679-90.

BEN-YEHUDA, S., RUDNER, D. Z. & LOSICK, R. 2003. RacA, a bacterial protein that anchors chromosomes to the cell poles. *Science,* 299**,** 532-6.

BETTEGOWDA, C., HUANG, X., LIN, J., CHEONG, I., KOHLI, M., SZABO, S. A., ZHANG, X., DIAZ, L. A., JR., VELCULESCU, V. E., PARMIGIANI, G., KINZLER, K. W., VOGELSTEIN, B. & ZHOU, S. 2006. The genome and transcriptomes of the anti-tumor agent *Clostridium novyi-NT*. *Nat Biotechnol,* 24**,** 1573-80.

BLAYLOCK, B., JIANG, X., RUBIO, A., MORAN, C. P., JR. & POGLIANO, K. 2004. Zipper-like interaction between proteins in adjacent daughter cells mediates protein localization. *Genes Dev,* 18**,** 2916-28.

BLEYMAN, M. & WOESE, C. 1968. Ribosomal Ribonucleic Acid Maturation During Bacterial Spore Germination.

BRANDT, L. J., ARONIADIS, O. C., MELLOW, M., KANATZAR, A., KELLY, C., PARK, T., STOLLMAN, N., ROHLKE, F. & SURAWICZ, C. 2012. Long-term follow-up of colonoscopic fecal microbiota transplant for recurrent *Clostridium difficil*e infection. *Am J Gastroenterol,* 107**,** 1079-87.

BRODER, D. H. & POGLIANO, K. 2006. Forespore engulfment mediated by a ratchet-like mechanism. *Cell,* 126**,** 917-28.

BROUSSOLLE, V., ALBERTO, F., SHEARMAN, C. A., MASON, D. R., BOTELLA, L., NGUYEN-THE, C., PECK, M. W. & CARLIN, F. 2002. Molecular and Physiological Characterisation of Spore Germination in *Clostridium botulinum* and *Clostridium sporogenes*. *Anaerobe,* 8**,** 89-100.

BUIST, G., STEEN, A., KOK, J. & KUIPERS, O. P. 2008. LysM, a widely distributed protein motif for binding to (peptido)glycans. *Mol Microbiol,* 68**,** 838-47.

BURBULYS, D., TRACH, K. A. & HOCH, J. A. 1991. Initiation of sporulation in *Bacillus subtilis* is controlled by a multicomponent phosphorelay. *Cell,* 64**,** 545-52.

BURKHOLDER, W. F., KURTSER, I. & GROSSMAN, A. D. 2001. Replication initiation proteins regulate a developmental checkpoint in *Bacillus subtili*s. *Cell,* 104**,** 269-79.

BURNS, D. A., HEAP, J. T. & MINTON, N. P. 2010a. The diverse sporulation characteristics of *Clostridium difficile* clinical isolates are not associated with type. *Anaerobe,* 16**,** 618-22.

BURNS, D. A., HEAP, J. T. & MINTON, N. P. 2010b. SleC is essential for germination of *Clostridium difficile* spores in nutrient-rich medium supplemented with the bile salt taurocholate. *J Bacteriol,* 192**,** 657-64.

CALABI, E. & FAIRWEATHER, N. 2002. Patterns of sequence conservation in the S-Layer proteins and related sequences in *Clostridium difficile*. *J Bacteriol,* 184**,** 3886-97.

CALABI, E., WARD, S., WREN, B., PAXTON, T., PANICO, M., MORRIS, H., DELL, A., DOUGAN, G. & FAIRWEATHER, N. 2001. Molecular characterization of the surface layer proteins from *Clostridium difficile*. *Mol Microbiol,* 40**,** 1187-99.

CAMP, A. H. & LOSICK, R. 2008. A novel pathway of intercellular signalling in *Bacillus subtilis* involves a protein with similarity to a component of type III secretion channels. *Mol Microbiol,* 69**,** 402-17.

CAMP, A. H. & LOSICK, R. 2009. A feeding tube model for activation of a cell-specific transcription factor during sporulation in *Bacillus subtilis*. *Genes Dev,* 23**,** 1014-24.

CARTER, G. P., DOUCE, G. R., GOVIND, R., HOWARTH, P. M., MACKIN, K. E., SPENCER, J., BUCKLEY, A. M., ANTUNES, A., KOTSANAS, D., JENKIN, G. A., DUPUY, B., ROOD, J. I. & LYRAS, D. 2011. The Anti-Sigma Factor TcdC Modulates Hypervirulence in an Epidemic BI/NAP1/027 Clinical Isolate of *Clostridium difficile*. *PLoS Pathog,* 7**,** e1002317.

CARTER, G. P., LYRAS, D., ALLEN, D. L., MACKIN, K. E., HOWARTH, P. M., O'CONNOR, J. R. & ROOD, J. I. 2007. Binary toxin production in *Clostridium difficile* is regulated by CdtR, a LytTR family response regulator. *J Bacteriol,* 189**,** 7290-301.

CARTMAN, S. T., KELLY, M. L., HEEG, D., HEAP, J. T. & MINTON, N. P. 2012. Precise Manipulation of the *Clostridium difficile* Chromosome Reveals a Lack of Association Between tcdC Genotype and Toxin Production. *Appl Environ Microbiol*.

CARTMAN, S. T. & MINTON, N. P. 2010. A mariner-based transposon system for in vivo random mutagenesis of *Clostridium difficile*. *Appl Environ Microbiol,* 76**,** 1103-9.

CHAMBON, P., DEUTSCHER, M. P. & KORNBERG, A. 1968. Biochemical studies of bacterial sporulation and germination. X. Ribosomes and nucleic acids of vegetative cells and spores of *Bacillus megaterium*. *J Biol Chem,* 243**,** 5110-6.

CHANG, J. Y., ANTONOPOULOS, D. A., KALRA, A., TONELLI, A., KHALIFE, W. T., SCHMIDT, T. M. & YOUNG, V. B. 2008. Decreased diversity of the fecal Microbiome in recurrent *Clostridium difficile*-associated diarrhea. *J Infect Dis,* 197**,** 435-8.

CHANG, T. W., GORBACH, S. L. & BARTLETT, J. B. 1978. Neutralization of *Clostridium difficile* toxin by *Clostridium sordellii* antitoxins. *Infect Immun,* 22**,** 418-22.

CHASTANET, A. & LOSICK, R. 2007. Engulfment during sporulation in *Bacillus subtilis* is governed by a multi-protein complex containing tandemly acting autolysins. *Mol Microbiol,* 64**,** 139-52.

CHESNOKOVA, O. N., MCPHERSON, S. A., STEICHEN, C. T. & TURNBOUGH, C. L., JR. 2009. The spore-specific alanine racemase of *Bacillus anthracis* and its role in suppressing germination during spore development. *J Bacteriol,* 191**,** 1303-10.

CHIANG, S. L. & MEKALANOS, J. J. 1998. Use of signature-tagged transposon mutagenesis to identify *Vibrio cholerae* genes critical for colonization. *Mol Microbiol,* 27**,** 797-805.

CHIRAKKAL, H., O'ROURKE, M., ATRIH, A., FOSTER, S. J. & MOIR, A. 2002. Analysis of spore cortex lytic enzymes and related proteins in *Bacillus subtilis* endospore germination. *Microbiology,* 148**,** 2383-92.

CHUNG, J. D. & STEPHANOPOULOS, G. 1995. Studies of transcriptional state heterogeneity in sporulating cultures of *Bacillus subtilis*. *Biotechnol Bioeng,* 47**,** 234-42.

COHEN, S. H., GERDING, D. N., JOHNSON, S., KELLY, C. P., LOO, V. G., MCDONALD, L. C., PEPIN, J., WILCOX, M. H., SOCIETY FOR HEALTHCARE EPIDEMIOLOGY OF, A. & INFECTIOUS DISEASES

SOCIETY OF, A. 2010. Clinical practice guidelines for *Clostridium difficile* infection in adults: 2010 update by the society for healthcare epidemiology of America (SHEA) and the infectious diseases society of America (IDSA). *Infect Control Hosp Epidemiol,* 31**,** 431-55.

COHN, F. 1877. Untersuchungen über Bacterien. IV. Beiträge zur Biologie der Bacillen. *Beiträge Biol. Pflanzen,* 7**,** 249-276.

COLEY, J., DUCKWORTH, M. & BADDILEY, J. 1975. Extraction and purification of lipoteichoic acids from Gram-positive bacteria. *Carbohydr Res,* 40**,** 41-52.

COSTA, T., ISIDRO, A. L., MORAN, C. P., JR. & HENRIQUES, A. O. 2006. Interaction between coat morphogenetic proteins SafA and SpoVID. *J Bacteriol,* 188**,** 7731-41.

COWAN, A. E., OLIVASTRO, E. M., KOPPEL, D. E., LOSHON, C. A., SETLOW, B. & SETLOW, P. 2004. Lipids in the inner membrane of dormant spores of *Bacillus* species are largely immobile. *Proc Natl Acad Sci U S A,* 101**,** 7733-8.

CROBACH, M. J., DEKKERS, O. M., WILCOX, M. H. & KUIJPER, E. J. 2009. European Society of Clinical Microbiology and Infectious Diseases (ESCMID): data review and recommendations for diagnosing *Clostridium difficile*-infection (CDI). *Clin Microbiol Infect,* 15**,** 1053-66.

CURRY, S. R., MARSH, J. W., MUTO, C. A., O'LEARY, M. M., PASCULLE, A. W. & HARRISON, L. H. 2007. tcdC genotypes associated with severe TcdC truncation in an epidemic clone and other strains of *Clostridium difficile*. *J Clin Microbiol,* 45**,** 215-21.

DANIEL, R. A. & ERRINGTON, J. 1993. Cloning, DNA sequence, functional analysis and transcriptional regulation of the genes encoding dipicolinic acid synthetase required for sporulation in *Bacillus subtilis*. *J Mol Biol,* 232**,** 468-83.

DAWSON, L. F., VALIENTE, E., DONAHUE, E. H., BIRCHENOUGH, G. & WREN, B. W. 2011. Hypervirulent *Clostridium difficile* PCR-ribotypes exhibit resistance to widely used disinfectants. *PLoS One,* 6**,** e25754.

DE HOON, M. J., EICHENBERGER, P. & VITKUP, D. 2010. Hierarchical evolution of the bacterial sporulation network. *Curr Biol,* 20**,** R735-45.

DE LA RIVA, L., WILLING, S. E., TATE, E. W. & FAIRWEATHER, N. F. 2011. Roles of cysteine proteases Cwp84 and Cwp13 in biogenesis of the cell wall of *Clostridium difficile*. *J Bacteriol,* 193**,** 3276-85.

DEAKIN, L. J., CLARE, S., FAGAN, R. P., DAWSON, L. F., PICKARD, D. J., WEST, M. R., WREN, B. W., FAIRWEATHER, N. F., DOUGAN, G. & LAWLEY, T. D. 2012. The *Clostridium difficile spo0A* gene is a persistence and transmission factor. *Infect Immun,* 80**,** 2704-11.

DEMBEK, M., REYNOLDS, C. B. & FAIRWEATHER, N. F. 2011. The *Clostridium difficile* cell wall protein CwpV undergoes enzyme-independent intramolecular autoproteolysis. *J Biol Chem*.

DOAN, T., MARQUIS, K. A. & RUDNER, D. Z. 2005. Subcellular localization of a sporulation membrane protein is achieved through a network of interactions along and across the septum. *Mol Microbiol,* 55**,** 1767-81.

DOAN, T., MORLOT, C., MEISNER, J., SERRANO, M., HENRIQUES, A. O., MORAN, C. P., JR. & RUDNER, D. Z. 2009. Novel secretion apparatus maintains spore integrity and developmental gene expression in *Bacillus subtilis*. *PLoS Genet,* 5**,** e1000566.

DRIKS, A. 1999. *Bacillus subtilis* spore coat. *Microbiol Mol Biol Rev,* 63**,** 1-20.

DUBBERKE, E. R. & OLSEN, M. A. 2012. Burden of *Clostridium difficile* on the healthcare system. *Clin Infect Dis,* 55 Suppl 2**,** S88-92.

DUBBERKE, E. R., RESKE, K. A., NOBLE-WANG, J., THOMPSON, A., KILLGORE, G., MAYFIELD, J., CAMINS, B., WOELTJE, K., MCDONALD, J. R., MCDONALD, L. C. & FRASER, V. J. 2007. Prevalence of *Clostridium difficile* environmental contamination and strain variability in multiple health care facilities. *Am J Infect Control,* 35**,** 315-8.

DWORKIN, J. & LOSICK, R. 2005. Developmental commitment in a bacterium. *Cell,* 121**,** 401-9.

EISEMAN, B., SILEN, W., BASCOM, G. S. & KAUVAR, A. J. 1958. Fecal enema as an adjunct in the treatment of pseudomembranous enterocolitis. *Surgery,* 44**,** 854-9.

EMERSON, J. & FAIRWEATHER, N. F. 2009. Surface structures of *Clostridium difficile* and other clostridia. *In:* BRUGGEMANN, H. & GOTTSCHALK, G. (eds.) *Clostridia - Molecular Biology in the Post-genomic Era.* Norfolk, UK: Caister Academic Press.

EMERSON, J. E., REYNOLDS, C. B., FAGAN, R. P., SHAW, H. A., GOULDING, D. & FAIRWEATHER, N. F. 2009. A novel genetic switch controls phase variable expression of CwpV, a *Clostridium difficile* cell wall protein. *Mol Microbiol,* 74**,** 541-556.

EMERSON, J. E., STABLER, R. A., WREN, B. W. & FAIRWEATHER, N. F. 2008. Microarray analysis of the transcriptional responses of *Clostridium difficile* to environmental and antibiotic stress. *J Med Microbiol,* 57**,** 757-64.

ERRINGTON, J. 1993. *Bacillus subtilis* sporulation: regulation of gene expression and control of morphogenesis. *Microbiol Rev,* 57**,** 1-33.

ERRINGTON, J. 2003. Regulation of endospore formation in *Bacillus subtilis*. *Nat Rev Microbiol,* 1**,** 117-26.

EYRE, D. W., CULE, M. L., WILSON, D. J., GRIFFITHS, D., VAUGHAN, A., O'CONNOR, L., IP, C. L., GOLUBCHIK, T., BATTY, E. M., FINNEY, J. M., WYLLIE, D. H., DIDELOT, X., PIAZZA, P., BOWDEN, R., DINGLE, K. E., HARDING, R. M., CROOK, D. W., WILCOX, M. H., PETO, T. E. & WALKER, A. S. 2013. Diverse sources of *Clostridium difficile* infection identified on whole-genome sequencing. *N Engl J Med,* 369**,** 1195-205.

FAGAN, R. P., ALBESA-JOVE, D., QAZI, O., SVERGUN, D. I., BROWN, K. A. & FAIRWEATHER, N. F. 2009. Structural insights into the molecular organization of the S-layer from *Clostridium difficile*. *Mol Microbiol,* 71**,** 1308-22.

FAGAN, R. P. & FAIRWEATHER, N. F. 2011. *Clostridium difficile* has two parallel and essential Sec secretion systems. *J Biol Chem,* 286**,** 27483-27493.

FAGAN, R. P. & FAIRWEATHER, N. F. 2014. Biogenesis and functions of bacterial S-layers. *Nat Rev Microbiol*.

FAGAN, R. P., JANOIR, C., COLLIGNON, A., MASTRANTONIO, P., POXTON, I. R. & FAIRWEATHER, N. F. 2011. A proposed nomenclature for cell wall proteins of *Clostridium difficile*. *J Med Microbiol,* 60**,** 1225-8.

FAWCETT, P., EICHENBERGER, P., LOSICK, R. & YOUNGMAN, P. 2000. The transcriptional profile of early to middle sporulation in *Bacillus subtilis*. *Proc Natl Acad Sci U S A,* 97**,** 8063-8.

FRANCIS, M. B., ALLEN, C. A., SHRESTHA, R. & SORG, J. A. 2013. Bile Acid Recognition by the *Clostridium difficile* Germinant Receptor, CspC, Is Important for Establishing Infection. *PLoS Pathog,* 9**,** e1003356.

FREDLUND, J., BRODER, D., FLEMING, T., CLAUSSIN, C. & POGLIANO, K. 2013. The SpoIIQ landmark protein has different requirements for septal localization and immobilization. *Mol Microbiol,* 89**,** 1053-68.

FUJITA, M. & LOSICK, R. 2005. Evidence that entry into sporulation in *Bacillus subtilis* is governed by a gradual increase in the level and activity of the master regulator Spo0A. *Genes Dev,* 19**,** 2236-44.

GALPERIN, M. Y., MEKHEDOV, S. L., PUIGBO, P., SMIRNOV, S., WOLF, Y. I. & RIGDEN, D. J. 2012. Genomic determinants of sporulation in Bacilli and Clostridia: towards the minimal set of sporulation-specific genes. *Environ Microbiol,* 14**,** 2870-90.

GARRICK-SILVERSMITH, L. & TORRIANI, A. 1973. Macromolecular syntheses during germination and outgrowth of *Bacillus subtilis* spores. *J Bacteriol,* 114**,** 507-16.

GEE, C. L., PAPAVINASASUNDARAM, K. G., BLAIR, S. R., BAER, C. E., FALICK, A. M., KING, D. S., GRIFFIN, J. E., VENGHATAKRISHNAN, H., ZUKAUSKAS, A., WEI, J. R., DHIMAN, R. K., CRICK, D. C., RUBIN, E. J., SASSETTI, C. M. & ALBER, T. 2012. A phosphorylated pseudokinase complex controls cell wall synthesis in mycobacteria. *Sci Signal,* 5**,** ra7.

GEORGE, R. H., SYMONDS, J. M., DIMOCK, F., BROWN, J. D., ARABI, Y., SHINAGAWA, N., KEIGHLEY, M. R., ALEXANDER-WILLIAMS, J. & BURDON, D. W. 1978. Identification of *Clostridium difficile* as a cause of pseudomembranous colitis. *Br Med J,* 1**,** 695.

GERDING, D. N., MUTO, C. A. & OWENS, R. C., JR. 2008. Measures to control and prevent *Clostridium difficile* infection. *Clin Infect Dis,* 46 Suppl 1**,** S43-9.

GHOSH, S., SCOTLAND, M. & SETLOW, P. 2012. Levels of germination proteins in dormant and superdormant spores of *Bacillus subtilis*. *J Bacteriol,* 194**,** 2221-7.

GHOSH, S. & SETLOW, P. 2009. Isolation and characterization of superdormant spores of *Bacillus species*. *J Bacteriol,* 191**,** 1787-97.

GHOSH, S. & SETLOW, P. 2010. The preparation, germination properties and stability of superdormant spores of *Bacillus cereus*. *J Appl Microbiol,* 108**,** 582-90.

GIEL, J. L., SORG, J. A., SONENSHEIN, A. L. & ZHU, J. 2010. Metabolism of bile salts in mice influences spore germination in *Clostridium difficile*. *PLoS One,* 5**,** e8740.

GONZALEZ-PASTOR, J. E., HOBBS, E. C. & LOSICK, R. 2003. Cannibalism by sporulating bacteria. *Science,* 301**,** 510-3.

GOUGH, E., SHAIKH, H. & MANGES, A. R. 2011. Systematic review of intestinal microbiota transplantation (fecal bacteriotherapy) for recurrent *Clostridium difficile* infection. *Clin Infect Dis,* 53**,** 994-1002.

GOVIND, R. & DUPUY, B. 2012. Secretion of *Clostridium difficile* toxins A and B requires the holin-like protein TcdE. *PLoS Pathog,* 8**,** e1002727.

GREHAN, M. J., BORODY, T. J., LEIS, S. M., CAMPBELL, J., MITCHELL, H. & WETTSTEIN, A. 2010. Durable alteration of the colonic microbiota by the administration of donor fecal flora. *J Clin Gastroenterol,* 44**,** 551-61.

GROSSMAN, A. D. 1995. Genetic networks controlling the initiation of sporulation and the development of genetic competence in *Bacillus subtilis*. *Annu Rev Genet,* 29**,** 477-508.

HALL, I. C. & O'TOOLE, H. 1935. Intestinal flora in newborn infants: with a description of a new pathogenic anaerobe, *Bacillus difficilis*. *Am. J. Dis. Child.***,** 390.

HAMON, M. A. & LAZAZZERA, B. A. 2001. The sporulation transcription factor Spo0A is required for biofilm development in *Bacillus subtilis*. *Mol Microbiol,* 42**,** 1199-209.

HANCOCK, I. & BADDILEY, J. 1976. In vitro synthesis of the unit that links teichoic acid to peptidoglycan. *J Bacteriol,* 125**,** 880-6.

HANDKE, L. D., SHIVERS, R. P. & SONENSHEIN, A. L. 2008. Interaction of *Bacillus subtilis* CodY with GTP. *J Bacteriol,* 190**,** 798-806.

HEAP, J. T., EHSAAN, M., COOKSLEY, C. M., NG, Y. K., CARTMAN, S. T., WINZER, K. & MINTON, N. P. 2012. Integration of DNA into bacterial chromosomes from plasmids without a counter-selection marker. *Nucleic Acids Res,* 40**,** e59.

HEAP, J. T., KUEHNE, S. A., EHSAAN, M., CARTMAN, S. T., COOKSLEY, C. M., SCOTT, J. C. & MINTON, N. P. 2010. The ClosTron: Mutagenesis in *Clostridium* refined and streamlined. *J Microbiol Methods,* 80**,** 49-55.

HEAP, J. T., PENNINGTON, O. J., CARTMAN, S. T., CARTER, G. P. & MINTON, N. P. 2007. The ClosTron: a universal gene knock-out system for the genus *Clostridium*. *J Microbiol Methods,* 70**,** 452-64.

HEAP, J. T., PENNINGTON, O. J., CARTMAN, S. T. & MINTON, N. P. 2009. A modular system for *Clostridium* shuttle plasmids. *J Microbiol Methods,* 78**,** 79-85.

HEEG, D., BURNS, D. A., CARTMAN, S. T. & MINTON, N. P. 2012. Spores of *Clostridium difficile* Clinical Isolates Display a Diverse Germination Response to Bile Salts. *PLoS One,* 7**,** e32381.

HENRIQUES, A. O., MELSEN, L. R. & MORAN, C. P., JR. 1998. Involvement of superoxide dismutase in spore coat assembly in *Bacillus subtilis*. *J Bacteriol,* 180**,** 2285-91.

HENRIQUES, A. O. & MORAN, C. P., JR. 2000. Structure and assembly of the bacterial endospore coat. *Methods,* 20**,** 95-110.

HENRIQUES, A. O. & MORAN, C. P., JR. 2007. Structure, assembly, and function of the spore surface layers. *Annu Rev Microbiol,* 61**,** 555-88.

HENSEL, M., SHEA, J. E., GLEESON, C., JONES, M. D., DALTON, E. & HOLDEN, D. W. 1995. Simultaneous identification of bacterial virulence genes by negative selection. *Science,* 269**,** 400-3.

HIGGINS, D. & DWORKIN, J. 2012. Recent progress in *Bacillus subtilis* sporulation. *FEMS Microbiol Rev,* 36**,** 131-48.

HILBERT, D. W. & PIGGOT, P. J. 2004. Compartmentalization of gene expression during *Bacillus subtilis* spore formation. *Microbiol Mol Biol Rev,* 68**,** 234-62.

HIRANO, Y., MATSUDA, M. & KAMEYAMA, T. 1991. Two-dimensional polyacrylamide gel electrophoresis of proteins synthesized during early germination of *Bacillus subtilis* 168 in the presence of actinomycin D. *J Basic Microbiol,* 31**,** 429-36.

HOWERTON, A., PATRA, M. & ABEL-SANTOS, E. 2013. A new strategy for the prevention of Clostridium difficile infection. *J Infect Dis,* 207**,** 1498-504.

HUANG, C. M., FOSTER, K. W., DESILVA, T. S., VAN KAMPEN, K. R., ELMETS, C. A. & TANG, D. C. 2004. Identification of *Bacillus anthracis* proteins associated with germination and early outgrowth by proteomic profiling of anthrax spores. *Proteomics,* 4**,** 2653-61.

HUDSON, K. D., CORFE, B. M., KEMP, E. H., FEAVERS, I. M., COOTE, P. J. & MOIR, A. 2001. Localization of GerAA and GerAC germination proteins in the *Bacillus subtilis* spore. *J Bacteriol,* 183**,** 4317-22.

HUEBNER, E. S. & SURAWICZ, C. M. 2006. Probiotics in the prevention and treatment of gastrointestinal infections. *Gastroenterol Clin North Am,* 35**,** 355-65.

HULLO, M. F., MOSZER, I., DANCHIN, A. & MARTIN-VERSTRAETE, I. 2001. CotA of *Bacillus subtilis* is a copper-dependent laccase. *J Bacteriol,* 183**,** 5426-30.

HUNDSBERGER, T., BRAUN, V., WEIDMANN, M., LEUKEL, P., SAUERBORN, M. & VON EICHEL-STREIBER, C. 1997. Transcription analysis of the genes *tcdA-E* of the pathogenicity locus of *Clostridium difficile*. *Eur J Biochem,* 244**,** 735-42.

HUSSAIN, H. A., ROBERTS, A. P. & MULLANY, P. 2005. Generation of an erythromycin-sensitive derivative of *Clostridium difficile* strain 630 (630Deltaerm) and demonstration that the conjugative transposon Tn916DeltaE enters the genome of this strain at multiple sites. *J Med Microbiol,* 54**,** 137-41.

INOUE, A., MURATA, Y., TAKAHASHI, H., TSUJI, N., FUJISAKI, S. & KATO, J. 2008. Involvement of an essential gene, *mviN*, in murein synthesis in *Escherichia coli*. *J Bacteriol,* 190**,** 7298-301.

JANK, T., GIESEMANN, T. & AKTORIES, K. 2007. Rho-glucosylating *Clostridium difficile* toxins A and B: new insights into structure and function. *Glycobiology,* 17**,** 15R-22R.

JANOIR, C., PECHINE, S., GROSDIDIER, C. & COLLIGNON, A. 2007. Cwp84, a surface-associated protein of *Clostridium difficile*, is a cysteine protease with degrading activity on extracellular matrix proteins. *J Bacteriol,* 189**,** 7174-80.

JENG, Y. H. & DOI, R. H. 1974. Messenger ribonucleic acid of dormant spores of *Bacillus subtilis*. *J Bacteriol,* 119**,** 514-21.

JIANG, M., SHAO, W., PEREGO, M. & HOCH, J. A. 2000. Multiple histidine kinases regulate entry into stationary phase and sporulation in *Bacillus subtilis*. *Mol Microbiol,* 38**,** 535-42.

JOHNSON, S., ADELMANN, A., CLABOTS, C. R., PETERSON, L. R. & GERDING, D. N. 1989. Recurrences of *Clostridium difficile* diarrhea not caused by the original infecting organism. *J Infect Dis,* 159**,** 340-3.

JOHNSON, S., SAMORE, M. H., FARROW, K. A., KILLGORE, G. E., TENOVER, F. C., LYRAS, D., ROOD, J. I., DEGIROLAMI, P., BALTCH, A. L., RAFFERTY, M. E., PEAR, S. M. & GERDING, D. N. 1999. Epidemics of diarrhea caused by a clindamycin-resistant strain of *Clostridium difficile* in four hospitals. *N Engl J Med,* 341**,** 1645-51.

JONES, A. L., KNOLL, K. M. & RUBENS, C. E. 2000. Identification of *Streptococcus agalactiae* virulence genes in the neonatal rat sepsis model using signature-tagged mutagenesis. *Mol Microbiol,* 37**,** 1444-55.

JONES, S. W., PAREDES, C. J., TRACY, B., CHENG, N., SILLERS, R., SENGER, R. S. & PAPOUTSAKIS, E. T. 2008. The transcriptional program underlying the physiology of clostridial sporulation. *Genome Biol,* 9**,** R114.

JUNCKER, A. S., WILLENBROCK, H., VON HEIJNE, G., BRUNAK, S., NIELSEN, H. & KROGH, A. 2003. Prediction of lipoprotein signal peptides in Gram-negative bacteria. *Protein Sci,* 12**,** 1652-62.

KARASAWA, T., IKOMA, S., YAMAKAWA, K. & NAKAMURA, S. 1995. A defined growth medium for *Clostridium difficile*. *Microbiology,* 141 (Pt 2)**,** 371-5.

KEIJSER, B. J., TER BEEK, A., RAUWERDA, H., SCHUREN, F., MONTIJN, R., VAN DER SPEK, H. & BRUL, S. 2007. Analysis of temporal gene expression during *Bacillus subtilis* spore germination and outgrowth. *J Bacteriol,* 189**,** 3624-34.

KHORUTS, A., DICKSVED, J., JANSSON, J. K. & SADOWSKY, M. J. 2010. Changes in the composition of the human fecal microbiome after bacteriotherapy for recurrent *Clostridium difficile*-associated diarrhea. *J Clin Gastroenterol,* 44**,** 354-60.

KIDWELL, M. G. & LISCH, D. R. 2001. Perspective: transposable elements, parasitic DNA, and genome evolution. *Evolution,* 55**,** 1-24.

KIM, J., SMATHERS, S. A., PRASAD, P., LECKERMAN, K. H., COFFIN, S. & ZAOUTIS, T. 2008. Epidemiological features of *Clostridium difficile*-associated disease among inpatients at children's hospitals in the United States, 2001-2006. *Pediatrics,* 122**,** 1266-70.

KIRBY, J. M., AHERN, H., ROBERTS, A. K., KUMAR, V., FREEMAN, Z., ACHARYA, K. R. & SHONE, C. C. 2009. Cwp84, a surface-associated, cysteine protease, plays a role in the maturation of the surface layer of *Clostridium difficile*. *J Biol Chem,* 284**,** 3466-34673.

KLOBUTCHER, L. A., RAGKOUSI, K. & SETLOW, P. 2006. The *Bacillus subtilis* spore coat provides 'eat resistance' during phagocytic predation by the protozoan Tetrahymena thermophila. *Proc Natl Acad Sci U S A,* 103**,** 165-70.

KOCH, R. 1876. Untersuchungen ueber Bakterien V. Die Aetiologie der Milzbrand-Krankheit, begruendent auf die Entwicklungsgeschichte des *Bacillus anthracis*. *Beitr. z. Biol. D. Pflanzen,* 2**,** 277-310.

KODAMA, T., TAKAMATSU, H., ASAI, K., KOBAYASHI, K., OGASAWARA, N. & WATABE, K. 1999. The *Bacillus subtilis yaaH* gene is transcribed by SigE RNA polymerase during sporulation, and its product is involved in germination of spores. *J Bacteriol,* 181**,** 4584-91.

KODAMA, T., TAKAMATSU, H., ASAI, K., OGASAWARA, N., SADAIE, Y. & WATABE, K. 2000. Synthesis and characterization of the spore proteins of *Bacillus subtilis* YdhD, YkuD, and YkvP, which carry a motif conserved among cell wall binding proteins. *J Biochem,* 128**,** 655-63.

KUEHNE, S. A., CARTMAN, S. T., HEAP, J. T., KELLY, M. L., COCKAYNE, A. & MINTON, N. P. 2010. The role of toxin A and toxin B in *Clostridium difficile* infection. *Nature,* 467**,** 711-3.

KUIJPER, E. J., COIGNARD, B. & TULL, P. 2006. Emergence of *Clostridium difficile*-associated disease in North America and Europe. *Clin Microbiol Infect,* 12 Suppl 6**,** 2-18.

KUIPERS, E. J. & SURAWICZ, C. M. 2008. *Clostridium difficile* infection. *Lancet,* 371**,** 1486-8.

LAABERKI, M. H. & DWORKIN, J. 2008. Role of spore coat proteins in the resistance of *Bacillus subtilis* spores to *Caenorhabditis elegans* predation. *J Bacteriol,* 190**,** 6197-203.

LAFORCE, F. M., BUMFORD, F. H., FEELEY, J. C., STOKES, S. L. & SNOW, D. B. 1969. Epidemiologic study of a fatal case of inhalation anthrax. *Arch Environ Health,* 18**,** 798-805.

LAMBERT, P. A., HANCOCK, I. C. & BADDILEY, J. 1977. Occurrence and function of membrane teichoic acids. *Biochim Biophys Acta,* 472**,** 1-12.

LAMONTAGNE, F., LABBE, A. C., HAECK, O., LESUR, O., LALANCETTE, M., PATINO, C., LEBLANC, M., LAVERDIERE, M. & PEPIN, J. 2007. Impact of emergency colectomy on survival of patients with fulminant *Clostridium difficile* colitis during an epidemic caused by a hypervirulent strain. *Ann Surg,* 245**,** 267-72.

LAMPE, D. J., AKERLEY, B. J., RUBIN, E. J., MEKALANOS, J. J. & ROBERTSON, H. M. 1999. Hyperactive transposase mutants of the Himar1 mariner transposon. *Proc Natl Acad Sci U S A,* 96**,** 11428-33.

LAMPE, D. J., CHURCHILL, M. E. & ROBERTSON, H. M. 1996. A purified mariner transposase is sufficient to mediate transposition *in vitro*. *EMBO J,* 15**,** 5470-9.

LAMPE, D. J., GRANT, T. E. & ROBERTSON, H. M. 1998. Factors affecting transposition of the Himar1 mariner transposon *in vitro*. *Genetics,* 149**,** 179-87.

LANCKRIET, A., TIMBERMONT, L., HAPPONEN, L. J., PAJUNEN, M. I., PASMANS, F., HAESEBROUCK, F., DUCATELLE, R., SAVILAHTI, H. & VAN IMMERSEEL, F. 2009. Generation of single-copy transposon insertions in *Clostridium perfringens* by electroporation of phage mu DNA transposition complexes. *Appl Environ Microbiol,* 75**,** 2638-42.

LANGRIDGE, G. C., PHAN, M. D., TURNER, D. J., PERKINS, T. T., PARTS, L., HAASE, J., CHARLES, I., MASKELL, D. J., PETERS, S. E., DOUGAN, G., WAIN, J., PARKHILL, J. & TURNER, A. K. 2009. Simultaneous assay of every *Salmonella typhi* gene using one million transposon mutants. *Genome Res,* 19**,** 2308-16.

LAWLEY, T. D., CLARE, S., WALKER, A. W., GOULDING, D., STABLER, R. A., CROUCHER, N., MASTROENI, P., SCOTT, P., RAISEN, C., MOTTRAM, L., FAIRWEATHER, N. F., WREN, B. W., PARKHILL, J. & DOUGAN, G. 2009a. Antibiotic treatment of *Clostridium difficile* carrier mice

triggers a supershedder state, spore-mediated transmission, and severe disease in immunocompromised hosts. *Infect Immun,* 77**,** 3661-9.

LAWLEY, T. D., CLARE, S., WALKER, A. W., STARES, M. D., CONNOR, T. R., RAISEN, C., GOULDING, D., RAD, R., SCHREIBER, F., BRANDT, C., DEAKIN, L. J., PICKARD, D. J., DUNCAN, S. H., FLINT, H. J., CLARK, T. G., PARKHILL, J. & DOUGAN, G. 2012. Targeted Restoration of the Intestinal Microbiota with a Simple, Defined Bacteriotherapy Resolves Relapsing *Clostridium difficile* Disease in Mice. *PLoS Pathog,* 8**,** e1002995.

LAWLEY, T. D., CROUCHER, N. J., YU, L., CLARE, S., SEBAIHIA, M., GOULDING, D., PICKARD, D. J., PARKHILL, J., CHOUDHARY, J. & DOUGAN, G. 2009b. Proteomic and genomic characterization of highly infectious *Clostridium difficile* 630 spores. *J Bacteriol,* 191**,** 5377-86.

LEWIS, J. C., SNELL, N. S. & BURR, H. K. 1960. Water Permeability of Bacterial Spores and the Concept of a Contractile Cortex. *Science,* 132**,** 544-5.

LIU, T. Y. & GOTSCHLICH, E. C. 1967. Muramic acid phosphate as a component of the mucopeptide of Gram-positive bacteria. *J Biol Chem,* 242**,** 471-6.

LONDONO-VALLEJO, J. A., FREHEL, C. & STRAGIER, P. 1997. SpoIIQ, a forespore-expressed gene required for engulfment in *Bacillus subtilis*. *Mol Microbiol,* 24**,** 29-39.

LOUIE, T. J., MILLER, M. A., MULLANE, K. M., WEISS, K., LENTNEK, A., GOLAN, Y., GORBACH, S., SEARS, P., SHUE, Y. K. & GROUP, O. P. T. C. S. 2011. Fidaxomicin versus vancomycin for *Clostridium difficile* infection. *N Engl J Med,* 364**,** 422-31.

LYERLY, D. M., SAUM, K. E., MACDONALD, D. K. & WILKINS, T. D. 1985. Effects of *Clostridium difficile* toxins given intragastrically to animals. *Infect Immun,* 47**,** 349-52.

LYRAS, D., O'CONNOR, J. R., HOWARTH, P. M., SAMBOL, S. P., CARTER, G. P., PHUMOONNA, T., POON, R., ADAMS, V., VEDANTAM, G., JOHNSON, S., GERDING, D. N. & ROOD, J. I. 2009. Toxin B is essential for virulence of *Clostridium difficile*. *Nature,* 458**,** 1176-9.

MAKINO, S. & MORIYAMA, R. 2002. Hydrolysis of cortex peptidoglycan during bacterial spore germination. *Med Sci Monit,* 8**,** RA119-27.

MCCLINTOCK, B. 1950. The origin and behavior of mutable loci in maize. *Proc Natl Acad Sci U S A,* 36**,** 344-55.

MCCOUBREY, J. & POXTON, I. R. 2001. Variation in the surface layer proteins of *Clostridium difficile*. *FEMS Immunol Med Microbiol,* 31**,** 131-5.

MCDONALD, L. C., KILLGORE, G. E., THOMPSON, A., OWENS, R. C., JR., KAZAKOVA, S. V., SAMBOL, S. P., JOHNSON, S. & GERDING, D. N. 2005. An epidemic, toxin gene-variant strain of *Clostridium difficile*. *N Engl J Med,* 353**,** 2433-41.

MCFARLAND, L. V. 2008. Antibiotic-associated diarrhea: epidemiology, trends and treatment. *Future Microbiol,* 3**,** 563-78.

MCFARLAND, L. V., BRANDMARKER, S. A. & GUANDALINI, S. 2000. Pediatric *Clostridium difficile*: a phantom menace or clinical reality? *J Pediatr Gastroenterol Nutr,* 31**,** 220-31.

MCKENNEY, P. T., DRIKS, A. & EICHENBERGER, P. 2013. The *Bacillus subtilis* endospore: assembly and functions of the multilayered coat. *Nat Rev Microbiol,* 11**,** 33-44.

MCKENNEY, P. T., DRIKS, A., ESKANDARIAN, H. A., GRABOWSKI, P., GUBERMAN, J., WANG, K. H., GITAI, Z. & EICHENBERGER, P. 2010. A distance-weighted interaction map reveals a previously uncharacterized layer of the *Bacillus subtilis* spore coat. *Curr Biol,* 20**,** 934-8.

MEI, J. M., NOURBAKHSH, F., FORD, C. W. & HOLDEN, D. W. 1997. Identification of *Staphylococcus aureus* virulence genes in a murine model of bacteraemia using signature-tagged mutagenesis. *Mol Microbiol,* 26**,** 399-407.

MEISNER, J., WANG, X., SERRANO, M., HENRIQUES, A. O. & MORAN, C. P., JR. 2008. A channel connecting the mother cell and forespore during bacterial endospore formation. *Proc Natl Acad Sci U S A,* 105**,** 15100-5.

MEKHJIAN, H. S., PHILLIPS, S. F. & HOFMANN, A. F. 1979. Colonic absorption of unconjugated bile acids: perfusion studies in man. *Dig Dis Sci,* 24**,** 545-50.

MESNAGE, S., FONTAINE, T., MIGNOT, T., DELEPIERRE, M., MOCK, M. & FOUET, A. 2000. Bacterial SLH domain proteins are non-covalently anchored to the cell surface *via* a conserved mechanism involving wall polysaccharide pyruvylation. *EMBO J,* 19**,** 4473-84.

MEYER, P., GUTIERREZ, J., POGLIANO, K. & DWORKIN, J. 2010. Cell wall synthesis is necessary for membrane dynamics during sporulation of *Bacillus subtilis*. *Mol Microbiol,* 76**,** 956-70.

MIRZA, J. & BAGNI, N. 1991. Effects of exogenous polyamines and difluoromethylornithine on seed germination and root growth of *Arabidopsis thaliana*. *Plant Growth Regulation,* 10**,** 163-168.

MOHR, G., SMITH, D., BELFORT, M. & LAMBOWITZ, A. M. 2000. Rules for DNA target-site recognition by a lactococcal group II intron enable retargeting of the intron to specific DNA sequences. *Genes Dev,* 14**,** 559-73.

MOIR, A. 2003. Bacterial spore germination and protein mobility. *Trends Microbiol,* 11**,** 452-4.

MONCRIEF, J. S., BARROSO, L. A. & WILKINS, T. D. 1997. Positive regulation of *Clostridium difficile* toxins. *Infect Immun,* 65**,** 1105-8.

MORI, H. & ITO, K. 2001. The Sec protein-translocation pathway. *Trends Microbiol,* 9**,** 494-500.

MULLANE, K. M., MILLER, M. A., WEISS, K., LENTNEK, A., GOLAN, Y., SEARS, P. S., SHUE, Y. K., LOUIE, T. J. & GORBACH, S. L. 2011. Efficacy of fidaxomicin versus vancomycin as therapy for *Clostridium difficile* infection in individuals taking concomitant antibiotics for other concurrent infections. *Clin Infect Dis,* 53**,** 440-7.

MULLANY, P., WILKS, M., PUCKEY, L. & TABAQCHALI, S. 1994. Gene cloning in *Clostridium difficile* using Tn916 as a shuttle conjugative transposon. *Plasmid,* 31**,** 320-3.

MULLANY, P., WILKS, M. & TABAQCHALI, S. 1991. Transfer of Tn916 and Tn916 delta E into *Clostridium difficile*: demonstration of a hot-spot for these elements in the *Clostridium difficile* genome. *FEMS Microbiol Lett,* 63**,** 191-4.

MURRELL, W. G. 1967. The biochemistry of the bacterial endospore. *Adv Microbiol Physiol,* 1**,** 133-251.

NELSON, D. L. & KORNBERG, A. 1970. Biochemical studies of bacterial sporulation and germination. XX. Phosphate metabolism during germination. *J Biol Chem,* 245**,** 1146-55.

NERANDZIC, M. M. & DONSKEY, C. J. 2010. Triggering germination represents a novel strategy to enhance killing of *Clostridium difficile* spores. *PLoS One,* 5.

NERANDZIC, M. M. & DONSKEY, C. J. 2013. Activate to eradicate: inhibition of *Clostridium difficile* spore outgrowth by the synergistic effects of osmotic activation and nisin. *PLoS One,* 8**,** e54740.

NG, Y. K., EHSAAN, M., PHILIP, S., COLLERY, M. M., JANOIR, C., COLLIGNON, A., CARTMAN, S. T. & MINTON, N. P. 2013. Expanding the Repertoire of Gene Tools for Precise Manipulation of the *Clostridium difficile* Genome: Allelic Exchange Using pyrE Alleles. *PLoS One,* 8**,** e56051.

NICHOLSON, W. L., SETLOW, B. & SETLOW, P. 1990. Binding of DNA in vitro by a small, acid-soluble spore protein from *Bacillus subtilis* and the effect of this binding on DNA topology. *J Bacteriol,* 172**,** 6900-6.

O'CONNOR, J. R., LYRAS, D., FARROW, K. A., ADAMS, V., POWELL, D. R., HINDS, J., CHEUNG, J. K. & ROOD, J. I. 2006. Construction and analysis of chromosomal *Clostridium difficile* mutants. *Mol Microbiol,* 61**,** 1335-51.

O'NEILL, G. L., BEAMAN, M. H. & RILEY, T. V. 1991. Relapse versus reinfection with *Clostridium difficile*. *Epidemiol Infect,* 107**,** 627-35.

OLMEDO, G., NINFA, E. G., STOCK, J. & YOUNGMAN, P. 1990. Novel mutations that alter the regulation of sporulation in *Bacillus subtilis*. Evidence that phosphorylation of regulatory protein SpoOA controls the initiation of sporulation. *J Mol Biol,* 215**,** 359-72.

PAIDHUNGAT, M., RAGKOUSI, K. & SETLOW, P. 2001. Genetic requirements for induction of germination of spores of *Bacillus subtilis* by Ca(2+)-dipicolinate. *J Bacteriol,* 183**,** 4886-93.

PAIDHUNGAT, M. & SETLOW, P. 2000. Role of ger proteins in nutrient and nonnutrient triggering of spore germination in *Bacillus subtilis*. *J Bacteriol,* 182**,** 2513-9.

PAIDHUNGAT, M. & SETLOW, P. 2001. Localization of a germinant receptor protein (GerBA) to the inner membrane of *Bacillus subtilis* spores. *J Bacteriol,* 183**,** 3982-90.

PANESSA-WARREN, B. J., TORTORA, G. T. & WARREN, J. B. 2007. High resolution FESEM and TEM reveal bacterial spore attachment. *Microsc Microanal,* 13**,** 251-66.

PAREDES-SABJA, D., SETLOW, P. & SARKER, M. R. 2009a. The protease CspB is essential for initiation of cortex hydrolysis and dipicolinic acid (DPA) release during germination of spores of *Clostridium perfringens* type A food poisoning isolates. *Microbiology,* 155**,** 3464-72.

PAREDES-SABJA, D., SETLOW, P. & SARKER, M. R. 2009b. SleC is essential for cortex peptidoglycan hydrolysis during germination of spores of the pathogenic bacterium *Clostridium perfringens*. *J Bacteriol,* 191**,** 2711-20.

PAREDES-SABJA, D., SETLOW, P. & SARKER, M. R. 2010. Germination of spores of *Bacillales* and *Clostridiales* species: mechanisms and proteins involved. *Trends Microbiol*.

PAREDES, C. J., ALSAKER, K. V. & PAPOUTSAKIS, E. T. 2005. A comparative genomic view of Clostridial sporulation and physiology. *Nat Rev Microbiol,* 3**,** 969-78.

PARADIS-BLEAU, C., MARKOVSKI, M., UEHARA, T., LUPOLI, T. J., WALKER, S., KAHNE, D. E. & BERNHARDT, T. G. 2010. Lipoprotein cofactors located in the outer membrane activate bacterial cell wall polymerases. *Cell,* 143**,** 1110-20.

PEGG, A. E. & MCCANN, P. P. 1982. Polyamine metabolism and function. *Am J Physiol,* 243**,** C212-21.

PEPIN, J., SAHEB, N., COULOMBE, M. A., ALARY, M. E., CORRIVEAU, M. P., AUTHIER, S., LEBLANC, M., RIVARD, G., BETTEZ, M., PRIMEAU, V., NGUYEN, M., JACOB, C. E. & LANTHIER, L. 2005. Emergence of fluoroquinolones as the predominant risk factor for *Clostridium difficile*-associated diarrhea: a cohort study during an epidemic in Quebec. *Clin Infect Dis,* 41**,** 1254-60.

PEPIN, J., VALIQUETTE, L., ALARY, M. E., VILLEMURE, P., PELLETIER, A., FORGET, K., PEPIN, K. & CHOUINARD, D. 2004. *Clostridium difficile*-associated diarrhea in a region of Quebec from 1991 to 2003: a changing pattern of disease severity. *CMAJ,* 171**,** 466-72.

PEREGO, M., HANSTEIN, C., WELSH, K. M., DJAVAKHISHVILI, T., GLASER, P. & HOCH, J. A. 1994. Multiple protein-aspartate phosphatases provide a mechanism for the integration of diverse signals in the control of development in *Bacillus subtilis*. *Cell,* 79**,** 1047-55.

PEREGO, M., SPIEGELMAN, G. B. & HOCH, J. A. 1988. Structure of the gene for the transition state regulator, *abrB*: regulator synthesis is controlled by the *spo0A* sporulation gene in *Bacillus subtilis*. *Mol Microbiol,* 2**,** 689-99.

PEREIRA, F. C., SAUJET, L., TOME, A. R., SERRANO, M., MONOT, M., COUTURE-TOSI, E., MARTIN-VERSTRAETE, I., DUPUY, B. & HENRIQUES, A. O. 2013. The Spore Differentiation Pathway in the Enteric Pathogen *Clostridium difficile*. *PLoS Genet,* 9**,** e1003782.

PERMPOONPATTANA, P., TOLLS, E. H., NADEM, R., TAN, S., BRISSON, A. & CUTTING, S. M. 2011. Surface Layers of *Clostridium difficile* Endospores. *J Bacteriol*.

PETROF, E., GLOOR, G., VANNER, S., WEESE, S., CARTER, D., DAIGNEAULT, M., BROWN, E., SCHROETER, K. & ALLEN-VERCOE, E. 2013. Stool substitute transplant therapy for the eradication of *Clostridium difficile* infection: 'RePOOPulating' the gut. *Microbiome,* 1**,** 3.

PLANCHE, T., AGHAIZU, A., HOLLIMAN, R., RILEY, P., POLONIECKI, J., BREATHNACH, A. & KRISHNA, S. 2008. Diagnosis of *Clostridium difficile* infection by toxin detection kits: a systematic review. *Lancet Infect Dis,* 8**,** 777-84.

POLISSI, A., PONTIGGIA, A., FEGER, G., ALTIERI, M., MOTTL, H., FERRARI, L. & SIMON, D. 1998. Large-scale identification of virulence genes from *Streptococcus pneumonia*e. *Infect Immun,* 66**,** 5620-9.

POPHAM, D. L., HELIN, J., COSTELLO, C. E. & SETLOW, P. 1996. Muramic lactam in peptidoglycan of *Bacillus subtilis* spores is required for spore outgrowth but not for spore dehydration or heat resistance. *Proc Natl Acad Sci U S A,* 93**,** 15405-10.

POPOFF, M. R. & BOUVET, P. 2009. Clostridial toxins. *Future Microbiol,* 4**,** 1021-64.

POTTATHIL, M. & LAZAZZERA, B. A. 2003. The extracellular Phr peptide-Rap phosphatase signaling circuit of *Bacillus subtilis*. *Front Biosci,* 8**,** d32-45.

PURDY, D., O'KEEFFE, T. A., ELMORE, M., HERBERT, M., MCLEOD, A., BOKORI-BROWN, M., OSTROWSKI, A. & MINTON, N. P. 2002. Conjugative transfer of clostridial shuttle vectors

from *Escherichia coli* to *Clostridium difficile* through circumvention of the restriction barrier. *Mol Microbiol,* 46**,** 439-52.

PUTNAM, E. E., NOCK, A. M., LAWLEY, T. D. & SHEN, A. 2013. SpoIVA and SipL are *Clostridium difficil*e spore morphogenetic proteins. *J Bacteriol,* 195**,** 1214-25.

RAHN-LEE, L., GORBATYUK, B., SKOVGAARD, O. & LOSICK, R. 2009. The conserved sporulation protein YneE inhibits DNA replication in *Bacillus subtilis*. *J Bacteriol,* 191**,** 3736-9.

RATNAYAKE-LECAMWASAM, M., SERROR, P., WONG, K. W. & SONENSHEIN, A. L. 2001. B*acillus subtilis* CodY represses early-stationary-phase genes by sensing GTP levels. *Genes Dev,* 15**,** 1093-103.

REYNOLDS, C. B., EMERSON, J. E., DE LA RIVA, L., FAGAN, R. P. & FAIRWEATHER, N. F. 2011. The *Clostridium difficile* Cell Wall Protein CwpV is Antigenically Variable between Strains, but Exhibits Conserved Aggregation-Promoting Function. *PLoS Pathog,* 7**,** e1002024.

RIEGLER, M., SEDIVY, R., POTHOULAKIS, C., HAMILTON, G., ZACHERL, J., BISCHOF, G., COSENTINI, E., FEIL, W., SCHIESSEL, R., LAMONT, J. T. & ET AL. 1995. *Clostridium difficile* toxin B is more potent than toxin A in damaging human colonic epithelium in vitro. *J Clin Invest,* 95**,** 2004-11.

RIESENMAN, P. J. & NICHOLSON, W. L. 2000. Role of the spore coat layers in *Bacillus subtili*s spore resistance to hydrogen peroxide, artificial UV-C, UV-B, and solar UV radiation. *Appl Environ Microbiol,* 66**,** 620-6.

RIGGS, M. M., SETHI, A. K., ZABARSKY, T. F., ECKSTEIN, E. C., JUMP, R. L. & DONSKEY, C. J. 2007. Asymptomatic carriers are a potential source for transmission of epidemic and nonepidemic *Clostridium difficile* strains among long-term care facility residents. *Clin Infect Dis,* 45**,** 992-8.

RILEY, T. V., BOWMAN, R. A. & GOLLEDGE, C. L. 1995. Usefulness of culture in the diagnosis of *Clostridium difficile* infection. *Eur J Clin Microbiol Infect Dis,* 14**,** 1109-11.

RODRIGUES, C. D., MARQUIS, K. A., MEISNER, J. & RUDNER, D. Z. 2013. Peptidoglycan hydrolysis is required for assembly and activity of the transenvelope secretion complex during sporulation in *Bacillus subtilis*. *Mol Microbiol,* 89**,** 1039-52.

ROUPHAEL, N. G., O'DONNELL, J. A., BHATNAGAR, J., LEWIS, F., POLGREEN, P. M., BEEKMANN, S., GUARNER, J., KILLGORE, G. E., COFFMAN, B., CAMPBELL, J., ZAKI, S. R. & MCDONALD, L. C. 2008. *Clostridium difficile*-associated diarrhea: an emerging threat to pregnant women. *Am J Obstet Gynecol,* 198**,** 635 e1-6.

RUBIO, A. & POGLIANO, K. 2004. Septal localization of forespore membrane proteins during engulfment in *Bacillus subtilis*. *EMBO J,* 23**,** 1636-46.

RUIZ, N. 2008. Bioinformatics identification of MurJ (MviN) as the peptidoglycan lipid II flippase in *Escherichia coli*. *Proc Natl Acad Sci U S A,* 105**,** 15553-7.

RUPNIK, M., WILCOX, M. H. & GERDING, D. N. 2009. *Clostridium difficile* infection: new developments in epidemiology and pathogenesis. *Nat Rev Microbiol,* 7**,** 526-36.

SAUJET, L., MONOT, M., DUPUY, B., SOUTOURINA, O. & MARTIN-VERSTRAETE, I. 2011. The key sigma factor of transition phase, SigH, controls sporulation, metabolism, and virulence factor expression in *Clostridium difficile*. *J Bacteriol,* 193**,** 3186-96.

SAUJET, L., PEREIRA, F. C., SERRANO, M., SOUTOURINA, O., MONOT, M., SHELYAKIN, P. V., GELFAND, M. S., DUPUY, B., HENRIQUES, A. O. & MARTIN-VERSTRAETE, I. 2013. Genome-Wide Analysis of Cell Type-Specific Gene Transcription during Spore Formation in *Clostridium difficile*. *PLoS Genet,* 9**,** e1003756.

SCANDELLA, C. J. & KORNBERG, A. 1969. Biochemical studies of bacterial sporulation and germination. XV. Fatty acids in growth, sporulation, and germination of *Bacillus megaterium*. *J Bacteriol,* 98**,** 82-6.

SCHAEFFER, P., MILLET, J. & AUBERT, J. P. 1965. Catabolic repression of bacterial sporulation. *Proc Natl Acad Sci U S A,* 54**,** 704-11.

SCHAFFER, C. & MESSNER, P. 2005. The structure of secondary cell wall polymers: how Gram-positive bacteria stick their cell walls together. *Microbiology,* 151**,** 643-51.

SCHWAN, C., STECHER, B., TZIVELEKIDIS, T., VAN HAM, M., ROHDE, M., HARDT, W. D., WEHLAND, J. & AKTORIES, K. 2009. *Clostridium difficile* toxin CDT induces formation of microtubule-based protrusions and increases adherence of bacteria. *PLoS Pathog,* 5**,** e1000626.

SEBAIHIA, M., PECK, M. W., MINTON, N. P., THOMSON, N. R., HOLDEN, M. T., MITCHELL, W. J., CARTER, A. T., BENTLEY, S. D., MASON, D. R., CROSSMAN, L., PAUL, C. J., IVENS, A., WELLS-BENNIK, M. H., DAVIS, I. J., CERDENO-TARRAGA, A. M., CHURCHER, C., QUAIL, M. A., CHILLINGWORTH, T., FELTWELL, T., FRASER, A., GOODHEAD, I., HANCE, Z., JAGELS, K., LARKE, N., MADDISON, M., MOULE, S., MUNGALL, K., NORBERTCZAK, H., RABBINOWITSCH, E., SANDERS, M., SIMMONDS, M., WHITE, B., WHITHEAD, S. & PARKHILL, J. 2007. Genome sequence of a proteolytic (Group I) *Clostridium botulinum* strain Hall A and comparative analysis of the Clostridial genomes. *Genome Res,* 17**,** 1082-92.

SEBAIHIA, M., WREN, B. W., MULLANY, P., FAIRWEATHER, N. F., MINTON, N., STABLER, R., THOMSON, N. R., ROBERTS, A. P., CERDENO-TARRAGA, A. M., WANG, H., HOLDEN, M. T., WRIGHT, A., CHURCHER, C., QUAIL, M. A., BAKER, S., BASON, N., BROOKS, K., CHILLINGWORTH, T., CRONIN, A., DAVIS, P., DOWD, L., FRASER, A., FELTWELL, T., HANCE, Z., HOLROYD, S., JAGELS, K., MOULE, S., MUNGALL, K., PRICE, C., RABBINOWITSCH, E., SHARP, S., SIMMONDS, M., STEVENS, K., UNWIN, L., WHITHEAD, S., DUPUY, B., DOUGAN, G., BARRELL, B. & PARKHILL, J. 2006. The multidrug-resistant human pathogen *Clostridium difficile* has a highly mobile, mosaic genome. *Nat Genet,* 38**,** 779-86.

SEKIGUCHI, J., AKEO, K., YAMAMOTO, H., KHASANOV, F. K., ALONSO, J. C. & KURODA, A. 1995. Nucleotide sequence and regulation of a new putative cell wall hydrolase gene, *cwlD*, which affects germination in *Bacillus subtilis*. *J Bacteriol,* 177**,** 5582-9.

SETLOW, B., COWAN, A. E. & SETLOW, P. 2003. Germination of spores of *Bacillus subtilis* with dodecylamine. *J Appl Microbiol,* 95**,** 637-48.

SETLOW, P. 1974. Polyamine levels during growth, sporulation, and spore germination of *Bacillus megaterium*. *J Bacteriol,* 117**,** 1171-7.

SETLOW, P. 1975. Protein metabolism during germination of *Bacillus megaterium* spores. II. Degradation of pre-existing and newly synthesized protein. *J Biol Chem,* 250**,** 631-7.

SETLOW, P. 2003. Spore germination. *Curr Opin Microbiol,* 6**,** 550-6.

SETLOW, P. 2006. Spores of *Bacillus subtilis*: their resistance to and killing by radiation, heat and chemicals. *J Appl Microbiol,* 101**,** 514-25.

SETLOW, P. 2007. I will survive: DNA protection in bacterial spores. *Trends Microbiol,* 15**,** 172-80.

SETLOW, P. & KORNBERG, A. 1970a. Biochemical studies of bacterial sporulation and germination. 23. Nucleotide metabolism during spore germination. *J Biol Chem,* 245**,** 3645-52.

SETLOW, P. & KORNBERG, A. 1970b. Biochemical studies of bacterial sporulation and germination. XXII. Energy metabolism in early stages of germination of *Bacillus megaterium* spores. *J Biol Chem,* 245**,** 3637-44.

SETLOW, P. & PRIMUS, G. 1975. Protein metabolism during germination of *Bacillus megaterium* spores. I. Protein synthesis and amino acid metabolism. *J Biol Chem,* 250**,** 623-30.

SHIMAMOTO, S., MORIYAMA, R., SUGIMOTO, K., MIYATA, S. & MAKINO, S. 2001. Partial characterization of an enzyme fraction with protease activity which converts the spore peptidoglycan hydrolase (SleC) precursor to an active enzyme during germination of *Clostridium perfringens* S40 spores and analysis of a gene cluster involved in the activity. *J Bacteriol,* 183**,** 3742-51.

SILHAVY, T. J., KAHNE, D. & WALKER, S. 2010. The bacterial cell envelope. *Cold Spring Harb Perspect Biol,* 2**,** a000414.

SILVA, J., JR., BATTS, D. H., FEKETY, R., PLOUFFE, J. F., RIFKIN, G. D. & BAIRD, I. 1981. Treatment of *Clostridium difficile* colitis and diarrhea with vancomycin. *Am J Med,* 71**,** 815-22.

SINGH, R. P. & SETLOW, P. 1979. Regulation of phosphoglycerate phosphomutase in developing forespores and dormant and germinated spores of *Bacillus megaterium* by the level of free manganous ions. *J Bacteriol,* 139**,** 889-98.

SIRANOSIAN, K. J. & GROSSMAN, A. D. 1994. Activation of *spo0A* transcription by sigma H is necessary for sporulation but not for competence in *Bacillus subtilis*. *J Bacteriol,* 176**,** 3812-5.

SLEYTR, U. B. & BEVERIDGE, T. J. 1999. Bacterial S-layers. *Trends Microbiol,* 7**,** 253-60.

SLEYTR, U. B. & MESSNER, P. 1983. Crystalline surface layers on bacteria. *Annu Rev Microbiol,* 37**,** 311-39.

SMITS, L. P., BOUTER, K. E., DE VOS, W. M., BORODY, T. J. & NIEUWDORP, M. 2013. Therapeutic potential of fecal microbiota transplantation. *Gastroenterology,* 145**,** 946-53.

SOGAARD-ANDERSEN, L. 2013. Stably bridging a great divide: localization of the SpoIIQ landmark protein in *Bacillus subtilis*. *Mol Microbiol,* 89**,** 1019-24.

SONENSHEIN, A. L. 2000. Control of sporulation initiation in Bacillus subtilis. *Curr Opin Microbiol,* 3**,** 561-6.

SORG, J. A. & SONENSHEIN, A. L. 2008. Bile salts and glycine as cogerminants for *Clostridium difficile* spores. *J Bacteriol,* 190**,** 2505-12.

SORG, J. A. & SONENSHEIN, A. L. 2009. Chenodeoxycholate is an inhibitor of *Clostridium difficile* spore germination. *J Bacteriol,* 191**,** 1115-7.

SORG, J. A. & SONENSHEIN, A. L. 2010. Inhibiting the initiation of *Clostridium difficile* spore germination using analogs of chenodeoxycholic acid, a bile acid. *J Bacteriol*.

STAMPER, P. D., ALCABASA, R., AIRD, D., BABIKER, W., WEHRLIN, J., IKPEAMA, I. & CARROLL, K. C. 2009. Comparison of a commercial real-time PCR assay for *tcdB* detection to a cell culture cytotoxicity assay and toxigenic culture for direct detection of toxin-producing *Clostridium difficile* in clinical samples. *J Clin Microbiol,* 47**,** 373-8.

STEIL, L., SERRANO, M., HENRIQUES, A. O. & VOLKER, U. 2005. Genome-wide analysis of temporally regulated and compartment-specific gene expression in sporulating cells of *Bacillus subtilis*. *Microbiology,* 151**,** 399-420.

STEINER, E., DAGO, A. E., YOUNG, D. I., HEAP, J. T., MINTON, N. P., HOCH, J. A. & YOUNG, M. 2011. Multiple orphan histidine kinases interact directly with Spo0A to control the initiation of endospore formation in *Clostridium acetobutylicum*. *Mol Microbiol,* 80**,** 641-54.

STEVENS, L. & WINTHER, M. D. 1979. Spermine, spermidine and putrescine in fungal development. *Adv Microb Physiol,* 19**,** 63-148.

STOCK, A. M., ROBINSON, V. L. & GOUDREAU, P. N. 2000. Two-component signal transduction. *Annu Rev Biochem,* 69**,** 183-215.

STRINGER, S. C., WEBB, M. D., GEORGE, S. M., PIN, C. & PECK, M. W. 2005. Heterogeneity of times required for germination and outgrowth from single spores of nonproteolytic *Clostridium botulinum*. *Appl Environ Microbiol,* 71**,** 4998-5003.

STUBBS, S., RUPNIK, M., GIBERT, M., BRAZIER, J., DUERDEN, B. & POPOFF, M. 2000. Production of actin-specific ADP-ribosyltransferase (binary toxin) by strains of *Clostridium difficile*. *FEMS Microbiol Lett,* 186**,** 307-12.

SUN, Y. L., SHARP, M. D. & POGLIANO, K. 2000. A dispensable role for forespore-specific gene expression in engulfment of the forespore during sporulation of *Bacillus subtilis*. *J Bacteriol,* 182**,** 2919-27.

TABOR, C. W. & TABOR, H. 1984. Polyamines. *Annu Rev Biochem,* 53**,** 749-90.

TAKUMI, K., ENDO, Y., KOGA, T., OKA, T. & NATORI, Y. 1992. In vitro self-assembly of the S-layer subunits from *Clostridium difficile* GAI 0714 into tetragonal arrays. *Tokushima J Exp Med,* 39**,** 95-100.

TEASLEY, D. G., GERDING, D. N., OLSON, M. M., PETERSON, L. R., GEBHARD, R. L., SCHWARTZ, M. J. & LEE, J. T., JR. 1983. Prospective randomised trial of metronidazole versus vancomycin for *Clostridium-difficil*e-associated diarrhoea and colitis. *Lancet,* 2**,** 1043-6.

TICEHURST, J. R., AIRD, D. Z., DAM, L. M., BOREK, A. P., HARGROVE, J. T. & CARROLL, K. C. 2006. Effective detection of toxigenic *Clostridium difficil*e by a two-step algorithm including tests for antigen and cytotoxin. *J Clin Microbiol,* 44**,** 1145-9.

TIPPER, D. J. & LINNETT, P. E. 1976. Distribution of peptidoglycan synthetase activities between sporangia and forespores in sporulating cells of *Bacillus sphaericu*s. *J Bacteriol,* 126**,** 213-21.

TOMAS, C. A., ALSAKER, K. V., BONARIUS, H. P., HENDRIKSEN, W. T., YANG, H., BEAMISH, J. A., PAREDES, C. J. & PAPOUTSAKIS, E. T. 2003. DNA array-based transcriptional analysis of

asporogenous, nonsolventogenic *Clostridium acetobutylicum* strains SKO1 and M5. *J Bacteriol,* 185**,** 4539-47.

TYPAS, A., BANZHAF, M., VAN DEN BERG VAN SAPAROEA, B., VERHEUL, J., BIBOY, J., NICHOLS, R. J., ZIETEK, M., BEILHARZ, K., KANNENBERG, K., VON RECHENBERG, M., BREUKINK, E., DEN BLAAUWEN, T., GROSS, C. A. & VOLLMER, W. 2010. Regulation of peptidoglycan synthesis by outer-membrane proteins. *Cell,* 143**,** 1097-109.

UNDERWOOD, S., GUAN, S., VIJAYASUBHASH, V., BAINES, S. D., GRAHAM, L., LEWIS, R. J., WILCOX, M. H. & STEPHENSON, K. 2009. Characterization of the sporulation initiation pathway of *Clostridium difficile* and its role in toxin production. *J Bacteriol,* 191**,** 7296-305.

VAN DEN BERG, R. J., KUIJPER, E. J., VAN COPPENRAET, L. E. & CLAAS, E. C. 2006. Rapid diagnosis of toxinogenic *Clostridium difficile* in faecal samples with internally controlled real-time PCR. *Clin Microbiol Infect,* 12**,** 184-6.

VAN OOIJ, C., EICHENBERGER, P. & LOSICK, R. 2004. Dynamic patterns of subcellular protein localization during spore coat morphogenesis in *Bacillus subtilis*. *J Bacteriol,* 186**,** 4441-8.

VEENING, J. W., HAMOEN, L. W. & KUIPERS, O. P. 2005. Phosphatases modulate the bistable sporulation gene expression pattern in *Bacillus subtilis*. *Mol Microbiol,* 56**,** 1481-94.

VIDAL, J. E., CHEN, J., LI, J. & MCCLANE, B. A. 2009. Use of an EZ-Tn5-based random mutagenesis system to identify a novel toxin regulatory locus in *Clostridium perfringens* strain 13. *PLoS One,* 4**,** e6232.

VOLLMER, W. 2008. Structural variation in the glycan strands of bacterial peptidoglycan. *FEMS Microbiol Rev,* 32**,** 287-306.

VOTH, D. E. & BALLARD, J. D. 2005. *Clostridium difficile* toxins: mechanism of action and role in disease. *Clin Microbiol Rev,* 18**,** 247-63.

WAGNER, J. K., MARQUIS, K. A. & RUDNER, D. Z. 2009. SirA enforces diploidy by inhibiting the replication initiator DnaA during spore formation in *Bacillus subtilis*. *Mol Microbiol,* 73**,** 963-74.

WALIGORA, A. J., HENNEQUIN, C., MULLANY, P., BOURLIOUX, P., COLLIGNON, A. & KARJALAINEN, T. 2001. Characterization of a cell surface protein of *Clostridium difficile* with adhesive properties. *Infect Immun,* 69**,** 2144-53.

WANG, G., ZHANG, P., PAREDES-SABJA, D., GREEN, C., SETLOW, P., SARKER, M. R. & LI, Y. Q. 2011. Analysis of the germination of individual *Clostridium perfringens* spores and its heterogeneity. *J Appl Microbiol,* 111**,** 1212-23.

WANG, L., GRAU, R., PEREGO, M. & HOCH, J. A. 1997. A novel histidine kinase inhibitor regulating development in *Bacillus subtilis*. *Genes Dev,* 11**,** 2569-79.

WARNY, M., PEPIN, J., FANG, A., KILLGORE, G., THOMPSON, A., BRAZIER, J., FROST, E. & MCDONALD, L. C. 2005. Toxin production by an emerging strain of *Clostridium difficile* associated with outbreaks of severe disease in North America and Europe. *Lancet,* 366**,** 1079-84.

WARTH, A. D. & STROMINGER, J. L. 1969. Structure of the peptidoglycan of bacterial spores: occurrence of the lactam of muramic acid. *Proc Natl Acad Sci U S A,* 64**,** 528-35.

WARTH, A. D. & STROMINGER, J. L. 1972. Structure of the peptidoglycan from spores of *Bacillus subtilis*. *Biochemistry,* 11**,** 1389-96.

WEIDENMAIER, C. & PESCHEL, A. 2008. Teichoic acids and related cell-wall glycopolymers in Gram-positive physiology and host interactions. *Nat Rev Microbiol,* 6**,** 276-87.

WELLS, C. L. & WILKINS, T. D. 1996. *Medical Microbiology. 4th edition,* Galveston, Texas, University of Texas Medical Branch at Galveston.

WHEAT, R. W. & GHUYSEN, J. M. 1971. Occurrence of glucomuramic acid in Gram-positive bacteria. *J Bacteriol,* 105**,** 1219-21.

WHEELDON, L., WORTHINGTON, T. & LAMBERT, P. 2011. Histidine acts as a co-germinant with glycine and taurocholate for *Clostridium difficile* spores. *J Appl Microbiol*.

WHEELDON, L. J., WORTHINGTON, T., HILTON, A. C., ELLIOTT, T. S. & LAMBERT, P. A. 2008. Physical and chemical factors influencing the germination of *Clostridium difficile* spores. *J Appl Microbiol,* 105**,** 2223-30.

WILCOX, M. H., SHETTY, N., FAWLEY, W. N., SHEMKO, M., COEN, P., BIRTLES, A., CAIRNS, M., CURRAN, M. D., DODGSON, K. J., GREEN, S. M., HARDY, K. J., HAWKEY, P. M., MAGEE, J. G., SAILS, A. D. & WREN, M. W. 2012. Changing epidemiology of *Clostridium difficile* infection following the introduction of a national ribotyping-based surveillance scheme in England. *Clin Infect Dis,* 55**,** 1056-63.

WILLEY, S. H. & BARTLETT, J. G. 1979. Cultures for *Clostridium difficile* in stools containing a cytotoxin neutralized by *Clostridium sordellii* antitoxin. *J Clin Microbiol,* 10**,** 880-4.

WILSON, K. H. 1983. Efficiency of various bile salt preparations for stimulation of *Clostridium difficile* spore germination. *J Clin Microbiol,* 18**,** 1017-9.

WILSON, K. H., KENNEDY, M. J. & FEKETY, F. R. 1982. Use of sodium taurocholate to enhance spore recovery on a medium selective for *Clostridium difficile*. *J Clin Microbiol,* 15**,** 443-6.

WREN, B. W., CLAYTON, C. L., MULLANY, P. P. & TABAQCHALI, S. 1987. Molecular cloning and expression of *Clostridium difficile* toxin A in *Escherichia coli* K12. *FEBS Lett,* 225**,** 82-6.

WRIGHT, A., DRUDY, D., KYNE, L., BROWN, K. & FAIRWEATHER, N. F. 2008. Immunoreactive cell wall proteins of *Clostridium difficile* identified by human sera. *J Med Microbiol,* 57**,** 750-6.

WRIGHT, A., WAIT, R., BEGUM, S., CROSSETT, B., NAGY, J., BROWN, K. & FAIRWEATHER, N. 2005. Proteomic analysis of cell surface proteins from *Clostridium difficile*. *Proteomics,* 5**,** 2443-52.

WU, L. J. & ERRINGTON, J. 1994. *Bacillus subtilis* SpoIIIE protein required for DNA segregation during asymmetric cell division. *Science,* 264**,** 572-5.

YASSIN, S. F. 2009. Pseudomembranous Colitis, Surgical Treatment. *eMedicine General Surgery*.

YI, X. & SETLOW, P. 2010. Studies of the commitment step in the germination of spores of *Bacillus species*. *J Bacteriol,* 192**,** 3424-33.

YOUNG, F. E. 1966. Fractionation and partial characterization of the products of autolysis of cell walls of *Bacillus subtilis*. *J Bacteriol,* 92**,** 839-46.

ZHONG, J., KARBERG, M. & LAMBOWITZ, A. M. 2003. Targeted and random bacterial gene disruption using a group II intron (targetron) vector containing a retrotransposition-activated selectable marker. *Nucleic Acids Res,* 31**,** 1656-64.

Appendix A

Table A1. *C. difficile* strains used in this study

Strain No.	Genomic background	Plasmid	Plasmid description	Designated name	Source
2001	630	N/A	N/A		Peter Mullany
2015	630 Δ*erm*	N/A	N/A		Peter Mullany
2347	630 Δ*erm* cwp10::*erm*	N/A	N/A	*cwp10*::CT	This study
2348	630 Δ*erm cwp29::erm*	N/A	N/A	*cwp29*::CT	This study
2356	630 Δ*erm cwp7::erm*	N/A	N/A	*cwp7*::CT	This study
2357	630 Δ*erm cwp7::erm*	pMLD024	pRPF144-*cwp7*	*cwp7*::CT + [pCwp7]	This study
2359	630 Δ*erm cwp7::erm*	pMLD026	pRPF144-$cwp7_{trunc}$	*cwp7::CT* + [$pCwp7_{trunc}$]	This study
2360	630 Δ*erm*	pMTL960	pMTL960	630 Δ*erm* + [pMTL960]	This study
2361	630 Δ*erm cwp7::erm*	pMTL960	pMTL960	*cwp7*::CT + [pMTL960]	This study
2366	630 Δ*erm cwp18::erm*	N/A	N/A	*cwp18*::CT	This study
2367	630 Δ*erm cwp27::erm*	N/A	N/A	*cwp27*::CT	This study
2411	630 Δ*erm*	pMLD024	pRPF144-*cwp7*	630 Δ*erm* + [pCwp7]	This study
2412	630 *Δerm cwp7::erm*	pMLD035	pRPF144-*cwp7-mCherry*	*cwp7::CT* + [$pCwp7_{mCherry}$]	This study
2428	630 Δ*erm*	pMLD052	pRPF185-*αCD2783*		This study
2429	630 Δ*erm cwp7::erm*	pMLD052	pRPF185-*αCD2783*		This study
2542	630 Δ*erm ΔpyrE*	N/A	N/A		Nigel Minton
2545	630 Δ*erm fliC::erm*	N/A	N/A		Susan Logan
2600	630 Δ*erm cwp7::erm*	pMLD063	pFT58-Pcwp2-cwp7-SNAP-Cdi		This study
2601	630 Δ*erm ΔpyrE Δcwp7*	N/A	N/A	*Δcwp7 ΔpyrE*	This study
2618	630 Δ*erm Δcwp7*	N/A	N/A	*Δcwp7*	This study
2619	630 Δ*erm Δcwp7::Pcwp2-cwp7*	N/A	N/A	*Δcwp7::cwp7*	This study
2642	630 Δ*erm ΔpyrE ΔCD3494*	N/A	N/A	*ΔCD3494 ΔpyrE*	This study
2643	630 Δ*erm ΔpyrE ΔCD0106*	N/A	N/A	*ΔCD0106 ΔpyrE*	This study
2644	630 Δ*erm ΔpyrE ΔCD3567*	N/A	N/A	*ΔCD3567 ΔpyrE*	This study
2645	630 Δ*erm ΔpyrE ΔCD0125*	N/A	N/A	*ΔCD0125 ΔpyrE*	This study
2646	630 Δ*erm ΔCD3494*	N/A	N/A	*ΔCD3494*	This study
2647	630 Δ*erm ΔCD0106*	N/A	N/A	*ΔCD0106*	This study
2648	630 Δ*erm ΔCD3567*	N/A	N/A	*ΔCD3567*	This study
2649	630 Δ*erm ΔCD0125*	N/A	N/A	*ΔCD0125*	This study
2654	630 Δ*erm ΔCD3494::Pnat-CD3494*	N/A	N/A	*ΔCD3494::CD3494*	This study
2655	630 Δ*erm ΔCD0106::Pnat-CD0106*	N/A	N/A	*ΔCD0106::CD0106*	This study
2656	630 Δ*erm ΔCD3567::Pnat-CD3567*	N/A	N/A	*ΔCD3567::CD3567*	This study
2657	630 Δ*erm ΔCD0125::Pnat-CD0125*	N/A	N/A	*ΔCD0125::CD0125*	This study
2621	630 Δ*erm cwp7::erm*	pMLD075	pFT58-Pcwp2-SNAP-Cdi	*cwp7::CT* + [pSNAP]	This study
2631	630 Δ*erm*	pMLD063	pFT58-Pcwp2-cwp7-SNAP-Cdi	*cwp7::CT* + [$pCwp7_{SNAP}$]	This study
2698	630 Δ*erm cwp7::erm*	pMLD089	pRPF144-cwp7-FLAG	*cwp7::CT* + [$pCwp7_{FLAG}$]	This study

Table A2. Plasmids used in this study

Official name	Descriptive name	Comments
pMLD011	pMTL007C-E5-cwp10 (42a)	ClosTron plasmid targeting cwp10 (CD2796)
pMLD012	pMTL007C-E5-cwp29 (45a)	ClosTron plasmid targeting cwp29 (CD2518)
pMLD013	pMTL007C-E5-cwp7 (207a)	ClosTron plasmid targeting cwp7 (CD2782)
pMLD023	pET28a-cwp7 26-323	heterologous expression of cwp7 fragment (aa 26-323) for antibody purification.
pMLD024	pRPF144-cwp7	cwp7 complementation under the control of a constitutive, Pcwp2 promoter
pMLD026	pRPF144-cwp7-trunc	cwp7 complementation under the control of a constitutive, Pcwp2 promoter, no transmembrane helix
pMLD027	pMTL007C-E5-cwp18 (346a)	ClosTron plasmid targeting cwp18 (CD1047)
pMLD028	pMTL007C-E5-cwp27 (82s)	ClosTron plasmid targeting cwp27 (CD0440)
pMLD035	pRPF144-cwp7-mCherry (XhoI/XhoI)	pMLD034 with mCherry from pZLS016 cloned into the XhoI site (XhoI/XhoI cloning)
pMLD061	pMTL-YN3-Δcwp7	660 bp deletion within the cwp7 ORF with 750 bp LHR and HR
pMLD062	pMTL84121-linker-SNAP-Cdi	made by adding a liner to pFT47 [2360/2361]. 6bp different form pFT58 (no second stop codon on C-terminus of SNAP-Cdi)
pMLD063	pFT58-Pcwp2-cwp7-SNAP-Cdi	cwp7 including Pcwp2 from pMLD024 cloned EcoRI/BamHI into pFT58 to fuse with SNAP-Cdi
pMLD064	pFT58-Pcwp7-cwp7-SNAP-Cdi	cwp7 including native promoter cloned SacI/BamHI into pFT58 to fuse with SNAP-Cdi
pMLD066	pMTL-YN3-ΔCD3494	150 bp deletion within the CD3494 ORF with 750 bp LHR and RHR (ΔpyrE system)
pMLD069	pMTL-YN3-ΔCD0106	390bp deletion within the cwlD ORF with 1200bp LHR and RHR (ΔpyrE system)
pMLD070	pMTL-YN3-ΔCD3567	1137bp deletion within the CD3567 ORF with 1200bp LHR and RHR (ΔpyrE system)
pMLD071	pMTL-YN3-ΔCD0125	390bp deletion within the cwlD ORF with 1200bp LHR and RHR (ΔpyrE system)
pMLD073	pMTL-YN1C-Pcwp2-cwp7	Entire cwp7 ORF with under the cotrol of Pcwp2 cloned EcoRI/BamHI
pMLD074	pMTL-YN1C-Ptet-cwp7	Entire cwp7 ORF with under the cotrol of Ptet cloned KpnI/BamHI
pMLD075	pFT58-Pcwp2-SNAP-Cdi	pMLD063 without the cwp7 ORF (effectively Pcwp2-SNAP-Cdi). Constructed via inverse PCR using primers [2464/2465]
pMLD077	pMTL-YN1C-Ptet-cwp7 (-SacI)	pMLD074 with a SacI site upstream of Ptet removed via inverse PCR using primers [2492/2493]
pMLD085	pMTL-YN1C-Pnat-CD3494	CD3494 under the control of its native promoter cloned into pMTL-YN1C via Gibson Assembly
pMLD086	pMTL-YN1C-Pnat-CD0106	CD0106 under the control of its native promoter cloned into pMTL-YN1C via Gibson Assembly
pMLD087	pMTL-YN1C-Pnat-CD3567	CD3567 under the control of its native promoter cloned into pMTL-YN1C via Gibson Assembly
pMLD088	pMTL-YN1C-Pnat-CD0125	CD0125 under the control of its native promoter cloned into pMTL-YN1C via Gibson Assembly
pMLD089	pRPF144-cwp7-FLAG	cwp7-FLAG fusion under the control of Pcwp2
pRPF215	pMTL960-Ptet-himar1 (Tnase) + ermB transposon	Codon-optimised himar1 transposase and a Mariner transposon carrying ermB cloned under the control of the inducible Ptet promoter

Figure A1. Maps of plasmids used in this study.

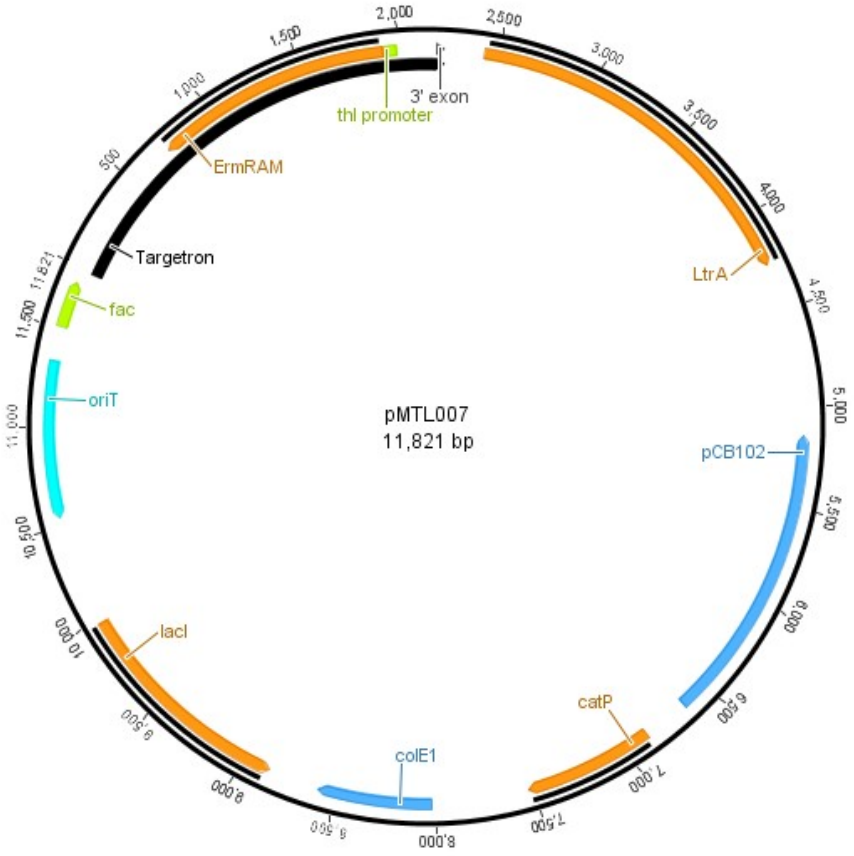

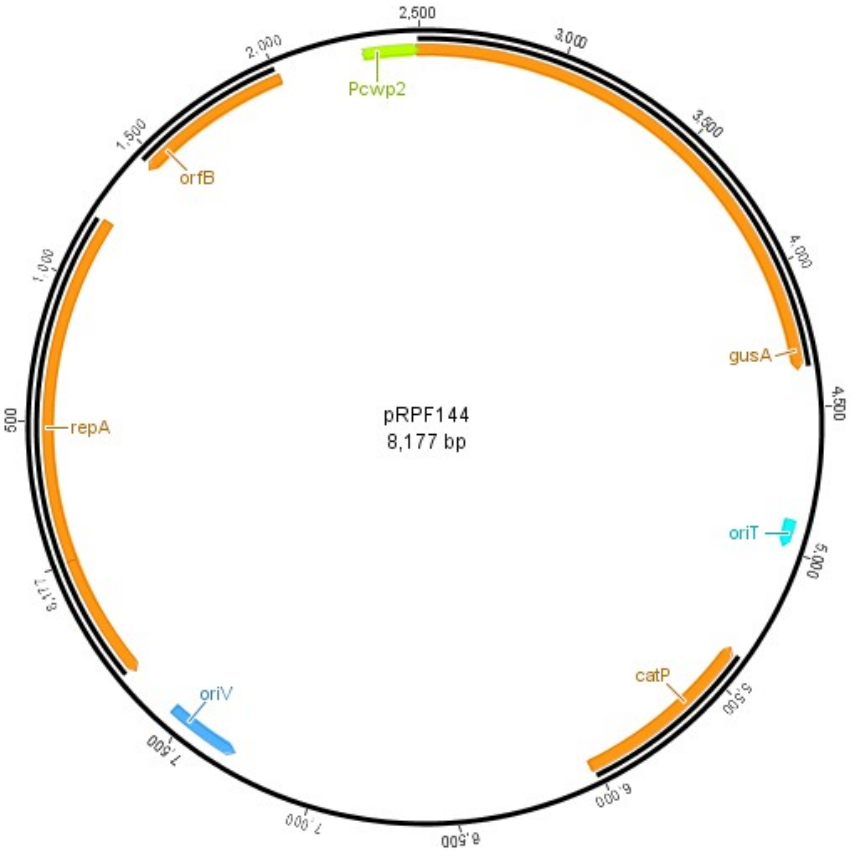

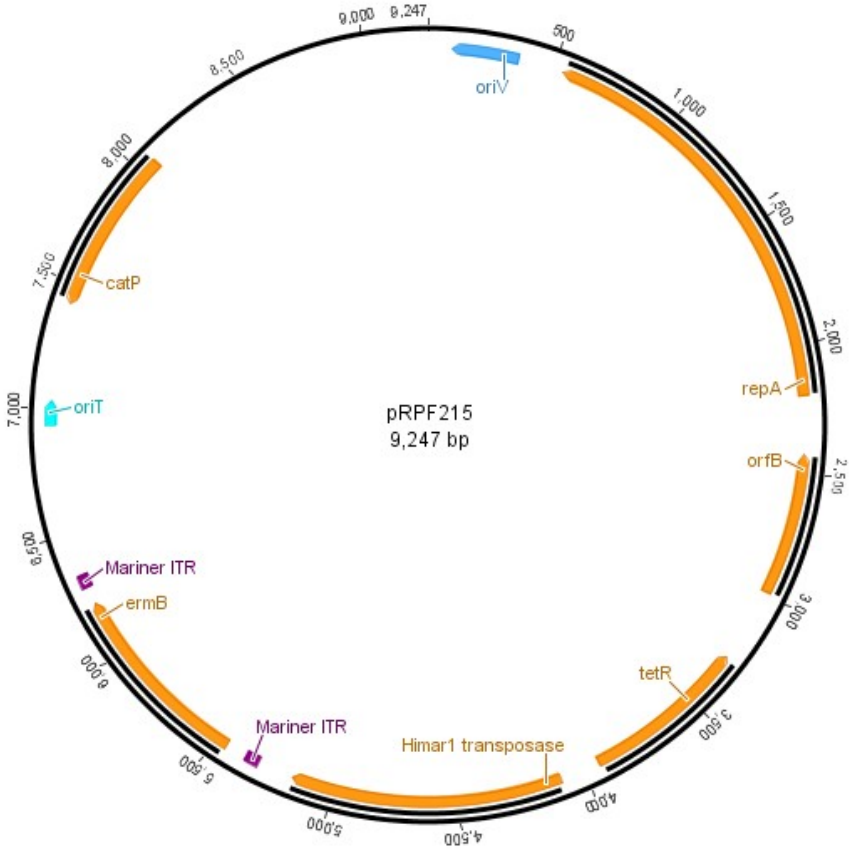
pRPF215
9,247 bp
oriV
repA
orfB
tetR
Himar1 transposase
Mariner ITR
ermB
Mariner ITR
catP
oriT

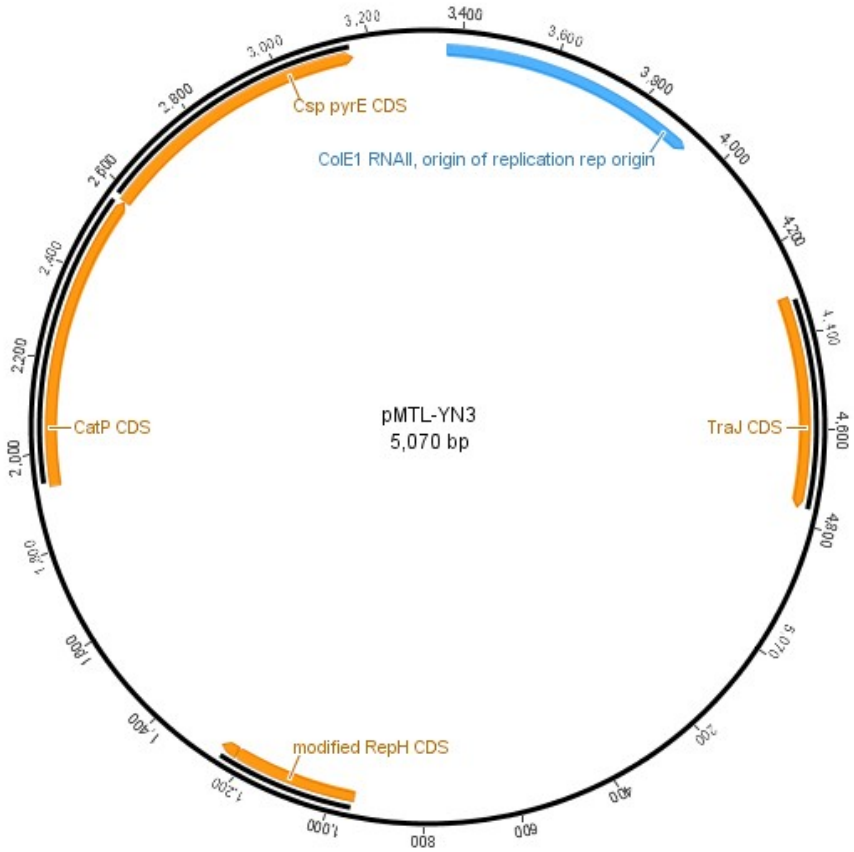
pMTL-YN3
5,070 bp
Csp pyrE CDS
ColE1 RNAII, origin of replication rep origin
TraJ CDS
modified RepH CDS
CatP CDS

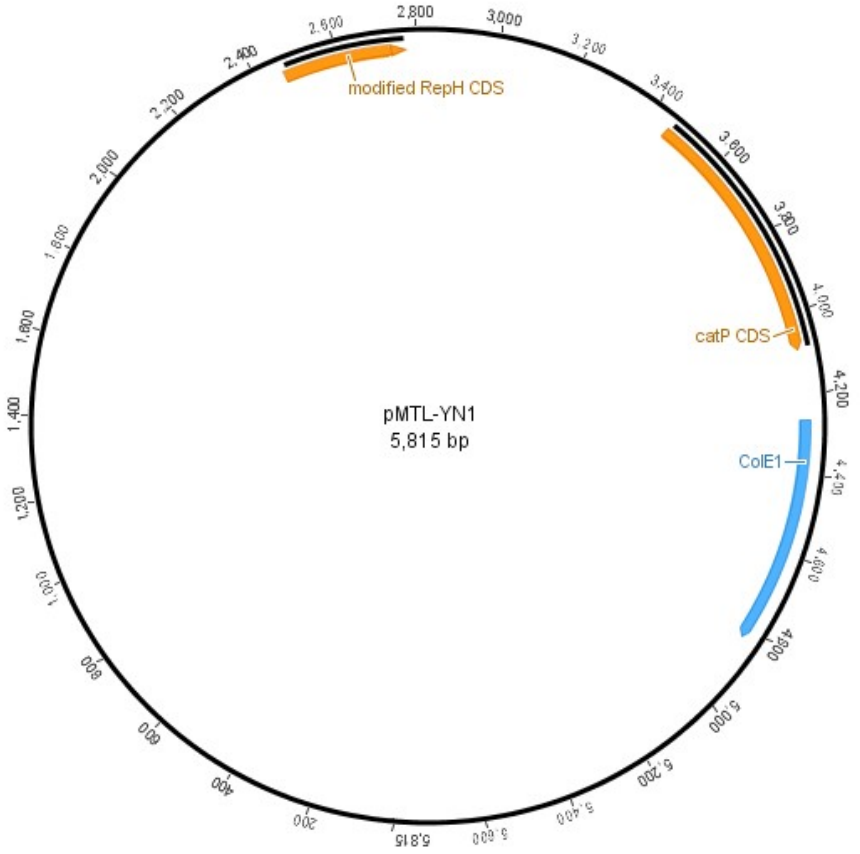
modified RepH CDS
catP CDS
ColE1
pMTL-YN1
5,815 bp

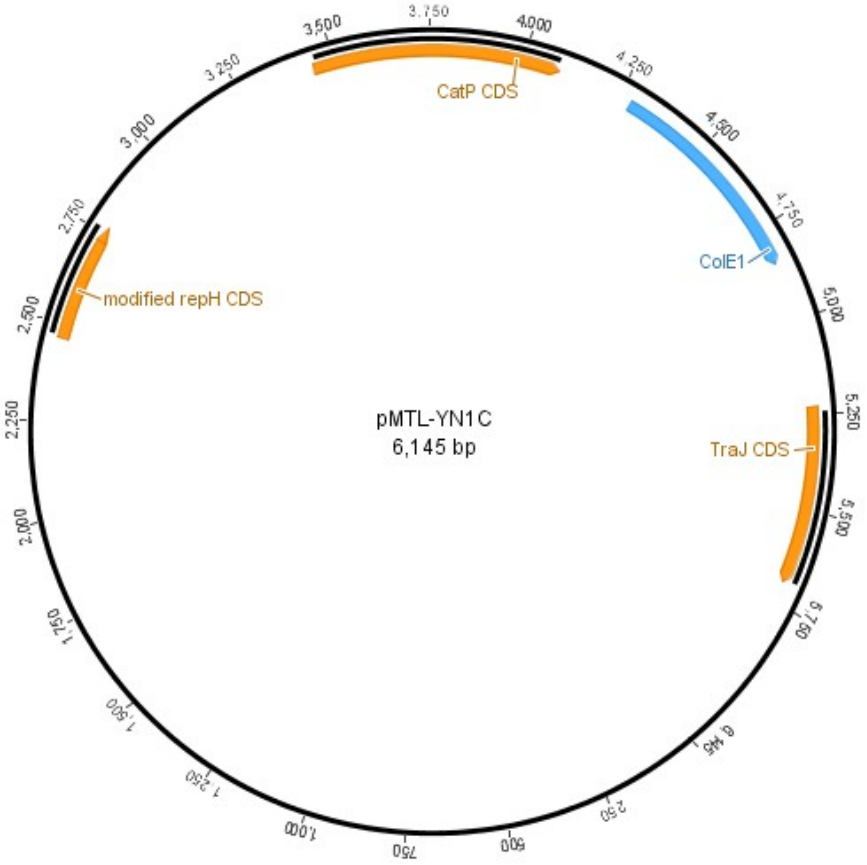
CatP CDS
ColE1
modified repH CDS
TraJ CDS
pMTL-YN1C
6,145 bp

Table A3. Primers used in this study.

Name	Orientation	Sequence (5' -> 3')	Restriction site	Comments
408	F	TCTTGAATATCAAAGGTGAGCCAGTACA		16S rRNA amplification for RT-PCR
409	R	TACAGCGTGGACTACCAGGGTATCTAAT		
722	F	ACGCGTTATATTGATAAAAATAATAATAGTGGG		RAM amplification for screening ClosTron mutants
723	R	ACGCGTGCGACTCATAGAATTATTTCCTCCCG		
793	F	CACCTCCTTTTTGACTTTAAGCCTACGAATACC		pRPF144 plasmid sequencing
794	R	CACCGACGAGCAAGGCAAGACCG		
1063	R	CGAAATTAGAAACTTGCGTTCAGTAAAC		ClosTron EBS universal primer
1322	F	CTG GAC TTC ATG AAA AAC TAA AAA AAA TAT TG		pRPF185 plasmid sequencing
1671	F	TCCCTCTTATTCTTTCTACTTTCATTCC		cwp7 (CD2782) amplification for RT-PCR (300bp product)
1672	R	GAAGGGAGTATACCAGAGATTTCG		
1673	F	GCTGGTTTATCACTTGTTCCTTTTCC		cwp10 (CD2796) amplification for RT-PCR (300bp product)
1674	R	TTCATTTCAAGCCAGTATAAAAGTACAAGG		
1675	F	TGATGAAGTACCACCTATTACATAACTTTC		cwp29 (CD2518) amplification for RT-PCR (300bp product)
1676	R	GCTTTATCAATAGAACTTTCTCCACCT		
1677	F	CCATCAAACAATGTAGAAGAAGCTGG		tcdA (CD0663) amplification for RT-PCR (300bp product)
1678	R	TAGCAAATTCGCTTGTGTTGAATTCATC		
1679	F	AGATTTATGATGGAACTAGGAAAGTATTTAAG		tcdB (CD0660) amplification for RT-PCR (300bp product)
1680	R	CACCAAGAGAACCTTCAAAATAATTCC		
1681	F	TCTAGCAAACGCTGCATGTGC		pfoR (CD2625) amplification for RT-PCR (300bp product)
1682	R	ACAACCACTAAATCCACTCCAGG		
1702	F	CTCACCTTGTACTTTTATACTGG		for screening *cwp10* ClosTron mutants
1703	R	AATAAAAGAAAATCTTTTATAAGAACTATAGC		
1704	F	CTTAATCCATCAGCCATTGTGC		for screening *cwp29* ClosTron mutants
1705	R	GTGAAATTAAAGAAATTATTATCACTAGG		
1718	F	GTATAAGTGCAACACCTTTAGC		for screening *cwp7* ClosTron mutants
1719	R	TCTTTAGATACTGCCTTTAAACC		
1762	F	GGATCCAAAAGCTTCCTTATAAATCAAAAAC	BamHI	for complementation of the *cwp7* ClosTron mutant using pRPF144
1763	R	GAGCTCAAAGAAAAGGAATGAGAAC	SacI	
1764	F	CTCGAGGCTCTTAAATAGACTATAATC	XhoI	for producing recombinant Cwp7 using pET-28a for antibody production
1790	R	CCA TGG ATG CAA ATC CCA AAA GAG	NcoI	
1791	F	GATC GG ATC CAA AAG CTT CCT TAT AAA TC	BamHI	for complementation of the *cwp7* ClosTron mutant using pRPF144
1792	R	GATC GA GCT CAA AGA AAA GGA ATG AG	SacI	
1804	F	GCT CTT AAA TAG ACT ATA ATC ACC TAC TG		to delete the C-terminal transmembrane helix in *cwp7* in pMLD024/025

1805	R	AGG GCA CTT AGA TAT GAG TCG AAA TAG		
1835	F	GACTCATATCTAAGTGCCCTAAATG		to amplify a fragment of transcript between *cwp7* and *mviN* via RT-PCR
1836	R	AATACTGATTTGTAGTGATAACTTAAGTCG		
1837	F	GTCTTTTCTTTGTCTCAAAGTACATAGG		to amplify a fragment of transcript between *cwp7* and *mviN* via RT-PCR
1838	R	AAAAACAGCTAAAGCAGCATTGTGG		
1843	F	CAATTTGAAAAATAGTTTTTGATTTATAAGGAAGC		to add a C-terminal StrepTag to *cwp7* in pMLD024
1844	R	TGGATGACTCCATTTCGACTCATAT		
1845	F	CACCACCACTAGTTTTTGATTTATAAGG		to add a C-terminal HisTag to *cwp7* in pMLD024
1846	R	GTGGTGGTGTTTCGACTCATATC		
1860	F	CTA TCT TCT AAG TAG TTT TTG TTT TCC TTT TC		to amplify a fragment of transcript between *cwp7* and *mviN* via RT-PCR
1861	F	ACA AAT AAT GCC ATA ACA AAC TCA TTT AGC		
1862	F	TCAAATTCATTGCCAGATGCATTGG		for screening *cwp18* ClosTron mutants
1863	R	AATTAAAATAACTTCTGCTGGATTAAGCC		
1864	F	CTGTTTCATTATTGATTGCTAGTTGTCC		for screening *cwp27* ClosTron mutants
1865	R	TTGCTGACAATCCATCAGATAATCC		
1951	F	GAGTAGTTTTTGATTTATAAGGAAGCTTTTGG		to add an XhoI site directly upstream of the *cwp7* stop codon in pRPF144-*cwp7*
1952	R	GAGTTTCGACTCATATCTAAGTGCCC		
1953	F	GATCCTCGAGGTGAGCAAGGGCGAGGAG	XhoI	to amplify mCherry from pZLS016 (adds XhoI on both sides)
1954	R	GATCCTCGAGCTACTTGTACAGCTCGTCCATG	XhoI	
1985	F	GATCCTCGAGCCCAAAAGAGAGTTGATAGAAG	XhoI	To add an N-terminal StrepTag to *cwp7* using pHAS007 construct
2109	F	GATCGAGCTCCTTTGGTACAAGTCGAATAAAAC	SacI	To amplify CD2783 for antisense RNA
2110	R	GATCGGATCCAATATGGAGGTAACTATGTCTG	BamHI	
2206	R	GATCGTCGACCTACTTGTACAGCTCGTCCATG	SalI	to amplify mCherry pZLS016 (adds SalI on 3' end)
2236	F	TTCTCCCGCATTTTCCTAGTC		CD2783 ClosTron screening primer (200bp product)
2237	R	ATTGCAAGTGAGATTGACTATAGC		
2280	R	GACCTACTTGTACAGCTCGT		to remove the XhoI site from pMLD054
2301	F	GATCGAATTCTGCATCAAGCTAGCTTG	EcoRI	to clone *Pcwp2-cwp7* from pMLD024 into pFT58 (EcoRI/BamHI)
2302	F	GGCGCGCCGCCATTATTTTTTTGAAC		to remove the fragment between SbfI/AscI in pMTL-YN3 for Gibson assembly purposes
2303	R	CCTGCAGGGGGCCCGATC		
2304	F	CGGGCCCCCTGCAGGAACAAATTGCTCTGTAAATAAAAG		Gibson assembly: pMTL-YN3 -> *cwp7* LHR
2305	R	AATCCCAAAATAAAGAAAATCTATACTGCTAGATTAG		Gibson assembly: *cwp7* LHR <- *cwp7* RHR
2306	F	ATTTTCTTTATTTTGGGATTTGCATCTGC		Gibson assembly: *cwp7* LHR -> *cwp7* RHR
2307	R	TAATGGCGGCGCGCCTGTACCAAAGAATTATGGATTTAG		Gibson assembly: *cwp7* RHR <- pMTL-YN3
2308	F	GTCGTTTCTAAATCCTGCTGC		for screening *pyrE cwp7* deletion mutants (anneals to the chromosome)
2309	R	TAGCATAGTAAAAGGAACAGTTTTATTCG		
2310	F	GGAGCTGGTGAAGTACATC		for pFT58 sequencing
2311	R	TAAGTTGGGTAACGCCAGG		
2317	F	CATGCGCTCCATCAAGAAG		for sequencing pMTL-YN3 vectors

2318	R	CTTTCTATTCAGCACTG		
2360	F	AGCTGCTGATAAAGATTGTGAAATGAAGAGAACC		pFT47 alteration to add a linker on the N-terminus of SNAP-Cdi
2361	R	GCGGATCCCCGGGTACC		
2368	F	CATCAAGAAGAGCGACTTCG		for *pyrE* mutant screening. Binds to pMTL-YN3 plasmid.
2369	R	TTCTTTCTATTCAGCACTGTTATGC		
2374	F	CGGGCCCCCTGCAGGGACTTGCTATTTCTTTTTTATATTCC		Gibson assembly: pMTL-YN3 -> CD3494 LHR
2375	R	GAAAGATAGAGGAACTATAAATTCTATGGTATATGC		Gibson assembly: CD3494 LHR F <- CD3494 RHR
2376	F	TATAGTTCCTCTATCTTTCAAAGTTATGTTCTG		Gibson assembly: CD3494 LHR F -> CD3494 RHR
2377	R	TAATGGCGGCGCGCCAAAATCTAGAACTTTTATCACAAAGATAG		Gibson assembly: CD3494 RHR <- pMTL-YN3
2429	R	TGCAAAAGTAGCTCCTACAGC		for *pyrE* screening. Flanks the *pyrE* locus to confirm WT/*pyrE* phenotype.
2430	F	GAATAAAAAGTTTAGACGAAATAAGAGG		
2431	F	CGGGCCCCCTGCAGGAATGGCTTGTAATTATCCAAG		Gibson assembly: pMTL-YN3 -> CD3567 LHR
2432	R	TAGACGGAATAATCGTATATATATGCAAAGAAGG		Gibson assembly: CD3567 LHR <- CD3567 RHR
2433	F	ATACGATTATTCCGTCTACATTAGAAATAGTATTTTTATC		Gibson assembly: CD3567 LHR -> CD3567 RHR
2434	R	TAATGGCGGCGCGCCCAGTATAAAGAAGTAAGAGCAC		Gibson assembly: CD3567 RHR <- pMTL-YN3
2435	F	TTTAATTTTCCTTCTAAGATTGCTTCTC		*pyrE* CD3567 screening
2436	R	AATACCTGCAGTAGGTGTAGC		
2437	F	CGGGCCCCCTGCAGGTTACAGATACCATACTGGTTATG		Gibson assembly: pMTL-YN3 -> CD0106 LHR
2438	R	GTTTGTCTTTTACTACTACTAGACATATCATTGC		Gibson assembly: CD0106 LHR <- CD0106 RHR
2439	F	GTAGTAGTAAAAGACAAACAAGACAGTAAAGAATTATC		Gibson assembly: CD0106 LHR -> CD0106 RHR
2440	R	TAATGGCGGCGCGCCACGCATTTCACCGCTACAC		Gibson assembly: CD0106 RHR <- pMTL-YN3
2441	F	GAGATTTTGTTGTTGTAGTAAATGCAG		*pyrE* CD0106 screening
2442	R	GCAACTGGTGTTCCTCCTAATATC		
2443	F	CGGGCCCCCTGCAGGTCCATCACTTATAACTTTAGTTTC		Gibson assembly: pMTL-YN3 -> CD0125 LHR F
2444	R	CACTTTCTATTTTATTAGAAGCCAATTTATCTACATTATTATTTG		Gibson assembly: CD0125 LHR <- CD0125 RHR R
2445	F	CTTCTAATAAAATAGAAAGTGAAGAAGGTATACATG		Gibson assembly: CD0125 LHR -> CD0125 RHR F
2446	R	TAATGGCGGCGCGCCCATCATCAAATCTATCTCCAC		Gibson assembly: CD0125 RHR <- pMTL-YN3 R
2447	F	TGTTTTGTTAGGATTTGTGACTTGC		*pyrE* CD0125 screening
2448	R	CTTTCTCCTATAAGAAGATTGTGTTG		
2449	F	AAGTTTATGAATCTGATGAGTGTCC		pMTL-YN1 screening
2450	R	AGGCGATTAAGTTGGGTAACG		
2462	F	CATGATATAGGTATGCC		for pMTL-YN1C and pMTL-YN1X sequencing
2463	R	GTGCTGCAAGGCGATTAAG		
2464	R	CATAAGTTCTCATTCCTTTTCTTTGAG		to remove *cwp7* from pMLD063
2465	F	GATAAAGATTGTGAAATGAAGAGAACC		
2466	F	AATCCCAAAAGAGAGTTGATAGAAG		to remove the Cwp7 signal peptide from pMLD063
2485	F	CTTTCTTTAAGCTGTTTATTTGTATTTCAG		*pyrE* CD3494 screening
2486	R	GATGGATGAGTTTTGGAATCAGG		

2492	F	GGTACCTTAAGACCCACTTTC		to remove SacI upstream of Ptet in pMLD074 *via* inverse PCR
2493	R	GAATTCGTAATCATGGTCATATGG		
2571	F	GGATCCTCTAGAGTCGACG		Gibson assembly: pMTL-YN1C-Pcwp2 linearisation
2572	R	GAGCTCTTATTATTTTTTCCTTATTTACC		
2621	R	GCGGCCGCTTATTACATCC		pMTL-YN1C linearisation. To be used with 2571
2622	F	GTAATAAGCGGCCGCGAGAGAAGAAGATGAAGTTTAAG		Gibson assembly: CD3494 native complementation via pMTL-YN1C
2623	R	CGACTCTAGAGGATCCTGCTTACATCTTGAGTAAAAGG		
2624	F	GTAATAAGCGGCCGCTTAAATAGGGGCAGAAATATAATATTATTAC		Gibson assembly: CD0106 native complementation via pMTL-YN1C
2625	R	CGACTCTAGAGGATCCCTTTAATACAAGCTATTTACATATTTAGAC		
2626	F	GTAATAAGCGGCCGCACATCTAATGTAAAGTTGCAAG		Gibson assembly: CD3567 native complementation via pMTL-YN1C
2627	R	CGACTCTAGAGGATCCGGTATTATAATACCCTATTATACTTAATTACTTTAAATTTTTTAATATTAATC		
2628	F	GTAATAAGCGGCCGCAGAAGGAATGGCAGAAGAG		Gibson assembly: CD0125 native complementation via pMTL-YN1C
2629	R	CGACTCTAGAGGATCCGCTTAACCAAATATGATTAAACTTG		
2630	F	GACGATGACAAGTAGTTTTTGATTTATAAG		to replace the HisTag in pMLD024 for FLAG *via* inverse PCR
2631	R	ATCCTTGTAATCTTTCGACTCATATC		

Table A4. Antibodies used in this study

1° antibody	Conjugate	Dilution		Species	Source
		Western blotting	Immunostaining		
anti-SLP LMW	N/A	1:200,000	1:20	rabbit	Robert Fagan, this laboratory
anti-SLP HMW	N/A	1:100,000	1:20	rabbit	Emanuella Calabi, this laboratory
anti-Cwp66 C-term	N/A	1:20,000	1:20	mouse	Simon Cutting, Royal Holloway
anti-Cwp2	N/A	1:50,000	1:20	mouse	Simon Cutting, Royal Holloway
anti-Cwp84	N/A	1:4,000	1:20	mouse	Simon Cutting, Royal Holloway
anti-Cwp7	N/A	1:10,000	1:20	mouse	This study
anti-FLAG	N/A	1:4,000	N/A	mouse	Sigma
2° antibody		**Dilution**		**Source**	
anti-rabbit IgG-HRP	horse radish peroxidase	1:5,000	N/A	goat	Dako Cytomation
anti-mouse IgG-HRP	horse radish peroxidase	1:10,000	N/A	rabbit	Dako Cytomation
anti-rabbit IgG-FITC	fluorescein	N/A	1:200	goat	Dako Cytomation
anti-mouse IgG-FITC	fluorescein	N/A	1:200	rabbit	Dako Cytomation
Anti-his-tag-HRP	horse radish peroxidase	1:2;000	N/A	N/A	Sigma

Appendix B

Table B1. Genes significantly up-regulated during germination ($p \leq 0.01$).

Systematic Name	Gene product	Fold change (30 vs. 180 min)	*p*-value
CD2270	putative 1-phosphofructokinase	+79.8	5.79E-03
CD2269	PTS system, IIbc component	+75.2	5.71E-03
CD0524	putative peptidase	+35.4	7.64E-03
CD2671	oligopeptide transporter, ATP-binding protein	+28.0	1.15E-03
CD2670	oligopeptide ABC transporter, ATP-binding protein	+24.7	1.22E-03
CD3019	putative transporter	+22.7	2.21E-03
CD2673	oligopeptide ABC transporter, permease protein	+21.1	1.46E-03
CD2541	sodium:dicarboxylate symporter family protein	+19.2	7.98E-03
CD3073	putative membrane protein	+19.1	1.81E-03
CD2966	aldehyde-alcohol dehydrogenase	+17.2	8.16E-03
CD2240	N-acetylneuraminate lyase	+16.6	6.58E-03
CD2674	oligopeptide ABC transporter, permease protein	+16.0	5.79E-03
CD1696	putative sodium:amino acid symporter	+13.8	5.71E-03
CD2548	putative sugar transporter, permease protein	+13.6	3.30E-03
CD2669a	putative Na(+)/H(+) antiporter	+13.2	5.05E-03
CD2239	putative sodium:solute symporter	+11.6	6.84E-03
CD1506	putative drug/sodium antiporters	+11.4	3.85E-03
CD2595	PyrR bifunctional protein	+10.9	6.58E-03
CD2040	MerR-family transcriptional regulator	+10.9	3.85E-03
CD1950	putative membrane protein	+10.8	4.93E-03
CD2177	probable amino-acid ABC transporter,substrate-binding protein	+10.6	6.42E-03
CD2594	uracil permease	+10.5	4.54E-03
CD1680	putative FMN-binding exported protein	+9.5	5.71E-03
CD2456	ABC transporter, ATP-binding protein	+9.5	2.15E-03
CD2238	conserved hypothetical protein	+9.4	5.96E-03
CD1679	putative flavodoxin	+9.4	3.77E-03
CD2145	DNA mismatch repair protein	+9.3	3.85E-03
CD3247	putative electron transfer protein	+9.2	6.42E-03
CD2617	putative membrane protein	+9.0	5.35E-03
CD2176	probable amino-acid ABC transporter, permease protein	+8.7	1.81E-03
CD3290	putative protein translocase	+8.2	5.59E-03
CD2107	putative xanthine/uracil permease	+7.6	2.78E-03
CD1408	D-alanine--D-alanine ligase B	+7.3	8.43E-03
CD1681	TetR-family transcriptional regulator	+6.9	5.71E-03
CD0672	conserved hypothetical protein	+6.7	2.78E-03
CD2041	putative regulatory protein	+6.7	5.59E-03
CD2042	putative transcriptional regulator	+6.6	2.00E-03
CD1677	putative membrane protein	+6.6	5.71E-03
CD2175	probable amino-acid ABC transporter, permease protein	+6.4	4.45E-03

CD2013	TetR-family transcriptional regulator	+6.2	3.77E-03
CD2012	putative hydrolase	+6.1	3.77E-03
CD1998	TetR-family transcriptional regulator	+6.1	8.27E-03
CD2703	conserved hypothetical pentapeptide repeat protein	+6.0	5.58E-03
CD1027	spermidine/putrescine ABC transporter,substrate-binding lipoprotein	+5.8	5.71E-03
CD2024	ABC transporter, ATP-binding protein	+5.7	4.67E-03
CD2471	conserved hypothetical protein	+5.7	8.53E-03
CD1273	putative competence protein	+5.5	5.76E-03
CD1025	spermidine/putrescine ABC transporter, permease protein	+5.2	6.37E-03
CD1617	GntR-family transcriptional regulator	+5.1	5.79E-03
CD1026	putative spermidine/putrescine ABC transporter,permease protein	+5.1	5.34E-03
CD2966A	putative membrane protein	+5.0	5.59E-03
CD1488	putative transcriptional regulator	+4.8	4.67E-03
CD0761	putative ATP-dependent RNA helicase	+4.7	9.13E-03
CD2152	putative glutamyl-aminopeptidase	+4.7	9.13E-03
CD2207	putative flavodoxin	+4.7	4.45E-03
CD1621	putative mechanosensitive ion channel protein	+4.7	4.24E-03
CD3646	GntR-family transcriptional regulator	+4.6	6.61E-03
CD2457	conserved hypothetical protein	+4.6	6.00E-03
CD1024	spermidine/putrescine ABC transporter,ATP-binding protein	+4.5	8.10E-03
CD3241	proline reductase	+4.4	4.41E-03
CD2208	MarR-family transcriptional regulator	+4.4	6.99E-03
CD1164	Spo0B-associated GTP-binding protein	+4.3	5.71E-03
CD2025	putative ABC transporter, permease protein	+4.3	5.79E-03
CD2023	GntR-family transcriptional regulator	+4.2	1.54E-03
CD2472	conserved hypothetical protein	+4.2	8.33E-03
CD2214	putative regulatory protein	+4.2	5.05E-03
CD1345	PadR-family transcriptional regulator	+4.2	6.98E-03
CD3243	hypothetical protein	+4.2	8.78E-03
CD2845	rubrerythrin	+4.2	2.78E-03
CD2056	putative membrane protein	+4.2	8.43E-03
CD0806	putative sigma-54-dependent transcriptional regulator	+4.1	5.42E-03
CD0471	penicillinase repressor	+4.1	5.18E-03
CD2215	putative regulatory protein	+4.1	5.71E-03
CD3219	chaperonin	+4.0	4.97E-03
CD3236	putative membrane protein	+4.0	5.76E-03
CD0470	putative beta-lactamase-inducing penicillin-binding protein	+3.9	6.80E-03
CD2840	seryl-tRNA synthetase	+3.9	6.30E-03
CD1676	pyrrolidone-carboxylate peptidase	+3.9	5.08E-03
CD3072	conserved hypothetical protein	+3.8	7.09E-03
CD2102	putative Na(+)/H(+) antiporter	+3.8	8.10E-03
CD1555	putative amino acid permease	+3.8	5.79E-03
CD2151	putative membrane protein	+3.8	5.71E-03
CD1618	ABC transporter, ATP-binding protein	+3.7	3.77E-03

CD1296	segregation and condensation protein B	+3.7	4.66E-03
CD1757	conserved hypothetical protein	+3.7	6.73E-03
CD2236	putative glucokinase	+3.7	8.62E-03
CD2781	putative transmembrane virulence factor MviN family protein	+3.5	4.45E-03
CD0320	two-component response regulator	+3.5	5.82E-03
CD2843	putative zinc-binding dehydrogenase	+3.5	5.59E-03
CD3286	putative sodium-dependent phosphate transporter	+3.5	4.41E-03
CD3289	hypothetical protein	+3.5	9.80E-03
CD3478	conserved hypothetical protein	+3.5	5.71E-03
CD2593	putative antibiotic resistance ABC transporter,ATP-binding protein	+3.4	5.00E-03
CD3592	orotidine 5'-phosphate decarboxylase	+3.4	5.34E-03
CD1229	putative penicillin-binding protein	+3.4	6.69E-03
CD0821	two-component sensor histidine kinase	+3.4	9.80E-03
CD3188	hypothetical protein	+3.4	9.91E-03
CD2792	preprotein translocase SecA subunit	+3.4	5.71E-03
CD2235	RpiR-family transcriptional regulator	+3.4	5.37E-03
CD1471	putative membrane protein (putative phage infection protein)	+3.4	5.96E-03
CD1438	putative multiprotein complex assembly protein	+3.4	6.42E-03
CD2888	ABC transporter, permease protein	+3.4	8.10E-03
CD2043	putative hydrolase	+3.3	4.41E-03
CD0998	putative radical SAM protein	+3.3	3.00E-03
CD2705	putative amidohydrolas	+3.3	8.62E-03
CD3077	phosphosugar-binding transcriptional regulator	+3.3	6.84E-03
CD3616	putative Na+/H+ exchanger	+3.3	5.79E-03
CD2368	hypothetical protein	+3.2	3.53E-03
CD2206	aldehyde dehydrogenase	+3.2	4.39E-03
CD1294	putative membrane-associated peptidase	+3.2	6.37E-03
CD2528	hypothetical protein	+3.2	5.76E-03
CD1326	radical SAM-superfamily protein	+3.1	9.51E-03
CD2171	putative Sodium:dicarboxylate symporter	+3.1	5.71E-03
CD0983	putative hydrolase	+3.1	8.37E-03
CD2103	putative ABC transporter, permease protein	+3.1	7.64E-03
CD2234	cAMP-binding regulatory protein	+3.1	6.56E-03
CD2972	hypothetical protein	+3.1	5.79E-03
CD0321	hypothetical protein	+3.1	3.85E-03
CD3678	putative sporulation membrane protein	+3.1	9.32E-03
CD2253	GntR-family transcriptioanl regulator	+3.0	1.81E-03
CD2782	cell surface protein	+3.0	5.71E-03
CD1625	two-component sensor histidine kinase	+3.0	8.33E-03
CD2057	conserved hypothetical protein	+3.0	5.05E-03
CD0427	putative DNA-binding protein	+3.0	5.79E-03
CD1201	N utilization substance protein B	+3.0	9.32E-03
CD0482	putative lantibiotic resistance two-component sensor kinase	+3.0	3.77E-03
CD1227	putative O-methyltransferase	+3.0	5.96E-03

CD1504	ABC transporter, ATP-binding protein	+3.0	6.42E-03
CD2100	putative [2Fe-2S]-binding subunit of oxidoreductase	+2.9	5.59E-03
CD1665	cysteine synthase A	+2.9	9.30E-03
CD0481	putative lantibiotic resistance two-component response regulator	+2.9	7.73E-03
CD1806	putative fructokinase	+2.8	4.41E-03
CD1736	putative transcriptional regulator	+2.8	5.08E-03
CD1624	two-component response regulator	+2.8	5.71E-03
CD0676	conserved hypothetical protein	+2.8	4.41E-03
CD2516	putative L-asparaginase	+2.8	5.08E-03
CD1258	putative GTPase	+2.8	3.50E-03
CD3677	SpoIIIJ-associated protein	+2.8	8.91E-03
CD3239	conserved hypothetical protein	+2.8	7.92E-03
CD2450	putative ribosomal protein L11 methyltransferase	+2.8	6.36E-03
CD2049	conserved hypothetical protein	+2.8	6.07E-03
CD2690	putative membrane-associated phosphatase	+2.7	5.71E-03
CD2592	fibronectin-binding protein	+2.7	7.02E-03
CD2766	putative penicillin-binding protein repressor	+2.7	5.08E-03
CD1270	two-component sensor histidine kinase	+2.7	4.63E-03
CD2780	putative phosphomannomutase/phosphoglycerate mutase	+2.7	6.36E-03
CD2015	putative membrane protein	+2.7	5.71E-03
CD2770	putative capsular polysaccharide biosynthesis glycosyl transferase	+2.7	6.56E-03
CD2689	putative lipoprotein	+2.7	5.74E-03
CD1046	peptidase T	+2.7	4.84E-03
CD1314	tRNA pseudouridine synthase B	+2.6	9.32E-03
CD1343	glutamine synthetase	+2.6	8.10E-03
CD2998	putative iron ABC transporter, permease protein	+2.6	5.96E-03
CD2597	lipoprotein signal peptidase	+2.6	5.79E-03
CD3582	putative pseudouridylate synthase	+2.5	8.33E-03
CD1574	conserved hypothetical protein	+2.5	6.84E-03
CD1542	conserved hypothetical protein	+2.5	1.81E-03
CD0521	two-component response regulator	+2.5	5.76E-03
CD1505	putative ABC transporter, permease protein	+2.5	7.52E-03
CD2265	putative membrane protein	+2.5	5.96E-03
CD0696	probable cation transport protein	+2.5	5.05E-03
CD1309	translation initiation factor IF-2	+2.5	9.51E-03
CD2615	TetR-family trancscriptional regulator	+2.5	7.55E-03
CD0517	putative membrane protein	+2.5	9.30E-03
CD0408A	putative membrane protein	+2.5	9.75E-03
CD2050	putative 23S RNA and tRNA pseudouridine synthase	+2.4	5.79E-03
CD2017	putative phage regulatory protein	+2.4	7.55E-03
CD2655	UDP-N-acetylmuramoyl-tripeptide--D-alanyl-D-alan ine ligase	+2.4	5.08E-03
CD1995	putative membrane protein	+2.4	9.53E-03
CD0670	putative regulatory protein	+2.4	7.33E-03
CD0316	putative ABC transporter, permease protein	+2.4	7.92E-03

CD2806	holliday junction DNA helicase	+2.4	5.76E-03
CD3520	putative cation efflux protein	+2.4	7.49E-03
CD2771	putative UDP-glucose 6-dehydrogenase	+2.4	6.81E-03
CD3647	PTS system, IIa component	+2.3	5.79E-03
CD0569	putative outer membrane lipoprotein	+2.3	8.69E-03
CD0336	ABC transporter, ATP-binding protein	+2.3	9.57E-03
CD0159	putative glyoxalase	+2.3	8.43E-03
CD2097	putative membrane protein	+2.3	8.27E-03
CD2345	LysR-family regulatory protein	+2.3	5.79E-03
CD0566	putative RNA methylase	+2.3	6.36E-03
CD0984	putative membrane protein	+2.3	8.82E-03
CD1281	putative tRNA (5-methylaminomethyl-2-thiouridylate)-methyltransferase	+2.3	5.59E-03
CD1297	putative membrane protein	+2.3	4.41E-03
CD3220A	small acid-soluble spore protein	+2.3	8.62E-03
CD2503	cation-transporting ATPase	+2.3	6.56E-03
CD1946	AraC-family transcriptional regulator	+2.2	8.06E-03
CD0781	penicillin-binding protein	+2.2	5.37E-03
CD3648	PTS system, IIb component	+2.2	9.32E-03
CD0822	putative lantibiotic ABC transporter,ATP-binding protein	+2.2	6.46E-03
CD1388	putative transcriptional regulator (pseudogene)	+2.2	5.79E-03
CD1311	putative RNA-binding protein	+2.2	6.42E-03
CD1041	ATP-dependent nuclease subunit A	+2.2	6.71E-03
CD0891	putative agmatinase	+2.2	5.79E-03
CD1996	AraC-family transcriptional regulator	+2.2	5.71E-03
CD3359	ABC transporter, ATP-binding protein	+2.1	2.78E-03
CD2995	ribonucleoside-diphosphate reductase alpha chain	+2.1	8.72E-03
CD0198	GMP synthase [glutamine-hydrolyzing]	+2.1	7.64E-03
CD0282	putative phosphoesterase	+2.1	8.30E-03
CD1268	ABC transporter, ATP-binding protein	+2.1	2.78E-03
CD2336	putative toxic anion resistance protein	+2.1	5.76E-03
CD0344	metallo-beta-lactamase superfamily protein	+2.1	6.71E-03
CD0796	LacI-family transcriptional regulator	+2.1	6.81E-03
CD2179	putative formate dehydrogenase	+2.1	7.92E-03
CD3055	putative ABC transporter, permease protein	+2.1	5.71E-03
CD2465	amino acid transporter	+2.1	6.42E-03
CD1467	ABC transporter, permease protein	+2.1	4.67E-03
CD1678	putative membrane protein	+2.1	5.79E-03
CD0350	conserved hypothetical protein	+2.1	4.84E-03
CD2359	putative hydrolase	+2.1	6.42E-03
CD1644	putative transcriptional regulator	+2.1	6.39E-03
CD2526	glycogen branching enzyme	+2.0	6.98E-03
CD1394	putative oxidoreductase	+2.0	8.62E-03
CD2994	ribonucleoside-diphosphate reductase beta chain	+2.0	5.42E-03
CD1813	hypothetical protein	+2.0	8.33E-03

CD2052	putative lipoprotein	+2.0	3.99E-03
CD2183	ATP-dependent RNA helicase	+2.0	5.37E-03
CD0888	arginine decarboxylase	+2.0	7.34E-03
CD2337	putative membrane protein	+2.0	8.29E-03
CD2818	ABC transporter, ATP-binding/permease protein	+2.0	5.71E-03

Table B2. Genes significantly down-regulated during germination ($p \leq 0.01$).

Systematic Name	Gene product	Fold change (30 vs 180 min)	*p*-value
CD2354	glycine reductase complex component B alpha and beta subunits	-100.0	4.67E-03
CD2352	glycine/sarcosine/betaine reductase complex component A	-100.0	5.59E-03
CD2349	glycine/sarcosine/betaine reductase complex component C beta subunit	-100.0	5.79E-03
CD2355	thioredoxin	-100.0	6.42E-03
CD2380	putative indolepyruvate oxidoreductase subunit	-88.5	6.16E-03
CD2356	thioredoxin reductase	-86.2	1.81E-03
CD2351	glycine reductase complex component B gamma subunit	-73.5	4.66E-03
CD2348	glycine/sarcosine/betaine reductase complex component C alpha subunit	-64.9	3.74E-03
CD2357	putative glycine reductase complex component	-38.6	6.36E-03
CD0804	electron transfer flavoprotein beta-subunit	-30.0	3.53E-03
CD2625	putative membrane protein	-29.8	5.71E-03
CD3027	PTS system, glucose-specific IIa component	-28.4	4.24E-03
CD3028	putative phosphosugar isomerase	-27.9	5.05E-03
CD0022	putative translation elongation factor	-27.8	4.67E-03
CD3136	6-phospho-beta-glucosidase	-26.5	5.96E-03
CD3137	PTS system, IIabc component	-26.2	9.51E-03
CD2693	putative sodium:dicarboxylate symporter	-25.3	1.87E-03
CD3029	putative bifunctional protein: repressor/cystathionine beta-lyase	-24.2	2.00E-03
CD3030	PTS system, maltose and glucose-specific IIbc component	-23.8	2.78E-03
CD0179	NAD-specific glutamate dehydrogenase	-23.8	7.80E-03
CD1125	nitroreductase-family protein	-23.5	6.56E-03
CD1692	ArsR-family transcriptional regulator	-21.2	3.77E-03
CD1745A	putative ferrous iron transport protein A	-18.3	4.67E-03
CD1693	putative dinitrogenase iron-molybdenum cofactor	-17.7	2.81E-03
CD2342	succinate-semialdehyde dehydrogenase [NAD(P)+]	-15.2	3.50E-03
CD2343	succinyl-CoA:coenzyme A transferase	-12.9	4.45E-03
CD0840	putative hydrolase	-12.0	7.98E-03
CD2339	4-hydroxybutyrate CoA transferase	-11.9	2.78E-03
CD2796	cell surface protein	-11.8	1.81E-03
CD1139	electron transport complex protein	-11.4	6.71E-03
CD0279	conserved hypothetical protein	-11.4	5.79E-03
CD2340	conserved hypothetical protein	-11.2	2.78E-03
CD0399	acyl-CoA dehydrogenase, short-chain specific	-11.1	4.66E-03
CD0855	oligopeptide ABC transporter, substrate-binding lipoprotein	-11.0	6.37E-03
CD0856	oligopeptide ABC transporter, ATP-binding protein	-10.5	2.40E-03
CD2338	NAD-dependent 4-hydroxybutyrate dehydrogenase	-10.5	4.76E-03
CD0142	putative RNA-binding protein	-10.4	6.42E-03
CD2341	gamma-aminobutyrate metabolism dehydratase/isomerase [includes: 4-hydroxybutyryl-coa dehydratase; vinylacetyl-coa-delta-isomerase]	-10.2	3.53E-03
CD0857	oligopeptide ABC transporter, ATP-binding protein (pseudogene)	-10.0	6.37E-03
CD1142	electron transport complex protein	-9.9	5.71E-03
CD2248	conserved hypothetical protein	-9.9	5.76E-03

CD1138	electron transport complex protein	-9.8	3.30E-03
CD1795	conserved hypothetical protein	-9.8	6.42E-03
CD1807	putative NADPH-dependent FMN reductase	-9.7	8.26E-03
CD2344	putative membrane protein	-9.2	6.68E-03
CD2600	putative carbon starvation	-9.1	9.95E-03
CD1140	electron transport complex protein	-9.0	3.70E-03
CD0398	subunit of oxygen-sensitive 2-hydroxyisocaproyl-CoA dehydratase	-8.6	5.71E-03
CD0718	formate--tetrahydrofolate ligase	-8.5	3.85E-03
CD0854	oligopeptide ABC transporter, permease protein	-8.4	2.78E-03
CD2249	putative ATPase	-8.3	9.80E-03
CD1142A	hypothetical protein	-8.3	4.67E-03
CD0397	subunit of oxygen-sensitive 2-hydroxyisocaproyl-CoA dehydratase	-8.1	8.43E-03
CD1137	electron transport complex protein	-8.1	8.91E-03
CD0180	hypothetical protein	-7.9	9.27E-03
CD3419	delta-aminolevulinic acid dehydratase	-7.5	5.08E-03
CD1141	electron transport complex protein	-7.2	3.77E-03
CD3407	putative iron-only hydrogenase, catalytic subunit	-7.1	4.41E-03
CD0396	activator of 2-hydroxyisocaproyl-CoA dehydratase	-7.1	7.02E-03
CD2378	putative membrane protein	-7.1	5.71E-03
CD0866	putative exported protein	-7.0	5.34E-03
CD0174	putative oxidoreductase, acetyl-CoA synthase subunit	-7.0	2.81E-03
CD2797	putative exported protein	-7.0	5.18E-03
CD3421	porphobilinogen deaminase	-6.9	5.79E-03
CD0267	putative exported protein	-6.9	8.43E-03
CD2444	putative sigma 54 modulation protein	-6.8	5.05E-03
CD0050	putative dual-specificity prolyl/cysteinyl-tRNA synthetase	-6.8	7.02E-03
CD2667	PTS system, glucose-specific IIbc component	-6.7	2.11E-03
CD0188	putative ketopantoate reductase	-6.7	2.78E-03
CD0270	putative flagellar motor switch protein	-6.7	9.53E-03
CD0268	flagellar basal-body rod protein FlgG	-6.6	7.80E-03
CD0176	putative oxidoreductase, NAD/FAD binding subunit	-6.6	5.14E-03
CD1897	hypothetical protein	-6.5	2.78E-03
CD1510	conserved hypothetical protein	-6.5	3.17E-03
CD0269	putative flagellar basal-body rod protein	-6.5	9.32E-03
CD0828	putative oxidative stress protein	-6.3	2.78E-03
CD3229	dihydrodipicolinate reductase	-6.1	6.98E-03
CD1896	putative lipoprotein	-6.0	5.37E-03
CD0255	flagellar hook protein	-6.0	8.33E-03
CD0720	putative FolD bifunctional protein [includes: methylenetetrahydrofolate dehydrogenase; methenyltetrahydrofolate cyclohydrolase]	-5.9	8.43E-03
CD3406	putative iron-only hydrogenase,electron-transferring subunit	-5.8	4.66E-03
CD0114	putative ATP/GTP-binding protein	-5.6	9.30E-03
CD2666	PTS system, glucose-specific IIa component	-5.5	5.71E-03
CD0716	putative bifunctional carbon monoxide dehydrogenase/acetyl-CoA synthase	-5.5	9.30E-03
CD0853	oligopeptide ABC transporter, permease protein	-5.3	5.79E-03

CD0588	hypothetical protein	-5.3	7.80E-03
CD0258	flagellar basal body-associated protein	-5.3	9.27E-03
CD1537	putative glutamate synthase [NADPH] small chain	-5.1	3.53E-03
CD2054	aspartokinase	-5.1	6.42E-03
CD2158	4-aminobutyrate aminotransferase	-5.1	8.33E-03
CD1461	putative membrane protein	-5.0	9.39E-03
CD0394	(R)-2-hydroxyisocaproate dehydrogenase	-5.0	2.78E-03
CD0118	putative subunit of oxidoreductase	-5.0	4.39E-03
CD1895	putative membrane protein	-5.0	5.96E-03
CD0177	cyclopropane-fatty-acyl-phospholipid synthase	-4.9	3.85E-03
CD3423	cobalt-precorrin-6a reductase	-4.9	6.71E-03
CD0776	LacI-family transcriptional regulator	-4.7	9.47E-03
CD2511	transcriptional antiterminator	-4.7	5.71E-03
CD3664	putative amino acid aminotransferase	-4.7	5.96E-03
CD0725	putative carbon monoxide dehydrogenase/acetyl-CoA synthase complex, small subunit	-4.5	5.71E-03
CD3669	putative exported protein	-4.5	5.79E-03
CD0296	hypothetical protein	-4.5	5.37E-03
CD2510	PTS system, IIbc component	-4.5	5.42E-03
CD0723	putative carbon monoxide dehydrogenase/acetyl-CoA synthase complex, dihydrolipoyl dehydrogenase subunit	-4.5	5.79E-03
CD2852	D-alanyl transferase	-4.5	6.56E-03
CD0178	putative ATP-binding protein	-4.5	8.16E-03
CD2828	putative aromatic amino acid aminotransferase	-4.4	5.91E-03
CD1365A	hypothetical protein	-4.2	6.42E-03
CD2512	PTS system, IIa component	-4.1	5.76E-03
CD3424	cobalt-precorrin-3b c(17)-methyltransferase	-4.1	5.98E-03
CD1333	putative tyrosine recombinase	-4.1	2.78E-03
CD2156	radical SAM-superfamily protein	-4.1	4.67E-03
CD1369	hypothetical protein	-4.0	7.41E-03
CD1953	conserved hypothetical protein	-4.0	7.34E-03
CD0402	sigma-54-dependent transcriptional regulator	-3.9	1.65E-03
CD3316	formate dehydrogenase accessory protein	-3.8	9.27E-03
CD1372	phage protein	-3.8	5.79E-03
CD1462	GntR-family transcriptional regulator	-3.8	9.13E-03
CD3150	conserved hypothetical protein	-3.8	5.71E-03
CD2591	low-specificity L-threonine aldolase	-3.8	6.84E-03
CD1371	phage protein	-3.7	9.10E-03
CD0389	6-phospho-beta-glucosidase	-3.7	5.80E-03
CD1448	conserved hypothetical protein	-3.7	5.59E-03
CD1363	putative phage protein	-3.7	9.47E-03
CD3033	thioredoxin	-3.7	3.05E-03
CD3510	putaive membrane protein	-3.7	5.71E-03
CD3649	conserved hypothetical protein	-3.6	4.46E-03
CD2118	threonine synthase	-3.6	6.36E-03
CD1493	putative 3-methyladenine DNA glycosylase	-3.5	5.05E-03

CD3315	electron transport protein	-3.5	8.33E-03
CD0727	putative carbon monoxide dehydrogenase/acetyl-CoA synthase complex,methyltransferase subunit	-3.5	5.05E-03
CD0726	putative carbon monoxide dehydrogenase/acetyl-CoA synthase complex, alpha subunit	-3.4	3.77E-03
CD2601	two-component response regulator	-3.3	8.92E-03
CD2377	NUDIX-family protein	-3.3	4.45E-03
CD0559	conserved hypothetical protein	-3.3	5.79E-03
CD3463	alanine racemase	-3.3	5.71E-03
CD3317	formate dehydrogenase H	-3.3	6.56E-03
CD1534	putative gamma-glutamyltranspeptidase	-3.2	6.42E-03
CD0631	conserved hypothetical protein	-3.2	4.67E-03
CD1771	conserved hypothetical protein	-3.2	5.59E-03
CD1261	putative ribonucleotide-diphosphate reductase	-3.2	4.21E-03
CD1082	molybdopterin-guanine dinucleotide biosynthesis protein B	-3.2	4.39E-03
CD1459	putative 5-nitroimidazole reductase	-3.2	5.98E-03
CD2996	hypothetical protein	-3.1	8.43E-03
CD0108	anaerobic ribonucleoside-triphosphate reductase	-3.1	9.91E-03
CD0825	rubrerythrin	-3.1	7.33E-03
CD2626	cinserved hypothetical protein	-3.1	7.57E-03
CD3405	putative iron-only hydrogenase,electron-transferring subunit	-3.1	4.41E-03
CD0834	putative isocitrate/3-isopropylmalate dehydrogenase	-3.1	9.00E-03
CD3464	putative lipoprotein	-3.0	6.84E-03
CD1081	molybdopterin biosynthesis protein	-3.0	4.45E-03
CD3315A	hypothetical protein	-3.0	9.13E-03
CD3465	conserved hypothetical protein	-3.0	3.89E-03
CD1262	ribonuclease HII	-3.0	9.32E-03
CD2119	homoserine kinase	-3.0	5.91E-03
CD0813	putative PTS system, IIb component	-2.9	5.79E-03
CD0750	amino acid ABC transporter, substrate-binding protein	-2.9	3.53E-03
CD2245	asparaginyl-tRNA synthetase	-2.9	3.77E-03
CD3512	type IV pilus assembly protein	-2.9	9.10E-03
CD2407	putative multidrug efflux pump, membrane protein	-2.9	5.96E-03
CD2443	conserved hypothetical protein	-2.8	9.13E-03
CD0243	conserved hypothetical protein	-2.8	9.80E-03
CD2376	putative membrane protein	-2.8	5.08E-03
CD1476	putative signaling protein	-2.8	5.79E-03
CD2124	putative transporter	-2.8	3.77E-03
CD2408	putative multidrug efflux pump, outer membrane protein	-2.7	5.71E-03
CD1304	putative mannosyl-glycoprotein endo-beta-N-acetylglucosamidase	-2.7	6.58E-03
CD2298	hypothetical protein	-2.7	3.85E-03
CD0341	conserved hypothetical protein	-2.7	4.45E-03
CD2627	conserved hypothetical protein	-2.6	5.71E-03
CD1969	putative regulatory protein	-2.6	5.79E-03
CD3466	holo-[acyl-carrier protein] synthase	-2.6	9.72E-03
CD3135	putative sugar-bisphosphate aldolase	-2.6	4.45E-03

CD0633	conserved hypothetical protein	-2.6	3.17E-03
CD0752	amino acid ABC transporter, ATP-binding protein	-2.5	5.79E-03
CD2155	radical SAM-superfamily protein	-2.5	5.37E-03
CD2053	diaminopimelate decarboxylase	-2.5	5.98E-03
CD1702A	putative thiamine biosynthesis protein	-2.5	5.71E-03
CD3507	putative type IV pilin	-2.5	5.79E-03
CD0807	hypothetical protein	-2.5	7.33E-03
CD2406	putative lipoprotein	-2.5	6.84E-03
CD3504	putative type IV prepilin leader peptidase	-2.4	3.85E-03
CD0467	putative hydrolase	-2.4	4.67E-03
CD2154	putative ATP/GTP-binding protein	-2.4	3.77E-03
CD1970	putative cyclase	-2.4	8.33E-03
CD2958	V-type sodium ATP synthase subunit E	-2.4	5.76E-03
CD2297	putative phage-related regulatory protein	-2.3	3.17E-03
CD1495	pyrroline-5-carboxylate reductase	-2.3	5.55E-03
CD2481	uracil-DNA glycosylase	-2.3	7.80E-03
CD2027	N-carbamoyl-L-amino acid hydrolase	-2.3	7.03E-03
CD0572	conserved hypothetical protein	-2.3	6.69E-03
CD0731	putative radical SAM superfamily protein	-2.2	9.32E-03
CD2161	putative membrane protein	-2.2	5.76E-03
CD1051	putative ABC transporter, permease protein	-2.2	9.80E-03
CD2061	conserved hypothetical protein	-2.2	6.84E-03
CD2060	conserved hypothetical protein	-2.2	5.71E-03
CD2296	hypothetical protein	-2.2	6.55E-03
CD2216	hypothetical protein	-2.2	6.42E-03
CD2622	conserved hypothetical protein	-2.2	6.47E-03
CD0728	putative carbon monoxide dehydrogenase/acetyl-CoA synthase complex, beta subunit	-2.2	7.33E-03
CD1538	putative signaling protein	-2.1	8.60E-03
CD0275	spore photoproduct lyase	-2.1	9.30E-03
CD2624	putative exported protein	-2.1	7.71E-03
CD2524	nicotinate-nucleotide adenylyltransferase	-2.1	7.02E-03
CD2795	cell surface protein	-2.1	6.37E-03
CD0810	putative flavodoxin	-2.0	7.85E-03
CD0879	putative carbohydrate kinase	-2.0	8.84E-03
CD0756	putative reductase	-2.0	9.10E-03
CD3670	putative selenocysteine lyase	-2.0	7.02E-03
CD0636	putative radical SAM superfamily protein	-2.0	9.51E-03
CD0635	conserved hypothetical protein	-2.0	9.32E-03
CD1135	putative cell wall hydrolase	-2.0	8.75E-03
CD2259	conserved hypothetical protein	-2.0	9.35E-03
CD1413	putative membrane protein	-2.0	4.00E-03

Table B3. Fifty most abundant transcripts present in the dormant spore ($p \leq 0.01$)

Systematic Name	Description	Fold change (0 vs 180min)	*p*-value
CD3249	small acid-soluble spore protein B	+595.2	0.00286
CD1631	putative superoxide dismutase [Mn]	+417.6	0.00034
CD1486	putative lipoprotein	+383.2	0.00141
CD2688	small acid-soluble spore protein A	+375.5	0.00141
CD1463	putative membrane protein	+365.3	8.08E-06
CD0783	putative stage IV sporulation protein	+337.3	0.00183
CD2112	hypothetical protein	+267.1	2.01E-05
CD0214	conserved hypothetical protein	+253.8	0.000157
CD2375	conserved hypothetical protein	+252.8	0.000134
CD0213	putative spore coat protein	+214	0.000932
CD2245A	conserved hypothetical protein	+177.1	0.000796
CD2809	conserved hypothetical protein	+86.89	0.000896
CD1880	hypothetical protein	+81.49	0.00355
CD1430	putative exported polysaccharide deacetylase	+29.15	0.00166
CD1290	putative small acid-soluble spore protein	+27.67	0.00886
CD1567	putative manganese-containing catalase	+25.05	0.00473
CD0446	D-ornithine aminomutase E component	+22.51	0.0064
CD1669	ABC transporter, ATP-binding protein	+22.28	0.0238
CD1487	hypothetical protein	+21.9	0.00668
CD3082	PTS system, IIb component	+21.28	0.00748
CD3164	ribonuclease R	+20.36	0.00615
CD2315	putative exported protein	+18.1	0.00485
CD3551A	conserved hypothetical protein	+17.74	0.0264
CD0424	putative single-strand binding protein	+17.73	0.0219
CD3258	iron-only hydrogenase	+16.2	0.0294
CD1904	ABC transporter, permease protein	+16.05	0.0263
CD1067	hypothetical protein	+15.73	0.000778
CD3371	conjugative transposon protein	+15.73	0.00871
CD0990	3-isopropylmalate dehydratase large subunit	+15.52	0.00628
CD1581	hypothetical protein	+15.37	0.00257
CD1291	D-alanyl-D-alanine carboxypeptidase	+15.15	0.0076
CD2374	hypothetical protein	+14.99	0.00558
CD3199	putative ABC transporter, permease protein	+14.84	0.0179
CD-16S-rRNA	Clostridium difficile 16S ribosomal RNA	+14.66	1.96E-23
CD0312	ArsR-family transcriptional regulator	+14.19	0.00459
CD2425	phosphate butyryltransferase	+14.16	0.00559
CD3446	endoglucanase	+14.07	0.026
CD2000	major intracellular serine protease	+14.02	0.0101
CD3305	ATP-dependent Clp protease proteolytic subunit	+13.52	0.00246
CD0413	putative single-strand binding protein	+13.4	0.0499
CD3130	putative 6-phospho-beta-glucosidase	+13.39	0.000731
CD0420	putative cell surface protein	+13.34	0.00137

CD1592	potassium-transporting ATPase B chain	+13.31	0.00595
CD0419A	hypothetical protein	+13.17	0.00694
CD3177	xanthine dehydrogenase, molybdenum binding and iron-sulfur binding subunits	+13.08	0.00974
CD0445	D-ornithine aminomutase S component	+12.87	0.00148
CD1197	putative stage III sporulation protein AF	+12.77	0.0201
CD0444	putative pyridoxal-phosphate dependent enzyme	+12.69	0.00362
CD1575	putative exported protein	+12.54	0.00442
CD3388	putative conjugative transposon replication initiation factor	+12.48	0.00116

Table B4. Genes required for sporulation ($p \leq 0.01$)

Systematic name	Descriptive name	Log fold change	*p*-value
CD0623	hypothetical protein	-7.86	4.09E-11
CD3473	ATP synthase C chain	-6.03	7.95E-80
CD3475	ATP synthase protein I	-5.85	6.30E-89
CD3272	putative membrane protein	-5.54	3.89E-79
CD0555	signal peptidase I	-5.21	4.35E-87
CD1428A	hypothetical protein	-4.94	8.65E-53
CD0714A	probable sugar O-acetyltransferase (partial)	-4.92	3.36E-10
CD3490	stage II sporulation protein e	-4.78	2.22E-83
CD0624	putative phage-related regulatory protein	-4.26	2.57E-10
CD0057	RNA polymerase sigma-H factor	-3.96	3.18E-55
CD1138	electron transport complex protein	-3.87	2.82E-40
CD0125	putative cell wall endopeptidase	-3.82	8.44E-60
CD3468	ATP synthase beta chain	-3.79	4.57E-55
CD1471	putative membrane protein (putative phage infection protein)	-3.78	7.73E-57
CD3447	putative transcription antiterminator	-3.75	1.93E-59
CD1653	putative lipoprotein	-3.74	4.47E-59
CD3474	ATP synthase A chain	-3.69	4.68E-40
CD1229	putative penicillin-binding protein	-3.61	5.47E-56
CD3198	multidrug resistance protein	-3.60	9.06E-49
CD3494	conserved hypothetical protein	-3.59	5.88E-37
CD2463	heat-inducible transcription repressor	-3.57	8.29E-45
CD0383	conjugative transposon FtsK/SpoIIIE-related protein	-3.57	2.15E-46
CD1320	putative peptidase	-3.47	6.56E-46
CD1610	putative membrane protein	-3.41	4.53E-22
CD3556	putative membrane protein	-3.41	5.37E-32
CD3303	chromate transport protein	-3.40	9.00E-37
CD1214	stage 0 sporulation protein A	-3.40	1.12E-36
CD2375	conserved hypothetical protein	-3.40	1.96E-09
CD2317	two-component sensor histidine kinase	-3.36	1.55E-47
CD1196	stage III sporulation-related protein	-3.36	1.56E-35
CD1136	putative membrane protein	-3.35	1.23E-42
CD3119	putative glycosyltransferase	-3.34	7.33E-46
CD3533	phosphonate ABC transporter, ATP-binding protein	-3.33	1.00E-38
CD3670	putative selenocysteine lyase	-3.32	7.06E-42
CD1344	putative cell wall biosynthesis protein	-3.30	1.86E-41
CD2644	sporulation sigma-E factor processing peptidase	-3.26	8.24E-34
CD1029	putative cell wall anchored protein	-3.25	2.49E-40
CD1678A	hypothetical protein	-3.21	4.67E-12
CD2766	putative penicillin-binding protein repressor	-3.19	8.80E-31
CD1464	two-component response regulator	-3.19	2.81E-42

CD2419	AraC-family transcriptional regulator	-3.12	1.08E-44
CD0459	ABC transporter, ATP-binding protein	-3.11	1.52E-15
CD0814	GntR-family transcriptional regulator	-3.09	4.86E-43
CD3250	conserved hypothetical protein	-3.08	8.29E-25
CD3302	chromate transport protein	-3.08	1.42E-35
CD0044	putative membrane protein	-3.06	3.29E-38
CD2232	anaerobic sulfite reductase subunit B	-3.05	6.12E-33
CD3276	PTS system, IId component	-3.04	1.72E-24
CD0653	ABC transporter, ATP-binding protein	-3.02	3.74E-38
CD1266	putative ABC transporter, permease protein	-3.00	7.40E-33
CD3441	putative aminotransferas	-2.97	4.63E-38
CD3388	putative conjugative transposon replication initiation factor	-2.96	6.62E-20
CD0637	putative acetyltransferase	-2.96	7.95E-17
CD3567	putative cell wall hydrolase	-2.94	1.01E-34
CD3624	putative ABC transporter, permease protein	-2.94	2.05E-31
CD1267	putative ABC transporter, permease protein	-2.91	1.15E-26
CD0409	putative replication initiation protein	-2.91	8.24E-40
CD2233	anaerobic sulfite reductase subunit A	-2.91	1.11E-38
CD1301	putative membrane protein	-2.90	1.01E-30
CD3225	dihydrodipicolinate synthase	-2.90	5.52E-35
CD0018	recombination protein	-2.89	3.99E-29
CD1631	putative superoxide dismutase [Mn]	-2.88	1.36E-08
CD0384	conjugative transposon protein	-2.88	1.91E-07
CD0867	putative membrane protein	-2.87	7.89E-35
CD1360	putative phage repressor	-2.86	1.67E-10
CD3633	putative membrane protein	-2.85	1.24E-21
CD1068	putative polysaccharide biosynthesis/sporulation protein	-2.85	1.23E-25
CD1128	DNA polymerase I	-2.85	3.69E-38
CD1324	putative DNA translocase	-2.84	4.04E-36
CD0161	putative lantibiotic ABC transporter,ATP-binding protein	-2.84	1.21E-35
CD0585	GntR-family transcriptional regulator	-2.79	6.69E-32
CD2969	putative AMP-binding protein	-2.79	7.14E-24
CD3110	putative phosphofructokinase	-2.78	2.63E-30
CD0618	putative transcriptional regulator	-2.77	1.41E-25
CD3448	putative tagatose-1,6-bisphosphate aldolase	-2.77	1.38E-34
CD3146	pseudogene	-2.76	8.14E-26
CD2496	selenide,water dikinase	-2.74	3.00E-27
CD1961	ABC transporter, ATP-binding protein	-2.71	2.34E-14
CD0440A	regulatory protein (partial)	-2.70	2.28E-06
CD2354	glycine reductase complex component B alpha and beta subunits	-2.70	1.82E-29
CD3362	ABC transporter, permease protein	-2.66	1.00E-18
CD0691	putative short chain dehydrogenase	-2.66	2.31E-26

CD2884	PTS system, lichenan-specific IIb component	-2.66	9.49E-22
CD2051	putative membrane protein	-2.64	1.77E-23
CD3150	conserved hypothetical protein	-2.63	5.59E-30
CD0335	hypothetical protein	-2.58	2.75E-14
CD2561	putative phosphatase	-2.57	3.36E-30
CD2104	putative ABC transporter, permease protein	-2.56	3.88E-26
CD2495	L-seryl-tRNA(Sec) selenium transferase (selenocysteinyl-tRNA(Sec) synthase)	-2.55	6.56E-28
CD3668	putative transcriptional regulator	-2.53	2.77E-29
CD2652	cell division/stage V sporulation protein	-2.53	9.76E-22
CD2493	selenocysteine-specific elongation factor	-2.51	1.11E-28
CD0032	putative beta-glucosidase	-2.51	4.20E-25
CD1170	conserved hypothetical protein	-2.48	2.40E-26
CD3144	putative transcriptional regulator	-2.48	3.75E-24
CD0775	stage V sporulation protein AE	-2.47	6.03E-12
CD2967	dipicolinate synthase, B chain	-2.46	1.40E-14
CD3147	putative DNA-methyltransferase	-2.45	2.15E-21
CD3079	6-phospho-beta-glucosidase	-2.43	1.46E-29
CD1692	ArsR-family transcriptional regulator	-2.42	3.75E-26
CD1311	putative RNA-binding protein	-2.42	8.80E-25
CD0629	putative transcriptional regulator	-2.41	7.47E-24
CD0627A	putative ferredoxin	-2.40	1.98E-12
CD0305	putative aminobenzoyl-glutamate utilization protein	-2.39	1.02E-22
CD2839	putative two-component sensor histidine kinase	-2.38	3.31E-19
CD3536	putative phosphonate metabolism protein	-2.37	1.46E-26
CD0619	conserved hypothetical protein	-2.37	8.50E-11
CD3632	putative isochorismatase	-2.34	3.19E-24
CD2021	hypothetical protein	-2.33	5.96E-21
CD3016	putative transcriptional antiterminator	-2.32	2.10E-24
CD3472	ATP synthase B chain	-2.31	1.93E-24
CD3148	hypothetical protein	-2.31	2.68E-26
CD1174	conserved hypothetical protein	-2.31	7.69E-21
CD3352	AraC-family transcriptional regulator	-2.30	8.59E-20
CD3559	cell division protein	-2.30	2.12E-24
CD0767	PTS system, glucitol/sorbitol-specific IIa component	-2.30	1.26E-24
CD1140	electron transport complex protein	-2.29	3.71E-13
CD2959	V-type sodium ATP synthase subunit K	-2.26	9.02E-20
CD3223	dihydrodipicolinate synthase	-2.25	8.54E-25
CD0314	putative membrane protein	-2.24	1.09E-10
CD3005	IclR-family transcriptional regulator	-2.23	1.15E-21
CD3368	putative GTPase	-2.21	1.56E-21
CD2554	transposase-like protein A	-2.20	1.37E-05
CD0210	putative hydrolase	-2.19	9.32E-20

CD0160	putative two-component response regulator	-2.19	4.43E-23
CD3048	PTS system, IIc component	-2.18	3.92E-24
CD1603	ABC transporter, permease protein	-2.17	8.07E-17
CD3399	putative exported protein	-2.16	5.20E-22
CD3063	putative exported protein	-2.15	2.44E-21
CD0394	(R)-2-hydroxyisocaproate dehydrogenase	-2.15	1.33E-19
CD0593	hypothetical protein	-2.14	2.60E-21
CD3070	PTS system, IIc component	-2.14	4.17E-21
CD2845	rubrerythrin	-2.13	3.11E-17
CD0907A	putative phage regulatory protein	-2.13	5.28E-09
CD0124	stage II sporulation protein D	-2.12	8.19E-22
CD0674	putative membrane protein	-2.12	8.42E-05
CD3341	pseudogene	-2.12	1.49E-05
CD3502	peptidyl-tRNA hydrolase	-2.11	3.76E-16
CD3290	putative protein translocase	-2.10	4.13E-22
CD1851	putative conjugal transfer protein (putative single-stranded dna binding protein)	-2.10	5.40E-11
CD0462	two-component response regulator	-2.09	9.81E-19
CD3146A	putative transposase (partial)	-2.09	7.30E-15
CD0783	putative stage IV sporulation protein	-2.08	2.28E-12
CD3613	conserved hypothetical protein	-2.08	1.45E-14
CD3617	conserved hypothetical protein	-2.07	3.85E-22
CD1270	two-component sensor histidine kinase	-2.07	1.32E-12
CD3353	GntR-family transcriptional regulator	-2.06	1.28E-14
CD2860	putative membrane protein	-2.06	3.73E-13
CD3255	two-component response regulator	-2.06	1.63E-21
CD3501	transcription-repair coupling factor	-2.06	1.32E-21
CD3469	ATP synthase subunit gamma	-2.06	8.16E-16
CD2996	hypothetical protein	-2.06	3.34E-19
CD1656	putative membrane protein	-2.06	8.52E-16
CD0552	putative spore-cortex-lytic protein	-2.05	9.07E-15
CD0889	S-adenosylmethionine decarboxylase proenzyme	-2.05	8.66E-14
CD0168	putative cyclic nucleotide-binding protein	-2.04	7.62E-16
CD1878	hypothetical protein	-2.04	1.16E-05
CD3266	two-component sensor histidine kinase	-2.04	8.74E-17
CD3470	ATP synthase alpha chain	-2.03	3.77E-15
CD3511	type IV pilus assembly protein	-2.03	2.23E-18
CD0031	AraC-family transcriptional regulator	-2.02	5.42E-20
CD1744	two-component sensor histidine kinase	-2.01	8.75E-14
CD0484	ABC transporter, ATP-binding protein	-2.01	9.97E-12
CD2357	putative glycine reductase complex component	-2.00	4.95E-12

TableB5. Genes required for germination ($p \leq 0.01$)

Systematic Name	Description	Log fold change	*p* value
CD2136A	hypothetical protein	-7.84	1.49E-09
CD1424	hypothetical protein	-7.41	1.27E-07
CD2043	putative hydrolase	-6.81	1.74E-05
CD2838	putative two-component response regulator	-6.78	1.74E-05
CD2809	conserved hypothetical protein	-6.67	5.00E-05
CD1699	riboflavin synthase alpha chain	-6.30	1.43E-04
CD1957	two-component response regulator	-6.30	1.43E-04
CD2150	putative endonuclease/exonuclease/phosphatase	-6.30	1.43E-04
CD1283	conserved hypothetical protein	-6.25	2.53E-04
CD2306	hypothetical protein	-6.25	2.53E-04
CD3630	putative PTS system, IIb component	-6.04	7.95E-04
CD1111	putative membrane protein	-5.98	1.41E-03
CD0435A	hypothetical protein	-5.86	2.50E-03
CD1256	tRNA (Guanine-n(1)-)-methyltransferase	-5.58	7.88E-03
CD2214	putative regulatory protein	-5.11	4.37E-18
CD1940	putative membrane protein	-4.92	2.22E-10
CD0670	putative regulatory protein	-4.77	3.75E-09
CD1668	putative membrane protein	-4.71	5.13E-14
CD2683	putative propanediol utilization protein	-4.30	1.13E-28
CD1019	conserved hypothetical protein	-4.28	5.01E-11
CD0782	putative exported protein	-4.25	4.53E-24
CD0770	anti-sigma F factor antagonist	-4.24	1.49E-10
CD2294	putative membrane protein	-4.23	2.05E-06
CD2048	RpiR-family transcriptional regulator	-4.16	1.29E-30
CD1322	aspartokinase	-4.15	1.07E-36
CD2808	putative membrane protein	-4.14	7.01E-16
CD2966A	putative membrane protein	-4.05	1.76E-05
CD3276	PTS system, IId component	-4.01	3.03E-29
CD1231	site-specific recombinase	-4.00	1.24E-48
CD2483	putative exported protein	-3.89	5.15E-35
CD0106	germination-specific N-acetylmuramoyl-L-alanine amidase	-3.82	2.06E-31
CD3471	ATP synthase subunit delta	-3.77	5.52E-21
CD1244	putative membrane protein	-3.72	2.91E-12
CD0771	anti-sigma F factor	-3.72	7.32E-16
CD2114	two-component system response regulator	-3.72	7.32E-16
CD1321	conserved hypothetical protein	-3.68	2.11E-15
CD3541	spore maturation protein B	-3.68	7.50E-12
CD0695	putative exported peptidase	-3.65	1.81E-24
CD2000	major intracellular serine protease	-3.65	1.23E-29
CD1945	putative glyoxalase	-3.59	4.88E-04

CD1142	electron transport complex protein	-3.56	1.23E-35
CD2745	adenine phosphoribosyltransferase	-3.56	2.05E-12
CD0101	ABC transporter, ATP-binding protein	-3.53	7.75E-19
CD2800	putative membrane protein	-3.53	7.59E-04
CD2304	putative regulatory protein	-3.49	3.48E-10
CD0382	hypothetical protein	-3.46	4.22E-04
CD0171	putative DNA-binding protein	-3.46	6.74E-32
CD1795	conserved hypothetical protein	-3.35	1.05E-07
CD2410	pyruvate, phosphate dikinase	-3.34	4.87E-36
CD3464	putative lipoprotein	-3.34	5.10E-27
CD1529	putative ABC transporter, permease protein	-3.32	1.85E-16
CD1831A	hypothetical protein	-3.31	1.07E-03
CD2411	conserved hypothetical protein	-3.30	2.84E-25
CD2169	iron-sulfur binding protein	-3.28	5.70E-16
CD3551	putative arginine decarboxylase	-3.28	2.63E-21
CD1480	putative exported protein	-3.28	1.70E-03
CD1627	putative D-alanyl-D-alanine carboxypeptidase	-3.28	1.70E-03
CD0696	probable cation transport protein	-3.26	1.14E-12
CD1753	ABC transporter, ATP-binding protein	-3.24	5.42E-11
CD2682	pyruvate-flavodoxin oxidoreductase	-3.19	4.94E-31
CD1139	electron transport complex protein	-3.18	1.43E-15
CD1786	hypothetical protein	-3.18	8.39E-05
CD2636	putative membrane protein	-3.15	4.04E-09
CD3667	conserved hypothetical protein	-3.14	5.72E-22
CD1002	putative regulatory protein	-3.13	2.58E-14
CD1045	putative membrane protein	-3.09	5.32E-11
CD0163	hypothetical protein	-3.09	2.64E-25
CD2446	putative tRNA binding protein	-3.09	2.21E-15
CD0102	ABC transporter, permease protein	-3.04	2.30E-16
CD1962	ABC transporter, permease protein	-3.03	2.36E-29
CD3194	AraC-family transcriptional regulator	-2.99	3.78E-12
CD3271	hypothetical protein	-2.98	3.50E-16
CD0397	subunit of oxygen-sensitive 2-hydroxyisocaproyl-CoA dehydratase	-2.97	3.66E-18
CD1613	hypothetical protein	-2.97	1.90E-13
CD3678	putative sporulation membrane protein	-2.97	6.72E-11
CD3153	putative phage DNA-binding protein	-2.96	4.13E-21
CD1974	HfQ protein	-2.96	6.90E-20
CD0925	hypothetical phage protein	-2.96	8.78E-11
CD1677	putative membrane protein	-2.95	6.58E-07
CD0802	putative CoA-transferase	-2.93	3.54E-16
CD1578	putative membrane-associated ribonuclease	-2.93	9.30E-07
CD1328	RecA protein (recombinase A)	-2.92	3.97E-21

CD0179	NAD-specific glutamate dehydrogenase	-2.92	1.05E-28
CD1174	conserved hypothetical protein	-2.90	5.51E-27
CD3078	putative membrane protein	-2.90	2.24E-05
CD2019	probable transporter	-2.90	1.02E-14
CD1703	putative thiamine biosynthesis protein	-2.89	1.02E-14
CD0485	two-component sensor histidine kinase	-2.89	1.36E-15
CD1737	putative gluconate permease	-2.88	5.61E-25
CD3294	putative type IV pilin	-2.88	2.18E-09
CD1274	DNA topoisomerase I	-2.87	9.37E-31
CD3476	putative ATP synthase protein	-2.86	3.25E-05
CD2805	holliday junction DNA helicase	-2.86	7.89E-20
CD3445	PTS system, IIa component	-2.82	4.31E-08
CD2392	conserved hypothetical protein	-2.79	1.03E-11
CD1485	conserved hypothetical protein	-2.79	6.82E-05
CD2105	ABC transporter, ATP-binding protein	-2.78	1.98E-12
CD1242	putative membrane protein	-2.77	1.30E-11
CD3379	conjugative transposon protein	-2.77	9.87E-05
CD1564	hypothetical protein	-2.76	1.28E-03
CD0395	isocaprenoyl-CoA:2-hydroxyisocaproateCoA-transferase	-2.76	1.97E-19
CD1617	GntR-family transcriptional regulator	-2.75	5.07E-20
CD1137	electron transport complex protein	-2.75	3.37E-19
CD1532	ABC transporter, ATP-binding protein	-2.73	1.91E-03
CD3492	putative septum formation protein	-2.72	1.51E-20
CD3666	conserved hypothetical protein	-2.72	4.35E-11
CD0979	putative phage regulatory protein	-2.72	9.37E-06
CD0403	putative fructose-bisphosphate aldolase	-2.72	1.23E-06
CD2539	ribonuclease Z	-2.69	5.73E-14
CD0311	hypothetical protein	-2.69	4.47E-32
CD3350	putative glycosyl transferase	-2.68	1.24E-14
CD1470	putative phage shock protein	-2.67	7.74E-12
CD0630	putative drug/sodium antiporter	-2.67	4.07E-11
CD3033	thioredoxin	-2.65	6.14E-14
CD2988	two-component system esponse regulator	-2.65	2.25E-13
CD0543	conserved hypothetical protein	-2.64	3.75E-14
CD3627	putative dihydrodipicolinate synthase	-2.64	1.91E-11
CD2570	two-component sensor histidine kinase	-2.63	1.45E-24
CD0449	Na+/H+ antiporter	-2.62	1.96E-15
CD3353	GntR-family transcriptional regulator	-2.62	1.81E-18
CD2551	hypothetical protein	-2.62	1.97E-04
CD1018	putative ABC transporter, permease/ATP-binding protein	-2.60	1.71E-25
CD1207	1-deoxy-D-xylulose 5-phosphate synthase	-2.60	7.00E-16
CD1767	glyceraldehyde-3-phosphate dehydrogenase 1	-2.59	4.50E-15

CD1204	exodeoxyribonuclease VII small subunit	-2.58	8.76E-06
CD3610	putative glyoxalase	-2.58	8.76E-06
CD3631	putative transcription antiterminator	-2.58	5.12E-23
CD2016	hypothetical protein	-2.57	2.85E-03
CD3059	putative membrane protein	-2.57	5.42E-05
CD2824	putative membrane protein	-2.57	8.76E-06
CD0863	PTS system, IIa component	-2.57	1.13E-06
CD2538	putative lipoprotein	-2.57	4.20E-15
CD2356	thioredoxin reductase	-2.56	6.09E-14
CD2656	stage V sporulation protein D (sporulation specific penicillin-binding protein)	-2.55	2.83E-19
CD2566	PTS system, IIa component	-2.55	1.55E-06
CD1537	putative glutamate synthase [NADPH] small chain	-2.53	6.17E-13
CD3262	putative phosphateABC transporter, permease protein	-2.53	6.24E-07
CD1943	conserved hypothetical protein	-2.52	3.25E-11
CD1981	putative transcriptional regulator	-2.52	7.67E-05
CD3477	putative cytidine and deoxycytidylate deaminase	-2.51	4.03E-11
CD1428	putative transcriptional regulator	-2.50	4.30E-03
CD1292	conserved hypothetical protein	-2.50	2.89E-06
CD2482	putative lipoprotein	-2.50	1.83E-07
CD1598	putative endonuclease	-2.48	3.94E-06
CD3312	probable transporter	-2.48	3.63E-17
CD2222	conserved hypothetical protein	-2.47	1.57E-05
CD2229	putative membrane protein	-2.45	7.80E-16
CD1240A	putative phage-related DNA-directed RNA polymerase 7 kDa polypeptide	-2.45	8.83E-04
CD1519	putative acetyltransferase	-2.45	7.35E-06
CD3195	putative excinuclease ABC subunit A	-2.44	1.35E-20
CD1422	MerR-family transcriptional regulator	-2.44	7.39E-13
CD2185	hypothetical protein	-2.44	1.89E-13
CD2197	putative subunit of oxidoreductase	-2.42	1.00E-05
CD0460	ABC transporter, permease protein	-2.42	1.67E-21
CD2254	putative amino acid recemase	-2.41	1.61E-10
CD3165	conserved hypothetical protein	-2.40	5.64E-08
CD0429	putative membrane protein	-2.39	8.51E-12
CD1536	putative dehydrogenase, electron transfer subunit	-2.39	1.81E-12
CD3677	SpoIIIJ-associated protein	-2.37	2.12E-10
CD1586	hypothetical protein	-2.37	3.70E-12
CD2358	putative oligoendopeptidase	-2.36	3.16E-13
CD0659	putative transcriptional regulator	-2.35	9.63E-03
CD1254	conserved hypothetical protein	-2.35	9.63E-03
CD3623	putative ABC transporter, ATP-binding protein	-2.33	1.54E-10
CD2807	crossover junction endodeoxyribonuclease RuvC	-2.33	6.17E-10
CD2144	putative membrane protein	-2.33	3.30E-17

CD0934	hypothetical phage protein	-2.32	1.14E-04
CD1126	AraC-family transcriptional regulator	-2.32	8.80E-07
CD3083	transcription antiterminator	-2.31	2.18E-09
CD1141	electron transport complex protein	-2.31	2.17E-06
CD0572	conserved hypothetical protein	-2.30	2.01E-10
CD2729	putative regulator of the sigma(E) factor	-2.30	5.29E-18
CD1678	putative membrane protein	-2.30	4.30E-04
CD1100	putative conjugative transposon protein	-2.29	3.82E-03
CD1505	putative ABC transporter, permease protein	-2.29	2.89E-06
CD1418A	putative integrase (partial)	-2.28	8.16E-07
CD3040	conserved hypothetical protein	-2.28	6.81E-20
CD2859	putative D-aminoacylase	-2.26	1.13E-16
CD3241	proline reductase	-2.25	2.06E-14
CD0398	subunit of oxygen-sensitive 2-hydroxyisocaproyl-CoA dehydratase	-2.25	6.60E-13
CD0336	ABC transporter, ATP-binding protein	-2.24	4.36E-16
CD1539	ABC transporter, ATP-binding protein	-2.23	5.46E-03
CD2097	putative membrane protein	-2.23	5.46E-03
CD2598	putative oligosaccharide deacetylase	-2.21	2.41E-10
CD2159	putative membrane protein	-2.20	2.76E-03
CD0674	putative membrane protein	-2.20	4.19E-04
CD1533	putative ABC transporter, permease protein	-2.19	1.76E-10
CD1312	transposase-like protein B	-2.19	2.32E-13
CD0613	ABC transporter, ATP-binding protein	-2.18	2.90E-07
CD2231	anaerobic sulfite reductase subunit C	-2.18	3.09E-17
CD3489	putative oligopeptidase	-2.17	7.58E-19
CD3197	MerR-family transcriptional regulator	-2.16	1.21E-08
CD0165	putative amino acid transporter	-2.16	7.50E-10
CD2585	peptide deformylase 2	-2.15	2.10E-06
CD3354	conserved hypothetical protein	-2.15	1.43E-12
CD1725	AraC-family transcriptional regulator	-2.15	2.36E-11
CD0826	putative oxidative stress regulatory protein	-2.15	1.59E-04
CD0315	hypothetical protein	-2.15	1.72E-03
CD1924	putative ethanolamine/propanediol transporter	-2.14	3.55E-08
CD2332	PTS system, mannitol-specific IIa component	-2.14	1.88E-20
CD3102	putative dipeptidase	-2.14	2.61E-19
CD2730	conserved hypothetical protein	-2.14	8.66E-12
CD1078	PTS system, IId component	-2.14	4.44E-08
CD3123	putative nitroreductase	-2.13	5.87E-11
CD0554	signal peptidase I	-2.12	1.59E-11
CD1743	two-component response regulator	-2.12	3.44E-09
CD1759	conserved hypothetical protein	-2.11	2.07E-05
CD2724	probable polysaccharide deacetylase	-2.11	2.70E-17

CD2287	putative membrane protein	-2.11	1.27E-05
CD3364	ABC transporter, ATP-binding protein	-2.10	2.27E-14
CD1525	putative iron-sulfur protein	-2.10	1.88E-07
CD0765	PTS system, glucitol/sorbitol-specific IIb component	-2.10	8.28E-19
CD2659	prolipoprotein diacylglyceryl transferase	-2.10	1.88E-17
CD2435	DNA repair protein	-2.10	2.54E-16
CD1793	putative membrane protein	-2.09	8.68E-05
CD1330	conserved hypothetical protein	-2.09	7.79E-14
CD2968	dipicolinate synthase, A chain	-2.09	1.79E-06
CD1956	two-component sensor histidine kinase	-2.08	2.31E-06
CD0547	putative penicillin-binding protein repressor	-2.08	2.00E-08
CD0233	conserved hypothetical protein	-2.07	3.39E-03
CD2464	oxygen-independent coproporphyrinogen III oxidase	-2.07	1.96E-12
CD1175	acetate kinase	-2.07	3.04E-13
CD3047	conserved hypothetical protein	-2.06	8.12E-10
CD1350	putative lantibiotic ABC transporter, permease protein	-2.06	2.99E-06
CD2160	putative membrane protein	-2.06	1.82E-11
CD3247	putative electron transfer protein	-2.05	5.29E-14
CD0664A	conserved hypothetical protein	-2.05	3.03E-08
CD1237	pseudogene	-2.05	8.21E-04
CD2563	conserved hypothetical protein (partial)	-2.05	8.21E-04
CD2806	holliday junction DNA helicase	-2.05	2.41E-11
CD3245	sigma-54-dependent transcriptional activator	-2.04	1.88E-19
CD2386	conserved hypothetical protein	-2.03	7.48E-08
CD1067	hypothetical protein	-2.03	2.07E-10
CD1039	conserved hypothetical protein	-2.03	2.80E-13
CD1813	hypothetical protein	-2.03	2.52E-06
CD1511	conserved hypothetical protein	-2.02	1.93E-07
CD2276	putative sodium:solute symporter	-2.02	1.59E-12
CD3564	stage II sporulation protein	-2.01	2.78E-12
CD2025	putative ABC transporter, permease protein	-2.01	2.45E-11
CD3568	conserved hypothetical protein	-2.00	2.54E-12
CD1812	putative two-component system response regulator (partial)	-2.00	7.11E-07
CD1754	putative ABC transporter, permease protein	-2.00	3.22E-06

Appendix C

Table D1. Summary of permissions for third party copyright works

Page no.	Type of work	Source	Copyright holder	Permission terms
15	Figure	Deaths Involving *Clostridium difficile*, England and Wales, 2012. Office for National Statstics.	© Crown copyright 2013	Open Government Licence
20	Adapted figure	RUPNIK, M., WILCOX, M. H. & GERDING, D. N. 2009. *Clostridium difficile* infection: new developments in epidemiology and pathogenesis. *Nat Rev Microbiol,* 7**,** 526-36.	© 2009 Macmillan Publishers Limited.	Individual Licence Agreement
28	Adapted figure	FAGAN, R. P. & FAIRWEATHER, N. F. 2014. Biogenesis and functions of bacterial S-layers. *Nat Rev Microbiol*.	© 2014 Macmillan Publishers Limited	Individual Licence Agreement
30	Adapted figure	ERRINGTON, J. 2003. Regulation of endospore formation in *Bacillus subtilis*. *Nat Rev Microbiol,* 1**,** 117-26.	© 2003 Macmillan Publishers Limited	Individual Licence Agreement
33	Adapted figure	HIGGINS, D. & DWORKIN, J. 2012. Recent progress in *Bacillus subtilis* sporulation. *FEMS Microbiol Rev,* 36**,** 131-48.	© 2011 Federation of European Microbiological Societies	Individual Licence Agreement
36	Adapted figure	SOGAARD-ANDERSEN, L. 2013. Stably bridging a great divide: localization of the SpoIIQ landmark protein in *Bacillus subtilis*. *Mol Microbiol,* 89**,** 1019-24.	© 2013 The Authors	Creative Commons Attribution Non-Commercial No Derivatives licence
37	Adapted figure	MCKENNEY, P. T., DRIKS, A. & EICHENBERGER, P. 2013. The *Bacillus subtilis* endospore: assembly and functions of the multilayered coat. *Nat Rev Microbiol,* 11**,** 33-44.	© 2013 Macmillan Publishers Limited	Individual Licence Agreement
39	Figure	POPHAM, D. L., HELIN, J., COSTELLO, C. E. & SETLOW, P. 1996. Muramic lactam in peptidoglycan of *Bacillus subtilis* spores is required for spore outgrowth but not for spore dehydration or heat resistance. *Proc Natl Acad Sci U S A,* 93**,** 15405-10.	© 1996 American Society for Microbiology	Permission granted without a license
49	Adapted figure	PAREDES-SABJA, D., SETLOW, P. & SARKER, M. R. 2010. Germination of spores of *Bacillales* and *Clostridiales* species: mechanisms and proteins involved. *Trends Microbiol*.	© 2010 Elsevier Ltd	Individual Licence Agreement
237	Full article	DEMBEK, M., STABLER, R. A., WITNEY, A. A., WREN, B. W. & FAIRWEATHER, N. F. 2013. Transcriptional Analysis of Temporal Gene Expression in Germinating Clostridium difficile 630 Endospores. *PLoS One,* 8, e64011.	© 2013 The Authors	Creative Commons Attribution Non-Commercial No Derivatives licence

NATURE PUBLISHING GROUP LICENSE
TERMS AND CONDITIONS

Feb 14, 2014

This is a License Agreement between Marcin Dembek ("You") and Nature Publishing Group ("Nature Publishing Group") provided by Copyright Clearance Center ("CCC"). The license consists of your order details, the terms and conditions provided by Nature Publishing Group, and the payment terms and conditions.

License Number 3327731080886
License date Feb 14, 2014
Licensed content publisher Nature Publishing Group
Licensed content publication Nature Reviews Microbiology
Licensed content title Clostridium difficile: infection: new developments in epidemiology and pathogenesis
Licensed content author Maja Rupnik, Mark H. Wilcox and Dale N. Gerding
Licensed content date Jul 1, 2009
Volume number 7
Issue number 7
Type of Use reuse in a dissertation / thesis
Requestor type academic/educational
Format print and electronic
Portion figures/tables/illustrations
Number of figures/tables/illustrations 1
High-res required no
Figures Figure 3 | Toxins produced by Clostridium difficile.
Author of this NPG article no
Your reference number None
Title of your thesis / dissertation Whole-genome analysis of sporulation and germination in Clostridium difficile
Expected completion date Mar 2014
Estimated size (number of pages) 250
Total 0.00 USD

NATURE PUBLISHING GROUP LICENSE
TERMS AND CONDITIONS

Feb 14, 2014

This is a License Agreement between Marcin Dembek ("You") and Nature Publishing Group ("Nature Publishing Group") provided by Copyright Clearance Center ("CCC"). The license consists of your order details, the terms and conditions provided by Nature Publishing Group, and the payment terms and conditions.

License Number 3327731381302
License date Feb 14, 2014
Licensed content publisher Nature Publishing Group
Licensed content publication Nature Reviews Microbiology
Licensed content title Biogenesis and functions of bacterial S-layers
Licensed content author Robert P. Fagan, Neil F. Fairweather
Licensed content date Feb 10, 2014
Volume number 12
Issue number 3
Type of Use
reuse in a dissertation / thesis
Requestor type academic/educational
Format print and electronic
Portion figures/tables/illustrations
Number of figures/tables/illustrations1
High-res required no
Figures Figure 1: Clostridium difficile and Bacillus anthracis cell surface protein families
Author of this NPG article no
Your reference number None
Title of your thesis / dissertation Whole-genome analysis of sporulation and germination in Clostridium difficile
Expected completion date Mar 2014
Estimated size (number of pages) 250
Total0.00 USD

NATURE PUBLISHING GROUP LICENSE
TERMS AND CONDITIONS

Feb 14, 2014

This is a License Agreement between Marcin Dembek ("You") and Nature Publishing Group ("Nature Publishing Group") provided by Copyright Clearance Center ("CCC"). The license consists of your order details, the terms and conditions provided by Nature Publishing Group, and the payment terms and conditions.

License Number3327860713393
License date Feb 14, 2014
Licensed content publisher Nature Publishing Group
Licensed content publication Nature Reviews Microbiology
Licensed content title Regulation of endospore formation in Bacillus subtilis
Licensed content author Jeff Errington
Licensed content date Nov 1, 2003
Volume number1
Issue number2
Type of Use reuse in a dissertation / thesis
Requestor type academic/educational
Format print and electronic
Portion figures/tables/illustrations
Number of figures/tables/illustrations1
High-res required no
Figures Figure 1 | The sporulation cycle of Bacillus subtilis
Author of this NPG article no
Your reference number None
Title of your thesis / dissertation Whole-genome analysis of sporulation and germination in Clostridium difficile
Expected completion date Mar 2014
Estimated size (number of pages) 250
Total0.00 USD

NATURE PUBLISHING GROUP LICENSE
TERMS AND CONDITIONS

Feb 14, 2014

This is a License Agreement between Marcin Dembek ("You") and Nature Publishing Group ("Nature Publishing Group") provided by Copyright Clearance Center ("CCC"). The license consists of your order details, the terms and conditions provided by Nature Publishing Group, and the payment terms and conditions.

License Number3327860713393
License date Feb 14, 2014
Licensed content publisher Nature Publishing Group
Licensed content publication Nature Reviews Microbiology
Licensed content title Regulation of endospore formation in Bacillus subtilis
Licensed content author Jeff Errington
Licensed content date Nov 1, 2003
Volume number1
Issue number2
Type of Use reuse in a dissertation / thesis
Requestor type academic/educational
Format print and electronic
Portion figures/tables/illustrations
Number of figures/tables/illustrations1
High-res required no
Figures Figure 1 | The sporulation cycle of Bacillus subtilis
Author of this NPG article no
Your reference number None
Title of your thesis / dissertation Whole-genome analysis of sporulation and germination in Clostridium difficile
Expected completion date Mar 2014
Estimated size (number of pages) 250
Total0.00 USD

JOHN WILEY AND SONS LICENSE
TERMS AND CONDITIONS

Feb 14, 2014

This is a License Agreement between Marcin Dembek ("You") and John Wiley and Sons ("John Wiley and Sons") provided by Copyright Clearance Center ("CCC"). The license consists of your order details, the terms and conditions provided by John Wiley and Sons, and the payment terms and conditions.

License Number3327860961581
License date Feb 14, 2014
Licensed content publisher John Wiley and Sons
Licensed content publication FEMS Microbiology Reviews
Licensed content title Recent progress in Bacillus subtilis sporulation
Licensed copyright line© 2011 Federation of European Microbiological Societies. Published by Blackwell Publishing Ltd. All rights reserved
Licensed content author Douglas Higgins, Jonathan Dworkin
Licensed content date Oct 25, 2011
Start page131
End page148
Type of use Dissertation/Thesis
Requestor type University/Academic
Format Print and electronic
Portion Figure/table
Number of figures/tables 1
Original Wiley figure/table number(s) Figure 3. Activation of SpoOA
Will you be translating? No
Title of your thesis / dissertation Whole-genome analysis of sporulation and germination in Clostridium difficile
Expected completion date Mar 2014
Expected size (number of pages) 250
Total0.00 USD

ELSEVIER LICENSE
TERMS AND CONDITIONS

Feb 14, 2014

This is a License Agreement between Marcin Dembek ("You") and Elsevier ("Elsevier") provided by Copyright Clearance Center ("CCC"). The license consists of your order details, the terms and conditions provided by Elsevier, and the payment terms and conditions.

Supplier Elsevier Limited, The Boulevard,Langford Lane Kidlington,Oxford,OX5 1GB,UK
Registered Company Number 1982084
Customer name Marcin Dembek
Customer address 38 Bullingdon Road, Oxford, None OX4 1QJ
License number3327710642697
License date Feb 14, 2014
Licensed content publisher Elsevier
Licensed content publication Trends in Microbiology
Licensed content title Germination of spores of Bacillales and Clostridiales species: mechanisms and proteins involved
Licensed content author Daniel Paredes-Sabja, Peter Setlow, Mahfuzur R. Sarker
Licensed content date February 2011
Licensed content volume number19
Licensed content issue number2
Number of pages 10
Start Page85
End Page94
Type of Use reuse in a thesis/dissertation
Portion figures/tables/illustrations
Number of figures/tables/illustrations1
Format both print and electronic
Are you the author of this Elsevier article? No
Title of your thesis/dissertation Whole-genome analysis of sporulation and germination in Clostridium difficile
Expected completion date Mar 2014
Estimated size (number of pages) 250
Total0.00 USD

OPEN ACCESS Freely available online

PLOS ONE

Transcriptional Analysis of Temporal Gene Expression in Germinating *Clostridium difficile* 630 Endospores

Marcin Dembek[1], Richard A. Stabler[2], Adam A. Witney[3], Brendan W. Wren[2], Neil F. Fairweather[1]*

1 MRC Centre for Molecular Bacteriology and Infection, Department of Life Sciences, Imperial College London, London, United Kingdom, **2** Faculty of Infectious and Tropical Diseases, London School of Hygiene and Tropical Medicine, London, United Kingdom, **3** Division of Clinical Sciences, St George's, University of London, London, United Kingdom

Abstract

Clostridium difficile is the leading cause of hospital acquired diarrhoea in industrialised countries. Under conditions that are not favourable for growth, the pathogen produces metabolically dormant endospores *via* asymmetric cell division. These are extremely resistant to both chemical and physical stress and provide the mechanism by which *C. difficile* can evade the potentially fatal consequences of exposure to heat, oxygen, alcohol, and certain disinfectants. Spores are the primary infective agent and must germinate to allow for vegetative cell growth and toxin production. While spore germination in *Bacillus* is well understood, little is known about *C. difficile* germination and outgrowth. Here we use genome-wide transcriptional analysis to elucidate the temporal gene expression patterns in *C. difficile* 630 endospore germination. We have optimized methods for large scale production and purification of spores. The germination characteristics of purified spores have been characterized and RNA extraction protocols have been optimized. Gene expression was highly dynamic during germination and outgrowth, and was found to involve a large number of genes. Using this genome-wide, microarray approach we have identified 511 genes that are significantly up- or down-regulated during *C. difficile* germination ($p \leq 0.01$). A number of functional groups of genes appeared to be co-regulated. These included transport, protein synthesis and secretion, motility and chemotaxis as well as cell wall biogenesis. These data give insight into how *C. difficile* re-establishes its metabolism, re-builds the basic structures of the vegetative cell and resumes growth.

Citation: Dembek M, Stabler RA, Witney AA, Wren BW, Fairweather NF (2013) Transcriptional Analysis of Temporal Gene Expression in Germinating *Clostridium difficile* 630 Endospores. PLoS ONE 8(5): e64011. doi:10.1371/journal.pone.0064011

Editor: Malcolm James Horsburgh, University of Liverpool, United Kingdom

Received January 16, 2013; **Accepted** April 8, 2013; **Published** May 15, 2013

Funding: This work was supported by a Wellcome Trust studentship 089875/Z/09/Z to M.D. The funders had no role in study design, data collection and analysis, decision to publish, or preparation of the manuscript.

Competing Interests: The authors have declared that no competing interests exist.

* E-mail: n.fairweather@imperial.ac.uk

Introduction

Clostridium difficile is a Gram-positive, anaerobic bacterium and a leading cause of antibiotic-associated diarrhoea in industrialised countries [1]. Infection typically occurs among hospitalized patients, whose natural intestinal microflora has been disrupted by prolonged treatment with broad-spectrum antibiotics, allowing the pathogen to colonize the compromised gastro-intestinal tract [2]. The resulting, toxin-mediated disease can range from mild, self-limiting diarrhoea through severe diarrhoea to the potentially lethal pseudomembraneus colitis and can progress to toxic megacolon and sepsis syndrome causing significant morbidity and mortality [3].

Under conditions that are not favourable for growth, *C. difficile* exits the vegetative growth cycle and triggers sporulation, producing metabolically dormant endospores (spores). These are thought to be the primary infectious agent as recent studies have shown that a mutant strain of *C. difficile* unable to produce SpoOA, a regulatory protein essential for spore formation, is unable to efficiently persist and transmit the disease [4]. Due to their multi-layered structure, spores are extremely robust and resistant to both chemical and physical insult, providing the mechanism by which *C. difficile* can evade the potentially fatal consequences of exposure to heat, oxygen, alcohol, and certain disinfectants [reviewed in 5,6]. Spores shed in faeces are therefore difficult to eradicate and can persist in healthcare facilities for extended periods of time leading to infection or re-infection of individuals through inadvertent ingestion of contaminated material [7,8].

In order to cause disease, spores need to return to vegetative growth through a process termed germination. In *Bacillus*, *Clostridium* and related species, spore germination is initiated upon binding of small molecules called germinants (often nutrients such as sugars and/or amino acids) to specific germination receptors (GRs). This triggers a series of irreversible biophysical events that lead to rehydration of the spore core and degradation of its protective layers. Once the constraints of spore outer layers are lifted, the cell enters a period of longitudinal growth, accompanied by re-establishment of cell metabolism during which DNA, RNA and protein synthesis resume [reviewed in 9]. While spore germination in *Bacillus* is well understood, and genes involved in this process have recently been identified in *Clostridium perfringens* [10–12], little is known about *C. difficile* germination and outgrowth. Even though many components of the spore germination machinery are conserved between spore forming members of *Bacillales* and *Clostridiales*, recent studies have revealed significant differences both in the proteins and in the signal transduction pathways involved [reviewed in 13]. Bioinformatic analysis of *C. difficile* genome has failed to reveal genes encoding known germination receptor subunits [14–16] even though a number of such genes were identified in other Clostridia. Furthermore, while

the *C. difficile* 630 spore proteome has recently been described [17], little homology has been found between *C. difficile* spore proteins and those present in other spore-formers. This would suggest that the aspects of germination in *C. difficile* are unique, a notion supported by the limited numbers of studies published so far [18–21].

We now know that bile salts (cholate, taurocholate, glycocholate and deoxycholate) stimulate *C. difficile* spore germination [21]. More recently glycine and histidine were shown to act as a co-germinants with these cholate derivatives [18,22,23], and kinetic studies suggest that there are distinct germination receptors for taurocholate and glycine [24]. Neither of these compounds has been previously described as a germinant for spores of *Bacillus* or *Clostridium* species, supporting the notion of a novel mode of germinant recognition in *C. difficile* spores. Furthermore, chenodeoxycholate, another bile salt, has been shown to inhibit *C. difficile* spore germination [19], adding a new level of regulation to the current model of *C. difficile* colonisation of the gut.

As limited as our insight into the mechanism of germination in *C. difficile* might be, even less is known about the events that follow initiation of germination and while transcriptomic analysis of gene expression during germination has been carried out in *B. subtilis* [*25*] and more recently *C. novyi-NT* [26] and *C. sporogenes* [*27*], no such data is available for *C. difficile*. To address this issue we use a combination of standard microbiology, microscopy and genome-wide transcriptome analysis to explore the morphological, physiological and transcriptional changes that occur during germination and subsequent outgrowth of *C. difficile* 630 spores and try to elucidate some of the processes that occur during the transformation of a metabolically dormant spore into an actively growing vegetative cell.

Results and Discussion

Characterization of Germination and Outgrowth Dynamics

C. difficile 630, an epidemic, virulent and multi-drug-resistant strain was selected for this analysis, as its complete genome sequence has been determined [15]. In order to obtain sufficient quantities of spores, free from vegetative cells and cell debris, a protocol for producing and purifying spores was developed. Growth of *C. difficile* 630 on solid SMC sporulation medium for 7 days ensured the highest sporulation rates (data not shown). Using these growth conditions, 10^7 - 10^8 endospores could be reproducibly obtained per ml of initial culture. Phase contrast microscopy confirmed the high purity of the purified spore suspensions, revealing fully developed, phase-bright endospores, free of vegetative cells and noticeable cell debris (Figure 1).

To ensure that the purification process does not detrimentally affect the spores, the viability and germination dynamics of the isolated spores were assessed. Spore germination is classically measured as a decrease in optical density (OD) of a spore suspension occurring concomitantly with the release of dipicolinic acid (DPA) from the spore core, rehydration of the core, and degradation of the cortex [9]. This is followed by an increase in OD_{600} correlated with outgrowth and cell division as the cells enter logarithmic growth phase. OD_{600} measurement of liquid cultures containing germinating spores combined with colony forming unit (CFU) counts and microscopy showed that >99.9999% of spores undergo germination when grown in nutrient medium (BHIS) supplemented with the germinant, sodium taurocholate (Tch) as indicated by a rapid decrease in OD_{600} (approx. 50% of initial value within 5 minutes of induction) and a 5-log drop in the number of spore CFUs (Figure 2A, 2B and 2C). Importantly, based on phase contrast and fluorescence microscopy analysis, spore germination in nutrient medium supplemented with an excess of Tch was synchronous and appeared to be complete within 180 min. This would be critical in subsequent transcriptomic analysis of gene expression during germination as it ensured that all spores were in the same phase of germination. Immediately upon induction of germination, the dormant spores lost their phase-bright appearance becoming susceptible to Hoechst 33258 DNA staining, presumably due to Ca^{2+}-DPA release and subsequent rehydration of the spore core resulting in a gradual increase in spore volume (0 - 30 min). This was followed by hydrolysis of cortex peptidoglycan and shedding of spore outer layers (45–60 min). Once these physical constraints were removed, germinating cells entered a phase of longitudinal growth which coincided with DNA replication followed by symmetric cell division (60–180 min) (Figure 3A and 3B). In contrast, no germination was observed among spores grown in medium devoid of the germinant as no changes in OD_{600}, spore CFU count or spore morphology could be observed throughout the 6 h incubation period (Figure 2A and 2D; Figure 3D). Unlike in *Bacillus,* where pre-treating spores with high temperature increases germination rates, we found that heat activation had no effect on germination dynamics of the isolated *C. difficile* endospores (data not shown). Interestingly, germination was not observed when liquid cultures were incubated aerobically, presumably due to the inhibitory presence of oxygen. Even though a decrease in OD_{600} and spore CFUs was observed immediately after induction with Tch and the spores lost their phase-bright appearance becoming susceptible to DNA staining (indicative of Ca^{2+}-DPA release and core rehydration), spores failed to progress fully to outgrowth and eventually were killed as indicated by the gradual drop in total CFUs (Figure 2A and 2C; Figure 3C). This is consistent with recent findings [28] and suggests that oxygen is a negative regulator of *C. difficile* endospore germination acting downstream of any signalling events that induce germination.

Optimization of RNA Extraction

RNA quality is of paramount importance in any transcriptional analysis of gene expression. It was therefore critical to develop a method for extracting RNA that would not only provide high yields, but would also ensure that the integrity of RNA was maintained. Mechanical disruption with silica beads followed by acid phenol-based extraction was shown to give the highest quality RNA. Using this method, between 2 and 10 μg of total RNA could be reproducibly isolated per 10^8 spores. The quantity of extracted RNA depended on the status of the spores and increased gradually as the spores went from dormancy through germination to outgrowth (Figure S1A). This could be attributed to the increasing susceptibility of the spore envelope to lysis during germination and/or the initiation of RNA synthesis [9]. All preparations were of high purity and integrity as indicated by a 260/280 nm absorption ratio in the range of 2.05 to 2.18 and Bioanalyzer electropherograms showing sharp and undegraded peaks (Figure S1B). Interestingly, we found that the ribosomal RNA (rRNA) of spores differed from that present in vegetative cells. In addition to the 16S and 23S rRNA species, two smaller rRNA species were identified in dormant spores, represented by small peaks on Bioanalyzer spectra (Figure S1C). These could only be discerned in dormant spores and reduced in intensity as germination progressed. A similar phenomenon has previously been reported in *Bacillus* [25] as well as the more closely related *Clostridium novyi* [26] and *Clostridium sporogenes* [27], although its significance remains unknown. These smaller species might

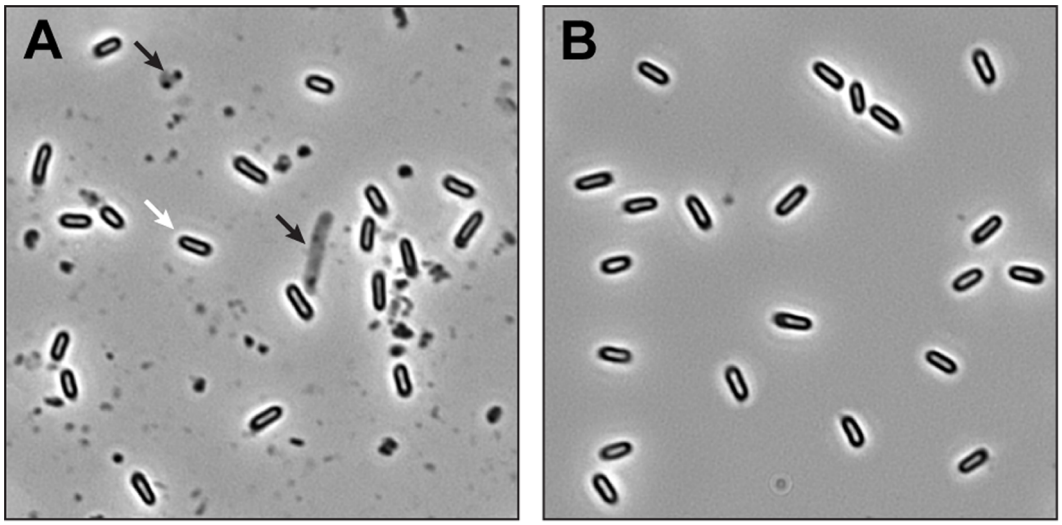

Figure 1. *C. difficile* spore purification. *C. difficile* was sporulated on SMC solid medium, washed extensively and purified *via* density gradient centrifugation. Samples taken before and after purification were analysed using phase contrast microscopy A) Crude spore preparation before purification. Phase-bright endospores (white arrow), vegetative cells and significant amount of cell debris (black arrows) are visible**.** B) Spore preparation after purification. Phase-bright endospores are visible, free of vegetative cells and cell debris.
doi:10.1371/journal.pone.0064011.g001

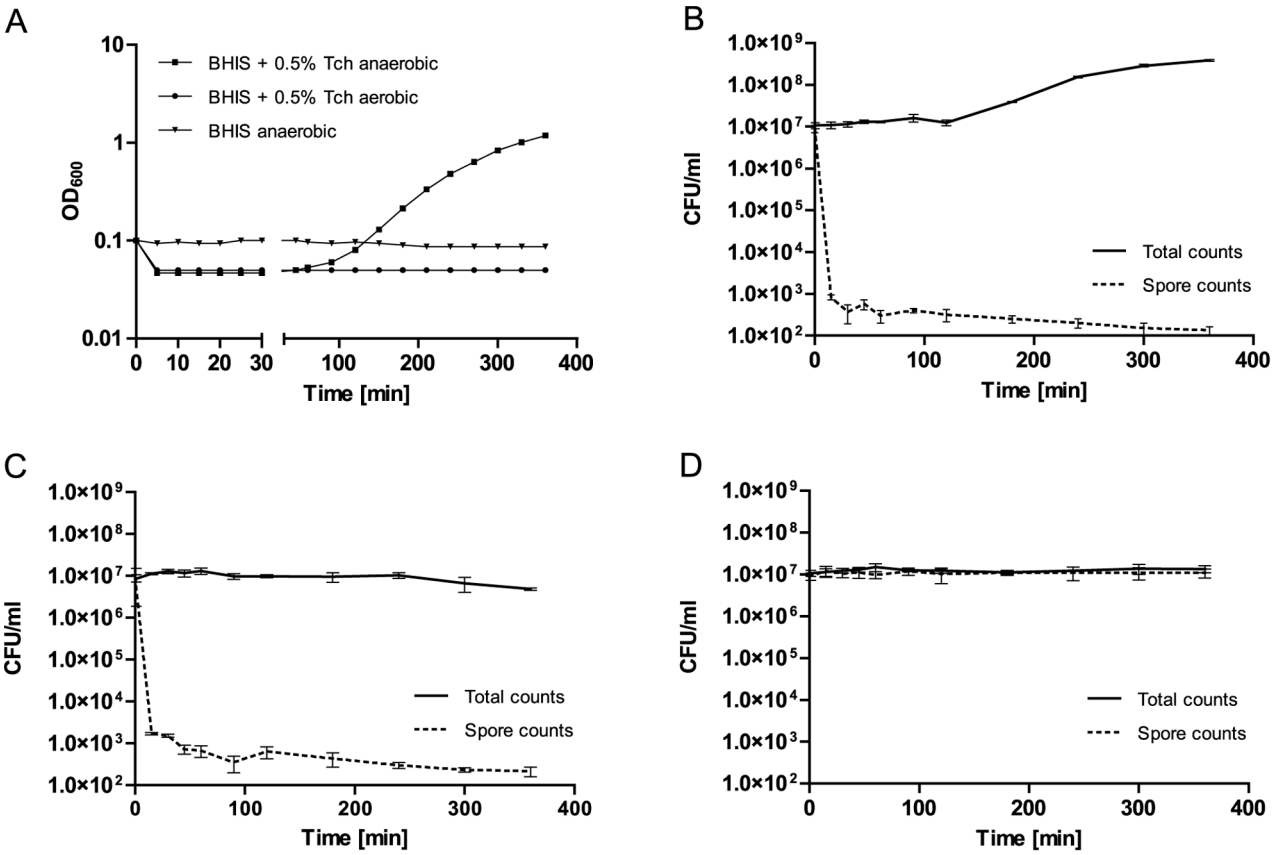

Figure 2. Growth characteristics during spore germination and outgrowth. Purified *C. difficile* 630 endospores were resuspended in BHIS $\pm$0.5% sodium taurocholate (Tch) to an OD_{600} of 0.1 and incubated either aerobically or anaerobically for 6 h at 37°C. Growth was monitored *via* OD_{600} measurements and CFU counts. A) *C. difficile* 630 germination dynamics growth curve. Spores incubated in the presence of 0.5% Tch showed a rapid decrease in OD_{600} immediately after resuspension, in both aerobic and anaerobic conditions. No decrease in OD_{600} was observed for spores incubated in the absence of Tch. B) CFU counts for spores germinated anaerobically in BHIS +0.5% Tch. C) CFU counts for spores germinated aerobically in BHIS +0.5% Tch. D) CFU counts for spores germinated anaerobically in BHIS. Data reported as means and standard deviations from three independent experiments.
doi:10.1371/journal.pone.0064011.g002

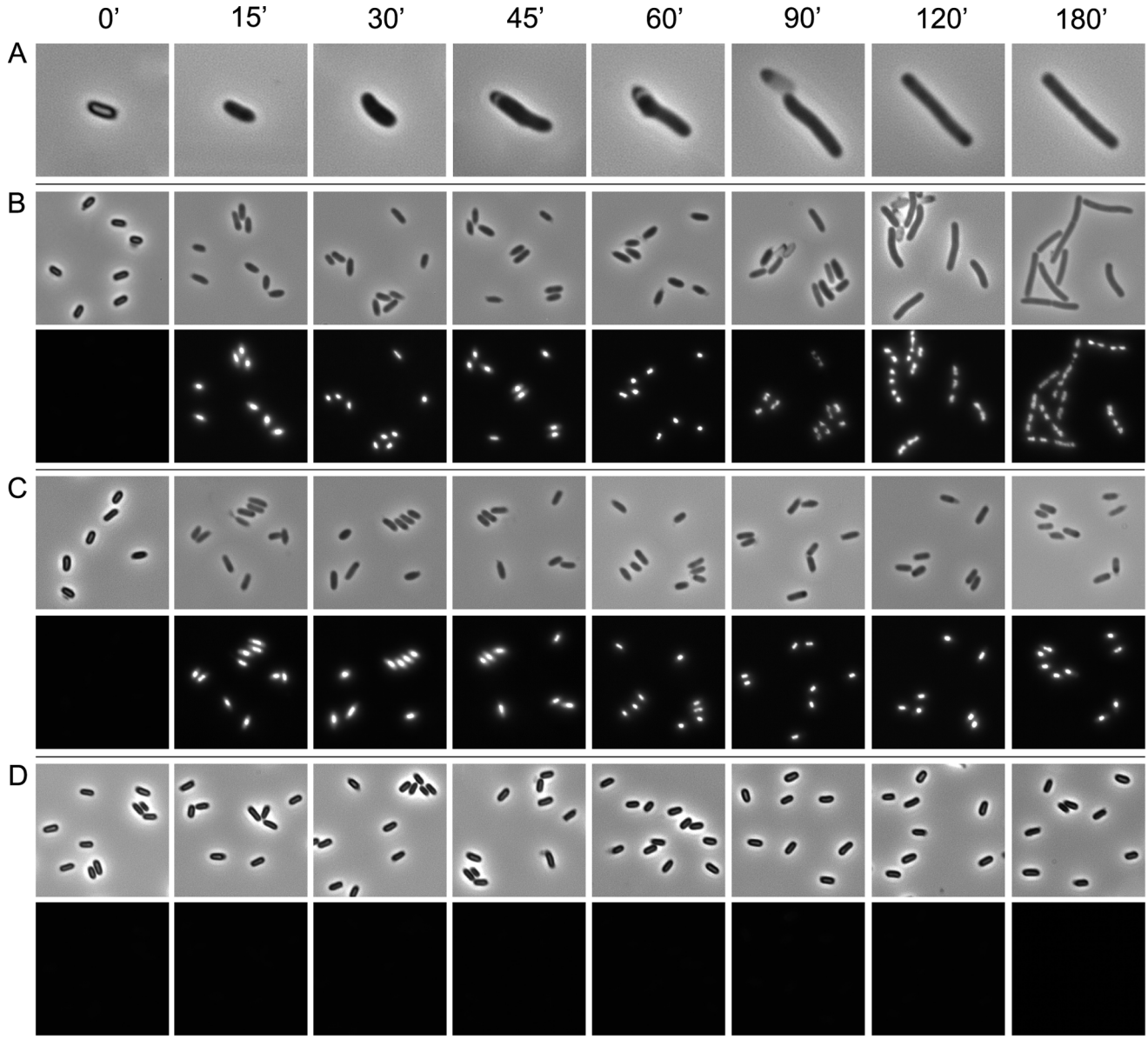

Figure 3. Morphological changes during spore germination and outgrowth. Purified *C. difficile* 630 endospores were resuspended in BHIS ±0.5% sodium taurocholate (Tch) to an OD_{600} of 0.1 and incubated either aerobically or anaerobically for 6 h at 37°C. At the given time points samples were formaldehyde-fixed and analysed using phase contrast microscopy and fluorescence microscopy following DNA staining with Hoechst 33258. A and B) Spores germinated anaerobically in BHIS +0.5% Tch. Upon induction of germination, dormant spores lose their phase-bright appearance and become susceptible to DNA staining. This is followed by a gradual increase in volume and shedding of spore outer layers which remain visible as empty 'shells'. Once the physical constraints of the outer spore layers are removed, the spore enters a phase of longitudinal growth coinciding with DNA replication followed by symmetric cell division. C) Spores germinated aerobically in BHIS +0.5% Tch. Following induction of germination, spores lose their phase-bright appearance and become susceptible to DNA staining but fail to progress to outgrowth. D) Spores germinated anaerobically in BHIS. No changes in spore appearance and no DNA staining could be observed.
doi:10.1371/journal.pone.0064011.g003

represent rRNA fragments or be indicative of RNA maturation within the germinating spore [29].

Microarray Analysis of Temporal Gene Expression during Spore Germination – General Observations

Total RNA extracted from germinating spores at eight time points representing dormancy (0 min), germination (15, 30, 45, 60 min) and outgrowth (90, 120, 180 min) was analysed by competitive RNA/DNA hybridisation using the BμG@S CDv2.0.1 microarray. Gene expression was highly dynamic during germination and outgrowth and was found to involve a large part of the genome. Relatively few transcripts were identified in dormant spores (see below), consistent with their metabolically silent state. In contrast, a significant up-regulation of gene expression was observed immediately after induction of germination, peaking at 30 min (Figure 4). In order to validate these results, semi-quantitative RT PCR was used to confirm the temporal expression pattern for a number of selected genes showing a wide range of distinct expression profiles being either significantly up- or down-regulated in the early or late stage of

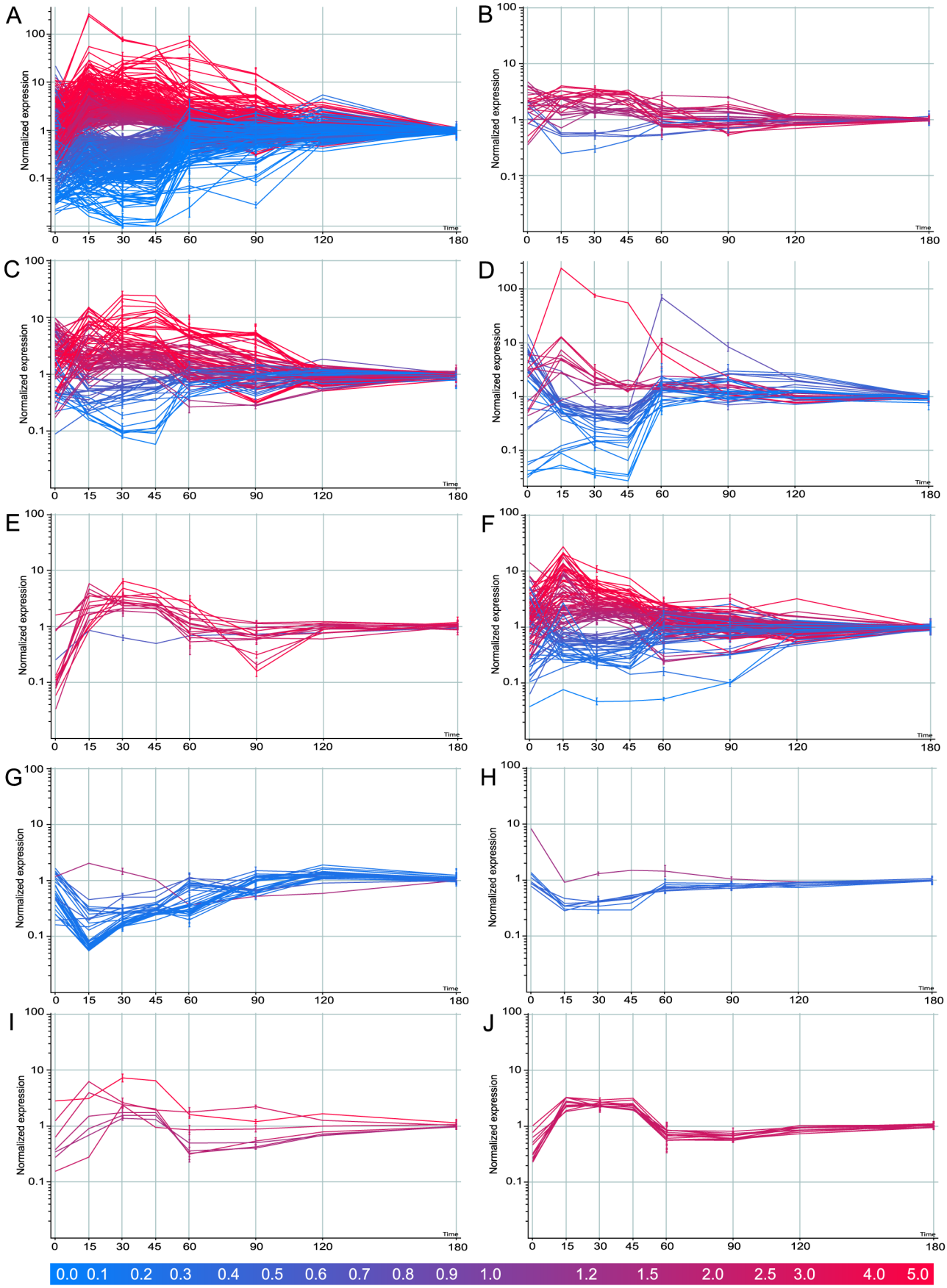
A
B
C
D
E
F
G
H
I
J
Normalized expression
Time
0 15 30 45 60 90 120 180
0.0 0.1 0.2 0.3 0.4 0.5 0.6 0.7 0.8 0.9 1.0 1.2 1.5 2.0 2.5 3.0 4.0 5.0

Figure 4. Temporal gene expression profiles in germinating *C. difficile* spores. A) All significantly, differentially regulated genes, B) two-component systems, C) ABC-transporters, D) phosphotransferase system, E) ribosomal proteins, F) transcriptional regulators, G) flagellar assembly and chemotaxis, H) type IV pili, I) peptidoglycan biosynthesis, J) secondary cell wall polymer (SCWP) biosynthesis are shown. Microarray gene expression data represented as normalised intensity with respect to control conditions. Analysed using 1-way ANOVA (A $p \leq 0.01$, B-J $p \leq 0.05$) and Benjamini-Hochberg multiple testing correction. Each line represents data for one gene. All graphs were generated using GeneSpring GX7.3.1.
doi:10.1371/journal.pone.0064011.g004

germination. In all cases the expression profiles obtained matched those seen in the microarray experiment (Figure 5).

We investigated in detail two time points: 30 min and 180 min post germination. At 30 min all spores are actively germinating in contrast to 180 min when normal vegetative growth has commenced. In total, 263 genes were up-regulated and 248 genes down-regulated at 30 min when compared to the 180 min time point ($p \leq 0.01$) (Figure 4A). The magnitude of change of the statistically up-regulated genes ranged from 1.3-fold to 80-fold, and that of down-regulated genes ranged from 1.3- to 100-fold. Many gene clusters encoding enzyme complexes or biochemical pathways appeared to be co-ordinately regulated. The Kyoto Encyclopedia of Genes and Genomes (KEGG) database was used to identify significantly differentially regulated pathways. Selected examples have been listed below and summarised in Table 1. Where appropriate, genes that marginally failed the stringent statistical cut-off ($0.01 \leq p \leq 0.05$) are also mentioned. Full lists of genes generated through this experiment are shown in supplementary data (Table S1).

Table 1. Numbers of genes differentially regulated during germination.

Functional group	Up-regulated	Down-regulated
Two-component systems	26	5
ABC-transporters	71	34
Phosphotransferase system	11	30
Ribosomal proteins	12	1
Transcriptional regulators	45	24
Flagellum and chemotaxis	0	34
Type IV pili	0	7
Peptidoglycan biosynthesis	9	1
Secondary cell wall polymers	12	0

The total number of genes within specific functional groups up-regulated or down-regulated at 30 min into germination was determined using microarray analysis (***p*≤0.05**).pone.0064011.g006.tif.
doi:10.1371/journal.pone.0064011.t001

Spore Transcripts

Despite early research hinting at the presence of mRNA in spores [30,31], for a long time it has been generally assumed that dormant spores do not contain functional transcripts. This view

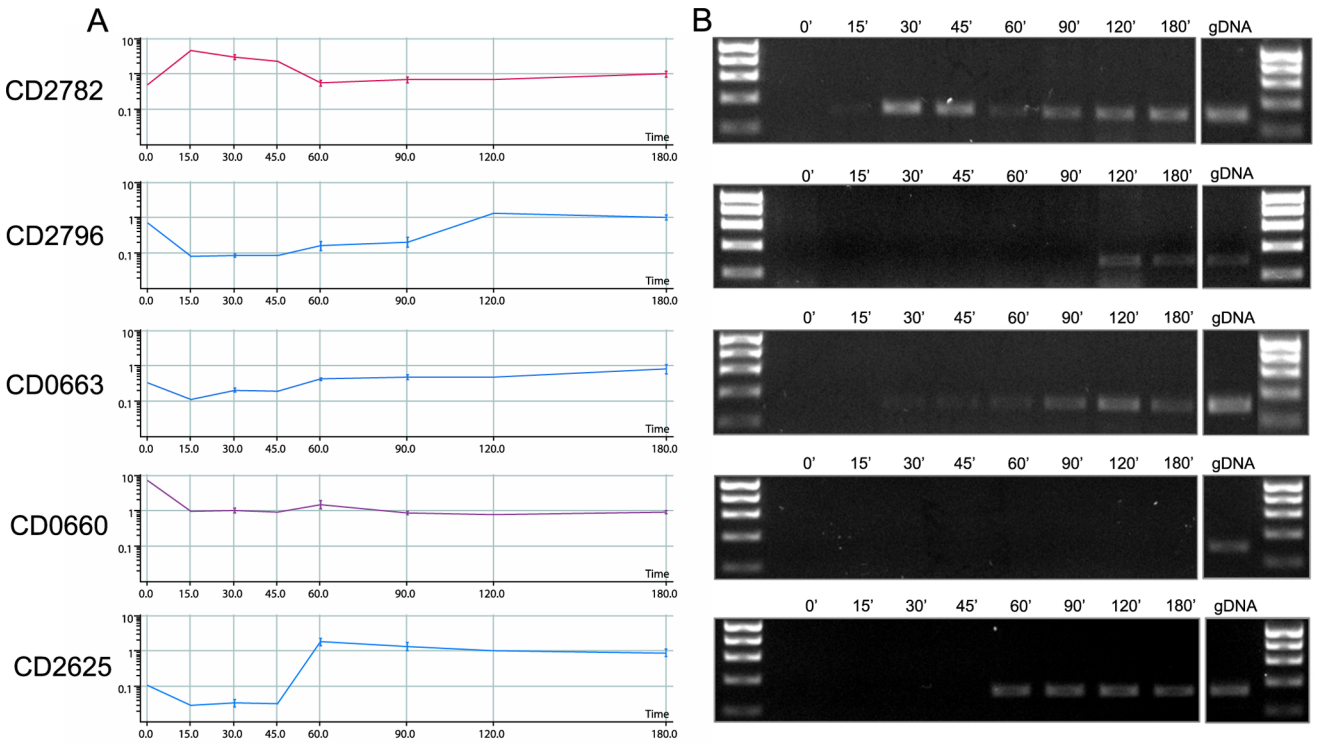

Figure 5. RT-PCR validation of microarray results. cDNA was prepared from total RNA using reverse transcription. Primers internal to five selected genes were used to amplify fragments of ~150 bp: (CD2782 - cell wall binding protein, CD2796 - cell wall binding protein, CD0663 - toxin A, CD0660 - toxin B, CD2625 - putative membrane protein). gDNA was used as template in a positive control reaction. 25 reaction cycles were carried out to ensure non-saturating conditions. A) microarray expression profile (normalised to 180 minutes), B) gel electrophoresis of the PCR amplicons.
doi:10.1371/journal.pone.0064011.g005

has now changed as recent studies conducted in *B. subtilis* [25], *C. novyi-NT* [26] and *C. sporogenes* [27] have shown that mRNA is abundant in spores and that its composition is dramatically different from that observed in vegetative cells. A number of explanations for this phenomenon have been proposed. Spore transcripts might represent mRNA that has been entrapped during the late phases of sporulation and is later degraded to act as a reservoir of nucleotides during germination. Indeed, five out of fifteen most abundant spore transcripts identified in this study represented late-sporulation genes such as those encoding small acid-soluble proteins A and B (CD2688 and CD3249 respectively) a putative spore coat protein (CD0213) and a stage IV sporulation protein (CD0783) (Table S2). Alternatively, transcripts might be stored to equip the spore with proteins that will become necessary during the transformation into a vegetative cell such as those involved in growth, protein synthesis, detoxification, metabolism, transport, secretion etc. Interestingly, the second most abundant transcript we have identified encodes a putative Mn-superoxide dismutase (CD1631). Other genes with redox activity whose transcripts were present at relatively high levels in dormant spores included two putative oxidoreductase complexes with ferrodoxin activity (CD2197-CD2199A and CD2427-CD2429A), a NADH oxidase (CD2540) and a NADH-dependent flavin oxidoreductase (CD2709). The inclusion of such a large number of redox genes within the spore transcriptome is intriguing, particularly in the light of the anaerobic life cycle of *C. difficile*. While *C. difficile* spores are resistant to ambient oxygen concentrations, vegetative cells can be killed by relatively short exposure to oxygen. It would thus be tempting to speculate that at least a subset of these genes might play a role in detoxification by scavenging reactive oxygen species (ROS). Finally, consistent with previous reports [26], we found that a large proportion of spore transcripts encode proteins with an unknown function (nine out of top fifteen hits). This not only underlines the difference in mRNA composition between spores and vegetative cells but also the need for more research into the spore transcriptome of major spore-forming bacteria.

Two-component Signal Transduction Systems

Two-component regulatory systems serve as a basic stimulus-response coupling mechanism to allow organisms to sense and respond to changes in many different environmental conditions. They typically consist of a membrane-bound histidine kinase that senses a specific environmental stimulus and a corresponding response regulator that mediates the cellular response, mostly through differential expression of target genes [reviewed in 32]. *C. difficile* 630 has fifty-one two-component sensor histidine kinases and fifty-four response regulators. Nine kinase genes and seventeen response regulator genes were up-regulated in germinating spores. Only five genes (three kinases and two response regulators) were down-regulated (Figure 4B).

Transport of Metabolites and Sugars

The germinating spore requires a large supply of metabolites and cofactors to facilitate re-establishment of cell metabolism. Consistent with this requirement, we found 100 out of 229 ABC-transporter genes were differentially regulated during germination. A majority of these (70 genes) were up-regulated during germination when compared to the vegetative state, including the entire *potABCD* locus (spermine/putrescine ABC-transporter). The spermidine/putrescine transporter is involved in polyamine trafficking, which in turn plays a crucial role in DNA replication, cell division and stress response. Interestingly, polyamines have previously been implicated in the shift from a quiescent to a proliferating state in bacteria, plants, fungi and other eukaryotic systems [reviewed in 33,34]. Similarly, the *appABC* operon (peptide/nickel ABC-transporter) and the *ssuABC* operon (sulfonate/nitrate/taurine ABC-transporter) were up-regulated. The latter is of particular interest as taurine conjugated with cholate yields taurocholate, the primary germinant for *C. difficile* spores. One could speculate that the up-regulation of this transporter might be a part of a positive feedback loop providing a constant supply of the germinant and the basis for commitment in germinating spores. Other ABC-transporters that had at least one significantly up-regulated gene included maltose/maltodextrin ABC-transporter (9.5-fold), lactose/L-arabinose ABC-transporter (13.6-fold) and iron complex ABC-transporter (2.6-fold). In contrast, two ABC-transporter complexes involved in cobalt and nickel transport and encoded by the *cbiMNOQ* operon were down-regulated (Figure 4C).

The PTS system is a complex phosphate translocation mechanism involved in the transport of sugars such as glucose, mannose and mannitol. As such it plays a key role in cell metabolism driving glycolysis. Unlike ABC-transporters, sugar transport was largely inactive during germination with the entire branch of the system responsible for glucose trafficking significantly down-regulated (from 1.9- to 23.8-fold) in germinating spores when compared to vegetative cells, including members of the *pstG-ABC* operon. In contrast, a number of genes involved in fructose and lactose metabolism were up-regulated in germinating spores. These included *fruABC* (fructose-specific phosphotransferase; 75.2-fold), CD2270 (putative 1-phosphofructokinase; 79.8-fold) and CD1806 (putative fructokinase; 2.8-fold) (Figure 4D). While this could simply reflect the composition of the culture medium, it could also indicate the preference for fructose as the main carbon source in early germination.

Ribosomal Proteins and Transcriptional Regulators

Exit from dormancy requires the bacterium to rebuild most of the structures found in a vegetative cell, necessitating large amounts of protein synthesis. It is not surprising then that a significant up-regulation of genes involved in transport, coincided with up-regulation of transcription and translation. In general, all genes encoding ribosomal proteins were up-regulated during germination. These included three genes encoding 30S subunit proteins and eight genes encoding 50S subunit proteins (Figure 4E). Similarly, genes encoding DNA-directed RNA polymerase were up-regulated, although only the genes encoding the β and β′ subunits of the polymerase had a p value ≤ 0.05. Furthermore, sixty-eight genes encoding transcriptional regulators were up-regulated (from 1.3- to 10.9-fold) while twenty-four genes were down-regulated (from 1.3- to 21.2-fold) in germinating spores (Figure 4F). These included members of the *gntR, tetR araC, marR, merR, rpiR, copR, deoR* and *lysR* gene families. On the whole, genes encoding tRNA synthetases were down regulated in germinating spores when compared to a vegetative cell. Similarly, enzymes involved in amino acid metabolism were largely down-regulated during germination, possibly reflecting the preferential catabolism of endogenous nutrients as a means for obtaining the necessary 'building blocks' for protein synthesis in early germination.

Secretion and Cell Wall Components

The Sec machinery provides a major pathway of protein translocation from the cytosol across the cytoplasmic membrane in bacteria [35]. A number of components of the *sec* secretory pathway can be identified in *C. difficile 630* including *secA1, secA2, secE and secY* [27]. In general, all genes within the *secAYEG* operon were up-regulated in germinating spores, although only *secA2* (3.4-fold) and *secE* (3.8-fold) significantly so. The lipoprotein signal-

peptidase *lspA* was also up-regulated (2.6-fold) as was the signal recognition particle encoded by *ffh* (4.16-fold) and prolipoprotein diacylglyceryl transferase encoded by *lgt* (3-fold).

The *C. difficile* flagellar assembly is encoded by thirty-five genes located within a single cluster. A vast majority of flagellar genes were inactive in germinating spores when compared to vegetative cells. In addition, five genes encoding components of the bacterial chemotaxis machinery including *motA*, *motB*, *cheY*, *cheD* and *cheW* were also found to be down-regulated in germinating spores (Table 2; Figure 4G) as were seven genes within two gene clusters encoding putative type IV pilus proteins (Table 3; Figure 4H). As cell motility is typically initiated upon nutrient deprivation in stationary phase, the overall inactivity of genes involved in motility during germination is in accordance with expectations, in that flagellar genes are dormant during germination and are transcribed in vegetative cells.

As a hallmark of cell expansion during germination and outgrowth, genes involved in cell wall biosynthesis were found to be significantly up-regulated in germinating spores. Peptidoglycan is produced from N-acetylglucosamine (GluNAc) and N-acetylemuramic acid (MurNAc) in a series of reactions involving incorporation of D-glutamine and D-alanyl-D-alanine. Genes encoding the enzymatic components of this pathway are largely located within the *mur-mra* cluster. Ten enzymes involved in peptidoglycan biosynthesis were up-regulated in germinating spores, including *ddl* (D-Ala D-Ala ligase B; 7.3-fold) *glnA* (glutamine synthase; 2.6-fold) and *murF* (UDP-MurNAc-pentapeptide synthase; 2.4-fold) as well as other members of the *mur-mra* cluster: *murGDE* and *mraYW* (Table 4; Figure 4I). In addition to peptidoglycan, the Gram-positive cell wall can also contain secondary cell wall polymers (SCWP) such as teichoic, teichuronic acids and lipoteichoic acids which can make up between 10 and

Table 2. List of differentially regulated flagellar assembly and chemotaxis genes.

Systematic name	Gene product	*p*-value	Fold change
CD0228	flagellar motor switch protein	0.0248	−1.9
CD0230	putative flagellar biosynthesis protein	0.0151	−3.7
CD0231	putative flagellar hook-associated protein	0.0204	−3.6
CD0232	flagellar hook-associated protein	0.0167	−5.0
CD0235	flagellar protein FliS	0.0106	−3.7
CD0236	flagellar protein	0.0161	−4.0
CD0237	flagellar cap protein	0.0165	−3.1
CD0239	flagellin subunit	0.0282	−2.0
CD0246	flagellar basal-body rod protein	0.0271	−3.1
CD0247	flagellar hook-basal body complex protein	0.0117	−3.8
CD0248	flagellar M-ring protein	0.0177	−3.9
CD0249	flagellar motor switch protein	0.0187	−4.8
CD0250	flagellar assembly protein	0.0115	−5.6
CD0251	flagellum-specific ATP synthase	0.0139	−5.7
CD0252	flagellar protein	0.0172	−6.1
CD0253	putative flagellar hook-length control protein	0.0177	−5.7
CD0255	flagellar hook protein	0.00833	−6.0
CD0255A	putative flagellar protein	0.0154	−6.2
CD0256	chemotaxis protein	0.0164	−6.4
CD0257	chemotaxis protein	0.0236	−6.0
CD0258	flagellar basal body-associated protein	0.00927	−5.3
CD0259	putative flagellar protein	0.0297	−4.9
CD0260	flagellar biosynthetic protein	0.0394	−4.4
CD0261	flagellar export protein	0.0393	−4.9
CD0262	flagellar export protein	0.0364	−5.4
CD0263	flagellar export protein	0.0232	−5.5
CD0265	flagellar number regulator	0.0284	−6.3
CD0268	flagellar basal-body rod protein FlgG	0.0078	−6.6
CD0269	putative flagellar basal-body rod protein	0.00932	−6.5
CD0270	putative flagellar motor switch protein	0.00953	−6.7
CD0271	putative flagellar motor switch protein	0.0475	−4.6
CD0533	chemotaxis protein	0.017	−1.8
CD0535	chemotaxis protein	0.0329	−1.9
CD0540	chemotaxis protein	0.0257	−1.6

doi:10.1371/journal.pone.0064011.t002

Table 3. List of differentially regulated type IV pilin genes.

Systematic name	Gene product	*p*-value	Fold change
CD3295	putative type IV pilus-assembly protein	0.0211	+1.3
CD3504	putative type IV prepilin leader peptidase	0.00385	−2.4
CD3505	putative type IV pilus retraction protein	0.0186	−2.5
CD3507	putative type IV pilin	0.00579	−2.5
CD3508	putative type IV pilin	0.0141	−2.3
CD3509	putative type IV pilus assembly protein	0.0191	−2.3
CD3511	type IV pilus assembly protein	0.0245	−3.4
CD3512	type IV pilus assembly protein	0.0091	−2.9

doi:10.1371/journal.pone.0064011.t003

60% of its structure. Although the genes specifying these components have not been identified in *C. difficile*, it might be relevant that a cluster of genes (CD2769-80) specifying glycotransferases and related enzymes was found to be significantly up-regulated in germinating spores (Table 5; Figure 4J).

Toxins

Of central importance in *C. difficile* is the pathogenicity locus (PaLoc) containing five genes encoding two large clostridial toxins: TcdA and TcdB as well as their regulators (*tcdC*, *tcdR*) and export machinery (*tcdE*) [36]. Both toxin A and B are represented by multiple probes on the microarray. *tcdA* was down-regulated during germination when compared to the vegetative cell. No transcripts for *tcdB* could be detected in either state, consistent with the observation that toxins are expressed in stationary phase.

Concluding Remarks

This study aims to give a genome-wide overview of the temporal gene expression during germination and outgrowth of *C. difficile* spores. We decided to focus on the events that follow initiation of germination and are critical in the transformation of a metabolically dormant spore into an actively growing vegetative cell. Our analysis was possible as we initially demonstrated the synchronous nature of germination in *C. difficile*. This is intriguing as germination in *Bacillus* species and even the more closely related *C. perfringens* and *C. botulinum* has been shown to be heterogenous [37–40]. While the vast majority of a spore population will enter germination upon exposure to germinants, a small proportion may not germinate for many hours or even days. This 'superdormancy' has been correlated with a low level of specific germination receptors in individual spores [41] and is thought to be an example of 'bet hedging', ensuring the survival of a given population in a rapidly changing environment. Under the conditions tested, 99.9999% of the *C. difficile* 630 spore population germinated synchronously. This might be a reflection of the unique germination mechanism present in *C. difficile* and/or the fact that the human gut is a relatively stable environment eliminating the need for super-dormancy.

Our results will give insight into how a dormant organism re-establishes its metabolism, re-builds the basic structures of the vegetative cell and resumes growth. Around 14% of genes (511 genes out of 3679) were found to be significantly differentially regulated at 30 min of germination when compared to the vegetative cell and a number of functional groups of genes appeared to be co-regulated. Further analysis of the genes and biochemical pathways identified here as important in germination will enable a more targeted investigation of germination in *C. difficile* endospores.

Experimental Procedures

Bacterial Strains and Culture Conditions

C. difficile 630 (*tcdA*+ *tcdB*+; epidemic strain isolated in 1985 from Zurich, Switzerland; PCR ribotype 012) was routinely cultured on

Table 4. List of differentially regulated peptidoglycan biosynthesis genes.

Systematic name	Gene product	*p*-value	Fold change
CD0784	putative N-acetylmuramoyl-L-alanine amidase	0.0195	+2.0
CD1343	glutamine synthetase	0.0081	+2.6
CD1408	D-alanine–D-alanine ligase B	0.00843	+7.3
CD2651	UDP-N-acetylglucosamine–N-acetylmuramyl-(penta peptide) pyrophosphoryl-undecaprenol N-acetylglucosamine transferase	0.022	+1.4
CD2653	UDP-N-acetylmuramoylalanine–D-glutamate ligase	0.0105	+1.5
CD2654	phospho-N-acetylmuramoyl-pentapeptide-transferase	0.0145	+1.7
CD2655	UDP-N-acetylmuramoyl-tripeptide–D-alanyl-D-alan ine ligase	0.00508	+2.4
CD2664	putative UDP-N-acetylmuramoylalanyl-D-glutamate–2,6-diaminopimelate ligase	0.0344	+2.4
CD3563	putative spore cortex-lytic enzyme	0.0245	+2.2
CD1898	putative phage-related cell wall hydrolase (endolysin)	0.0174	−6.1

doi:10.1371/journal.pone.0064011.t004

Table 5. List of differentially regulated putative secondary cell wall polymer (SCWP) biosynthesis genes.

Systematic name	Gene product	*p*-value	Fold change
CD2769	capsular polysaccharide biosynthesis protein	0.0201	+2.9
CD2770	putative capsular polysaccharide biosynthesis glycosyl transferase	0.00656	+2.7
CD2771	putative UDP-glucose 6-dehydrogenase	0.00681	+2.4
CD2772	putative teichuronic acid biosynthesis glycosyl transferase	0.016	+2.2
CD2773	putative beta-glycosyltransferase	0.0115	+2.3
CD2774	putative teichuronic acid biosynthesis glycosyl transferase	0.019	+2.2
CD2775	putative minor teichoic acid biosynthesis protein	0.016	+2.3
CD2776	putative glycosyl transferase	0.0408	+2.4
CD2777	putative polysaccharide polymerase	0.0182	+2.5
CD2778	putative polysaccharide biosynthesis protein	0.0311	+2.5
CD2779	putative mannose-1-phosphate guanylyltransferase	0.0116	+2.2
CD2780	putative phosphomannomutase/phosphoglycerate mutase	0.00636	+2.7

doi:10.1371/journal.pone.0064011.t005

blood agar base II (Oxoid) supplemented with 7% horse blood (TCS Biosciences), brain-heart infusion (BHI) agar (Oxoid) or in BHI broth (Oxoid). Cultures were grown statically in an anaerobic cabinet (Don Whitley Scientific) at 37°C in an anaerobic atmosphere (10% CO_2, 10% H_2 and 80% N_2). The strain has been fully sequenced [15] and its genome sequence is available at http://www.sanger.ac.uk/resources/downloads/bacteria/clostridium-difficile.html).

Genomic DNA Extraction

C. difficile 630 was collected from 10 ml late-log-phase culture by centrifugation at 5,000×g for 10 min. Genomic DNA was purified through subsequent incubations with lysozyme (1 h at 37°C), pronase (1 h at 55°C), 10% N-lauroylsarcosine (1 h at 37°C) and RNase (1 h at 37°C) followed by phenol/chloroform extraction and ethanol precipitation.

Sporulation

C. difficile 630 sporulation was induced as described previously [42]. Briefly, 10 ml of TGY broth (3% tryptic soy broth; 2% glucose; 1% yeast extract; 0.1% L-cysteine) was inoculated with a single colony of *C. difficile* 630 grown on BHIS agar (brain heart infusion agar supplemented with 0.1% L-cysteine and 5 mg/ml yeast extract). Following over-night static incubation, bacteria were sub-cultured 1:10 in SMC broth (9% Bacto peptone, 0.5% proteose peptone, 0.15% Tris base, 0.1% ammonium sulphate), incubated until the culture reached OD_{600} of 0.6 and spread out on SMC agar plates. After 7 days of anaerobic incubation at 37°C, spores were harvested in 2 ml of ice-cold sterile water.

Spore Purification

Crude spore suspensions were washed five times with ice-cold sterile water and vortexed for 10 min in between washes. The resulting pellets were re-suspended in 500 µl of 20% HistoDenz (Sigma) and layered over 1 ml of 50% HistoDenz in a 1.5 ml tube. Tubes were centrifuged at 14,000×g for 15 min. The spore pellet was recovered and washed three times with ice-cold sterile water to remove residual HistoDenz. Spore purity was assessed *via* phase contrast microscopy. Spore yields in individual preparations were estimated by counting colony forming units (CFU) on BHI agar plates supplemented with 0.1% sodium taurocholate (Tch). Purified spores were stored in water at 4°C until further analysis.

Germination Assay

Purified *C. difficile* 630 spores were re-suspended to and OD_{600} of 0.1 in BHIS ±0.5% Tch and incubated under aerobic or anaerobic conditions for 6 h at 37°C. Growth was monitored *via* OD_{600} measurements. CFU enumeration was carried out by plating 10-fold dilutions of the germinating cultures on BHIS +0.1% Tch. For spore enumeration, samples were heated at 70°C for 30 min prior to plating.

Phase Contrast and Fluorescence Microscopy

Samples were spun down (5,000×g; 10 min; 4°C), washed with 1 ml of PBS and fixed with 3.7% formaldehyde for 15 min at RT. Following fixation, samples were washed with PBS once more and dried onto glass slides. DNA staining was carried out by adding Hoechst 33258 dye to the mounting medium to a final concentration of 20 µg/ml. Phase contrast and fluorescence microscopy were carried out according to standard procedures on an Eclipse E600 microscope (Nikon) using a 100× oil immersion lens. Images were captured using a Retiga-400R Charge Coupled Device (Q-Imaging).

RNA Extraction and RT-PCR

RNA was extracted using the FastRNA Pro Blue Kit (MP Biosciences). Briefly, 5 ml cultures containing 5×10^9 endospores (OD_{600} 10) at various stages of germination were mixed with 10 ml of RNA Protect (Qiagen) and incubated for 5 min at RT. Samples were centrifuged (5,000×g; 10 min; 4°C), resuspended in 1 ml of RNA Pro solution and transferred to a lysing matrix tube containing 0.1 mm silica beads. Tubes were processed in a FastPrep-24 instrument (MP Biosciences) (3×45 s at 6.5 ms^{-1} with 2 min of cooling on ice between cycles). The efficiency of spore rupture was evaluated *via* phase contrast microscopy as well as by plating spore samples prior to and post processing, indicating that only 0.0001% of the spore population remains intact. Following disruption, samples were centrifuged to remove spore debris and silica beads from suspension (16,000×g; 10 min; 4°C). Approx. 700 µl of liquid was transferred to an RNase-free tube and incubated at RT for 5 min. 300 µl of chloroform was added. The sample was vortexed for 10 s and centrifuged (16,000×g; 15 min; 4°C) to separate the phases. The aqueous phase was transferred to a fresh tube containing 200 µl of 95% EtOH and placed on ice. The mixture was transferred to a spin column

assembly (SV Total RNA isolation system; Promega) and centrifuged (16,000×g; 1 min). Columns were washed twice with 600 µl and 250 µl of RNA wash solution. RNA was eluted in 45 µl of RNase-free water. DNase treatment was carried out using the Turbo DNase kit (Ambion) according to manufacturers protocol. The enzymatic reaction was cleaned-up using the RNeasy Mini Kit (Qiagen) RNA purity and quantity was determined by nanodrop UV spectroscopy. RNA integrity was confirmed on a RNA 6000 nano lab-Chip using a Bioanalyzer 2100 instrument (Agilent). Samples were stored at −80°C until further analysis.

Reverse Transcriptase PCR

For conventional RT-PCR, first strand cDNA was synthesized from total RNA using random decamers as primers and the RETROscript Kit (Ambion) according to manufacturer's instructions and then used in standard Taq (Sigma) PCR reactions using gene specific primers (Table S3).

Microarray Analysis

The microarray was constructed by determining all unique genes from the predicted coding sequences of *C. difficile* strains 630, QCD-32g58, 196, R20291 plasmid pCD630. Multiple optimal hybridisation 60-mer oligonucleotide sequences were designed (Oxford Gene Technologies), from which a minimal non-redundant subset of oligonucleotides were selected with a target coverage of three 60-mers per gene. Arrays were manufactured on the Inkjet *in situ* synthesized platform (Agilent) using the 8×15 k format.

Competitive genomic DNA/RNA hybridizations were carried out according to standard Agilent protocols. Briefly, 5 µg of total RNA was labelled with Cy3 *via* reverse transcription using SuperScript II (Invitrogen). 1 µg of gDNA was labelled with Cy5 using Exo-Klenow fragment. Both labelling reactions were cleaned-up using the PCR Purification MiniElute Kit (Qiagen). Cy3-labeled cDNA and Cy5-labeled gDNA were mixed with 10× blocking agent and hybridization buffer and incubated for 3 min at 95°C and 30 min at 37°C. Samples were then applied to a *C. difficile* OGT array CDv2.0.1 (BµG@S) and incubated for 24 h in a hybridization oven set to 65°C. The microarray slide was washed, fixed in acetonitryl, dried and scanned using an Agilent G2565CA Scanner. Microarray data extraction was performed using ImaGene software (BioDiscovery), and further processed using MAVI Pro software (MWG Biotech). Normalization and statistical analysis were performed using GeneSpring v7.3.1 software (Agilent Technologies). Briefly, gene specific data was derived from average intensity of between 1 and 5 oligonucleotide reporters. Gene values below 0.01 were set to 0.01. Each gene's measured intensity was divided by its control channel value in each sample; if the control channel was below 10 then 10 was used instead. If the control channel and the signal channel were both below 10 then no data was reported. Each measurement was divided by the 50th percentile of all measurements in that sample. Replicate time points were normalized to the 180 minute time point: each measurement for each gene was divided by the median of that gene's measurements in the corresponding control samples. Following the initial experiment covering eight time points (0′, 15′, 30′, 45′, 60′, 90′, 120′ and 180′), two additional biological replicates were carried out for time points 30′, 60′, 90′ and 180′. Each time point was independently tested versus 180 min using 1-way ANOVA using Benjamini-Hochberg multiple testing correction and $p = 0.01$ or 0.05.

Accession Numbers

The array design (CDv2.0.1) is deposited in BµG@Sbase (Accession No. A-BUGS-49; http://bugs.sgul.ac.uk/A-BUGS-49) and ArrayExpress (Accession No. A-BUGS-49). Fully annotated microarray data have been deposited in BµG@Sbase (accession number E-BUGS-145; http://bugs.sgul.ac.uk/E-BUGS-145) and also ArrayExpress (accession number E-BUGS-145).

Supporting Information

Figure S1 RNA quality control. A) Gradual increase in RNA yield observed during spore germination. B) Bioanalyzer pseudogel with RNA Integrity (RIN) values C) Bioanalyzer electropherograms showing two distinct peaks corresponding to 16S and 23S rRNA. In addition, two smaller rRNA species were identified in dormant spores and in early germination, represented by small peaks on Bioanalyzer spectra. 5S rRNA peak visible at retention time 23 seconds.
(DOCX)

Table S1 List of genes up and down regulated during germination.
(XLS)

Table S2 Abundant spore transcripts.
(XLS)

Table S3 Primers used in this study.
(DOCX)

Acknowledgments

We would like to thank Simon Cutting for expert advice on sporulation, Robert Fagan for his insight and advice, Melissa Martin for her help with carrying out the microarray experiments and the Wellcome Trust for funding a studentship to M.D.

Author Contributions

Conceived and designed the experiments: MD NF AAW. Performed the experiments: MD. Analyzed the data: MD NF RS BW. Wrote the paper: MD NF RS.

References

1. Rupnik M, Wilcox MH, Gerding DN (2009) *Clostridium difficile* infection: new developments in epidemiology and pathogenesis. Nat Rev Microbiol 7: 526–536.
2. Carroll KC, Bartlett JG (2011) Biology of *Clostridium difficile*: Implications for Epidemiology and Diagnosis. Annu Rev Microbiol: 501–521.
3. Deneve C, Janoir C, Poilane I, Fantinato C, Collignon A (2009) New trends in *Clostridium difficile* virulence and pathogenesis. Int J Antimicrob Agents 33 Suppl 1: S24–28.
4. Deakin LJ, Clare S, Fagan RP, Dawson LF, Pickard DJ, et al. (2012) The *Clostridium difficile* spo0A gene is a persistence and transmission factor. Infect Immun 80: 2704–2711.
5. Setlow P (2006) Spores of *Bacillus subtilis*: their resistance to and killing by radiation, heat and chemicals. J Appl Microbiol 101: 514–525.
6. Setlow P (2007) I will survive: DNA protection in bacterial spores. Trends Microbiol 15: 172–180.
7. Gerding DN, Muto CA, Owens RC, Jr. (2008) Measures to control and prevent *Clostridium difficile* infection. Clin Infect Dis 46 Suppl 1: S43–49.
8. Riggs MM, Sethi AK, Zabarsky TF, Eckstein EC, Jump RL, et al. (2007) Asymptomatic carriers are a potential source for transmission of epidemic and nonepidemic *Clostridium difficile* strains among long-term care facility residents. Clin Infect Dis 45: 992–998.
9. Setlow P (2003) Spore germination. Curr Opin Microbiol 6: 550–556.
10. Paredes-Sabja D, Udompijitkul P, Sarker MR (2009) Inorganic phosphate and sodium ions are cogerminants for spores of *Clostridium perfringens* type A food poisoning-related isolates. Appl Environ Microbiol 75: 6299–6305.

11. Paredes-Sabja D, Setlow P, Sarker MR (2009) GerO, a putative Na+/H+-K+ antiporter, is essential for normal germination of spores of the pathogenic bacterium *Clostridium perfringens*. J Bacteriol 191: 3822–3831.
12. Paredes-Sabja D, Torres JA, Setlow P, Sarker MR (2008) *Clostridium perfringens* spore germination: characterization of germinants and their receptors. J Bacteriol 190: 1190–1201.
13. Paredes-Sabja D, Setlow P, Sarker MR (2010) Germination of spores of *Bacillales* and *Clostridiales* species: mechanisms and proteins involved. Trends Microbiol. 19: 85–94.
14. Sebaihia M, Peck MW, Minton NP, Thomson NR, Holden MT, et al. (2007) Genome sequence of a proteolytic (Group I) *Clostridium botulinum* strain Hall A and comparative analysis of the clostridial genomes. Genome Res 17: 1082–1092.
15. Sebaihia M, Wren BW, Mullany P, Fairweather NF, Minton N, et al. (2006) The multidrug-resistant human pathogen *Clostridium difficile* has a highly mobile, mosaic genome. Nat Genet 38: 779–786.
16. Xiao Y, Francke C, Abee T, Wells-Bennik MH (2011) Clostridial spore germination versus bacilli: genome mining and current insights. Food Microbiol 28: 266–274.
17. Lawley TD, Croucher NJ, Yu L, Clare S, Sebaihia M, et al. (2009) Proteomic and genomic characterization of highly infectious *Clostridium difficile* 630 spores. J Bacteriol 191: 5377–5386.
18. Sorg JA, Sonenshein AL (2008) Bile salts and glycine as cogerminants for *Clostridium difficile* spores. J Bacteriol 190: 2505–2512.
19. Sorg JA, Sonenshein AL (2009) Chenodeoxycholate is an inhibitor of *Clostridium difficile* spore germination. J Bacteriol 191: 1115–1117.
20. Sorg JA, Sonenshein AL (2010) Inhibiting the initiation of *Clostridium difficile* spore germination using analogs of chenodeoxycholic acid, a bile acid. J Bacteriol. 19: 4983–4990.
21. Wilson KH (1983) Efficiency of various bile salt preparations for stimulation of *Clostridium difficile* spore germination. J Clin Microbiol 18: 1017–1019.
22. Wheeldon L, Worthington T, Lambert P (2011) Histidine acts as a co-germinant with glycine and taurocholate for *Clostridium difficile* spores. J Appl Microbiol. 110: 987–994.
23. Wheeldon LJ, Worthington T, Hilton AC, Elliott TS, Lambert PA (2008) Physical and chemical factors influencing the germination of *Clostridium difficile* spores. J Appl Microbiol 105: 2223–2230.
24. Ramirez N, Abel-Santos E (2010) Requirements for germination of *Clostridium sordellii* spores in vitro. J Bacteriol 192: 418–425.
25. Keijser BJ, Ter Beek A, Rauwerda H, Schuren F, Montijn R, et al. (2007) Analysis of temporal gene expression during *Bacillus subtilis* spore germination and outgrowth. J Bacteriol 189: 3624–3634.
26. Bettegowda C, Huang X, Lin J, Cheong I, Kohli M, et al. (2006) The genome and transcriptomes of the anti-tumor agent *Clostridium novyi*-NT. Nat Biotechnol 24: 1573–1580.
27. Bassi D, Cappa F, Cocconcelli PS (2013) Array-based transcriptional analysis of *Clostridium sporogenes* UC9000 during germination, cell outgrowth and vegetative life. Food Microbiol 33: 11–23.
28. Nerandzic MM, Donskey CJ (2010) Triggering germination represents a novel strategy to enhance killing of *Clostridium difficile* spores. PLoS One 5: e12285.
29. Bleyman M, Woese C (1968) Ribosomal ribonucleic acid maturation during bacterial spore germination. J. Bacteriol 97: 27–31.
30. Chambon P, Deutscher MP, Kornberg A (1968) Biochemical studies of bacterial sporulation and germination. X. Ribosomes and nucleic acids of vegetative cells and spores of *Bacillus megaterium*. J Biol Chem 243: 5110–5116.
31. Jeng YH, Doi RH (1974) Messenger ribonucleic acid of dormant spores of *Bacillus subtilis*. J Bacteriol 119: 514–521.
32. Stock AM, Robinson VL, Goudreau PN (2000) Two-component signal transduction. Annu Rev Biochem 69: 183–215.
33. Setlow P (1974) Polyamine levels during growth, sporulation, and spore germination of *Bacillus megaterium*. J Bacteriol 117: 1171–1177.
34. Ruiz-Herrera J (1994) Polyamines, DNA methylation, and fungal differentiation. Crit Rev Microbiol 20: 143–150.
35. Mori H, Ito K (2001) The Sec protein-translocation pathway. Trends Microbiol 9: 494–500.
36. Voth DE, Ballard JD (2005) *Clostridium difficile* toxins: mechanism of action and role in disease. Clin Microbiol Rev 18: 247–263.
37. Ghosh S, Setlow P (2009) Isolation and characterization of superdormant spores of *Bacillus* species. J Bacteriol 191: 1787–1797.
38. Ghosh S, Setlow P (2010) The preparation, germination properties and stability of superdormant spores of *Bacillus cereus*. J Appl Microbiol 108: 582–590.
39. Stringer SC, Webb MD, George SM, Pin C, Peck MW (2005) Heterogeneity of times required for germination and outgrowth from single spores of nonproteolytic *Clostridium botulinum*. Appl Environ Microbiol 71: 4998–5003.
40. Wang G, Zhang P, Paredes-Sabja D, Green C, Setlow P, et al. (2011) Analysis of the germination of individual *Clostridium perfringens* spores and its heterogeneity. J Appl Microbiol 111: 1212–1223.
41. Ghosh S, Scotland M, Setlow P (2012) Levels of germination proteins in dormant and superdormant spores of *Bacillus subtilis*. J Bacteriol 194: 2221–2227.
42. Permpoonpattana P, Tolls EH, Nadem R, Tan S, Brisson A, et al. (2011) Surface Layers of *Clostridium difficile* Endospores. J Bacteriol. 23: 6491–6470.